AFRL-PR-WP-TR-1998-2067

COMBUSTION AND HEAT TRANSFER; VOLUME 1 - ADVANCED JET FUELS DATA STUDIES

S. Zabarnick
G. L. Dieterle
S. P. Heneghan
W. A. Rubey
T. F. Williams
D. R. Ballal
J. S. Ervin
D. H. Kalt
R. C. Striebich
K. E. Binns
R. R. Grinstead
R. E. Kauffman
M. D. Vangsness

University of Dayton Research Institute
300 College Park
Dayton, OH 45469-0001

APRIL 1998

FINAL REPORT FOR PERIOD JUNE 8, 1992 – DECEMBER 31, 1997

Approved for public release; distribution unlimited

PROPULSION DIRECTORATE
AIR FORCE RESEARCH LABORATORY
AIR FORCE MATERIEL COMMAND
WRIGHT-PATTERSON AIR FORCE BASE, OH 45433-7251

NOTICE

USING GOVERNMENT DRAWINGS, SPECIFICATIONS, OR OTHER DATA INCLUDED IN THIS DOCUMENT FOR ANY PURPOSE OTHER THAN GOVERNMENT PROCUREMENT DOES NOT IN ANY WAY OBLIGATE THE US GOVERNMENT. THE FACT THAT THE GOVERNMENT FORMULATED OR SUPPLIED THE DRAWINGS, SPECIFICATIONS, OR OTHER DATA DOES NOT LICENSE THE HOLDER OR ANY OTHER PERSON OR CORPORATION; OR CONVEY ANY RIGHTS OR PERMISSION TO MANUFACTURE, USE, OR SELL ANY PATENTED INVENTION THAT MAY RELATE TO THEM.

THIS REPORT IS RELEASABLE TO THE NATIONAL TECHNICAL INFORMATION SERVICE (NTIS). AT NTIS, IT WILL BE AVAILABLE TO THE GENERAL PUBLIC, INCLUDING FOREIGN NATIONS.

THIS TECHNICAL REPORT HAS BEEN REVIEWED AND IS APPROVED FOR PUBLICATION.

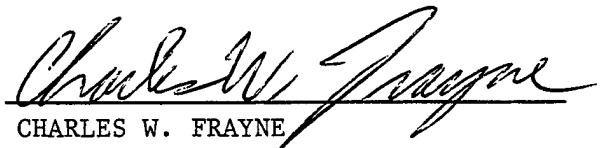

CHARLES W. FRAYNE
Combustion Branch
Propulsion Sciences and
Advanced Concepts Division

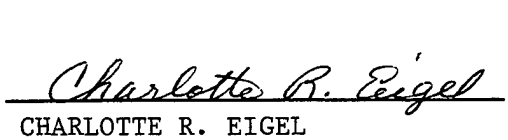

CHARLOTTE R. EIGEL
Chief, Combustion Branch
Propulsion Sciences and
Advanced Concepts Division

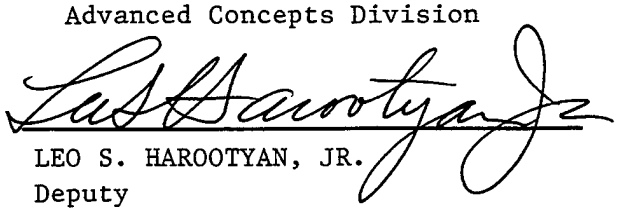

LEO S. HAROOTYAN, JR.
Deputy
Propulsion Sciences and
Advanced Concepts Division

Do not return copies of this report unless contractual obligations or notice on a specific document requires its return.

REPORT DOCUMENTATION PAGE

Form Approved OMB No. 0704-0188

1. AGENCY USE ONLY (Leave blank)	2. REPORT DATE	3. REPORT TYPE AND DATES COVERED
	April 1998	Final 6/8/92 – 12/31/97

4. TITLE AND SUBTITLE
COMBUSTION AND HEAT TRANSFER; VOLUME 1 – ADVANCED JET FUELS STUDIES

5. FUNDING NUMBERS
C-F33615-92-C-2207
PE: 62203
PR: 3048
TA: 05
WU: AH

6. AUTHOR(S)
S. Zabarnick, D.R. Ballal, K.E. Binns, G.L. Dieterle, J.S. Ervin, R.R. Grinstead, S.P. Heneghan, D.H. Kalt, R.E. Kauffman, W.A. Rubey, R.C Striebich, M.D. Vangsness, and T.F. Williams

7. PERFORMING ORGANIZATION NAME(S) AND ADDRESS(ES)
University of Dayton Research Institute
300 College Park
Dayton, OH 45469-0110

8. PERFORMING ORGANIZATION REPORT NUMBER
UDR-TR-1998-00035

9. SPONSORING/MONITORING AGENCY NAME(S) AND ADDRESS(ES)
Propulsion Directorate
Air Force Research Laboratory
Air Force Materiel Command
Wright-Patterson AFB, OH 45433-7251
POC: Charles W. Frayne, AFRL/PRSC, 937-255-6250

10. SPONSORING/MONITORING AGENCY REPORT NUMBER
AFRL-PR-WP-TR-1998-2067

11. SUPPLEMENTARY NOTES

12. DISTRIBUTION / AVAILABILITY STATEMENT
Approved for public release; distribution is unlimited

12b. DISTRIBUTION CODE

13. ABSTRACT (Maximum 200 words)

This report highlights studies performed in support of the development of advanced jet fuels, including JP-8+100, JP-900, and endothermic fuels. For the development of JP-8+100 fuel, we have tested hundreds of additives in both small and large scale test devices. We formulated combinations of the best additives (detergent/dispersant, hindered phenol antioxidant, and metal deactivator) and demonstrated their efficacy in reducing deposition under realistic aircraft conditions in large-scale simulator rigs. We optimized the concentrations of these additives for maximum effectiveness and minimum cost. We performed extensive studies of the compatibility of these fuel additives with current and future aircraft fuel system materials. We determined that the current best additives show no negative effects on both metallic and non-metallic fuel system materials. We also performed extensive studies on the fundamental processes of fuel oxidation, deposition, and pyrolysis. We made progress in support of development of future fuels such as JP-900 and endothermic fuels. Data set summaries of the much of the data obtained during the contract period are contained in the accompanying volume entitled, "Combustion and Heat Transfer; Volume 2 – Advanced Jet Fuels Data Sets."

14. SUBJECT TERMS
Jet Fuel, JP-8, JP-8+100, Fuel Additives, Autoxidation, Thermal Stability, Deposition, Fuel Systems

15. NUMBER OF PAGES
214

16. PRICE CODE

17. SECURITY CLASSIFICATION OF REPORT	18. SECURITY CLASSIFICATION OF THIS PAGE	19. SECURITY CLASSIFICATION OF ABSTRACT	20. LIMITATION OF ABSTRACT
UNCLASSIFIED	UNCLASSIFIED	UNCLASSIFIED	SAR

THIS PAGE LEFT INTENTIONALLY BLANK

TABLE OF CONTENTS

LIST OF FIGURES

LIST OF TABLES

PREFACE

This final report was submitted by the University of Dayton Research Institute (UDRI) under Contract No. F33615-92-C-2207, sponsored by the U.S. Air Force Research Laboratory, Propulsion Directorate, Wright-Patterson AFB, OH. Mr. Charles Frayne of AFRL/PRSC was the Contract Monitor and Dr. D.R. Ballal of the Aerospace Mechanics Division, UDRI was the Principal Investigator. This report covers work performed during the period June 8, 1992 through December 31, 1997.

The authors would like to acknowledge the support and encouragement of Dr. Mel Roquemore and Mr. Bill Harrison of the U.S. Air Force.

1. SUMMARY

This report highlights studies performed in support of the development of advanced jet fuels, including JP-8+100, JP-900, and endothermic fuels. For the development of JP-8+100 fuel, we have tested hundreds of additives in both small and large scale test devices. We formulated combinations of the best additives (detergent/dispersant, hindered phenol antioxidant, and metal deactivator) and demonstrated their efficacy in reducing deposition under realistic aircraft conditions in large-scale simulator rigs. We optimized the concentrations of these additives for maximum effectiveness and minimum cost. We performed extensive studies of the compatibility of these fuel additives with current and future aircraft fuel system materials. We determined that the current best additives show no negative effects on both metallic and non-metallic fuel system materials.

We also performed extensive studies on the fundamental processes of fuel oxidation, deposition, and pyrolysis. We developed chemical kinetic mechanisms which can simulate the oxidation and deposition processes. We performed experimental and modeling studies on fuel cooling which shows that deposition which occurs in fuel cooling heat exchangers can be a significant problem in fuel system design. We demonstrated an inverse relationship between oxidation and deposition over a range of fuels, and showed that our chemical kinetic mechanism can be used to explain this seemingly anomalous result. We developed statistical techniques to assist the evaluation of jet fuel additives, thermal stability measurements, and aircraft field performance. We developed a wide variety of fuels analysis techniques for measurement of the following: dissolved oxygen, detergent/dispersant capacity, antioxidants and phenolics, hydroperoxides, trace jet fuel compounds, metal deactivators, products of endothermic reforming, dissolved and free water in fuel, BHT, Betz dispersant, and elemental metals. We explored alternative techniques for reducing jet fuel deposition including: removal of dissolved oxygen, silylating agents, oxygen scavenging additives, and solid-phase extraction.

We also made progress in support of development of future fuels such as JP-900 and endothermic fuels. We explored the effect of supercritical fluid properties on high temperature fuels. We have begun to study the pyrolysis of fuel in catalytic and non-catalytic reaction systems.

Data set summaries of much of the data obtained during the contract period are contained in the accompanying volume entitled, "Combustion and Heat Transfer: Volume 2 – Advanced Jet Fuels Data Sets."

2. INTRODUCTION

Emerging environmental and technological demands of the 21st century imposed on the Air Force, the aircraft manufacturers, and the jet engine companies require the jet fuel to accomplish a variety of non-combustion related tasks. In particular, jet fuel is the primary coolant for aircraft hydraulics, environmental control subsystems, and the engine. Future high performance, high thermal efficiency engines will not only produce *more* excess heat, but also will have less fuel available with which to manage that heat. The end result is that jet fuel will be exposed to significantly higher temperatures for longer periods of time causing the fuel to degrade and foul aircraft and engine components.

In 1990, an Aircraft Thermal Management Working Group of Wright Research and Development Center (WRDC) investigated the cooling requirements for current, next generation, and future aircraft (Harrison, 1990). The estimated heat loads for various future aircraft and aircraft subsystems show a three-fold increase in the heat-loads for future aircraft as compared to the F4 aircraft. Also, the estimated worst case temperatures, pressures, and residence times experienced by fuel in typical modern engine and airframe components can be well into conditions where significant autoxidation of jet fuel occurs. After examining these and other projected requirements, the WRDC working group reached an alarming conclusion: "aircraft development in the near future will suffer performance penalties as tremendous quantities of ram air or excess fuel will be required to meet the heat sink requirements." To resolve the problem, the WRDC working group recommended the development of high thermal stability fuels, such as: (i) a high temperature thermally stable "JP-8+100" fuel which provides a 50% improvement in heat sink capability over conventional JP-8 fuel, and (ii) a new JP-900 fuel that has a 482C (900F) thermal stability and could eliminate the need to recirculate fuel onboard an aircraft.

Toward meeting these goals, the Air Force Wright Laboratory, Aero Propulsion and Power Directorate (WL/PO) initiated a 5 year program of research with the University of Dayton Research Institute (UDRI) beginning June 8, 1992. This program consisted of two phases: Phase I, Advanced Fuels, and Phase II, Advanced Combustion. This report will address only the Phase I, Advanced Fuels part of the program (the Phase II, Advanced Combustion program is addressed in a separate report). The objectives of the program were three-fold:

(1) To develop the research tools and perform the research needed to provide the basic understanding of the fundamental processes occurring in aircraft fuel system components that are required to develop JP-8+100, endothermic, and JP-900 thermally stable fuels.

(2) To develop laboratory and aircraft fuel system simulation tests and use them to evaluate the performance of additives required to increase the effective operating temperature of JP-8 fuels by 100F.

(3) To establish and utilize a database to evaluate fuel thermal deposition, combustor, and turbine models that can be used as an aid in designing hot components for 21st century aircraft.

In September 1996, three additional tasks were added to the program including: fuel/material compatibility tests, fuel system simulator development and additive evaluation tests, and advanced cooling studies.

To address these objectives we developed a variety of small and large scale fuel tests, analytical chemistry methods, and advanced modeling techniques. These newly developed techniques, and the studies performed with them, are the subject of this report. Our contributions to, and the success of, the JP-8+100 program have also been described in previous publications (Heneghan et al., 1996b; Heneghan et al., 1996c).

3. HIGHLIGHTS OF JET FUEL STUDIES

3.1 Quartz Crystal Microbalance Studies

The Quartz Crystal Microbalance (QCM) was developed and first used for the study of jet fuel thermal stability by Sandia National Labs (Klavetter et al., 1993). It enables the real-time, *in situ* measurement of extremely low amounts of deposits (<100 ng/cm^2). We originally acquired a QCM system in 1993 from Sandia and made numerous additions and operating modifications. As a result of these changes the QCM system has been used extensively for evaluating additives and for fundamental studies of fuel oxidation and deposition (Zabarnick, 1994b). These modifications include the addition of a pressure transducer and oxygen sensor to enable the direct *in situ* monitoring of the oxidation process (Zabarnick and Whitacre, 1998). For most testing we have chosen to operate the device under relatively low oxygen availability which more closely approximates that of real fuel systems (Zabarnick and Grinstead, 1994).

During the contract period, we utilized the QCM system for over 1,300 fuel tests encompassing additive testing and fundamental studies. Hundreds of JP-8+100 additive candidates were tested with the device. These test results are compiled in a series of UDR technical reports (Zabarnick, 1994a; Zabarnick et al., 1997; Zabarnick et al., 1995). The QCM was also used extensively for additive concentration optimization and additive package development (Zelesnik, 1995). In fact, the current JP-8+100 dispersant-antioxidant-metal deactivator combination was first tested and proven successful in the QCM (Zabarnick and Grinstead, 1994). The device has also been used extensively for testing of JP-8 and JP-8+100 fuel samples from the Air National Guard (ANG) field trials; these tests have confirmed that the JP-8+100 additive package has shown significant improvement in oxidation and deposition properties for fuels used in actual ANG aircraft. Highlights of some of the fundamental fuel studies performed using the QCM are summarized below.

We noted an inverse relationship between oxidation and deposition when looking at a range of different fuel samples using various fuel tests (Heneghan and Zabarnick, 1994). This behavior was readily confirmed using the QCM (Zabarnick, 1994b). These observations led us to develop a chemical kinetic mechanism to explain this apparent anomaly. We have shown that small amounts of easily oxidizable species present in fuel can result in a slowing of the oxidation rate of the fuel (Heneghan and Zabarnick, 1994; Zabarnick, 1993). These species, which are mostly heteroatomic (containing sulfur, nitrogen, and oxygen atoms), also contribute to the formation of deposits. Thus high depositing fuels, which contain these species, tend to oxidize slowly, while low deposition fuels, which lack these species, tend to oxidize rapidly.

We studied the temperature dependence of deposition and oxidation using the QCM system. Over the temperature range 140 to 180C, while oxidation increases with temperature, surface deposition peaks at an intermediate temperature (Zabarnick et al., 1996a). This observation was rationalized with previous observations in flowing and static tests of increasing deposition with temperature by analysis of the local oxygen availability of the system. We also measured the temperature dependence of the bulk insolubles and noted that these insoluble increase with temperature, as does the sum of the surface and bulk deposits.

We studied the effects on oxidation and deposition of blending a low depositing/fast oxidizing fuel ("good fuel") with a high depositing/slow oxidizing fuel ("bad fuel") (Zabarnick et al., 1996a). We found that adding small quantities (<10%) of the bad fuel to the good fuel had the positive effect of delaying oxidation while not significantly increasing deposition. Thus the resulting fuel has improved oxygen consumption characteristics and storage stability. We also found that diluting the bad fuel with the good fuel by 50% resulted in significant reduction in deposition with little change in oxidation rate. Thus the resulting fuel has better thermal stability. These blending techniques provide potential methods to inexpensively improve fuel properties. This blending study and others (Balster et al., 1996; Jones et al., 1996) have also been used for the development of improved chemical kinetic models of fuel autoxidation and antioxidant action.

Using the QCM, we studied the effect of materials on deposition (Zabarnick et al., 1996a). We used quartz crystals with various electrode surface materials including gold, aluminum, platinum, and silver. We found the gold and aluminum surfaces yield identical deposition amounts in two fuels. The platinum surface increased deposition in one fuel, but not the other. This shows that gold and aluminum are relatively non-catalytic under these conditions, while platinum is probably catalytically decomposing hydroperoxides, thereby increasing deposition. We found that the silver electrodes rapidly reacted with elemental sulfur present in some fuels. The result was extremely large mass deposition from the formation of silver sulfide on the electrode surface. Taking advantage of this reaction, we developed an extremely sensitive technique, using the QCM and silver electrode surfaces, for the detection and measurement of elemental sulfur in jet fuels (Zabarnick et al., 1996b). This technique may also be used for the detection of hydrogen sulfide in fuels and may also be used in other hydrocarbon liquids.

We studied the effect of oxygen availability on deposition in the QCM (Zabarnick et al., 1996a). We found that under complete oxygen consumption conditions, deposition is proportional to oxygen availability. But, under conditions of partial oxygen consumption, lower amounts of oxygen can actually result in increased deposition. This result has important implications for fuel systems which employ on-board inert gas generating systems (OBIGGS) to lower the oxygen concentration in fuel tanks. Studies which confirm these results are also reported in the Phoenix rig section.

We observed a strong correlation between oxidation and deposition for various fuels in the QCM (Zabarnick and Whitacre, 1998). Figure 1 shows an example of this correlation for fuel POSF-3145 with 3.0 mg/L MDA at 140C. The figure shows that the fuel begins to deposit near 2 hours, and deposition levels off at 4.3 $\mu g/cm^2$ after 7 hours. Correspondingly, oxygen removal begins near 2 hours and is complete near 6 to 7 hours. Also shown are pressure measurements, demonstrating the good agreement between the two techniques for following the fuel oxidation. This correlation between oxidation and deposition is strong and graphic confirmation of the common wisdom that deposition results from fuel oxidation.

We pioneered the use of pressure transducers and oxygen sensors in the QCM system for monitoring of fuel oxidation (Zabarnick, 1994b; Zabarnick and Whitacre, 1998). The pressure transducer technique provides an indirect measure of the extent of fuel oxidation, while the oxygen sensor is a direct measure of the headspace oxygen concentration. The development of these *in situ* techniques has provided substantial insight for both additive development and fundamental studies.

We studied the action of the JP-8+100 additive components BHT and MDA by following their concentration during fuel autoxidation in the QCM system (Zabarnick and Whitacre, 1998). To follow these additive concentrations, analysis techniques for determining their concentrations were developed using combinations of solid-phase extraction, gas chromatography, and mass spectrometry. The results indicate that both BHT and MDA are consumed during fuel oxidation. Presumably BHT reacts with alkylperoxy radicals, while the removal pathways for MDA are as yet unknown. We also noted that oxidation rates increase upon reduction of these additives below some critical level. In the case of MDA, significant increases were observed when the MDA concentration dropped below that required to complex the dissolved copper present as shown in Figure 2. These results are important for the design of additive packages.

We performed QCM tests on a series of 28 JP-8 and JP-5 fuels from military bases world-wide (Zelesnik, 1995). This "world survey" fuels study was conducted to determine the range of expected fuel behavior and the type of improvements expected from the addition of the JP-8+100 additive package. It was found that the addition of MDA to the Betz-Dearborn dispersant/BHT combination resulted in significant improvement for many of the fuels. The neat world survey fuels were found to, as a group, oxidize more rapidly and deposit more heavily than the typical fuels previously tested (Grinstead et al., 1994).

In testing a variety of fuels with the QCM we have noted that fuels can be classified in three general categories (Zabarnick, 1994b). The first class exhibits very good thermal stability and consumes oxygen rapidly. This first class includes hydrotreated fuels and pure solvents; these fuels contain few naturally occurring inhibitors to slow oxidation. The second class exhibits poor thermal stability and oxidizes slowly. This second class includes POSF-2827 fuel; these fuels contain naturally occurring inhibitors which slow oxidation and increase deposition. The third class exhibits relatively poor

thermal stability and also consumes oxygen readily. This third class includes POSF-3119 fuel; these fuels do not contain an optimum concentration of naturally occurring inhibitors and/or have relatively high concentrations of catalytic metals. These fuels do contain species which promote deposit formation. This classification of fuel types is useful for understanding fuel deposition and oxidation and for designing techniques to decrease deposition and slow oxidation.

We have used solid-phase extraction techniques for a variety of studies of jet fuel. In particular, we have shown that passing jet fuel through a silica gel solid-phase extraction cartridge can significantly improve fuel thermal stability (Zabarnick, 1994b). The species that adsorb to the silica gel can be desorbed by treatment with methanol. These species extracted from a high depositing fuel and subsequently added to a low depositing, will increase the deposition of the low depositing fuel. This result is significant as it shows we can remove and concentrate the "bad actors" which increase jet fuel deposition. It also indicates these bad actors are polar in character, relative to the bulk of the jet fuel. Much work has also been performed on the attempted analysis of these species with only limited success. They appear to be composed mostly of phenolic compounds and unidentified polar sulfur compounds.

3.2 Isothermal Corrosion Oxidation Test Studies

The Isothermal Corrosion-Oxidation Tester (ICOT) is a static test that has been employed extensively for the measurement of the thermal stability of jet fuels and jet fuel additive blends. The ICOT has become one of the primary screening tests for JP-8+100 additives. In this test a fuel sample is stressed in a glass tube at 180C for 5 hours with air flowing through a glass blower tube at 1.3L/hr. After the fuel sample has cooled completely, it is filtered through a 1 μm glass microfiber filter. The amount of solids is measured gravimetrically and reported as mg of solid/liter of fuel. The fuels thermal stability, or tendency to form deposits, is determined by the amount of solids collected on the filter.

Hundreds of fuels from the laboratory and the field have been characterized in the ICOT. Some fuels, such as JPTS produce no deposits under these testing conditions. Therefore, the ultimate goal for the JP-8+100 additive program is to have no deposits. A fuel with moderate thermal stability, 2827, was chosen to evaluate all incoming additives. Hundreds of additives were tested during the course of this program. Some of these results have been summarized in a report (Grinstead, 1994). Promising additives were blended in additional fuels. Additives that performed well in a variety of fuels were recommended for further testing in other testing rigs. The end result of this work is that one additive, Betz 8Q405, performed well in a variety of fuels in a variety of tests. Thus, it is currently being used in the additive package for JP-8+100 jet fuel in the field with

excellent results. The ICOT has been an economical way to evaluate many additives due to the short test duration, low fuel consumption, and quantitative results produced.

A recent modification will extend the usefulness of this test. The ICOT setup was modified to include an Ingold Oxygen Sensor (Grinstead, 1997). The sensor measures the amount of oxygen in the headspace in real time. Other modifications include using a blower tube with a sintered tip to facilitate the uptake of oxygen into the fuel. Also, the fuel is sparged with nitrogen instead of air during the heat up time. This prevents oxidation reactions from occurring until the desired temperature is reached. This technique will be especially useful for evaluating antioxidants because delays in oxidation can be observed. Also the total amount of oxygen consumed during a run relative to the amount of deposits is a new way to compare fuels. Now, the relationship between a fuels oxidation behavior and deposition can be studied in the ICOT.

3.3 Phoenix Rig Studies

The Phoenix Rig was a flowing system developed by UDRI and used for the study of jet fuel thermal and oxidative stabilities (Heneghan et al., 1993). Fuel was pumped at relatively high pressure (up to 3.45 MPa) through stainless-steel tubing held within copper blocks (Figure 3) that were used for both the heating and cooling of jet fuel. For heating, the copper blocks contained internal heating elements. For cooling, passages were machined within the copper blocks through which either water or air passed. Bulk fuel temperatures up to 625C and Reynolds numbers up to 11,000 could be attained. As found in actual aircraft, the oxygen availability was limited, and the oxygen concentration was measured at three different locations by gas chromatography. In addition, the mass of surface deposits were measured by carbon burnoff analysis. The Phoenix Rig was used for additive evaluation and fundamental studies of fuel oxidation and surface deposition. The capabilities of dissolved oxygen, deposition, and temperature measurement were extremely fruitful in the development of global (Chin et al., 1994; Ervin et al., 1996b; Heneghan et al., 1993; Heneghan et al., 1995; Katta et al., 1993) and pseudo-detailed chemical kinetic models (Ervin and Zabarnick, 1998; Zabarnick, 1998) for computational fluid dynamics simulations.

Several JP-8+100 additive candidates were tested using the Phoenix Rig (Heneghan et al., 1995; Heneghan et al., 1996b) with some results presented in a series of technical reports (Williams et al., 1994a; Williams et al., 1994b). The Phoenix Rig was also used in the development of an on-line technique to measure dissolved oxygen concentration in a flowing system (Rubey et al., 1995) and in the testing of coatings designed to reduce deposition. Important results from some of the fundamental fuel studies performed using the Phoenix Rig are summarized below.

We performed experiments using JP-8 and other additives to obtain baseline data on the structure and chemical compositions of surface deposits after different time

periods (Ervin et al., 1996a). The observed transient oxidation behavior was related to measured time-dependent changes in the surface deposits. Increasing dissolved oxygen concentrations and large changes in surface deposition were found to be characteristic of the "induction" time. Spectroscopic analysis showed that deposits which formed at heated walls are chemically different from those which form at cooled walls (Table 1). In addition, the microstructure of the deposits formed at heated walls generally consisted of microspherical particles while those formed in cooled regions appeared to be more uniform as the result of once-soluble species becoming insoluble at relatively low temperatures (Ervin and Williams, 1996; Heneghan et al., 1995). Certain JP-8 additives significantly reduced fouling in the heated section, but their effectiveness in the cooled section, especially after long periods was unclear.

We conducted flowing experiments at relatively large flow rates (62 and 100 mL/min) in order to gain a fundamental understanding of the effect of low dissolved oxygen concentration on fuel thermal stability under conditions of partial oxygen consumption (Ervin et al., 1995a; Ervin and Williams, 1996; Ervin et al., 1997). In air-saturated fuel at low temperatures, it is commonly accepted that deposits form from a series of free-radical chain reactions, but these reactions are not understood. Furthermore, it has long been thought that reducing the dissolved oxygen would decrease the resulting deposition, and this has been experimentally observed for complete oxygen depletion. However, little work was previously performed concerning partial oxygen consumption. Experiments were conducted in which the dissolved oxygen concentration at the flow inlet was varied, and the high flow rates allowed for incomplete oxygen consumption. We found that low inlet oxygen concentrations may sometimes actually result in increased surface fouling and is a very important discovery for future fuel system design (Table 2). Although not well understood, this observation is seemingly contrary to nearly all previous observations concerning the relationship between oxygen consumption and deposit formation (Hazlett, 1991). We suspect that surface deposits which formed from degassed fuel and partial oxygen consumption arise from reactions different from those with air-saturated fuel and complete oxygen consumption as suggested by the difference in chemical composition. To get significantly reduced deposition under conditions of partial oxygen consumption (which is generally found in actual engines), these studies indicate that the dissolved oxygen concentration must be very low, the actual concentration depending on the fuel, temperature, flow rate and surface material.

Some theories (Hazlett, 1991) for the formation of deposits assume that particles, nucleate, grow, and agglomerate within the bulk and then adhere to heated surfaces. However our non-isothermal experiments conducted at high flow rates, suggest that adherence of bulk particles alone does not adequately describe the deposition process. We found that the dependence of deposition on wall temperature in the heated sections suggests the preferential deposition at the stainless-steel walls, the radial location of maximum temperature in the tube (Ervin and Williams, 1996; Ervin et al., 1997). Because of the greater temperatures existing there together with potential catalytic effects of the stainless-steel, the fuel oxidation may be greatest there.

We used the Phoenix Rig to show that fluid dynamics and heat transfer can strongly influence fuel oxidation and deposition (Blust, 1993; Katta et al., 1995). We explored the influence of buoyancy on the flow typical of that found in thermal stability studies, and we found that buoyancy forces had a significant effect on heat transfer and oxygen consumption for Reynolds numbers up to 2300. It was hypothesized that buoyancy forces normal to the flow direction increase the heat and mass transport, develop three-dimensionality, and thus make the flow turbulent. In addition, flow instabilities were observed when the fuel was flowing downward in a vertically mounted test section.

3.4 Extended Duration Thermal Stability Test Studies (EDTST)

The Extended Duration Thermal Stability Test was developed by us to provide fuel thermal stability information for designers in addition to evaluating fuels. This system was established by modifying an existing facility that was originally a "hydrotreater" for processing fuels. A schematic of the Extended Duration Thermal Stability Test system is shown in Figure 4. The system consists of a 60 gallon feed tank, an electrical motor driven gear pump, two clamshell furnace heaters, and a scrap tank. The first furnace heater (preheater) in the system is used to establish the desired fuel bulk temperature into the second heater and to establish the desired fuel bypass temperature. The fuel bulk temperature represents the temperature that results from aircraft and engine heat loads. The maximum bulk temperature used for present day JP-8 fuel systems is 300F (149C). A goal for JP-8+100 fuel is to provide a capability to operate at 400F (204C) bulk fuel temperatures. Temperature is established in the second furnace heater (main heater) to represent the wetted wall temperatures associated with engine injection nozzles. A goal for JP-8+100 fuel is to provide a wetted wall temperature increase from 400F (204C), the present limit of JP-8, to 500F (260C) for engine fuel injection nozzle design.

Both furnace heaters are 0.81 meters long and resistance heated. They each have five heating element zones that are independently controlled. The fuel flows upward through a single stainless steel tube in each heater. The tube in the preheater has an outside diameter of 1.27 cm and a wall thickness of 0.0889 cm. The tube in the main heater has an outside diameter of 0.32 cm and a wall thickness of 0.0889 cm. Each tube is assembled inside a thick walled furnace tube that has an inside diameter of 2.54 cm and an outside diameter of 5.08 cm. The tubes have thermocouples attached to the outer wall for measuring wetted wall temperatures. The annular space between the furnace tube and heater tube is filled with sand. A typical main heater assembly is shown in Figure 5. During the test, the center section of this heater is controlled to achieve the highest temperature as measured by the thermocouples on the outside wall of the tube. A typical temperature profile for this tube is shown in Figure 6. A fuel bypass line is installed downstream of the preheater to represent the aircraft recirculation line from the engine to

the airframe tanks. A water/fuel cooler is installed in this line to represent the aircraft ram air heat exchanger cooler. A 2μ filter is also installed in the line for 4 hours to measure particles in the recirculated bulk fuel. Since effects of recirculation are one of the purposes of this test, the filter is installed for only a short duration. Aircraft fuel systems will probably not have a filter in the recirculation line. A 7μ filter is also installed downstream of the heater. This filter provides an indication of particles that the fuel nozzles will experience in an advanced fuel system design. After each test the preheater and heater tubes are cut up into 2-inch segments. The carbon on these segments and the filters are then measured using the LECO Carbon Analyzer.

A flow rate out of the system of 1 gallon per hour (gph) and duration of 96 hours have been used for most tests. Approximately 100 gallons of fuel is required for a 96 hour test. At the 1 gph flow rate and a bypass flow also at 1 gph, the residence time from the inlet of the preheater to the outlet of the main heater is 50 seconds. Similarly, the residence time from the inlet to the outlet of the main heater is 1.1 seconds with a Reynolds number of 2,400. These residence times are representative of those in aircraft and engine fuel systems. The Extended Duration Thermal Stability Test system is computer controlled and can run unattended for long periods of time. Over 18,000 hours of testing was conducted on this test system during this program.

3.4.1 Sensitivity Tests

Initially, sensitivity type tests were conducted in the EDTST system to establish the relationship of various system design factors in regards to thermal stability. The following sensitivity tests were conducted:

a. Carbon deposits versus wetted wall temperature

b. Thermal stability effects of fuel bulk temperature at various wetted wall temperatures

c. Thermal stability effects of high temperature fuel recirculation.

d. Thermal stability effects of various fuels.

A comparison of heater tube carbon deposits at various wetted wall temperatures (WWT) is shown in Figure 7 (Harrison et al., 1993). For the three temperatures, 450F (232C), 500F (260C), and 550F (288C), tested, the carbon deposits increased exponentially as the temperature was increased. A test duration of 72 hours, POSF-2926 (Jet-A) fuel, and a bulk fuel temperature of 300F (149C) into the heater were used for this test series.

A comparison of heater tube carbon deposits at various bulk fuel inlet conditions with a wetted wall of 500F (260C) is shown in Figure 8. The deposits at bulk temperatures below 350F (177C) were very similar in magnitude. However, above 350F (177C) the heater deposits increased. This indicates that at higher bulk temperatures there is a coupling effect between bulk fuel temperatures and wetted wall temperatures for

forming deposits. The test duration and fuel were the same as used for the previous discussed test series.

The effect of fuel recirculation was evaluated in two system configurations. The first configuration (two-pass recirculation) consisted of flowing all of the fuel through the preheater at the desired outlet bulk fuel temperature, then, flowing this fuel through the preheater and heater (Dieterle and Binns, 1994). This method insures that all of the fuel has been recirculated at high temperatures. The other configuration (active recirculation) consisted of bypassing fuel back to the fuel tank downstream of the preheater. This is representative of advanced aircraft fuel systems such as the F-22. A comparison of the heater carbon deposits that resulted from tests of these two methods along with a no recirculation test is shown in Figure 9. These tests were conducted at a bulk inlet temperature of 350F (177C) and a wetted wall temperature of 500F (260C). POSF-2980 fuel was used for this test with a test duration of 96 hours. The results indicate a significant increase in deposits with both recirculation methods when compared to the no bypass test. The two-pass method did produce higher deposits than the other method. However, it takes twice as much time as the other method and does not represent actual fuel system conditions. Therefore, the active recirculation method was selected for evaluating the JP-8+100 fuel candidates (Dieterle and Binns, 1995).

Throughout the program, eight fuels have been used for the various tests. A comparison of the heater deposits of four of these fuels is shown in Figure 10. Since the fuels were tested at different phases of the program, the same test conditions were not used for all fuels. The fuels shown in Figure 10 were tested in a recirculation type test for 96 hours. A bulk fuel temperature of 350 F (177C) and a wetted wall temperature of 500F (260C) were the conditions for these tests. The average deposit for the segment where the maximum deposit occurred for the four fuels was 8,700 ug/cm^2. A thickness of over 0.003 inch is estimated for this average deposit.

3.4.2 Test Results of JP-8+100 Additives Evaluations

The EDTST was identified by WL/POSF as one of the significant tests of the JP-8+100 additives because of its capability for evaluating fuels at realistic fuel system temperature conditions. The preliminary evaluation of the additives has been accomplished at two temperature conditions. A bulk temperature of 350F (177C) and a wetted wall temperature of 500F (260C) with active recirculation were used for prescreening the additives. The additives that perform satisfactory at these conditions were then tested at a 400F (204C) bulk fuel temperature and the same wetted wall temperature. The satisfactory additives at this condition were deemed as candidates for JP-8+100 fuel and were then subjected to material compatibility and ARSFSS testing.

Preliminary screening tests of the JP-8+100 additives were conducted in the QCM, ICOT, and HLPS (Binns et al., 1995). The additives that were determined to be promising based on these test results were then tested in the EDTST. Betz 8Q405 with

BHT was the first additive package tested. MDA was added later in the program and the package is referred to as Betz 8Q462 (Binns and Dieterle, 1996). This additive has provided the desired thermal stability increase for all of the fuel tested in the EDTST except for bulk fuel temperature. Some of the JP-8 fuels with this additive had slight deposits form in the bulk fuel at temperatures above 375F (191C) with active recirculation. Since it is envisioned that close tolerance valves will be exposed to fuel at these high bulk temperatures, even slight deposits are not desirable. A comparison of the deposits formed, on the tube segment with maximum heater deposit, for five fuels with the Betz additive at a wetted wall of 500F (260C) and bulk temperatures of 350F (191C) and 400F (204C) is shown in Figure 11. A significant reduction in deposit is provided by this additive compared to the unadditized fuels (shown in Figure 10) tested at the same wetted wall temperature and 350F (191C) bulk temperature. A test was attempted on a POSF-3166 (JP-8) fuel at 400F (204C) bulk temperatures, but it was terminated after 24 hours due to excessive carbon deposits forming on filter, lines, thermocouples and flow meters. Test of other JP-8 fuels at this higher bulk temperature was not attempted because of the extensive effort required to replace tubes and other components. The problem with 400F (204C) bulk temperatures is depicted by the preheater deposits as shown in Figure 12. The preheater deposits for the same fuels with and without the Betz additive at 350F (191C) are included for comparison purposes. These results indicate that four of the five fuels tested produce deposits at the higher bulk temperature. The JP-8 fuels all had higher deposits than with the Betz additive at 350F (191C) bulk temperatures and three of the fuels had higher deposits than the Betz additive at 400F (204C) bulk. The other JP-8+100 additive candidates had similar deposits at 400F (204C) bulk fuel temperatures. Test of JP-TS fuel at these conditions indicated that it also produced deposits at the 400F (204C) bulk conditions.

A comparison of the heater tube carbon deposits at the two screening test conditions for the additives that are considered to be acceptable based on the EDTST is shown in Figure 13. These additives are Betz 8Q462, Mobil 147b/BHT/MDA, SDA/BHT/MDA, and Ethyl 3407. A similar comparison of the preheater deposits for these fuels is shown in Figure 14. Further evaluation of these additives was then conducted in the ARSFSS as discussed in the following section.

3.5 Advanced Reduced Scale Fuel System Simulator (ARSFSS) Studies

The Advanced Reduced Scale Fuel System Simulator has more extensive capabilities than the Extended Duration Thermal Stability Test. It is capable of simulating thermal and flow profiles of aircraft fuel systems. It also has valves that are representative of actual aircraft. The simulator consists of three major systems. These systems are the fuel conditioning system, the airframe fuel system simulator and the engine fuel system simulator. A schematic of this simulator is shown in Figure 15. The simulator is configured for simulating an F-22 aircraft with an F119 engine. The flow

established for the simulator is approximately 1/72 scale of the F119 engine. The burn flow for the simulator is 1/3 of the flow for a single F119 fuel nozzle. The total flow that is required for each test is approximately 1,500 gallons.

The primary test articles of the simulator are (1) the Fuel Cooled Oil Cooler (FCOC), (2) the flow divider valve, (3) the Burner Feed Arm (BFA), and (4) servovalves #1 and 2. The fuel cooled oil cooler represents the engine lube system cooler. It consists of an induction heater and a steel manifold with three, 3/8-inch diameter, 0.035-inch thick wall tubes and associated thermocouples. The tubes are connected to provide for three passes through the heater. The tube that is used for the final pass through the heater is removed after each test. It is, then, cut into 2-inch long segments and subjected to carbon analysis. The flow divider valve (Figure 16) is an actual F119 valve that has been modified by changing the slot width for the reduced flow. The materials, clearances, and function are representative of the F119 flow divider valve. The performance of this valve is evaluated by a hysteresis test and visual inspection. The burner feed arm is RF induction heated. It consists of a steel clamshell with a 1/8-inch, 0.020-inch thick wall stainless steel tube installed in the middle of the clamshell. Thermocouples on the outside of the tube are located along the entire length to measure the temperature profile of the tube. At the end of the tests, this tube is cut up into 1-inch long sections and subjected to carbon burnoff. The servovalves (Figure 17) are modified F119 engine control valves. They are the second stage valves of electrohydraulic valves used in the engine control system. The materials and clearances are representative of the actual engine valves. The performance of these valves is evaluated by a hysteresis test and visual inspection.

The preliminary testing for this program was conducted to evaluate potential fuel thermal stability problems with the F-22 aircraft fuel system. Recirculation of high temperature fuel back to the fuel tanks was one of the major concerns for this fuel system. This series of tests was conducted at 300F (149C) out of the FCOC and a wetted wall temperature of 450F (232C) in the BFA. A generic F-22 duty cycle (Figure 18) established by Pratt and Whitney was also used for these tests. The initial two tests were conducted with Jet-A fuel (POSF-2980). These tests resulted in significant hysteresis increases in the servo and flow divider valves. Disassembly of the valves revealed a light brown residue on the valve parts. Analysis of the deposits revealed that the deposit consisted of 7 percent copper. The only known source for this copper was the gear pump's bronze bearings. Another type pump (vane) that did not contain any copper was purchased to avoid this problem in subsequent tests. Before the replacement pump was available, another test was conducted with no bypass line back to the airframe fuel tanks to determine if recirculation of the 300F (149C) fuel was a contributor to the valve deposits. Disassembly of the valves revealed a similar deposit as the initial tests. Based on this test it was concluded that recirculation of 300F (149C) fuel back to the tanks was not a major contributor to the valve deposits. The next two tests were conducted at the same conditions as the initial test with the addition of the JP-8 additives with and without a JP-8+100 additive. There were no observable deposits on the valves after either of these tests. This was expected with the JP-8+100 additive, but not for the addition of the JP-8

additive only. Another test was conducted with the JP-8 additive, which resulted in the same results. Particles of rust (iron oxide) were also observed on the filters and on disassembled components. Therefore, the deposits with the Jet-A fuel may have resulted from reactions due to the iron. The rust inhibitor in the JP-8 fuel is suspected to eliminate these reactions. A comparison of the heater carbon deposits for these five test runs is shown in Figure 19. The JP-8+100 additive had at least a ten-fold reduction in deposit compared with the other test runs.

For the next series of tests, the new vane pump and a 1-micron filter in the fuel supply line were installed into the simulator. The filter was installed to eliminate the iron oxide from the system. Test of the Jet-A fuel with and without the JP-8 additives was repeated to determine the effects of these changes. As shown in Figure 20, the carbon deposits were greatly reduced for the fuel with or without the JP-8 additives. Another test of the same fuel was conducted at an FCOC outlet temperature of 325F (163C) and a wetted wall temperature of 450F (232C). The valves did not have any significant deposits after any of these tests.

Tests to evaluate the high temperature capability of JP-8+100 additives were conducted at an FCOC outlet temperature of 350F (177C) and a wetted wall temperature of 500F (260C). The fuel used for this test was POSF-3119 with the JP-8 additives. The JP-8+100 additives tested were Betz 8Q462, Mobil 147b/BHT/MDA, and SDA/BHT/MDA. The fuel was tested with and without the JP-8+100 additives. A comparison of the BFA carbon deposits for these tests is shown in Figure 21. There were significant deposits for fuel without the JP-8+100 additive and essentially no deposits with the additives. The flow divider and servo #2 valves also had significant deposits without the additive and essentially no deposits with the additive. There also was unacceptable hysteresis of servo valve#2 after the test without the additive. Tests of the Betz additive were conducted with FCOC outlet temperatures of 375F (191C) and 400F (204C) and a BFA wetted wall temperature of 500F (260C) to verify the problem with deposits at the higher bulk temperatures. The comparison of carbon deposits on the FCOC and BFA after these tests is shown in Figure 22 and Figure 23. At the higher FCOC outlet temperature, there were larger deposits on the FCOC tube. This correlates with the larger deposits on the preheater tube for the EDTST at similar temperature conditions. The flow divider valve and servo valve #2 also had significant deposits after the higher temperature test and had no observable deposits after the 375F (191C) bulk tests.

A series of tests in the EDTST and the ARSFSS were conducted on higher concentrations of the Betz additive package to increase the bulk temperature capability to at least 400F (204C) (Dieterle and Binns, 1997). However, the Betz 8Q462 additive was found to be as good or better than the higher additive concentrations.

3.6 Fuels/Materials Compatibility Studies

This program has involved several tasks and activities in support of the Air Force fuels contract. These tasks include: Higher Acid Number Fuel/Materials Compatibility Studies, Fuel System Materials (Airframe/Engine) Listing/Cataloging, KC-135 Refueling Accident Support, Fuel/Materials Compatibility Testing for the JP-8+100 Fuel Additive Packages, Fuel/Materials Compatibility Testing for the F-16 Additive, and the Fuel/Materials Compatibility Applications Test Stand. This report will highlight the accomplishments pertaining to the JP-8+100 Fuel Additive Package studies. This work is also detailed in a separate technical report (Kalt, 1997) and on the World-Wide Web at https://posfbbs.appl.wpafb.af.mil/.

To date, the JP-8+100 (Betz 8Q462) thermal stability additive (TSA) package has been tested and/or evaluated in comparison to a JP-8 fuel (baseline) for more than 225 fuel system materials. The test results have shown this TSA package to be fully compatible with those tested/evaluated materials. This TSA package exhibited, in a fuel flow application test stand, improved test results over JP-8 fuel with the materials associated with an F-16/15 aircraft (F-100 engine) gear pump, i.e., bronze leaded bearings, CPM 10V gears, and 356T6 housings.

The JP-8+100 (Mobil MCP-1750) TSA package also has been tested and evaluated with most of the same materials and has exhibited the same compatible fuel system material results as the Betz TSA package. It also exhibited improved test results over JP-8 baseline fuel with the F-100 engine gear pump in the same fuel flow test stand and equivalent test conditions as the Betz TSA package. Many of the metallics, although tested, have not been fully evaluated with the Mobil TSA package and the final conclusions are pending further test evaluation.

The Ethyl 3424 TSA package testing and an F-16 additive package is complete; however, evaluations will continue and be reported in a subsequent report.

Further testing of the TSA packages as required in component applications also will be reported in a subsequent report.

The test of the Betz TSA package is described in detail below. The accompanying volume of data sets of this final report contains a summary of the test results with a few samples of data sheets for non-metallics and metallics.

3.6.1 Test Program Development

Prior to the initiation of the thermal stability additive fuel package materials evaluation, several weeks of preliminary development tests were completed. It was considered necessary to establish a method of evaluating a large number of materials at elevated temperatures up to 400F for aging periods of 28 days with a minimum number of fuel change-outs. A schedule of four fuel soaks (initial fuel and three changes-outs) during

the 28 day test was considered an acceptable and reasonable goal that did not incur a major program schedule impact.

Fuel deterioration was a primary concern over the sustained period of time under static temperatures of 325F and up to 400F. Fuel color was used as a qualitative method of judging the fuel after 7 days at a sustained high temperature. An initial temperature of 325F resulted in a fuel color change similar to that of simulated aircraft recirculated engine fuel test rig results (light amber). Experiments indicated that the factors that affected fuel color (the indicator for fuel deterioration) were: a) pressure; b) limiting introduction of oxygen/air; c) thermal cycling; and d) inclusion in the test chamber of an open container of fuel soaked sand.

Minimizing oxygen introduction into the fuel/material container successfully maintained fuel at a light amber color at 325F, and preliminary tests at 365F provided a reasonable indication that the fuel could retain a light amber color at 400F temperatures. Those techniques which minimized oxygen introduction into the fuel/material container thus minimizing fuel deterioration were documented and used throughout the program.

3.6.2 Experimental Methodology

Stainless steel pressure vessels equipped with exterior heating jackets were selected as test chambers. The pressure vessels were maintained in an unpressurized condition and vented by a check valve to the test cell (room) low pressure vent. The pressure vessel structural integrity was also protected with a low setting pressure relief valve. Ovens were used for fuel temperatures of 225F or less, and at those temperatures, minimizing fuel deterioration (very light amber color) was not a problem for the 7 day fuel change-out.

Later in the program, in order to increase material testing at 325F, a large oven was equipped with a fuel containment insert to insure fuel/vapors did not come in contact with the oven heating coils. A nitrogen blanket was maintained by bleeding nitrogen around the oven interior continuously throughout the test duration. This provided a slight positive pressure exterior to the fuel containment insert to avoid any possibility of fuel/vapor leaks into the hot oven heating coils.

Standard *Ball* brand canning jars were selected to hold the test material samples and the test fuel in which they were immersed. Rounds cut from thin, rigid Teflon sheet to the exact dimensions of the tops of the jars were used as covers and held in place with standard *Ball* jar rings. This provided the fuel/material container a safe fuel expansion/contraction method while maintaining the jar seal, thereby minimizing air/oxygen entry into the fuel. Non-metallic tests at UDRI at 200F (and lower temperatures) utilized aluminum foil in lieu of thin Teflon.

The fuel system test materials identified and selected for this test were those which come in contact with fuel on a continuous basis. Materials which may only be wetted inadvertently and on an intermittent basis were not included in this test program

due to the absence of a validated test method and the absence of baseline fuel data. Aircraft airframe and engine fuel systems and refueling equipment are the primary sources of test material identification. These materials are found in aircraft fuel containment system components and lines up through the engine fuel nozzles and combustion chamber, as well as the aircraft ground and aerial refueling systems. Due to the potentially wide use of fuel and associated fuel additives, it was necessary not only to consider materials of future aircraft (the original program objective) but also of current and older aircraft. In view of having a standard battlefield fuel and aerial refueling tanker operations involving both the intra-service and international communities, all military aircraft fuel system materials are potentially impacted by this program. As a result of this potential, a wide scope investigation for fuel system material identity was pursued. The Society of Automotive Engineers (SAE)/AE-5 committee, airframe/engine manufacturers, DOD personnel and fuel system component manufacturers were contacted to assist in identifying fuel system materials. The original list of fewer than 30 materials has grown to 227 materials, including 100 metallics and 127 non-metallics. Some of these materials may be located on both the lower airframe temperature range, 160 to 225F, and the engine with a temperature range from 250 to 400F.

Two primary test temperatures were selected for this fuel additive compatibility test program. An airframe temperature of 200F was chosen since engine fuel recirculation back to the airframe fuel tanks is likely on new high performance aircraft. A temperature up to 325F is currently experienced by many aircraft engines and associated fuel system component materials. Other test temperatures were evaluated when materials were unable to sustain the higher temperatures, i.e., 275/250/180/160F. A 400F temperature was evaluated when a material exhibited successful tolerance to 325F.

The test duration of 28 days was considered the most practical test period to assess such a large number of materials. Also, early evaluations accomplished at 7 and 28 days indicated significant material property changes after this intermediate time period. Some 7 day material property test data is included in this program to illustrate the material property changes between the 7 and 28 day periods. The correlation of 28 day static material exposure tests at a specific temperature to an actual aircraft fuel system component environment is not known to be established. However, the results of this test are primarily intended as a comparison of fuels with and without a thermal stability additive package and any negative or positive effects of that additive package. Material temperature limitations at a specified test duration also may be gleaned from the test results.

For this materials compatibility test program, Jet A fuels were used as the baseline/control fuels and also as the fuel for the thermal stability additives tests. The fuels selected for this evaluation are POSF-2980 and POSF-2926. These two fuels have physical properties which fall generally into a nominal fuel with no extreme characteristics. All testing after December 1996 will be accomplished with POSF-2926 fuel, since the Air Force POSF-2980 supply of Jet A fuel has been depleted. All Jet A fuel for this test program was converted to JP-8 by incorporating JP-8 additives. These

additives included an icing inhibitor, DiEGME, 0.12 volume %; a corrosion inhibitor, 15 mg/L; and a static dissipater, Stadis 450, 2 mg/l. Although testing of the fuel for conductivity (pS/m) indicates that in many cases the fuel did not meet the minimum of 150 pS/m, absolute conductivity of the fuel was not considered critical. Rather, maintaining the same amount of Stadis 450 in all test fuels was considered crucial.

The thermal stability additive test package for this program was provided by the Betz/Dearborn Company. The additive is identified as Spec Aid 8Q462. This thermal stability additive package includes a dispersant/detergent, a metal deactivator (MDA) at 10 mg/L, and an anti-oxidant (BHT) at 25 mg/L. All testing involved: 1) a baseline JP-8 fuel as a control, 2) JP-8 +100 (with thermal stability additive in normal concentrations), 3) and JP-8 +100 x4 (with thermal stability additive in four times normal concentrations).

The test equipment for higher temperature evaluations (325 to 400F) consisted of four pressure vessels with heating jackets, programmable digital temperature controllers, and separate over-temperature controllers. These pressure vessels are designed for safe operation over 400F. The vessels were fitted with a removable flat shelf for accommodating six quart-size jars around the circumference and one in the center (filled with fuel-soaked sand) for a total of seven jars. Additional heating chambers (ovens) were utilized to accommodate lower temperature fuel tests, i.e., 225F and lower. One environmental chamber equipped with a specially designed fuel/vapor isolation insert in the fuel/materials laboratory, B-490 WPAFB, was utilized for testing up to 325F. With this modification, the oven could accommodate considerably more test materials than the pressure vessels at this higher temperature.

Non-metallic materials test samples were placed and/or suspended in 700 mL of fuel in Teflon-capped (or aluminum foil capped, at 200F or lower), quart-size jars. The samples were marked for identification with silver pencils. Generally, five material test samples were used for non-metallic materials. An average of the five test sample test readings was used in the test reporting data. An exception was the compression set data for O-rings which involved two specimens. With some materials, only one test specimen (data point) was required, e.g. foam resistivity.

Metallic material test samples were placed in separate 30 mL beakers and marked with sample identification information. The metallics materials test coupons were 1 x 2 x 0.063 inch specimens. Three test specimens (placed in separate marked beakers) of a given metallic test material generally were used in this test. The beakers were placed inside Teflon-capped, quart-size jars. Weight measurements of the material test samples were made before and after fuel soak (28 day test) periods. An average of the weights of the three test samples was used in the test reporting data. A test iteration for metallics included a total of 10 specimens, 3 specimens of a given material in each of the 3 test fuels, and 1 specimen as a control (new) material The four pressure vessels could accommodate eight materials to be tested simultaneously.

3.6.3 Material/Fuel Property Tests

Properties of non-metallic materials are measured to determine the materials' ability to perform in component applications. The magnitude of this test program demanded that only a limited number of properties could be evaluated for each material. Those properties were measured for the new, unstressed material samples (control materials). Then, they were measured for material samples after thermal aging in: 1) the control fuel (JP-8); 2) in JP-8 +100 (with additive in normal concentrations); and 3) in JP-8 +100 x4 (with additive in 4 times normal concentration). The material sample properties after 28 day aging in JP-8 +100 and in JP-8 +100 x4 were compared to its properties after 28 day aging in the JP-8 control fuel and to the properties of new, unstressed material samples. Any negative/positive effects of the +100 additive were noted. Material specifications provide some property guidance after thermal aging and were used in this evaluation to assist in determining allowable limits for changes in material properties.

The tests selected were designed to give an indication of materials degradation with a minimal amount of testing. Tests of common physical properties of the materials related to the degradation of the function of the materials were selected. For example, in the case of coatings, pencil hardness was selected as an easy test that demonstrated whether the additive weakened the coating. For O-rings, tensile/elongation, volume change, and compression set were chosen as indicators of degradation. The materials types and properties tested are listed in Table 3. The test specifications employed are listed in Table 4.

Several physical property tests were conducted with the fuel before and after material thermal aging tests (Table 5). The two test fuels (+100 and +100 x4) and the JP-8 control fuel were subjected to measurement of acid no, gums, hydroperoxides, conductivity and visual color changes when subjected to non-metallic (elastomeric) materials. The fuel conductivity, color, and graphite furnace/inductive coupled plasma (ICP) test equipment were employed to evaluate the test fuel and control fuel after subjected to thermal aging of metallic materials. The graphite furnace/ICP proved to be of value in evaluating the metallic alloy elements which may be extracted into the fuel by the fuel's chemical/corrosive attack on the metallic (alloy).

3.6.4 Fuel System Component Materials Application Test Rig

We recently constructed a material compatibility flow rig to investigate the sealing properties of O-rings in a controlled environment. Provisions were also included to allow running actual aircraft fuel pumps at elevated temperatures with additized fuel. Fuel was supplied at 40 to 55 psig to a prototype Argo-Tech pump, similar to pumps used by the Air Force. Temperatures were controlled to 325F during 118 hours of operation at 500 psig for each test. JP8 blends were used for three tests. Neat JP8 was run for background information prior to one run each of JP8 with four times the normal concentration of the

BETZ and Mobil packages. Temperatures and pressures were logged during the test, At the end of each test the pump was returned to Argo-Tech for disassembly and examination.

3.6.5 Conclusions and Recommendations

On the basis of a comparative evaluation with JP-8, and of the materials tested and evaluated *to date*, the Betz/Dearborn 8Q462 thermal stability fuel additive is compatible with the materials found in Air Force aircraft fuel systems. The Betz/Dearborn 8Q462 thermal stability fuel additive actually improves the material properties of many non-metallic materials. In addition the Betz/Dearborn 8Q462 thermal stability fuel additive generally results in cleaner metallics. Numerous materials were determined to have temperature limitations independent of their exposure to the +100 additive. We recommend that the following materials not be used beyond the listed temperature: fluorosilicone O-rings 225F, fluorocarbon O-rings 325-400F, nitrile 160F, PR-1776 fuel tank sealant 160F. The following compounds should not be used in contact with fuel and fuel vapors: nitrile O-rings designed for hydraulic fluids and polysulfide potting compounds (e.g., CS-3100).We recommend maintaining the prohibition of fuel contact with the following metallic materials: copper, zinc, lead, and cadmium.

3.7 Fuel Modeling

We conducted a variety of modeling studies which explored the use of a variety of techniques to allow prediction of fuel oxidation and deposition in various systems. These techniques include: global chemistry modeling, pseudo-detailed chemical kinetic modeling, computational fluid dynamic simulations (CFD) with pseudo-detailed chemical kinetic mechanisms, CFD with global mechanisms, analysis of the meaning of activation energy and reaction order in fuel oxidation, and the modeling of deposition during fuel cooling. The highlights of these modeling studies are summarized below.

3.7.1 Autoxidation and Global Chemistry Model

We developed a free radical mechanism for oxidation and deposit formation in jet fuel (Heneghan and Zabarnick, 1994). Analysis of this mechanism showed the rate of oxygen consumption to be independent of the oxygen concentration (i.e., zeroth order in oxygen). At sufficiently low oxygen concentration the oxidation rate will become first order. This mechanism shows that methane production in the Phoenix rig is due to alkyl radical decomposition upon the complete consumption of oxygen.

We studied the use of global reactions for the simulation of jet fuel oxidation and deposition. We showed that the global rate constants used for oxidation are neither constant in time nor Arrhenius in form (Heneghan, 1994). This result explained the

activation energy change with temperature observed in previous global model studies (Katta et al., 1993). To incorporate such behavior into global models, we developed a time-dependent rate expression which allows the correct prediction of early oxygen consumption over a range of conditions (Chin et al., 1994). This new global model, which includes autoacceleration, was incorporated into a CFDC (computational fluid dynamics with chemistry) code. The model correctly predicts the shape and amount of deposition in flowing systems at various temperatures and flow conditions.

3.7.2 Pseudo-detailed Chemical Kinetic Modeling

We developed a pseudo-detailed chemical kinetic mechanism for fuel oxidation and the effect of antioxidants and hydroperoxide decomposers (Zabarnick, 1993; Zabarnick, 1998). As jet fuels are comprised of hundreds of compounds, it is impractical to model the chemical changes of all components of the mixture. Thus, the bulk fuel is modeled as a single compound, RH, which has the chemical properties of a normal alkane, such as *n*-dodecane. This "fuel" can also contain dissolved oxygen (O_2), an alkylperoxy radical inhibiting antioxidant (AH), an initiating species (I), and a hydroperoxide decomposing species (SH). The chemical kinetic mechanism is shown in Table 6. The activation energies and Arrhenius A-factors for each reaction were estimated via comparison with measured rate parameters of similar reactions and Benson style "thermochemical kinetics." This reaction mechanism has exhibited remarkable success in reproducing fuel oxidation behavior over a wide range of temperatures. The reactions employed in the mechanism are groupings of real reactions which actually occur in jet fuel oxidation and the estimated rate constants are obtained from real elementary rate data. Thus, the use of this mechanism for modeling of jet fuel oxidation and for comparison with measured oxidation profiles provides chemical insight into actual reaction processes. This is in contrast to global models which do not use real reactions and are simply empirical fits to measured data; such global models do provide insight into the chemistry which occurs.

This mechanism has been used for the study of antioxidants and hydroperoxide decomposers in a static system (Zabarnick, 1998). The mechanism was "calibrated" using isothermal oxidation data and demonstrated good agreement with experiment over the temperature range 140 to 185C. The model demonstrated excellent agreement with oxygen profiles obtained at various concentrations of added BHT antioxidant at 140C as shown in Figure 24. The model was also able to reproduce the behavior exhibited during the blending of fuel and show the behavior expected due to the presence of hydroperoxide decomposing species. The model also predicted a synergism between these alkylperoxy radical inhibiting antioxidants and hydroperoxide decomposers. This synergism has been previously observed experimentally (Scott, 1963).

A slightly modified version of the mechanism was incorporated into a computational fluid dynamics model for the study of flowing systems (Ervin and Zabarnick, 1998). The mechanism was able to successfully model oxygen and alkyl hydroperoxide concentration profiles in flowing tubes over a wide range of temperatures

and flow rates/residence times. This work is proof that pseudo-detailed chemical kinetic mechanisms can be successfully used in such two-dimensional CFD codes.

3.7.3 Reaction Order and Global Kinetic Modeling

Analysis and numerical simulation of low temperature oxidation of a hydrocarbon fuel have been used to show that a single overall activation energy and observed order are functions of the fuel's initial conditions, time, and temperature (Ervin and Heneghan, 1998). For example, Figure 25 shows how the observed reaction order for oxygen consumption changes as the dissolved oxygen is consumed at a temperature of 185C and in the presence of an antioxidant which acts to remove alkyl peroxy radicals. The activation energy and the reaction order both depend on the initial concentration of dissolved oxygen and the concentration remaining. Applying the operator for activation energy and reaction order to the rate law for a complicated (autoaccelerating) rate does not necessarily yield a simple activation energy or reaction order as might be expected from a simple global reaction rate law. Consequently, the activation energy or the reaction order of such a reaction process are not well defined concepts. These findings have important implications for the careful use of global parameters in engineering computational fluid dynamics models which simulate autoaccelerating systems.

3.7.4 Modeling of Deposits Formed in Cooled Regions of a Flowing System

Two categories of surface deposits which form in the autoxidative regime have been identified. The first forms in heated regions as the fuel is oxidized. The second accumulates in cooled regions as certain compounds within the reacted fuel become insoluble at reduced temperatures. We developed a global chemistry model that can be used in computational fluid dynamics codes to simulate fouling in cooled regions of flowing systems (Ervin et al., 1996b). In addition, experiments were conducted in the Phoenix Rig using JP-8 fuel with different thermal stability additives. Some thermal stability additives reduced fouling in heated regions but were not as effective in cooled regions. The deposition and oxidation measurements obtained for specific flow conditions were used to calibrate a chemical kinetics model which uses global reactions to simulate deposition. The calibrated model yielded reasonable predictions within the thermal and flow regimes considered.

3.8 Inverse Relationship Between Oxidation and Deposition

During studies of various jet fuels in many tests, we noted an inverse relationship between oxidation and deposition for a range of fuels. We noted that fuels that oxidize slowly, such as some straight-run fuels, tend to deposit relatively heavily, while fuels that oxidize rapidly, such as hydrotreated fuels and pure hydrocarbon solvents, tend to

produce relatively small quantities of deposits. This inverse relationship is illustrated in Figure 26.

In a chemical kinetic analysis of fuel autoxidation, we showed that the observed inverse behavior was consistent with the well known free radical autoxidation mechanism (Heneghan and Zabarnick, 1994). We proposed that naturally occurring antioxidant molecules were necessary to the formation of deposits. The larger the concentration of antioxidant molecules, the slower the fuel would oxidize and the more deposits it would form. Several possible characteristics of proton donating antioxidant molecules were discussed. In particular, the necessary concentration was discussed in relation to the activation energy for proton metathesis. Interestingly, an easily oxidized molecule (one that has a weakly bonded proton) can act as an antioxidant molecule when present in sufficiently small quantities. We proposed various species which, when present in jet fuel, may provide this observed behavior.

3.9 Statistical Studies

We developed a variety of statistical techniques to assist in the evaluation of jet fuel additives and jet fuel thermal stability measurements. These statistical analyses are detailed below.

We performed a non-parametric statistical analysis of the thermal stability test results for 12 fuels and 6 test techniques (Heneghan and Kauffman, 1995). The six tests were the ICOT, MCRT, QCM (at two different reaction times), JFTOT breakpoint, and HLPS. The result of the analysis is an average thermal stability scale which can be compared against the ranking of the fuels by the individual test techniques. Table 7 shows the resulting ranking of these 12 fuels. It shows that most of the thermal stability tests can readily delineate good and bad fuels. This average thermal stability scale represents a good test independent scale by which new analytical or physical tests can be evaluated, and the scale can be used to quantify improvement in jet fuel thermal stability. We also compared several quantitative analytical tests with the average thermal stability scale. The phenol tests, by both UV absorption and cyclic voltammetry, did the best job in reproducing the average thermal stability scale. These results implicate phenols as major "bad actors" in jet fuel deposition. This observation, the importance of phenolic material, is in agreement with the solid phase extract/QCM studies and the initial models proposed to explain the oxidation/deposition behavior of jet fuels (Heneghan and Zabarnick, 1994; Zabarnick, 1994b).

We developed a Poisson technique for analysis of the aircraft failures during the JP-8+100 additive field tests. This technique correctly determines the uncertainties in the running average in observed field anomalies. This improved technique greatly increases our ability to detect real changes in field performance as a result of the JP-8+100 additive package. Figure 27 shows the average failure rates (augmentor bang anomalies per thousand flight hours) and the upper and lower error bounds (2 sigma) versus time for

operations using JP-8 and JP-8+100. As shown in the figure, the upper error bound on the JP8+100 failure rate is well below the average failure rate experienced by those aircraft using JP-8. That is, the decrease due JP-8+100 is more than two failures per thousand flight hours at the 95% confidence level.

We developed an analysis of variance technique for the analysis of data from the fuels/materials interaction study. This technique provides a method of determining the significance of the materials data particularly for the non-metallic materials. We determined that, of the JP-8 additives, DiEGME was primarily responsible for any adverse effects observed in viton and teflon elastomers (Gracki, 1996).

3.10 Development of Fuels Analysis Techniques

We developed a variety of analytical techniques for determination of species important for the study of jet fuel. These techniques are crucial in allowing the study of the chemical processes which occur in fuel. These include methods for the measurement of oxygen, hydroperoxides, detergent/dispersant capacity, phosphorous, MDA, BHT, and water in fuel. Highlights of these analysis techniques are detailed below.

We developed two techniques for the measurement of dissolved oxygen in jet fuels and other hydrocarbon liquids. The first method is usually performed on-line and utilizes gas chromatography and a thermal conductivity detector for separation and detection of oxygen, nitrogen, and argon (Rubey et al., 1995). The chromatographic system is backflushed to prevent contamination of the column. The second method utilizes gas chromatography and a mass spectrometry in single-ion monitoring mode for separation and detection of oxygen (Striebich and Rubey, 1994). In this technique, oxygen is not separated chromatographically, but is separated from the non-retained chromatographic peak by mass spectral monitoring of its parent ion. This technique is rapid and accurate and has mostly been used for off-line analysis using syringe injection of the fuel.

We developed a technique for measuring the detergent/dispersant capacity of jet fuel containing the JP-8+100 additive package (Kauffman, 1997b). This test is based upon the capability of the selected fuel to suspend water and inorganic particles (black copper oxide powder). This powder will settle quickly in the absence of dispersant and remain suspended in the presence of dispersant. The settling rate of the suspended powder is a function of the dispersant concentration. This provides a rapid, inexpensive, and non-selective technique for measuring the dispersant concentration in fuels.

A cyclic voltammetry technique was developed to quantitate the antioxidants added to stored jet fuels and the phenolic type compounds produced during the oxidation of jet fuels (Kauffman and Tirey, 1992). The phenolic analyses were combined with voltammetric analyses of the amino-type compounds present in stored fuels to rank the tendency of the jet fuels to undergo thermal oxidation and produce deposits (Kauffman, 1994b).

A rapid, portable voltammetric technique was developed to quantitate the hydroperoxides in jet fuels (Kauffman, 1994a). The voltammetric technique is referred to as the Peroxide in Fuel Evaluation Concentration Technique (PERFECT) and will replace the current ASTM D-3703 test procedure once the balloting process for approval has been completed. The PERFECT and other voltammetric analytical techniques were used in combination to analyze oxidized fuels in order to gain a better understanding of how different sulfur compounds effect the oxidation/deposition mechanisms of jet fuels (Kauffman, 1997a).

Due to the inherent chemical complexity of jet aircraft fuels, the ability to separate and detect each and every compound is an impossible task with conventional gas chromatography. Consequently, we developed a multi-dimensional gas chromatographic system (MDGC) to provide an increased level of separation power for determination of each and every component. In this system, a portion of the column effluent (heart cut) is directed to a second column instead of being directed to the detector. The second more polar column provided a secondary separation. Where 1 or 2 peaks were detectable in the primary column, 10 or 20 peaks may be present after a multidimensional separation. This system was used to detect sulfur containing compounds which were not detectable with conventional GC-MS (Anderson et al., 1995).

We developed an Inverse Liquid Chromatography (ILC) technique (Striebich and Ohler, 1997) to investigate the interaction of selected fuel components with various surfaces: silane-treated glass (non-adsorptive), stainless steel type 304, and silco-steel coated stainless steel. In this technique, dilute solutions of metal deactivator additive (MDA) are pulsed into an n-decane mobile phase, flowing through a packed bed of powder simulating a surface. A uv-vis detector was used to record the residence time distribution in the packed bed. Metal deactivator additive has both a bulk effect (tying up free metals) and a surface passivation effect. This passivation effect was studied at two different temperatures (23 and 100C). Results verify the surface interaction of MDA with stainless steel; the inerting effect of coatings such as silco-steel was also observed. Temperature did not appear to cause a major change in the adsorptive nature of the MDA onto surfaces.

Advanced fuels are expected to crack into low molecular weight products upon exposure to extreme temperatures and pressures. The ability to detect all of the important products of thermal and catalytic cracking is critical for the calculation of endothermic cooling potentials and the prediction of combustion species input. The difficulty in the analysis is the wide range of compounds (hydrogen gas to hydrocarbons of approximately 100 amu) and the detection of both trace and percent level gases in the same analysis. We developed a sampling and analysis procedure for light gases which consists of filling a mylar sampling bag and injecting part of this gas into a GC equipped with thermal conductivity detection (TCD) and flame ionization detection (FID). A parallel, two column system is used to separate all of the major components for quantitative detection. Initial results from cracking experiments indicate hydrogen levels between 1 and 4%, methane 20%, ethane plus ethylene approximately 40%, propane plus propylene

approximately 25% with the balance distributed among C4 and higher compounds. We expect this analysis will be automated and widely used among the high temperature cracking experiments.

We developed a gas chromatographic method for accurately and precisely measuring dissolved and free water in jet fuels and other hydrocarbon matrices (Rubey et al., 1997). A special chromatographic column with a low phase ratio permits rapid and complete separation of water from other fuel species. The technique is capable of detecting sub-ppm levels of water. It is anticipated that with the use of a backflushing technique and a valve arrangement that this method can be scaled down for field use.

We developed three techniques for measurement of MDA in jet fuels. The first utilizes solid-phase extraction (SPE) and GC-MS (Striebich, 1997). MDA is concentrated by passing 10 mL of fuel through a silica gel SPE cartridge. The retained MDA is eluted with methanol, which is subsequently evaporated and dissolved in toluene. The toluene solution is injected into a GC-MS operated with a base deactivated injector liner and column. Single ion monitoring of the 161 amu fragment ion and 282 amu parent ion is used for quantitation. In the second technique a silylating agent is used to treat the MDA containing fuel (Striebich, 1997). The resulting silylated MDA compound is readily chromatographed without the need for preconcentration techniques. The third technique utilizes the ability of MDA to complex with iron compounds (Kauffman, 1997b). Ferric chloride and/or iron caprate complex with MDA to form colored species which are readily detected either visually by comparison with a color chart, or spectrophotometrically by measuring absorbance at 490 nm.

We developed a technique to measure BHT (the primary antioxidant species in the JP-8+100 package) in jet fuels (Striebich, 1997). First the BHT is extracted from the fuel via a liquid-liquid extraction with methanol. An autosampling GC-MS is used to withdraw the bottom methanol layer for injection into the chromatograph. Single ion monitoring of the 205 amu fragment ion and the 220 amu parent ion is used for quantitation.

A Leeman Labs inductively coupled plasma-atomic emission spectrometer (ICP-AES) was installed to analyze material test fuels for the presence of metallic corrosion products, wear metals, phosphorus, and sulfur. The metal content can then be used to judge the condition of fuel handling components or corrosion test coupons and flag systems with high values for further evaluation. While currently working in the range of 100 ppb for lower detection limit it is possible to quantify in the range of 1 – 10 ppb with several enhancements.

Samples of jet fuels, from the world survey of fuels, both with and without the +100 additive, have been studied with the ICP-AES in order to determine appropriate protocols and lower limits of quantification for copper and phosphorus (Vangsness and Heneghan, 1997). Copper quantification is important to the EDTEST and material compatibility programs as copper readily goes into solution with kerosene type fuels and strongly affects the fuel's deposition and oxidation rate at elevated temperatures.

Phosphorus is an important ingredient in the Betz additive package currently in limited use by the Air Force. Quantifying the phosphorus in fuels allows us to determine if a fuel sample contains the Betz additive and the amount of additive present. We have shown that the ICP can determine an unknown fuels phosphorus content to within 10% of the amount present in JP8+100 (8Q462), the current Betz additive package. Including copper and phosphorus, we have calibration standards for 26 metals and can identify 71 elements in kerosene at this time.

3.11 Additive Testing and Formulation

3.11.1 JP-8+100 Additives

The prime goal of the "JP-8+100" development program was to find an additive or additive combination that will improve the thermal stability of JP-8 fuel by 55C (100F). Additives were supplied by many additive manufacturers for testing. Several classes of additives were tested. These additive classes include: antioxidants, detergents, dispersants, stabilizers and metal deactivators. The QCM, ICOT, and HLPS (HLPS test performed by Pratt & Whitney) tests were used for screening each of the submitted additives (Anderson et al., 1994; Grinstead, 1994; Zabarnick, 1994a). Tests were generally run at the manufacturer's recommended concentration. The initial screening was performed on a single jet fuel; additives which performed satisfactorily where then tested in three additional jet fuels. Those additives that performed "best" were selected for follow-on testing, including concentration optimization (Zelesnik, 1995). During the course of testing various additive combinations, it was discovered that the combination of a good dispersant/detergent additive with an antioxidant provided excellent performance over a wide range of fuel types (Zabarnick and Grinstead, 1994). We then studied the performance of the best dispersant/antioxidant package in a "world survey" of 28 fuels acquired worldwide. These tests were performed with and without added metal deactivator. We found that the addition of a metal deactivator to the package resulted in significant improvement in many of these world survey fuels. To date, detergents/dispersant additives from Betz-Dearborn, Mobil, Ethyl, and Octel have performed satisfactorily in packages with the antioxidant BHT, 2,6 di-tert-butyl-4-methylphenol, and the metal deactivator, N,N'-disalicylidene-1,2-propanediamine.

After showing good performance in the screening tests, the additives were than tested extensively in flowing test rigs, such as the Extended Duration Thermal Stability Test (EDTST) and the Advanced Reduced Scale Fuel System Simulator (ARSFSS). These tests are described in separate sections of this report. These and other tests have shown that the proposed additive packages can achieve the original thermal stability improvement goal as measured by deposit formation in test rigs.

Fuel-materials compatibility tests were conducted with the proposed additive packages. The purpose of this testing is to identify fuel system materials which may experience significant adverse interactions as a result of prolonged contact with the JP-8+100 jet fuel. This testing was performed in three distinct phases: identification of the possible materials and temperatures conditions, establishment of testing procedures, and finally, testing and comparison with baseline data. Details of the tests, materials tested, and the test results are contained in the Fuels/Materials Compatibility section of this report. To date, more than 120 materials have been tested with the proposed additive packages without identifying any detrimental effects due to the additives.

3.11.2 Other Additives

We have also explored the use of other additive types to improve the performance of jet fuel, including oxygen scavengers and silylating agents. Oxygen scavengers are used to remove dissolved oxygen from the fuel via chemical reaction; this removal of molecular oxygen would result in a fuel with much improved thermal stability characteristics. We performed studies on one oxygen scavenger candidate, triphenylphosphine (TPP) (Beaver et al., 1997). TPP is known to react with atmospheric oxygen at elevated temperatures. These studies show an increase in oxidation rate and a decrease in deposition with TPP present, but at the present time it is unclear if TPP is directly reacting with molecular oxygen in jet fuel. Lack of understanding of the mechanism, and the high concentration of TPP needed to react with all of the dissolved oxygen, sulfur, and peroxides, limit the usefulness of TPP as a JP-8+100 additive. However, TPP shows promise in low oxygen systems, and as an analytic aid for jet fuels (Heneghan et al., 1996a).

We also explored the use of silylating agents to improve jet fuel thermal stability. Silylation agents such as hexamethyldisilazane (HMDS) and N-trimethylsilylimidazole (TMSI) have been used for many years for derivatization treatment in gas chromatography (GC). Such treatment converts polar compounds such as phenols, thiols, amides, alcohols, amines, and acids to relatively non-polar derivatives. In GC this improves the analytical efficiency and increases the detectability. As it is well known that such oxygen, nitrogen, and sulfur containing compounds contribute to deposit formation in jet fuel, we proposed that treatment of jet fuels with these compounds could significantly improve thermal stability. Figure 28 shows plots of deposition and headspace oxygen vs time for runs of fuel POSF-3119 with 1.0 mL HMDS/60 mL fuel run at 140C in the QCM. It is apparent that the additive significantly lowers deposition while also increasing the oxidation rate of the fuel. This is in marked contrast to JP-8+100 additives which would result in a decrease in the oxidation rate. Note that the deposition level with the silylation agent is significantly lower than that obtained with the Betz JP-8+100 package (8Q462 at 256 mg/L). Due to these promising results we tested a variety of silylation agents including: HMDS, TMSI, and N,O-bis(trimethlysilyl)acetamide (BSA). We also varied the concentration of HMDS to help elucidate its action in jet fuel.

The use of silylating agents (such as HMDS) to improve thermal stability is currently being developed.

3.12 Studies of Ultrasonic Removal of Dissolved Oxygen

The removal of dissolved oxygen by physical means has been considered in the past using methods which require prohibitively large facilities or are limited to very low flow rates. We explored the novel use of ultrasound to remove dissolved oxygen from flowing JP-8 jet fuel (Hanchak, 1995). Using a commercially available ultrasonic horn and a test cell fabricated from glass, we measured relatively low dissolved oxygen concentrations over a wide range of volumetric flow rates as shown in Figure 29 (Hanchak, 1995). For the flow rates considered in our studies, the fuel flow rate had little effect on ultrasonic removal of dissolved oxygen. The degassed fuel was later passed through a single-pass heat exchanger similar to that of the Phoenix Rig for thermal stability studies. Ultrasonically degassed fuel was found to have deposit-producing tendencies similar to that of fuel degassed by nitrogen sparging. Using gas chromatography with mass spectroscopy, it was found that ultrasound essentially did not change the original chemical composition of the jet fuel. As discussed earlier, removing only some of the oxygen may not produce the desired benefit in real fuel system (under conditions of partial oxygen consumption). The use of ultrasonic energy to remove oxygen on-line will probably not achieve the needed low levels of dissolved oxygen.

3.13 Electrical Conductivity Testing of O-Rings

Conventional material compatibility tests involving O-rings immersed in heated fuel may require 1 to 3 months for each additive package. Consequently, because of the large number of additives and different fuels to be tested, there is a need to rapidly pre-screen fuel and O-ring combinations. We developed a novel *in situ* electrical conductivity measurement used to monitor changes in nitrile, fluorocarbon, and fluorosilicone O-rings which were aged in heated jet fuel (Ervin et al., 1995b; Gracki, 1996). The electrical conductivity method detected changes in aged O-rings, which coincided with certain chemical changes measured by x-ray photoelectron spectroscopy of interior O-ring surfaces and physical alterations detected by mechanical compression testing.

3.14 Advanced Fuels Studies

We performed a variety of studies pertaining to the development of advanced fuels, such as JP-900 and endothermic fuels. Highlights of some of these studies are summarized below.

We studied deposition in supercritical fuels to determine if deposition profiles are controlled by the supercritical properties of the fuel or by chemical processes (Edwards and Zabarnick, 1992). The deposition property of interest was the decrease in deposition observed as fuel reaches its supercritical temperature. We tested fuels and pure hydrocarbons with widely varying critical temperatures and showed that the deposition behavior did not correlate with critical temperature. Also, the temperature at which the deposition decrease occurs could be shifted by varying the flow rate, which shows that the decrease is not solely a temperature effect. We believe that the deposition decrease is primarily due to the complete consumption of the dissolved oxygen present.

We developed a modified System for Thermal Diagnostic Studies (STDS) for the study of thermal cracking of fuels and model fuel compounds (Striebich, 1997). The modification involves the injection of a pulse (or plug) of liquid fuel into a high-temperature, pressurized flowing gas stream in capillary tubes (0.02 in ID). The use of such a pulsed injection has numerous advantages over the continuous flow of fuel. In particular, pulsed injection minimizes tube plugging due to fouling, allows fuel cracking under near-isothermal conditions, and minimizes fuel consumption (2 mL of fuel used per test). Timed liquid sampling is used to sample the flowing stream with subsequent on-line analysis using GC-MS or GC-TCD. Figure 30 shows results of initial experiments for heptane at 600C and 500 psig.

To allow the study of the cracking of advanced fuels we developed techniques for the quantitative detection of the products of thermal and catalytic cracking processes (Striebich, 1997). This analysis is difficult due to the wide range of compounds (hydrogen gas to approximately 100 molecular weight hydrocarbons) and the detection of both trace and percent level gases in the same sample. We developed a sampling and analysis procedure for light gases which consists of filling a mylar sampling bag and injecting this gas into a GC equipped with thermal conductivity detection (TCD) and flame ionization detection (FID). A parallel, two column system is used to separate all of the major components for quantitative detection. Initial results from cracking experiments indicate hydrogen levels between 1 and 4%, methane 20%, ethane plus ethylene approximately 40%, propane plus propylene approximately 25%, with the balance distributed among C_4 and higher compounds. We expect this analysis will be automated and widely used among the high temperature cracking experiments.

3.14.1 Advanced Aircraft Fuel System Simulator (AAFSS)

We are in the process of developing a unique system for studies of advanced endothermic/pyrolytic fuel systems. The Advanced Aircraft Fuel System Simulator (AAFSS) is a flowing system which will be used to study endothermic reactions at elevated pressures and temperatures and the effects of flow and temperature cycles on thermal deposition over long periods (500 hours). The AAFSS is designed for unattended operation with flow rates up to 315 mL/min. at 1000 psig and with temperatures up to 1200F. Figure 31 is a schematic of the AAFSS. In this arrangement, a 50-gallon fuel tank is sparged with gaseous nitrogen and oxygen to control the dissolved oxygen concentration within the fuel. A band heater with thermostat maintains the supply fuel at a temperature similar to that of aircraft fuel tanks. A positive displacement pump together with a bypass control valve controls the flow rate. A pressurized nitrogen line is attached to the fuel feed line upstream of the preheater by means of a shut-off valve in order to provide a safe flushing technique and an inert environment for system startup. After heating, the fuel can be cooled upstream or downstream of the backpressure control valve. Downstream of this valve, a separator is incorporated to allow on-line analysis of gas products using a GC-FID/TCD system. The liquid portion of the stressed fuel is analyzed off-line by conventional GC-MS techniques. Thus, fuel system simulator tests and GC-MS analyses will be used to provide a quantitative analysis of the endothermic reaction effluent. Sample lines between heating sections are monitored by a modified on-line GC for dissolved oxygen content in the fuel. The instrumentation and controls provide for continuous monitoring of pressure, differential pressure, flow rate, temperatures, voltages, currents, fuel levels, and safety devices.

The system has the unique capability of heating the fuel in several different ways, including near constant wall temperature, constant heat flux or combinations thereof. Thus, three different types of heaters will be used in the simulator: (1) a copper block (nickel plated) heater in which a tube can be heated with a nearly constant wall temperature, (2) a split-tube furnace with multi-zone, radiant, and convective heating, and (3) a resistive heater providing a constant heat flux to the test section. The total available power for heating the fuel exceeds 82 kW. Each test section can be operated over a large temperature range with, and without, a catalyst. Some experiments will require a combination of different heating sections. As illustrated in Figure 32, a split tube furnace may be used as a guard heater, eliminating heat losses. In addition, the AAFSS was designed, built and located to allow for integration of a small-scaled combustor. Issues of safety have necessitated an enclosure surrounding the heaters and a CO_2 fire suppression system that includes a UV/IR flame detection sensor.

4. CONCLUSIONS

This report has presented the highlights of studies performed in support of the development of advanced jet fuels, including JP-8+100, JP-900, and endothermic fuels. For the development of JP-8+100 fuel, we have tested hundreds of additives in both small and large scale test devices. We formulated combinations of the best additives (detergent/dispersant, hindered phenol antioxidant, and metal deactivator) and demonstrated their efficacy in reducing deposition in realistic aircraft conditions in large-scale simulator rigs. We optimized the concentrations of these additives for maximum effectiveness and minimum cost. We performed extensive studies of the compatibility of these fuel additives with current and future aircraft fuel system materials. We determined that the current best additives show no negative effects on both metallic and non-metallic fuel system materials.

We also performed extensive studies on the fundamental processes of fuel oxidation, deposition, and pyrolysis. We developed chemical kinetic mechanisms which can simulate the oxidation and deposition processes. We performed experimental and modeling studies on fuel cooling which shows that deposition which occurs in fuel cooling heat exchangers can be a significant problem in fuel system design. We demonstrated an inverse relationship between oxidation and deposition over a range of fuels, and showed that our chemical kinetic mechanism can be used to explain this seemingly anomalous result. We developed statistical techniques to assist the evaluation of jet fuel additives, thermal stability measurements, and aircraft field performance. We developed a wide variety of fuels analysis techniques for measurement of the following: dissolved oxygen, detergent/dispersant capacity, antioxidants and phenolics, hydroperoxides, trace jet fuel compounds, metal deactivators, products of endothermic reforming, dissolved and free water in fuel, BHT, Betz dispersant, and elemental metals. We explored alternative techniques for reducing jet fuel deposition including: removal of dissolved oxygen, silylating agents, oxygen scavenging additives, and solid-phase extraction.

We also made progress in support of development of future fuels such as JP-900 and endothermic fuels. We explored the effect of supercritical fluid properties on high temperature fuels. We have begun to study the pyrolysis of fuel in catalytic and non-catalytic reaction systems.

5. REFERENCES

Anderson, S., Garver, J., Rubey, W., Striebich, R., and Grinstead, R., 1995, "The Separation and Identification of Trace Heteroatomic Species in Jet Fuel by Sample Enrichment and Multidimensional Gas Chromatography with Mass Selective Detection (MDGC-MSD)," Presented at the Seventeenth International Symposium on Capillary Chromatography and Electrophoresis, Wintergreen, VA.

Anderson, S. D., Harrison, W. E., and Roquemore, W. M., 1994, "Development of Thermal Stability Additive Packages for JP-8," *Proceedings of the 5th International Conference on Stability and Handling of Liquid Fuels,* Vol. 1, pp. 255-273.

Balster, L. J., Balster, W. J., and Jones, E. G., 1996, "Thermal Stability of Jet-Fuel/Paraffin Blends," *Energ. Fuels,* Vol. 10, pp. 1176-1180.

Beaver, B., DeMunshi, R., Heneghan, S. P., Whitacre, S. D., and Neta, P., 1997, "Model Studies Directed at the Development of New Thermal Oxidative Stability Enhancing Additives for Future Jet Fuels," *Energ. Fuels,* Vol. 11, pp. 396-408.

Binns, K. E., and Dieterle, G. L., 1996, "Evaluation of the JP-8+100 Additive Candidates in the Extended Duration Thermal Stability Test System," *Prepr.-Am. Chem. Soc., Div Pet. Chem.,* Vol. 41, pp. 457-460.

Binns, K. E., Dieterle, G. L., and Williams, T. F., 1995, "System Evaluation of Improved Thermal Stability Jet Fuels," Presented at the 5th International Conference on Stability and Handling of Liquid Fuels, Rotterdam, the Netherlands.

Blust, J., 1993, "Effects of Buoyancy on Heat Transfer, Oxygen Consumption, and Carbon Deposition from Aviation Turbine Fuels," M.S. Thesis, University of Dayton.

Chin, L. P., Katta, V. R., and Heneghan, S. P., 1994, "Computer Modeling of Deposits Formed in Jet Fuels," *Prepr.-Am. Chem. Soc., Div Pet. Chem.,* Vol. 39, pp. 19-25.

Dieterle, G. L., and Binns, K. E., 1994, "Evaluation of High Thermal Stability Fuels for Future Aircraft," 30th AIAA/ASME/SAE/ASEE Joint Propulsion Conference, AIAA Paper No. 94-3171.

Dieterle, G. L., and Binns, K. E., 1995, "Extended Duration Thermal Stability Test of Improved Thermal Stability Jet Fuel," ASME, ASME Paper No. 95-GT-69.

Dieterle, G. L., and Binns, K. E., 1997, "System Evaluation of JP-8+100 Additives at High Bulk Temperatures," ASME Turbo Expo '97, ASME Paper No. 97-GT-071.

Edwards, T., and Zabarnick, S., 1992, "Supercritical Fuel Deposition Mechanisms," Presented at the 1992 AIChE National Meeting, Miami Beach, FL; paper 58d.

Ervin, J. S., and Heneghan, S. P., 1998, "The Meaning of Activation Energy and Reaction Order in Autoaccelerating Systems," *J. Eng. Gas Turbines Power,* Vol. 120, pp. 468-473.

Ervin, J. S., Heneghan, S. P., Martel, C. R., and Williams, T. F., 1996a, "Surface Effects on Deposits from Jet Fuels," *J. Eng. Gas Turbines Power,* Vol. 118, pp. 278-285.

Ervin, J. S., Heneghan, S. P., Williams, T. F., and Hanchak, M. A., 1995a, "Reduced Dissolved Oxygen and Jet Fuel Deposition," Presented at the 30th Intersociety Energy Conversion Engineering Conference, .

Ervin, J. S., Kauffman, R. E., and Kalt, D. H., 1995b, "Effects of Thermally Stressed Jet Fuels on O-Rings," Presented at the 33rd Aerospace Sciences Meeting, Reno, NV.

Ervin, J. S., and Williams, T. F., 1996, "Dissolved Oxygen Concentration and Jet Fuel Deposition," *Ind. Eng. Chem. Res.,* Vol. 35, pp. 899-904.

Ervin, J. S., Williams, T. F., Heneghan, S. P., and Zabarnick, S., 1997, "The Effects of Dissolved Oxygen Concentration, Fractional Oxygen Consumption, and Additives on JP-8 Thermal Stability," *J. Eng. Gas Turbines Power,* Vol. 119, pp. 822-829.

Ervin, J. S., Williams, T. F., and Katta, V. R., 1996b, "Global Kinetic Modeling of Aviation Fuel Fouling in Cooled Regions in a Flowing System," *Ind. Eng. Chem. Res.,* Vol. 35, pp. 4028-4032.

Ervin, J. S., and Zabarnick, S., 1998, "Computational Fluid Dynamics Simulations of Jet Fuel Oxidation Incorporating Pseudo-Detailed Chemical Kinetics," *Energ. Fuels,* Vol. 12, pp. 344-352.

Gracki, J., 1996, "The Effects of Thermally Stressed Additized Jet Fuel on O-Rings," M.S. Thesis, University of Dayton.

Grinstead, R., 1994, "Evaluation of JP-8+100 Additives by the Isothermal Corrosion Oxidation Test and the Microcarbon Residue Test," University of Dayton Research Institute, UDR-TR-94-63.

Grinstead, R., 1997, "Studies of Jet Fuel Thermal Stability, Oxidation, and Additives Using an Isothermal Oxidation Apparatus Equipped with an Oxygen Sensor," pp. manuscript in preparation.

Grinstead, R. R., Heneghan, S. P., Striebich, R. C., and Zabarnick, S., 1994, "Jet Fuel Thermal Stability and Analytic Test Data," University of Dayton Research Institute, UDR-TR-94-20.

Hanchak, M. A., 1995, "Ultrasonic Removal of Dissolved Oxygen from Flowing JP-8 Fuel," M.S. Thesis, University of Dayton.

Harrison, W. E., III, 1990, "Aircraft Thermal Management: Report of the Joint WRDC/ASD Aircraft Thermal Management Working Group," Wright Laboratory, WRDC-TR-90-2021.

Harrison, W. E., Binns, K. E., Anderson, S. D., and Morris, R. W., 1993, "High Heat Sink Fuels for Improved Aircraft Thermal Management," Presented at the International Conference on Environmental Systems, Colorado Springs, CO.

Hazlett, R. N., 1991, "Thermal Oxidation Stability of Aviation Turbine Fuels," ASTM, Philadelphia.

Heneghan, S. P., 1994, "Determining and Understanding the Global Oxidation Parameters of Jet Fuels," *Prepr.-Am. Chem. Soc., Div Pet. Chem.,* Vol. 39, pp. 14-18.

Heneghan, S. P., and Kauffman, R. E., 1995, "Analytic Tests and their Relation to Jet Fuel Stability," Presented at the 5th International Conference on Stability and Handling of Liquid Fuels, Rotterdam, the Netherlands.

Heneghan, S. P., Martel, C. R., Williams, T. F., and Ballal, D. R., 1993, "Studies of Jet Fuel Thermal Stability in a Flowing System," *J. Eng. Gas Turbines Power,* Vol. 115, pp. 480-490.

Heneghan, S. P., Martel, C. R., Williams, T. F., and Ballal, D. R., 1995, "Effects of Oxygen and Fuel Additives on the Thermal Stability of Jet Fuels," *J. Eng. Gas Turbines Power,* Vol. 117, pp. 120-124.

Heneghan, S. P., Williams, T., Whitacre, S. D., and Ervin, J. S., 1996a, "The Effects of Oxygen Scavenging on Jet Fuel Thermal Stability," *Prepr.-Am. Chem. Soc., Div Pet. Chem.,* Vol. 41, pp. 469-473.

Heneghan, S. P., and Zabarnick, S., 1994, "Oxidation of Jet Fuels and the Formation of Deposits," *Fuel,* Vol. 73, pp. 35-43.

Heneghan, S. P., Zabarnick, S., Ballal, D. R., and Harrison, W. E., 1996b, "JP-8+100: Development of a Thermally Stable Jet Fuel," *J. Energy Res. Tech.,* Vol. 118, pp. 170-179.

Heneghan, S. P., Zabarnick, S., Ballal, D. R., and Harrison, W. E., 1996c, "JP-8+100: The Development of High Thermal Stability Jet Fuel," AIAA, 96-0403.

Jones, E. G., Balster, L. M., and Balster, W. J., 1996, "Thermal Stability of Jet-A Fuel Blends," *Energ. Fuels,* Vol. 10, pp. 509-515.

Kalt, D. H., 1997, "Fuel and Fuel System Materials Compatibility Test Program for a JP-8+100 Fuel Additive," University of Dayton Research Institute, UDR-TR-97-01.

Katta, V. R., Blust, J., Williams, T. F., and Martel, C. R., 1995, "Role of Buoyancy in Fuel Thermal Stability Studies," *J. Thermophysics Heat Transfer,* Vol. 9, pp. 159-168.

Katta, V. R., Jones, E. G., and Roquemore, W. M., 1993, "Development of Global-Chemistry Model for Jet Fuel Thermal Stability Based on Observations from Static and Flowing Experiments," Presented at the 81st AGARD Symposium on Fuels and Combustion Technology for Advanced Aircraft Engines, .

Kauffman, R. E., 1994a, "Development of a Rapid, Portable Hydroperoxide Test for Jet Fuels," *Prepr.-Am. Chem. Soc., Div Pet. Chem.,* Vol. 39, pp. 42-46.

Kauffman, R. E., 1994b, "New, Rapid Techniques for Determining the Hydro-peroxide Content, Oxidation Stability, and Thermal Stability of Jet Fuels," ASME, 94-GT-346.

Kauffman, R. E., 1997a, "The Effects of Different Sulfur Compounds on Jet Fuel Oxidation and Deposition," *J. Eng. Gas Turbines Power,* Vol. 119, pp. 322-327.

Kauffman, R. E., 1997b, "Simple Analytical Techniques to Determine the Dispersant Capacity and Metal Deactivator Additive Concentration of JP-8+100 and Other Jet Fuels," ASME, 97-GT-77.

Kauffman, R. E., and Tirey, D. A., 1992, "New Techniques to Predict and Evaluate the Effectiveness of Antioxidants in Jet Fuels," *Prepr.-Am. Chem. Soc., Div Pet. Chem.,* Vol. 37, pp. 412-419.

Klavetter, E. A., Martin, S. J., and Wessendorf, K. O., 1993, "Monitoring Jet Fuel Thermal Stability Using a Quartz Crystal Microbalance," *Energ. Fuels,* Vol. 7, pp. 582-588.

Rubey, W. A., Striebich, R. C., and Anderson, S. A., 1997, "Water Measurement Techniques," Presented at the JP-8+100 User Review, Wright-Patterson AFB, OH.

Rubey, W. A., Striebich, R. C., Tissandier, M. D., Tirey, D. A., and Anderson, S. D., 1995, "Gas Chromatographic Measurement of Trace Oxygen and Other Dissolved Gases in Thermally Stressed Jet Fuel," *J. Chrom. Sci.,* Vol. 33, pp. 433-437.

Scott, G., 1963, "Antioxidants," *Chem. and Ind.,* pp. 271-281.

Striebich, R., 1997, University of Dayton Research Institute, unpublished results.

Striebich, R. C., and Ohler, B., 1997, "Surface Adsorption of Jet Fuel Metal Deactivator using Inverse Liquid Chromatography," Presented at the Ohio Valley Chromatography Symposium, Hueston Woods, OH.

Striebich, R. C., and Rubey, W. A., 1994, "Analytical Method for the Detection of Dissolved Oxygen," *Prepr.-Am. Chem. Soc., Div. Pet. Chem.,* Vol. 39, pp. 47-50.

Vangsness, M. D., and Heneghan, S. P., 1997, "Determining Additive Concentration and Additive Stability in JP-8+100/Metal Alloy Systems at Elevated Temperatures," Presented at the 6th International Conference on Stability and Handling of Liquid Fuels, Vancouver, BC.

Williams, T. F., Martel, C. R., and Blust, J., 1994a, "Studies of Thermal Stability of Jet Fuels, Vol. I: Experimental Work," University of Dayton Research Institute, UDR-TR-94-10.

Williams, T. F., Martel, C. R., and Blust, J., 1994b, "Studies of Thermal Stability of Jet Fuels, Vol. II: Data Sets," University of Dayton Research Institute, UDR-TR-94-11.

Zabarnick, S., 1993, "Chemical Kinetic Modeling of Jet Fuel Autoxidation and Antioxidant Chemistry," *Ind. Eng. Chem. Res.,* Vol. 32, pp. 1012-1017.

Zabarnick, S., 1994a, "Evaluation of Jet Fuels and Jet Fuel Additives Using the Quartz Crystal Microbalance and Pressure Measurements," University of Dayton Research Institute, UDR-TR-94-63.

Zabarnick, S., 1994b, "Studies of Jet Fuel Thermal Stability and Oxidation Using a Quartz Crystal Microbalance and Pressure Measurements," *Ind. Eng. Chem. Res.,* Vol. 33, pp. 1348-1354.

Zabarnick, S., 1998, "Chemical Kinetic Modeling of Antioxidant Chemistry for Jet Fuel Applications," *Energ. Fuels,* Vol. 12, pp. 547-553.

Zabarnick, S., and Grinstead, R. R., 1994, "Studies of Jet Fuel Additives Using the Quartz Crystal Microbalance and Pressure Monitoring at 140C," Presented at the 5th International Conference on Stability and Handling of Liquid Fuels, Rotterdam, the Netherlands.

Zabarnick, S., and Whitacre, S. D., 1998, "Aspects of Jet Fuel Oxidation," *J. Eng. Gas Turbines Power,* Vol. 120, pp. 519-525.

Zabarnick, S., Whitacre, S. D., and Mick, M. S., 1997, "Evaluation of Jet Fuels and Jet Fuel Additives Using the Quartz Crystal Microbalance and Pressure Measurements. Part III.," University of Dayton Research Institute, UDR-TR-97-108.

Zabarnick, S., Zelesnik, P., and Grinstead, R. R., 1996a, "Jet Fuel Deposition and Oxidation: Dilution, Materials, Oxygen, and Temperature Effects," *J. Eng. Gas Turbines Power,* Vol. 118, pp. 271-277.

Zabarnick, S., Zelesnik, P., and Whitacre, S. D., 1995, "Evaluation of Jet Fuels and Jet Fuel Additives Using the Quartz Crystal Microbalance and Pressure Measurements. Part II.," University of Dayton Research Institute, UDR-TR-95-98.

Zabarnick, S., Zelesnik, P., and Whitacre, S. D., 1996b, "Silver Corrosion and Sulfur Detection Using a Quartz Crystal Microbalance with Silver Electrode Surfaces," *Ind. Eng. Chem. Res.,* Vol. 35, pp. 2576-2580.

Zelesnik, P., 1995, "Studies of Jet Fuel Thermal Stability, Oxidation and Additives Using the Quartz Crystal Microbalance and Oxygen Monitoring," M.S. Thesis, University of Dayton.

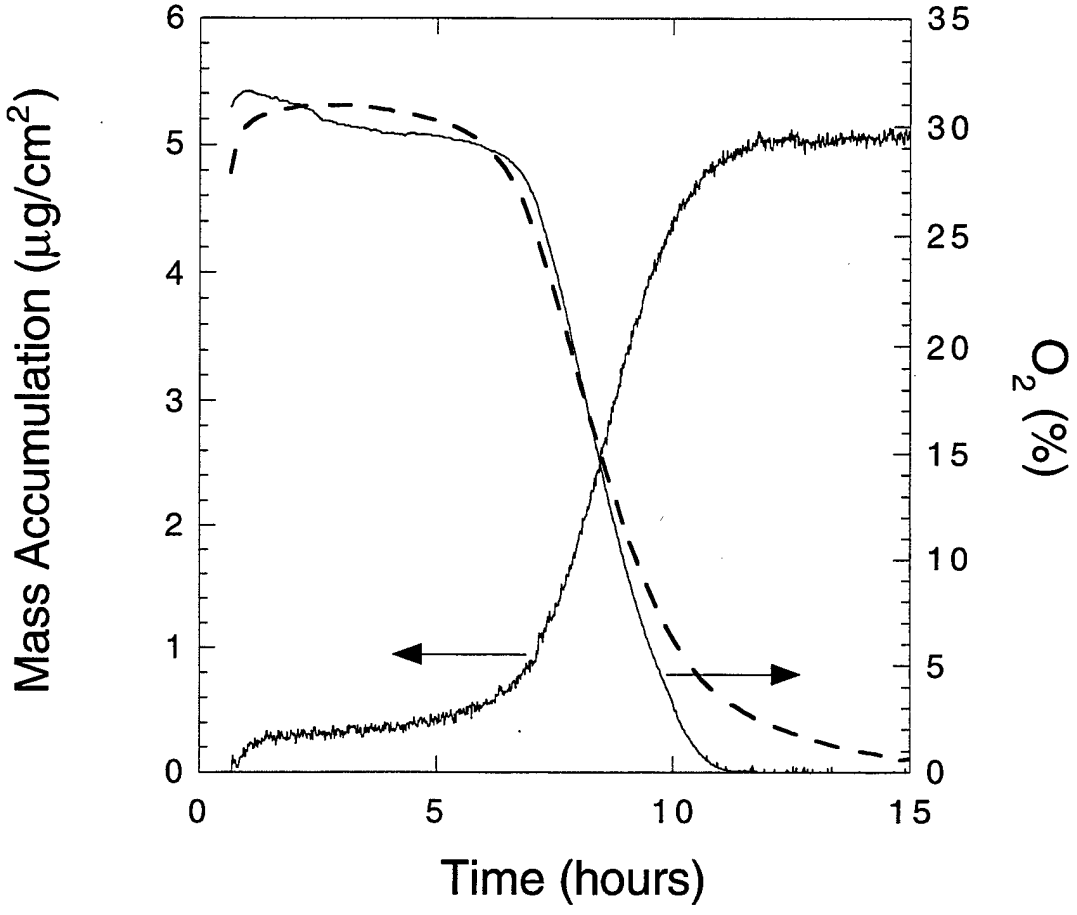

Figure 1. QCM studies. Plots of mass accumulation, oxygen percent, and relative pressure (---) for fuel POSF-3145 with 3.0 mg/L MDA.

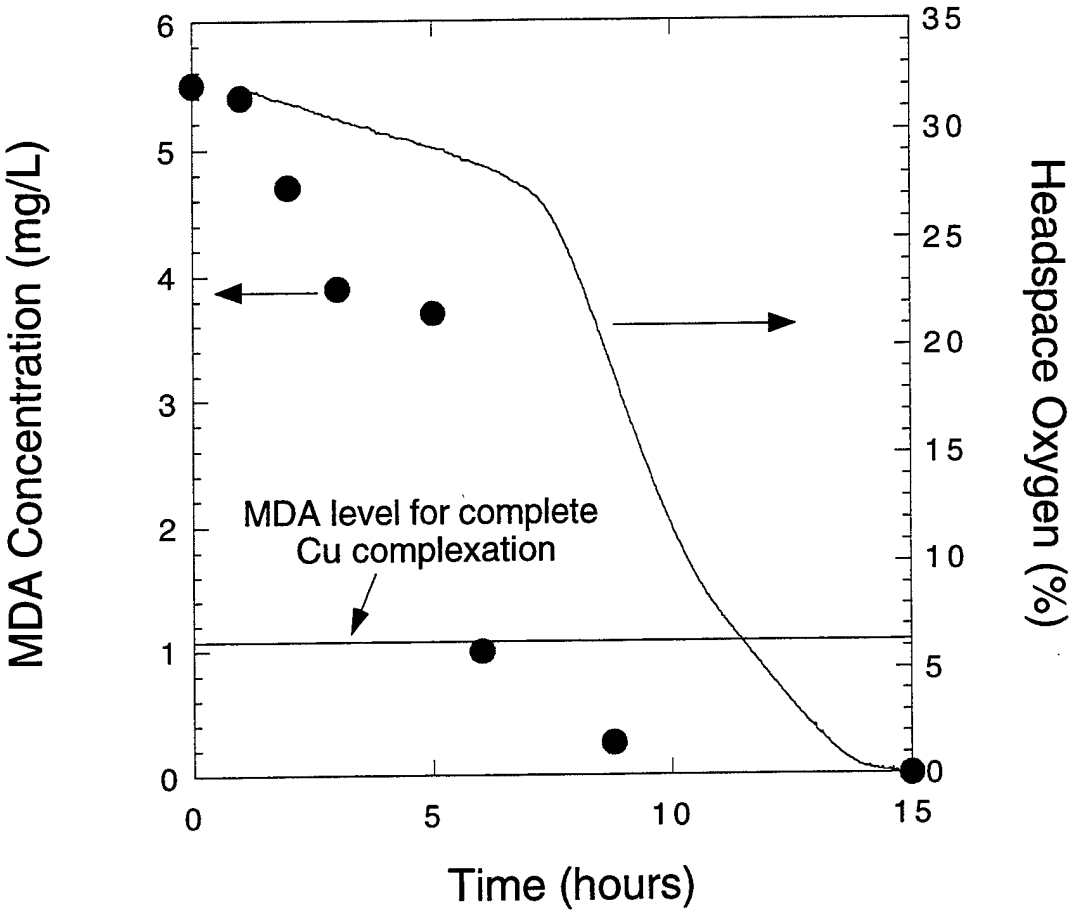

Figure 2. QCM studies. Plots of MDA (●) and headspace oxygen (line) concentrations versus time for fuel POSF-3145 with 5.8 mg/L MDA at 140C. Dashed line is oxygen profile for fuel POSF-3145 neat.

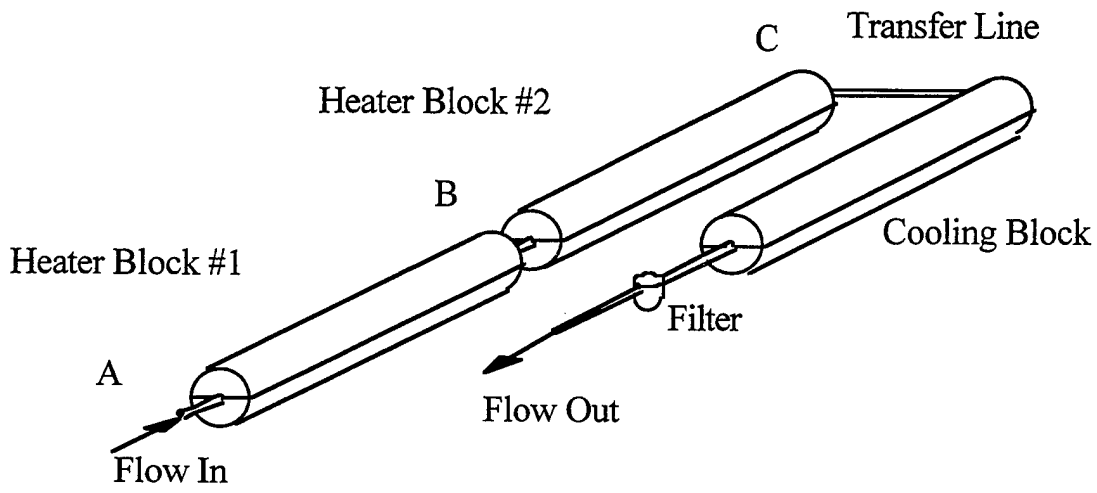

Figure 3. Phoenix Rig. Dissolved oxygen and bulk temperatures measured at locations A, B, and C.

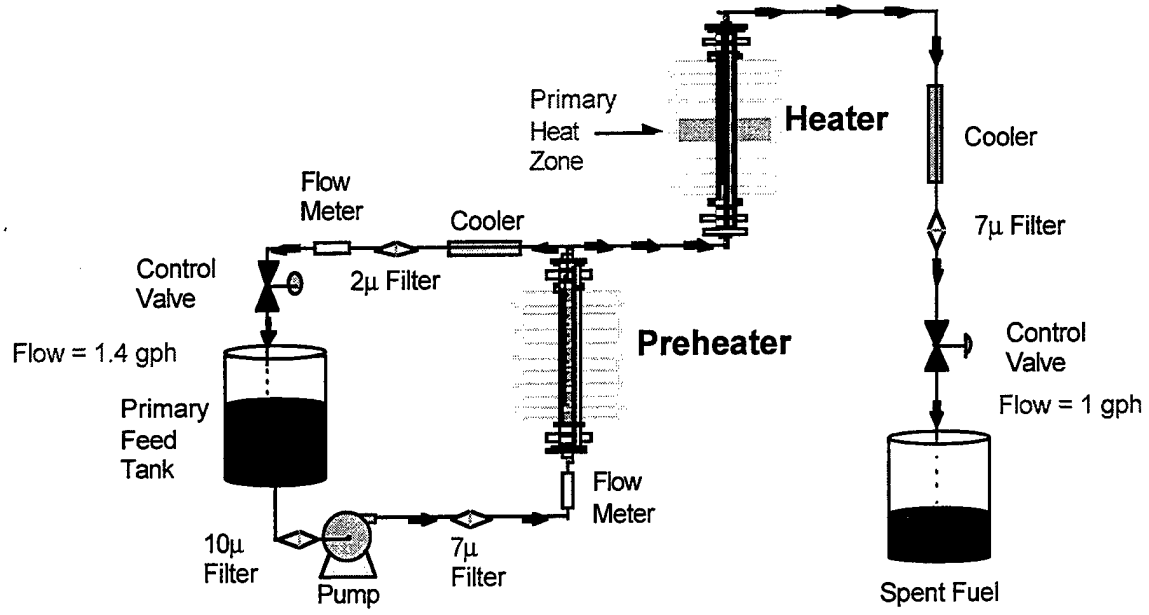

Figure 4. EDTST schematic.

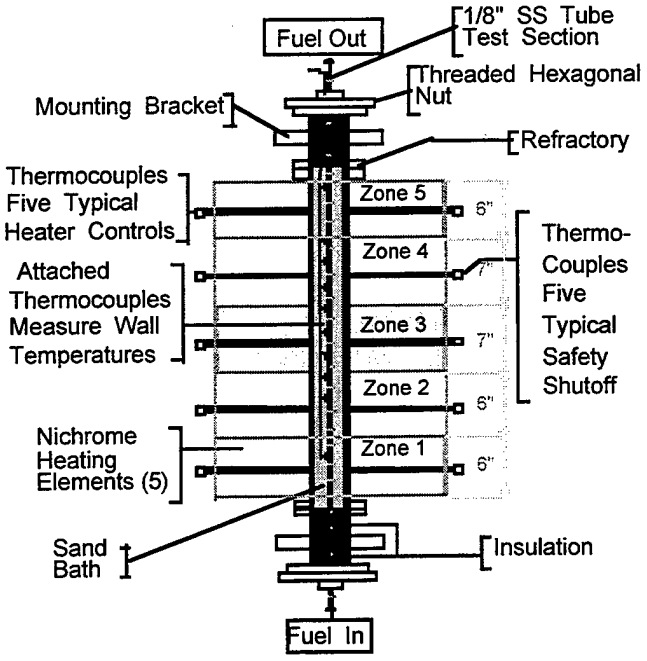

Figure 5. EDTST heater diagram.

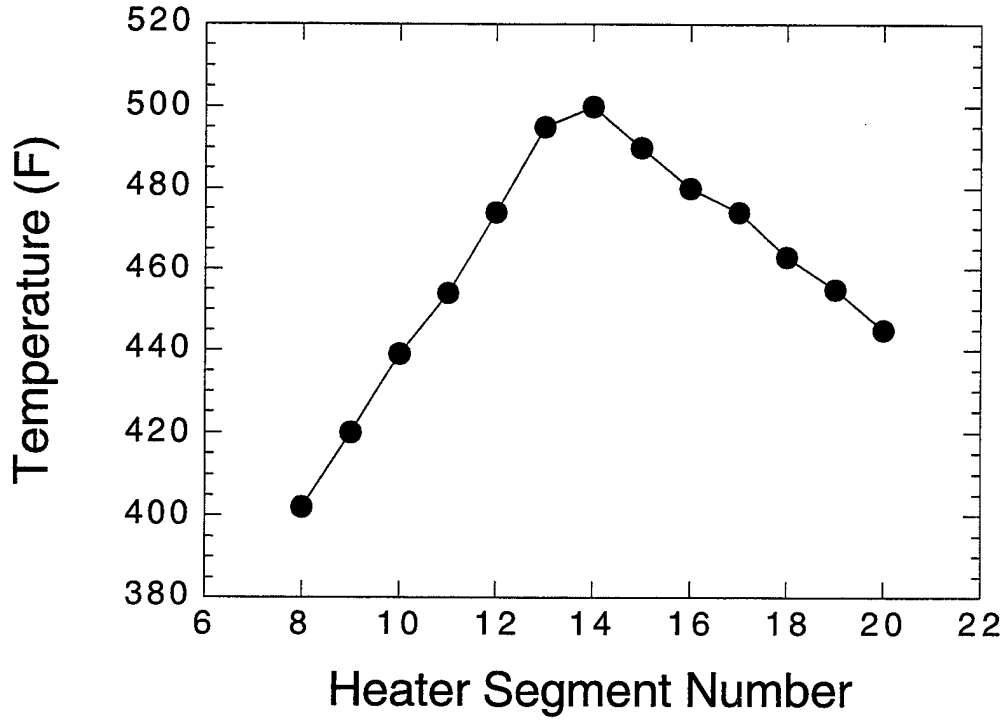

Figure 6. EDTST studies. Typical temperature profile.

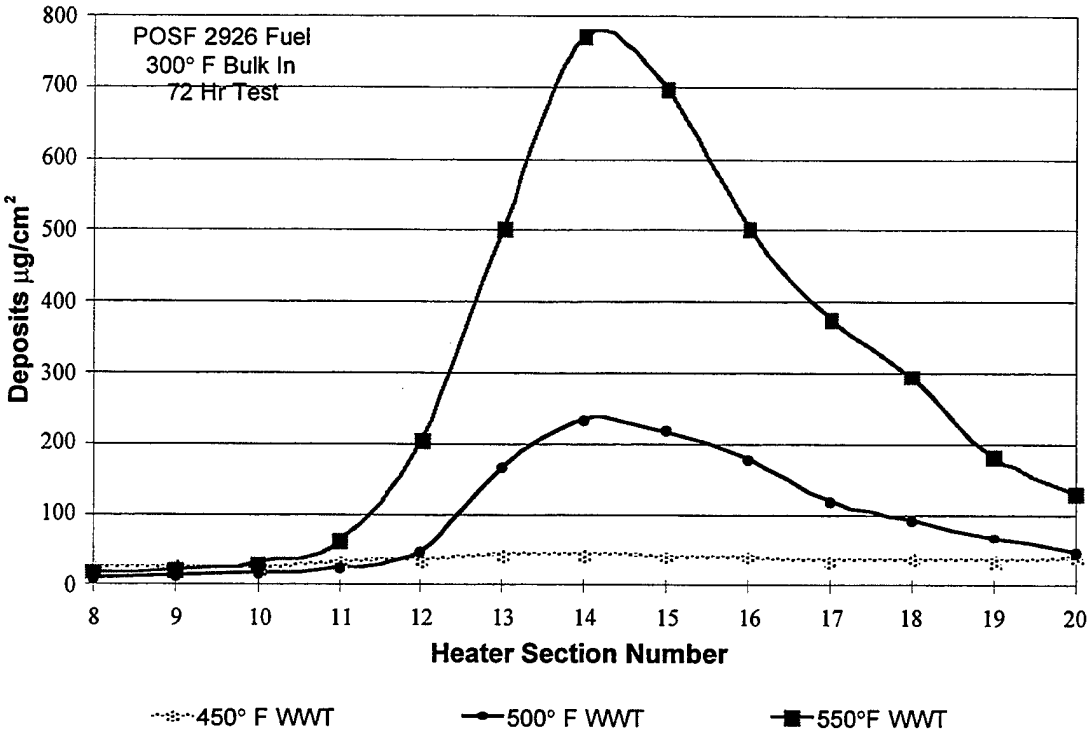

Figure 7. EDTST studies. Heater tube deposits at various wetted wall temperatures.

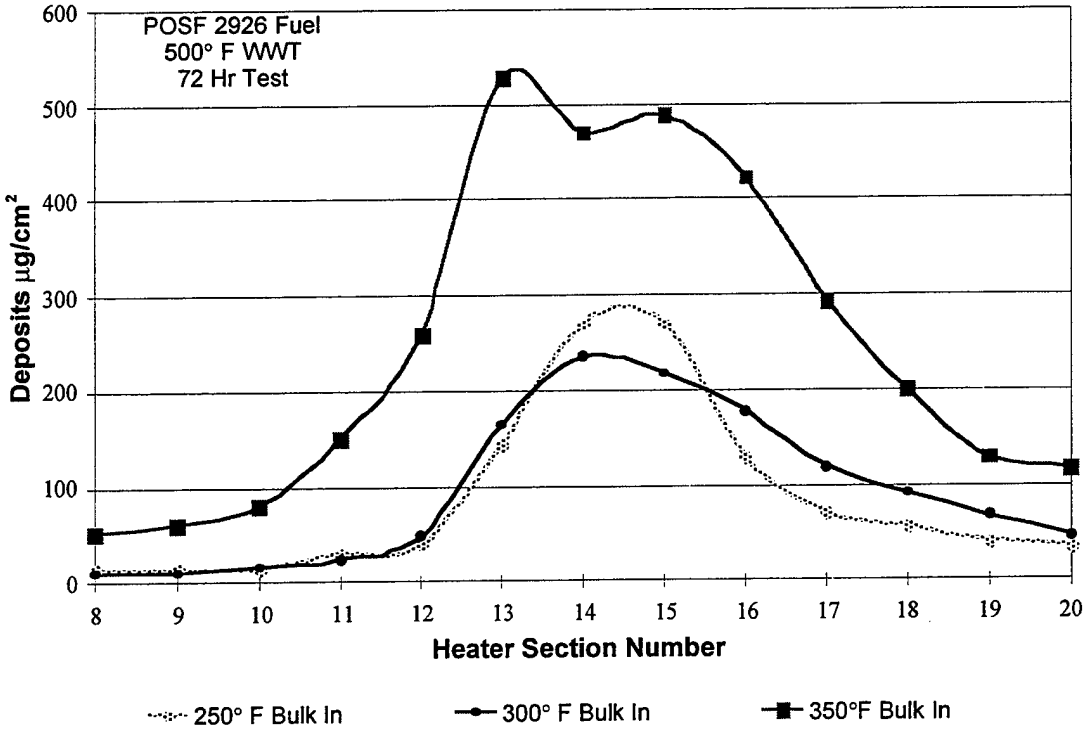

Figure 8. EDTST studies. Heater tube deposits at various bulk in temperatures.

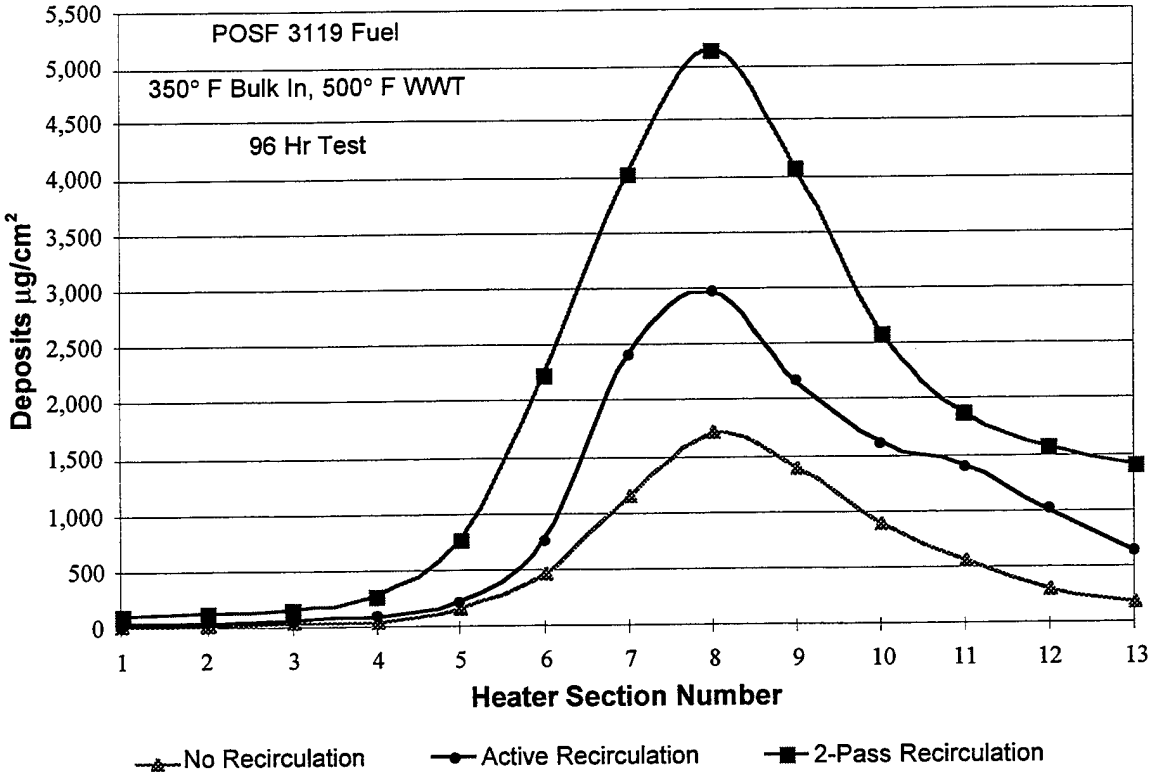

Figure 9. EDTST studies. A comparison of recirculation methods.

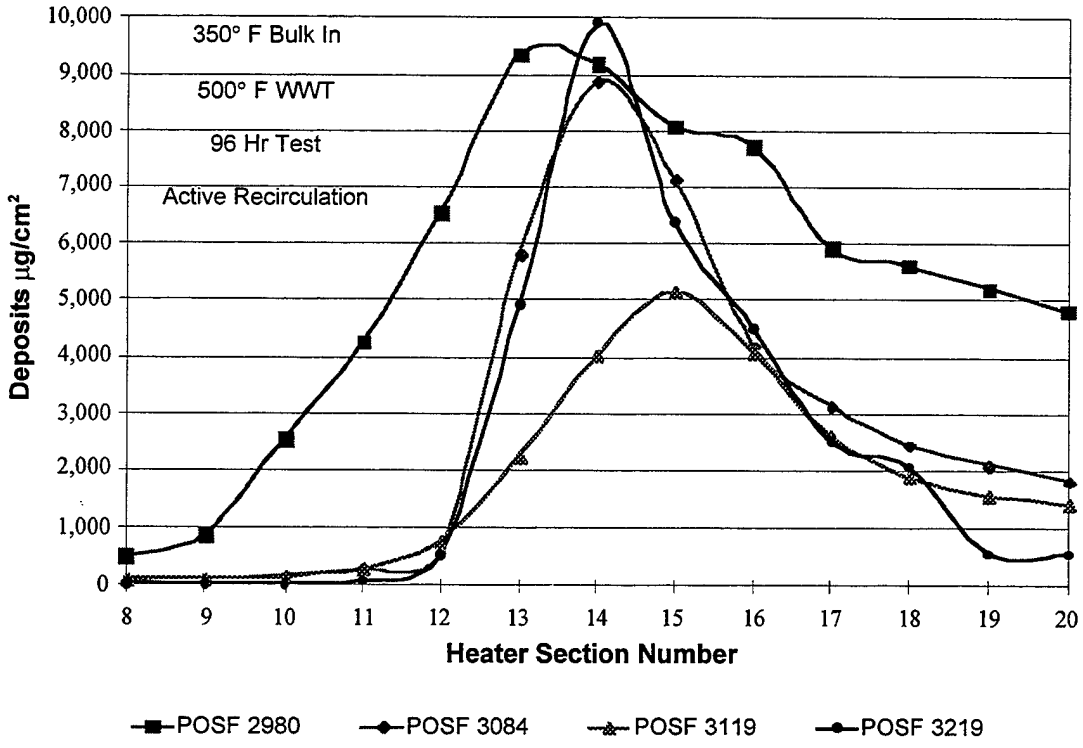

Figure 10. EDTST studies. A comparison of deposits between different fuels.

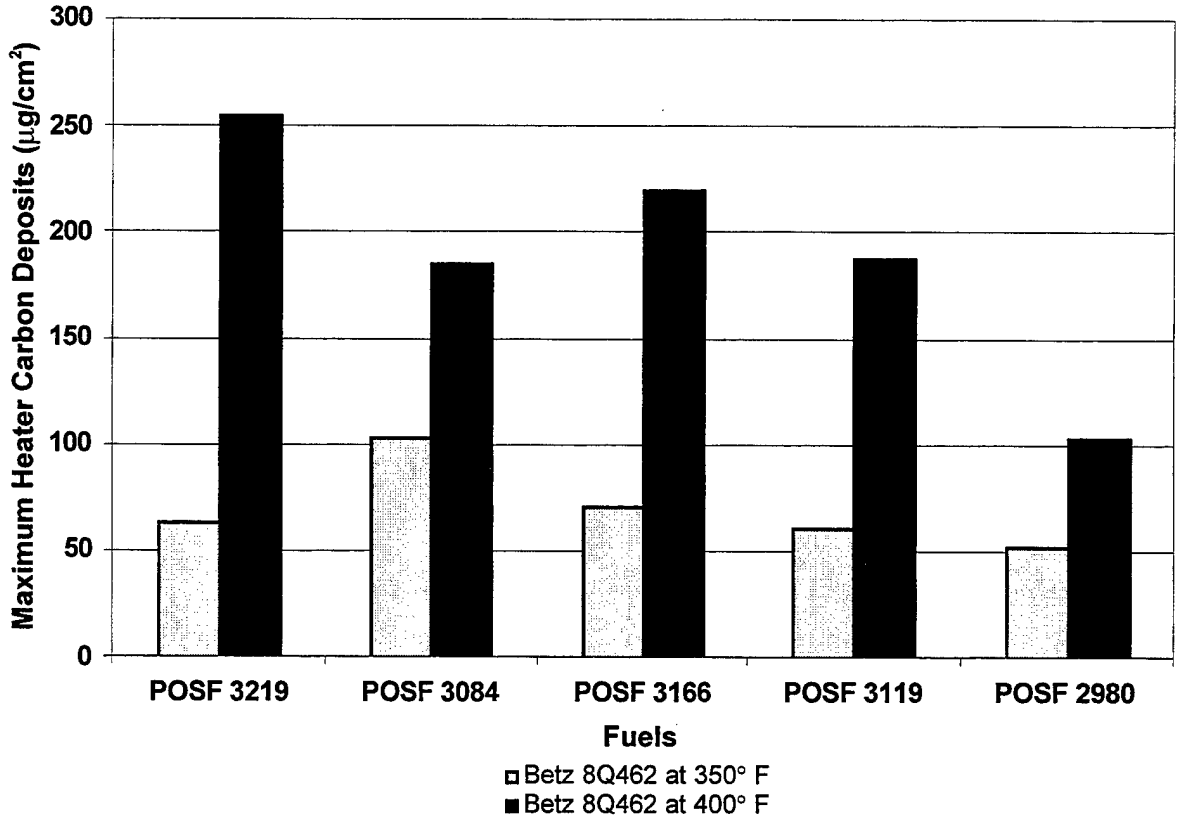

Figure 11. EDTST studies. Maximum heater deposits of various fuels at two bulk temperatures.

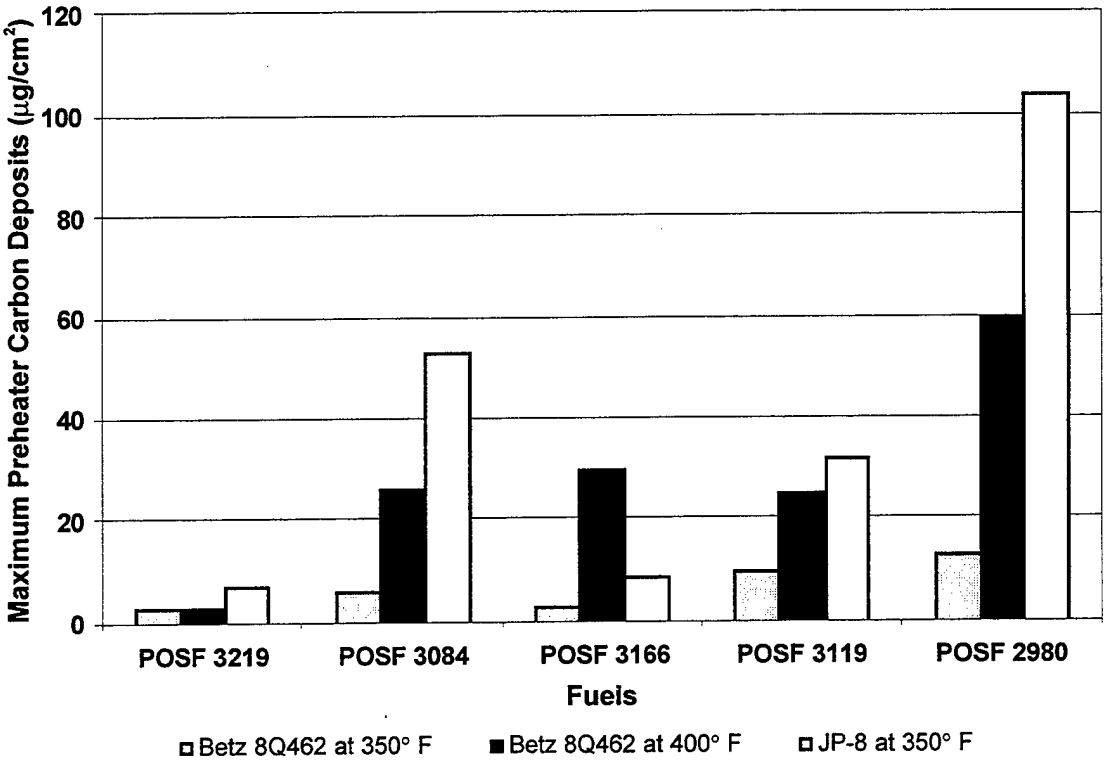

Figure 12. EDTST studies. Maximum preheater deposits of various fuels at two bulk temperatures.

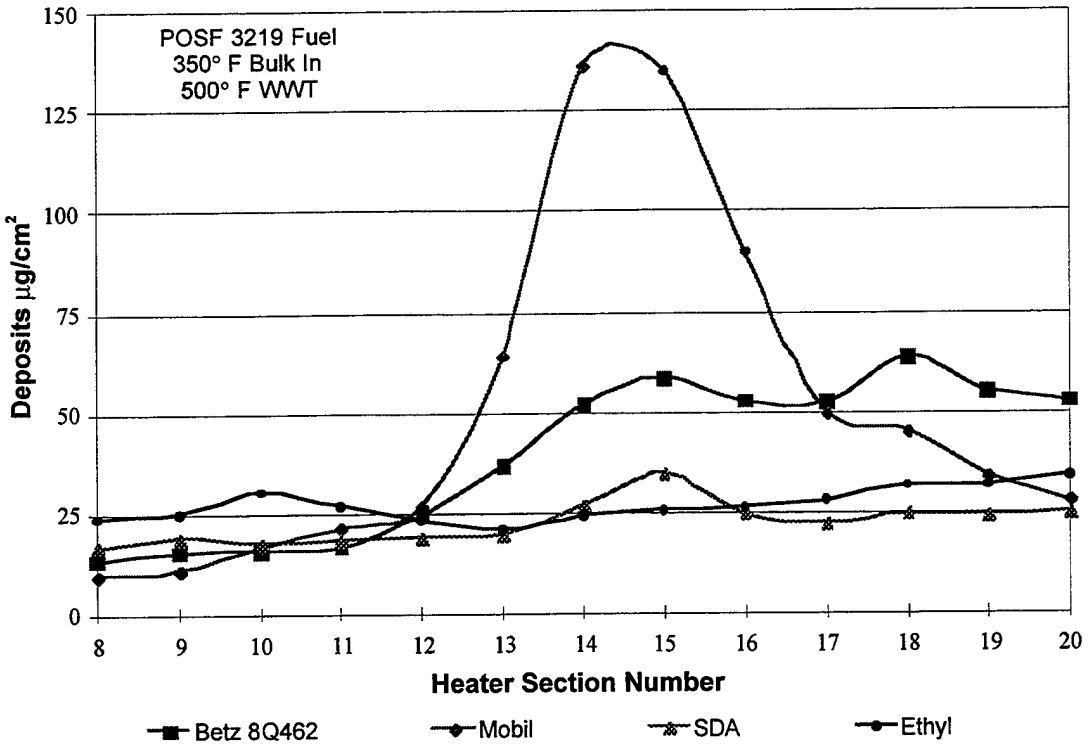

Figure 13. EDTST studies. Heater deposits of JP-8+100 additives.

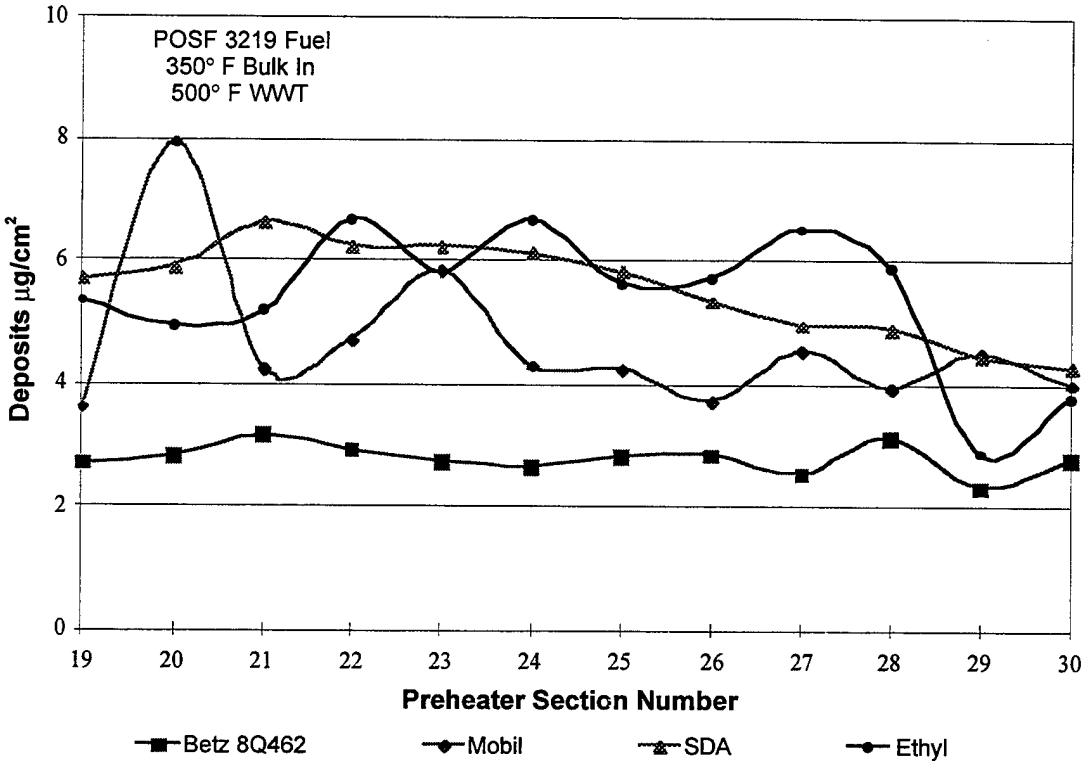

Figure 14. EDTST studies. Preheater deposits of JP-8+100 additives.

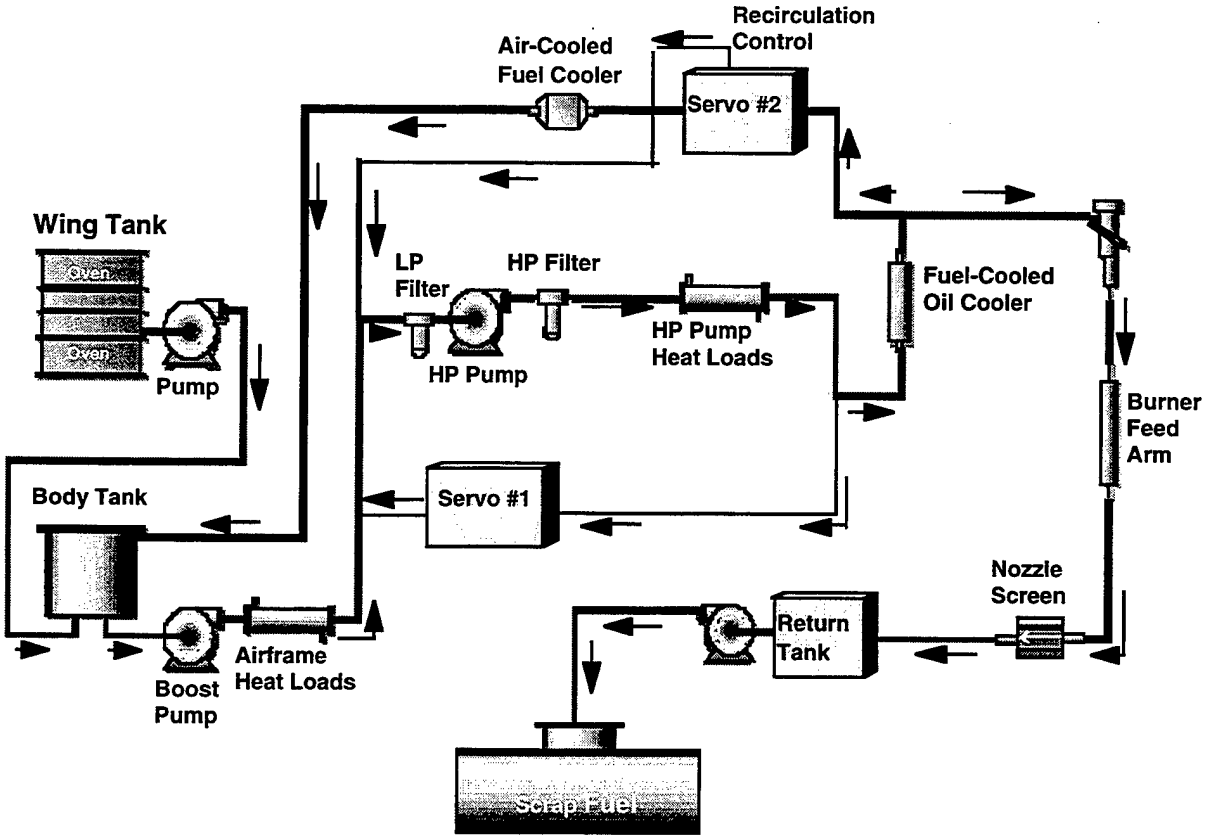

Figure 15. Advanced reduced scale fuel system simulator schematic.

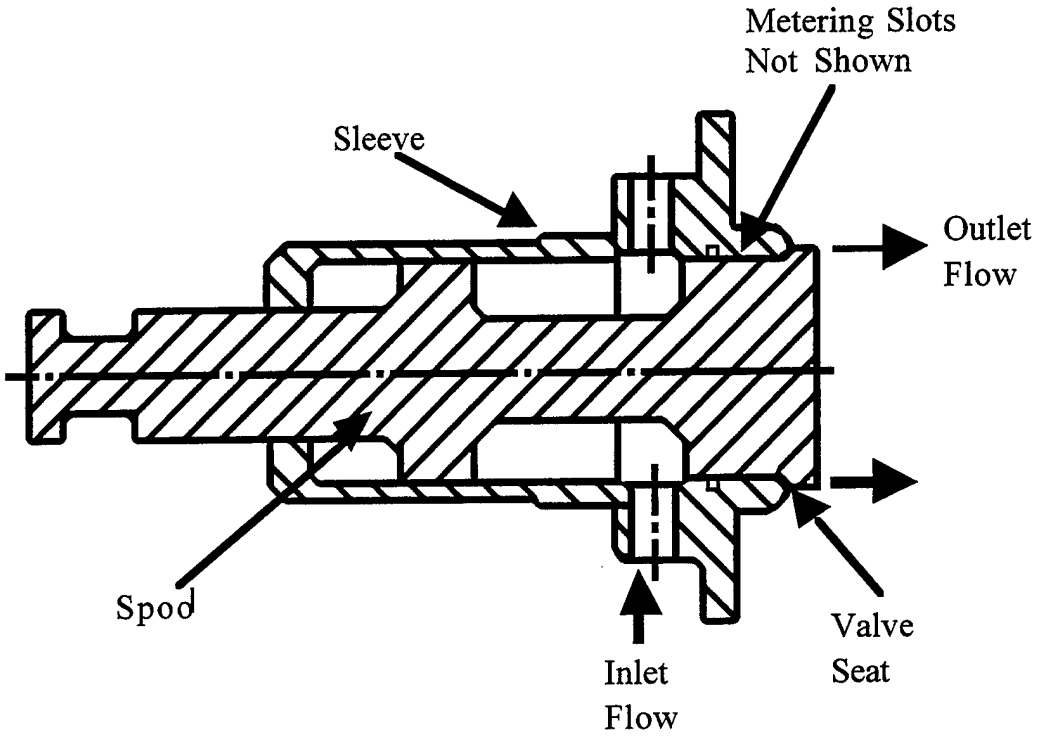

Figure 16. ARSFSS studies. Flow divider valve.

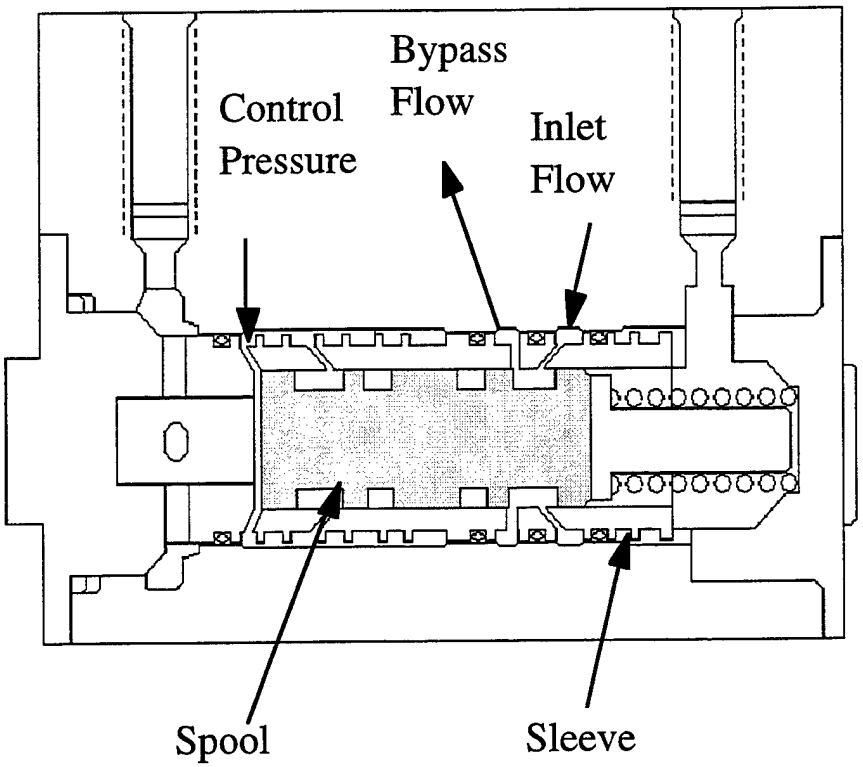

Figure 17. ARSFSS studies. Servovalve schematic.

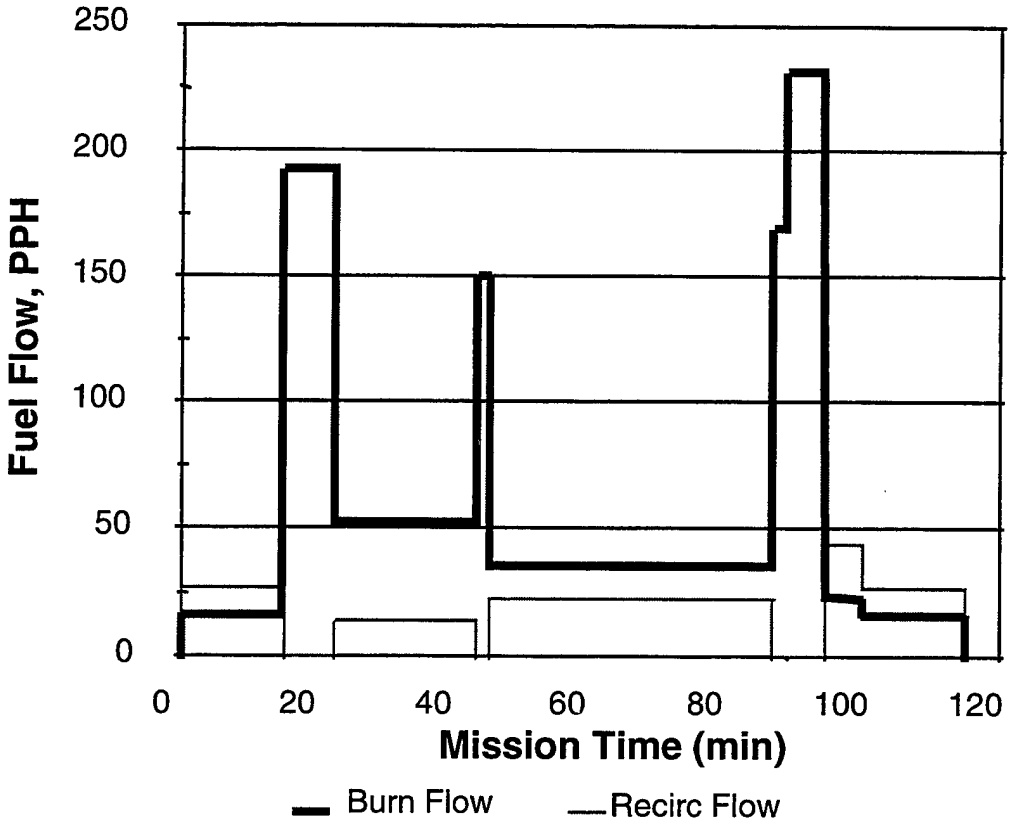

Figure 18. ARSFSS studies. Generic mission profile.

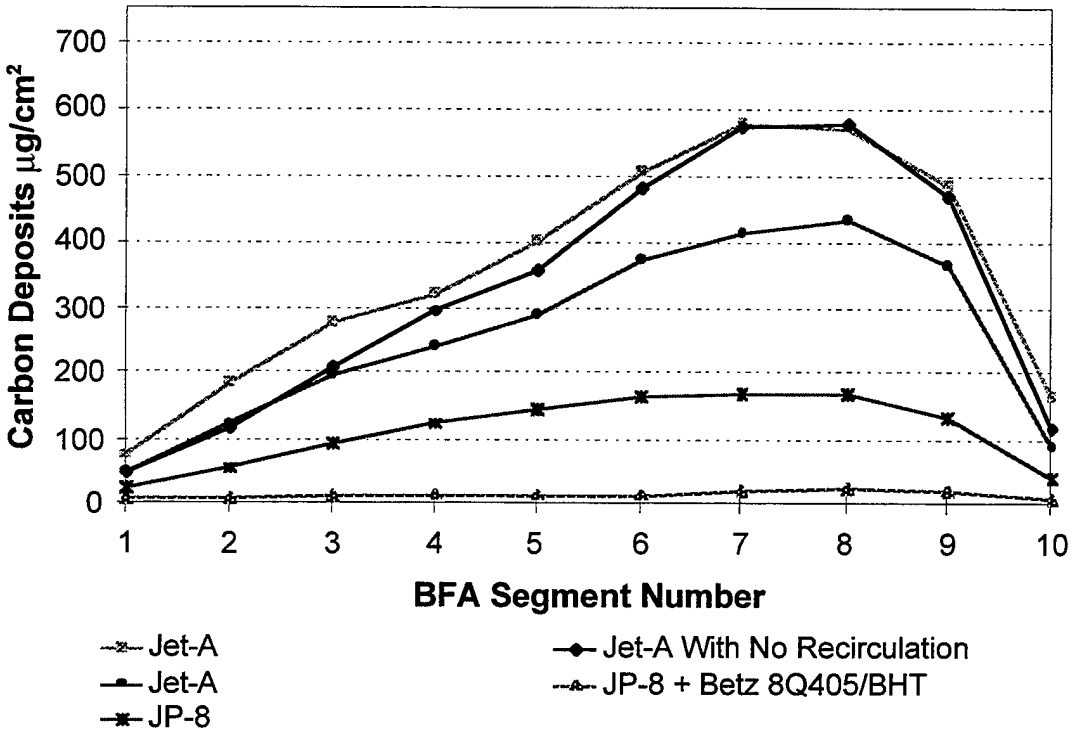

Figure 19. ARSFSS studies. Carbon deposits with and without recirculation.

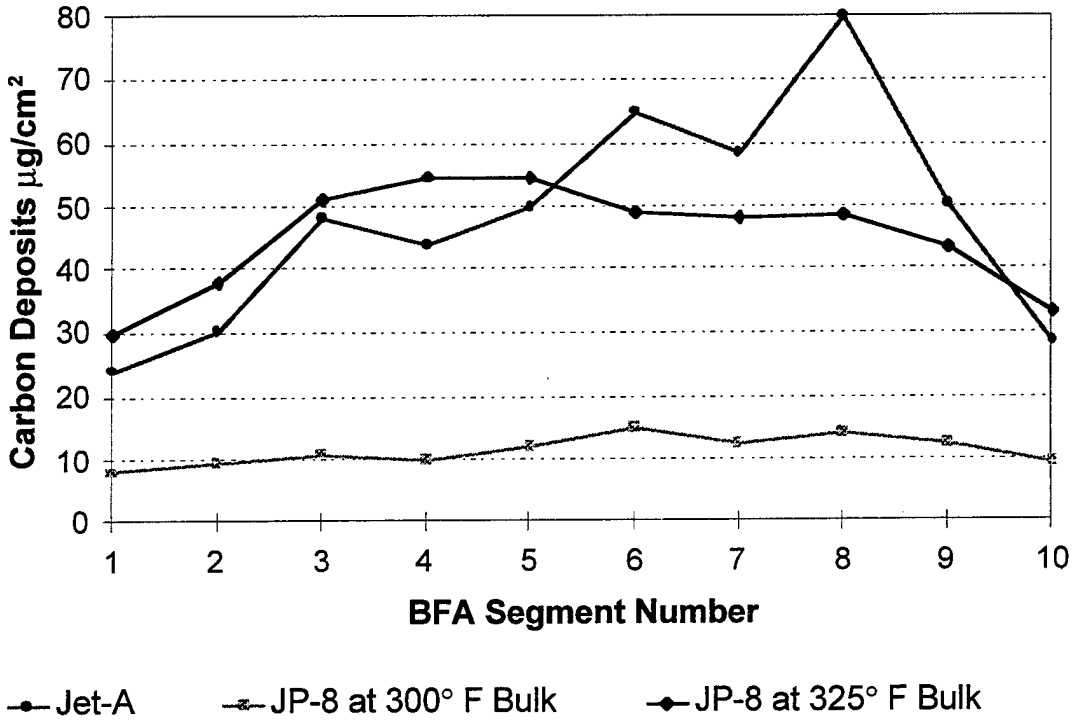

Figure 20. ARSFSS studies. Burner feed arm deposits after pump/filter change.

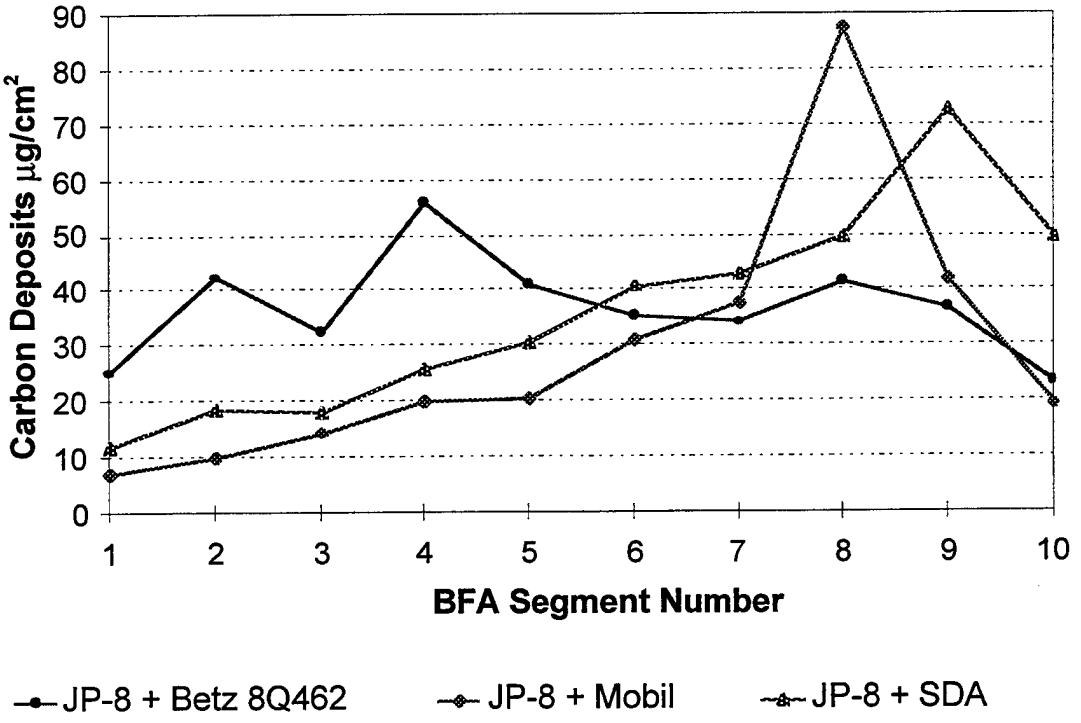

Figure 21. ARSFSS studies. Carbon deposit comparisons of JP-8+100 test results.

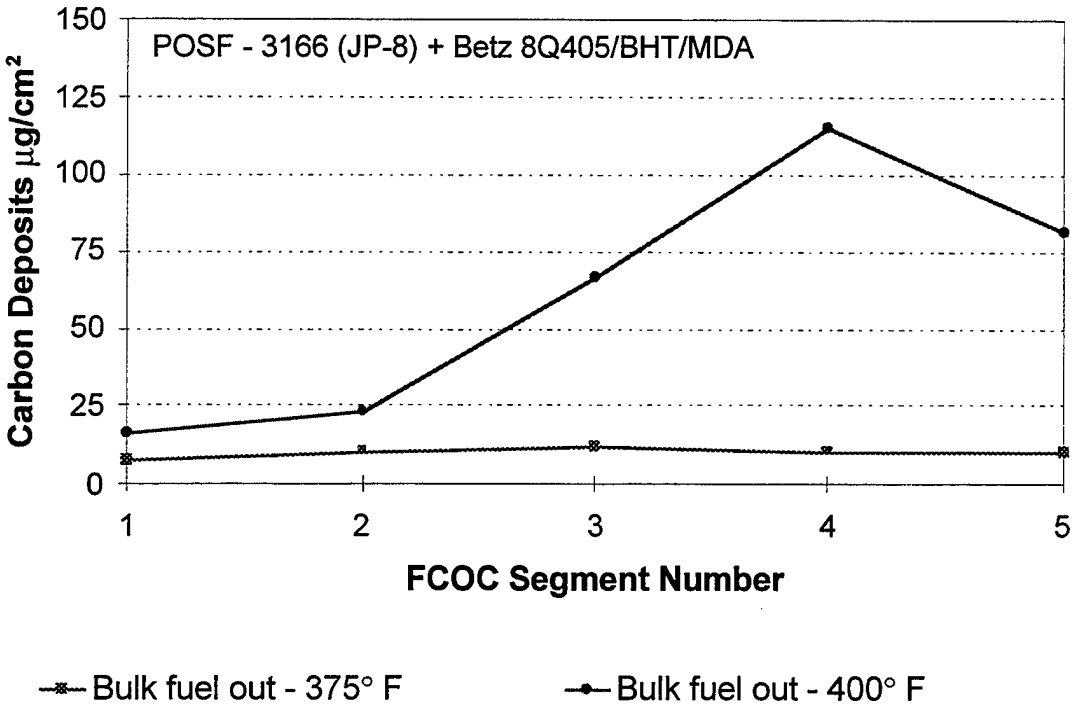

Figure 22. ARSFSS studies. Fuel cooled oil cooler deposits at various temperatures.

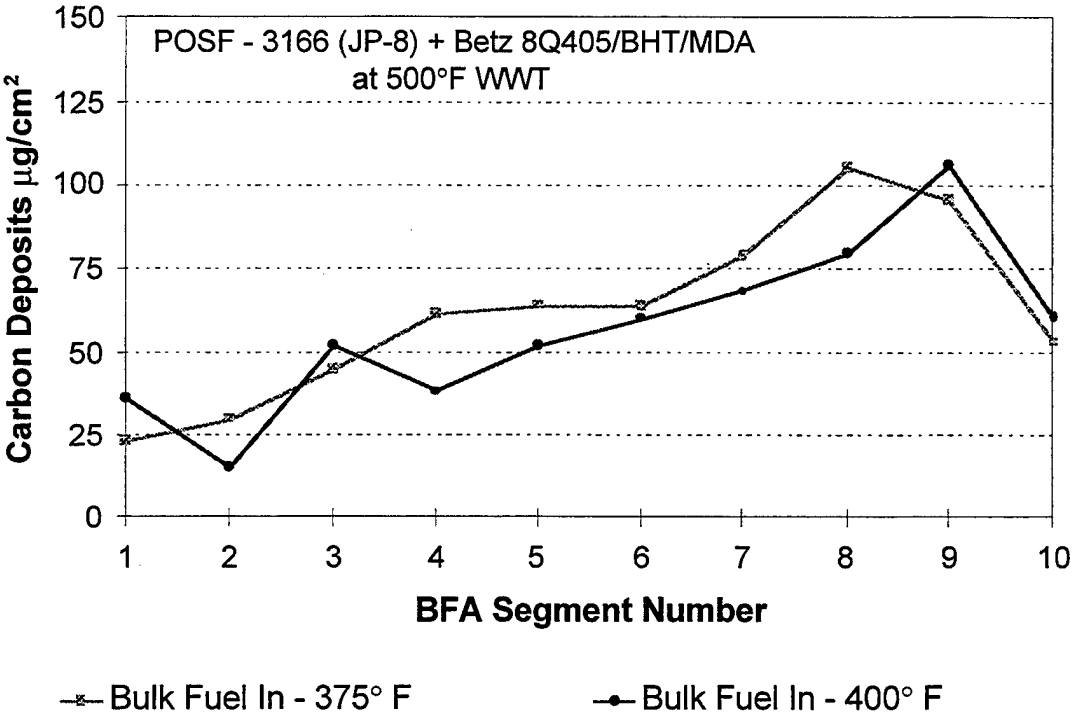

Figure 23. ARSFSS studies. Burner feed arm deposits at various temperatures.

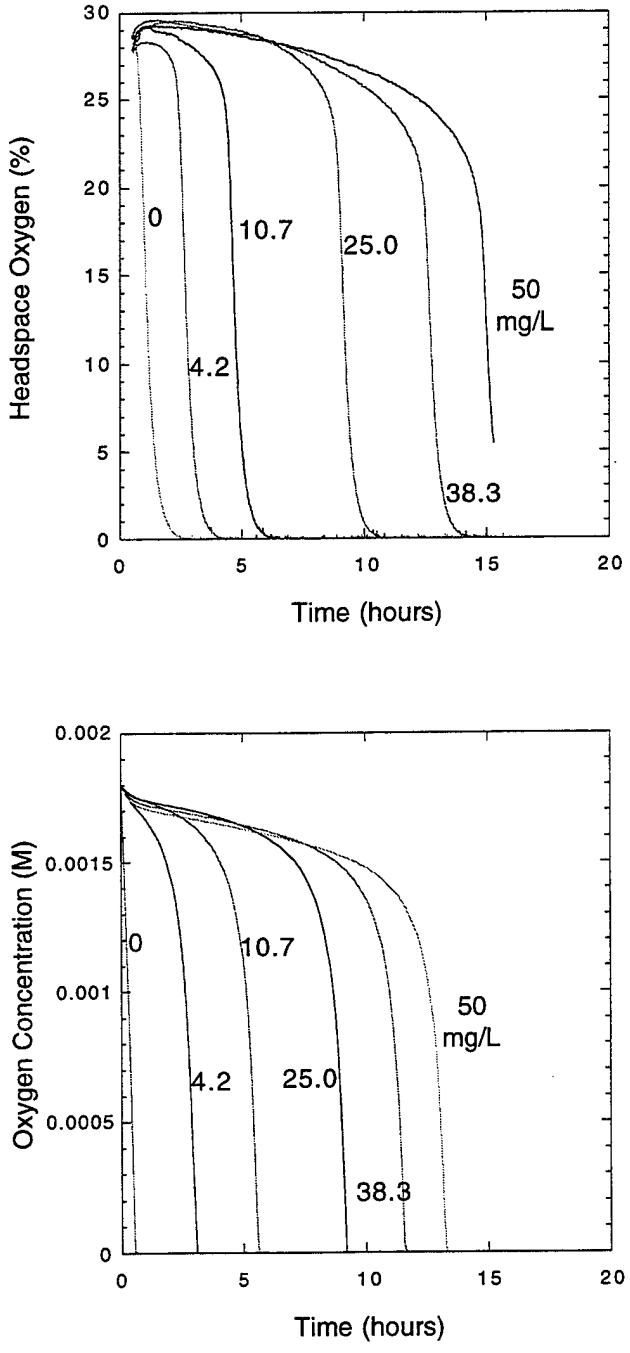

Figure 24. Fuel modeling. Plots of headspace oxygen concentration vs time for the oxidation of Exxsol D-110 at 140C in the QCM at various concentrations of added BHT (top); Plots of calculated oxygen concentration vs time at various concentrations of added BHT (bottom).

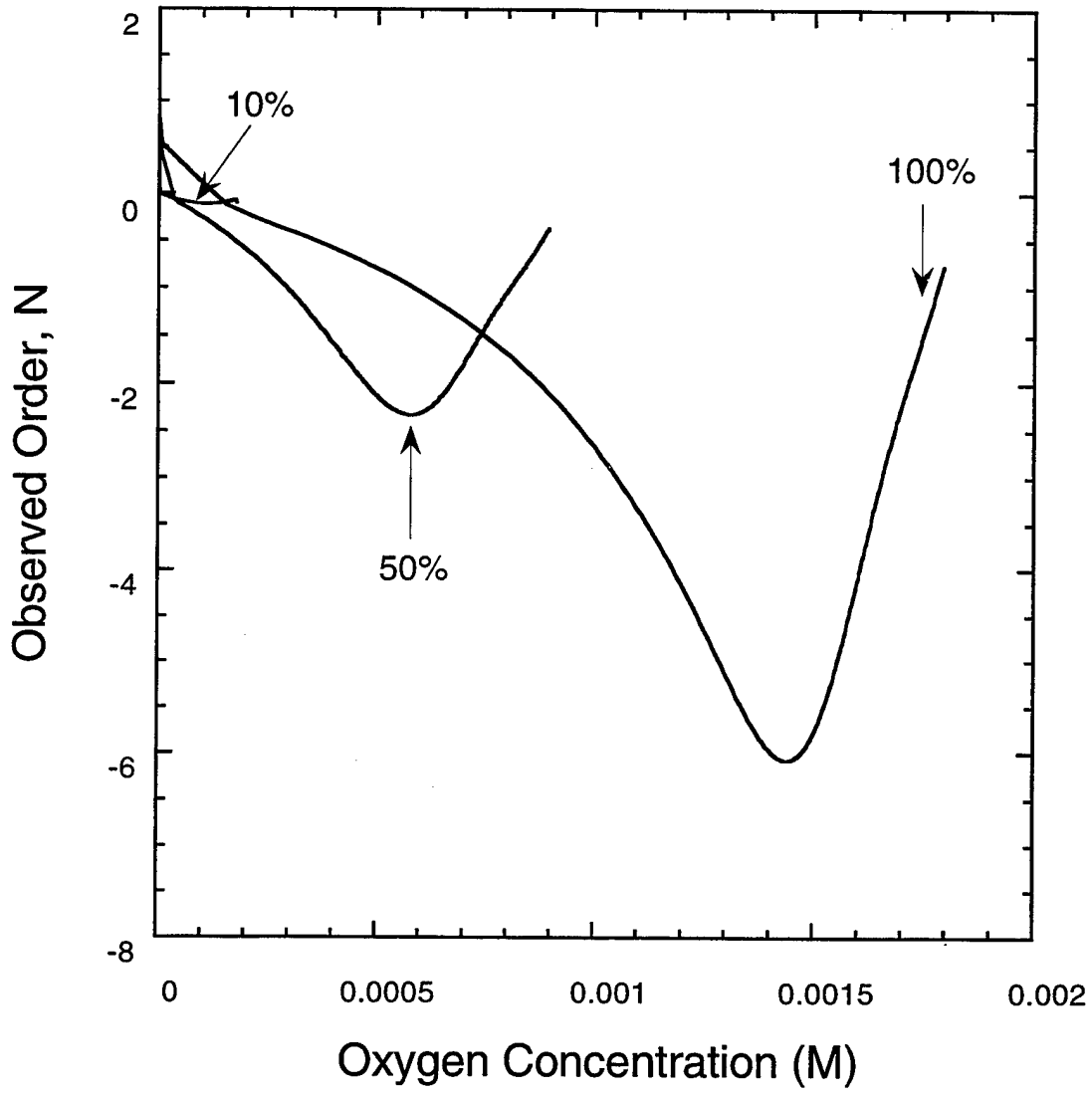

Figure 25. Fuel modeling. Variation of reaction order, N, with oxygen consumption for different initial oxygen concentrations at 185C with antioxidant concentration of 2.3 x 10^{-4}M.

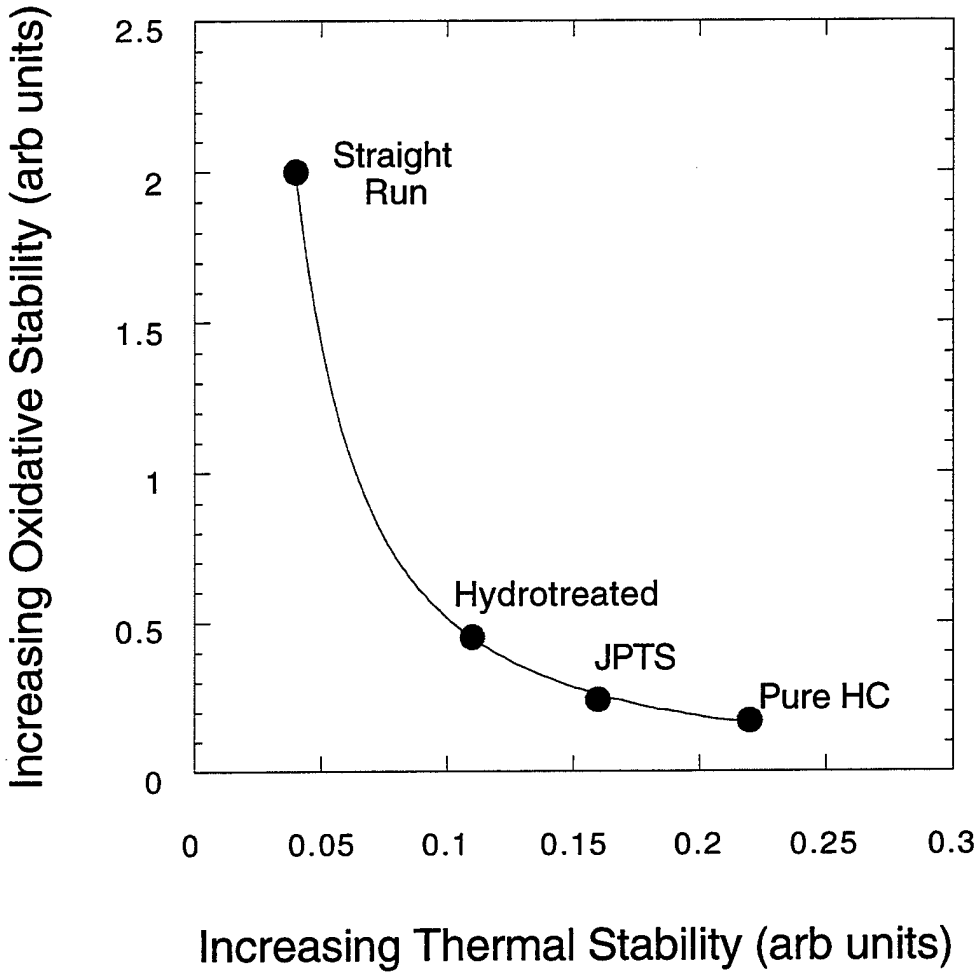

Figure 26. Inverse relationship between thermal stability and oxidative stability for various jet fuels and a pure hydrocarbon (HC)

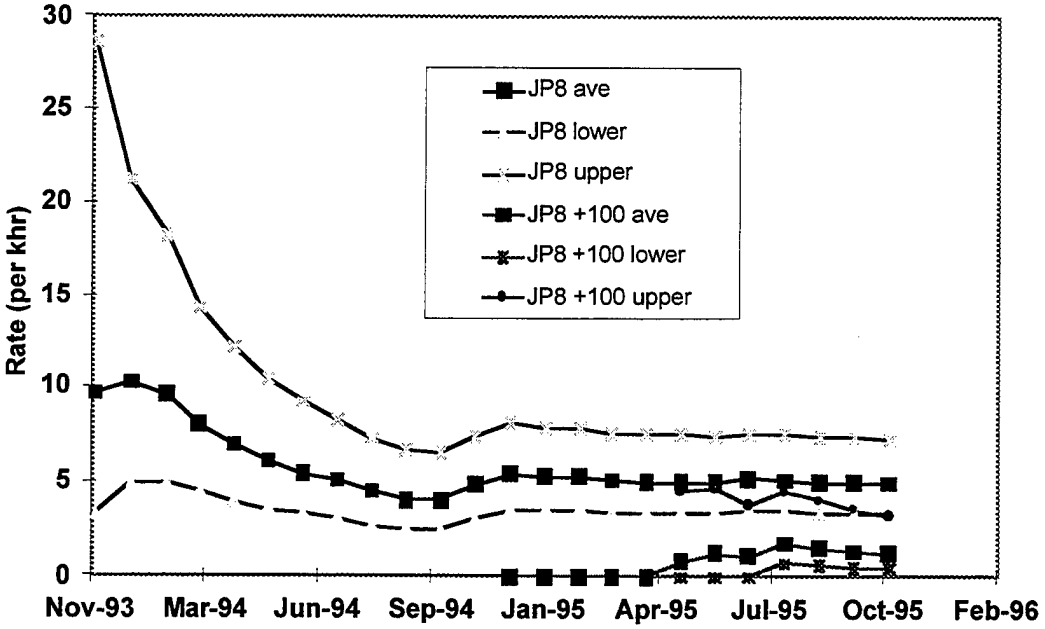

Figure 27. Mean rate of occurrences, upper and lower bounds for the mean for JP-8 and JP-8+ 100 at Kingsley AFB.

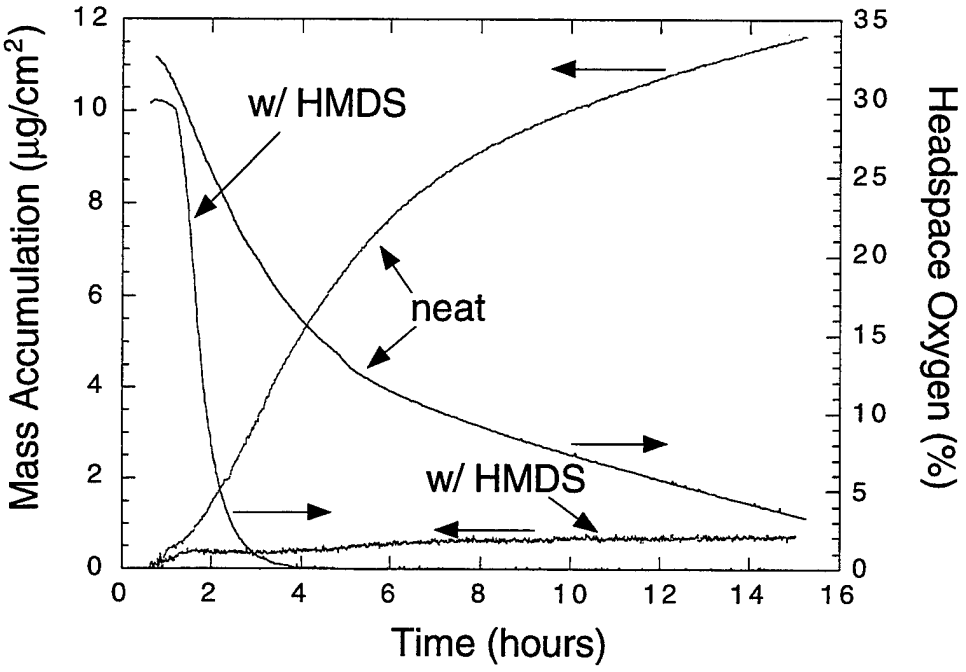

Figure 28. Plots of deposition and headspace oxygen concentration in QCM runs at 140C for fuel POSF-3119 neat and with 1 mL of HMDS.

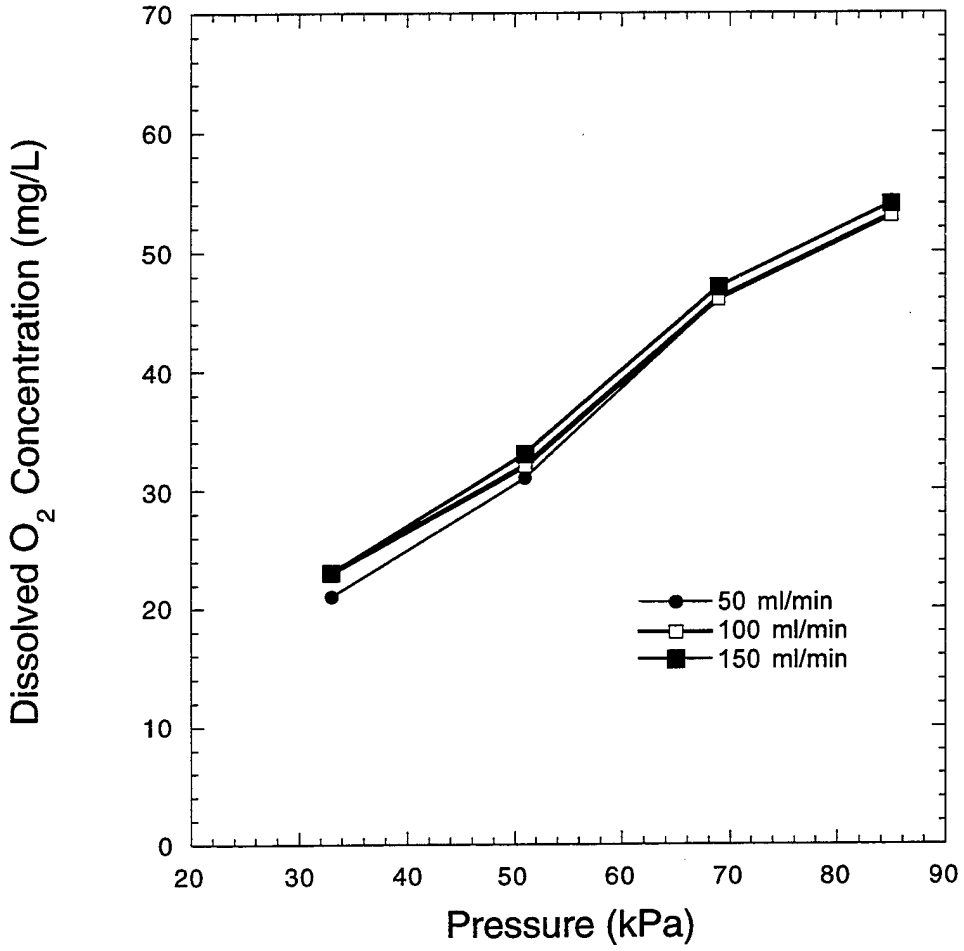

Figure 29. Ultrasonic removal of dissolved oxygen in fuel. Measured dissolved O_2 concentrations at different volumetric flow rates at 25C.

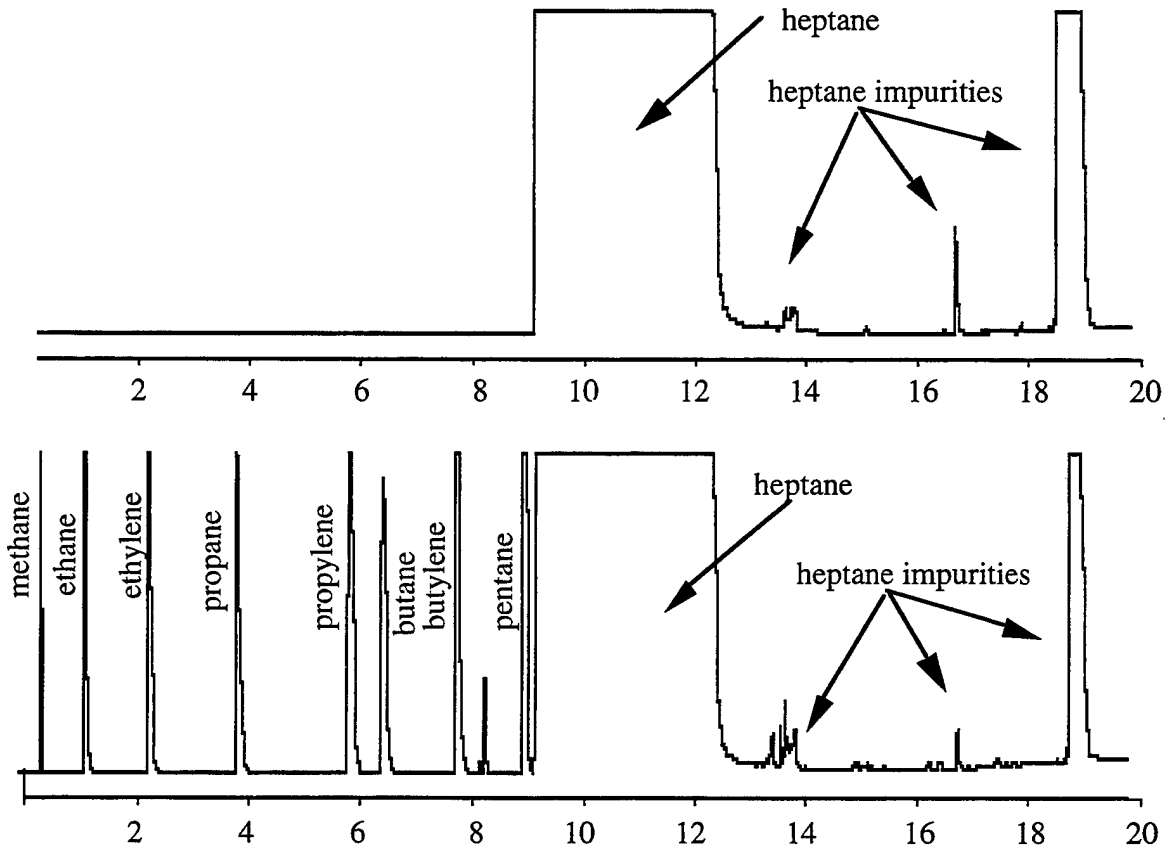

Figure 30. Chromatograms of n-heptane cracking in the pulsed STDS at 20C (top) and 600C (bottom).

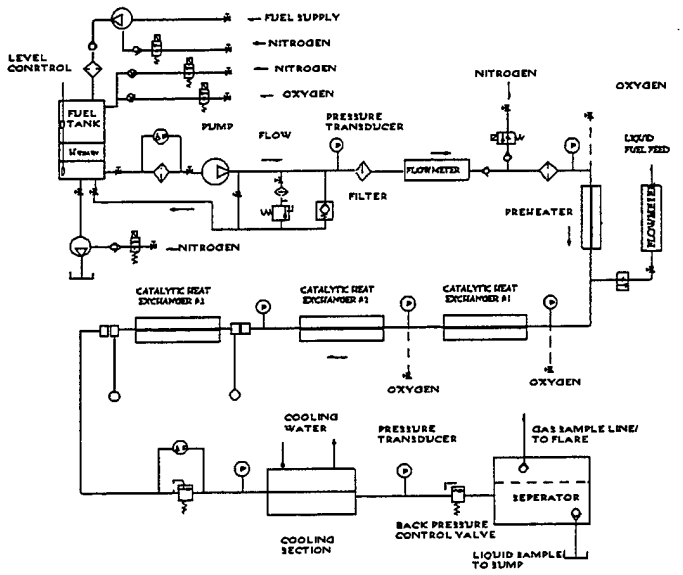

Figure 31. AAFSS studies. The advanced aircraft fuel system simulator.

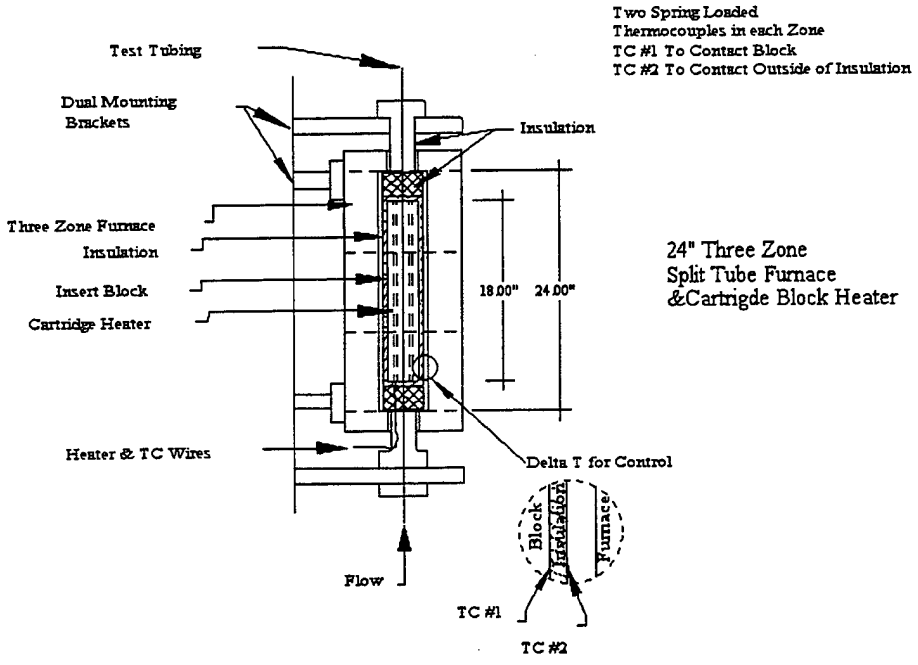

Figure 32. AAFSS studies. Split furnace functioning as a guard heater.

Table 1. XPS-Determined Percent Atomic Composition: JP-8 Fuel Deposits in Phoenix Rig

Hours	O-C=O	C=O	C-O	CH,C	O	Fe	N	S-O	C-S	Si	Cr	Total C	Total S	Total
Heated Section														
0	4.8	1.9	5.4	30.2	30.1	14.6	<0.7	0.9	<0.2	7.1	4.1	42.3	<1.1	99.1
0.5	3.7	4.4	5.7	45.1	30.6	5.5	2.4	2.2	0.46	-	-	58.9	2.7	100.1
1.5	4.1	4.6	7.8	49.9	26.1	3.4	1.8	1.6	0.53	-	-	66.4	2.1	99.8
3	4	4.8	6.8	50.4	27.2	2.8	2.1	1.5	0.34	-	-	66	1.8	99.9
6	4.5	4.6	7.3	51	26.2	2.5	1.8	1.7	0.37	-	-	67.4	2.1	100
Cooled Section														
0	4.8	1.9	5.4	30.2	30.1	14.6	<0.7	0.90.	<0.2	7.1	4.1	42.3	<1.1	99.1
0.5	1.6	1.7	4.5	25.5	44.8	6.8	1.3	1.4	<0.2	8.3	3.9	33.3	<1.6	99.8
1.5	1.7	2.4	4.1	36.4	36.4	5.3	1.7	1.7	0.44	5.5	4.4	44.6	2.1	100
3	1.4	3.1	6.1	58.6	22.2	2.7	3	2.4	0.35	-	-	69.2	2.8	99.9
6	1.4	2.8	6.6	56.4	23.2	3.8	3.1	2.4	0.33	-	-	67.2	2.7	100

O-C=O, acids and esters; C=O, aldehydes and ketones; C-O, alcohols and ethers; CH and C, hydrocarbons and carbon; S-O, sulfur oxides; C-S, sulfides

Table 2. Carbon Deposits & Consumed Dissolved O_2 Partial Consumption Conditions, 62 mL/min Fuel F2980.

inlet O_2 concn. (ppm)	O_2 consumed heated block 1 (ppm)	O_2 consumed heated block 2 (ppm)	total O_2 consumed (ppm)	deposits-heated blocks (μg)	deposits-cooled block (μg)
JP-8					
70	5	11	16	4057	4774
30	4	6	10	5800	2976
6	1	3	4	6007	1400
1	0.7	0.3	1	482	183
JP-8A					
70	5	6	11	1366	2909
30	5	6	11	1177	923

Table 3. List of Material Categories and Physical Property Tests

Category	Material	Physical Properties Tested
I.A.	Adhesives	Lap Shear
I.B.	Bladders	Tensile/Elongation/Volume Swell
I.C.	Coatings	Pencil Hardness/Tape Adhesion
I.C./I.D.	Coatings/Sealants	Tensile/Elongation/Volume Swell/Shore A Hardness/Peel Strength
I.D.	Sealants (non-curing)	Rupture Pressure/Volume Swell
I.E.	Composites	Inner Laminar Shear
I.F.	Foam (ESM)	Tensile/Elongation/Resistivity
I.G/II.G.	Gaskets (O-rings)	Tensile/Elongation/Volume Swell /Shore Hardness/Compression Set
I.H.	Hoses	Tensile/Elongation/Volume Swell/Shore A Hardness
I.I.	Electrical Wire	Tensile/Elongation/Insulation
I.J	Joining Materials	
I.K.	Miscellaneous	Visual Observations and Other
I.L.	Locking Compounds	Torque
I.M/II.M	Metallics	SCC/Weight Loss-Gain/Cleaning/Pitting
I.O.	Floats	Float Ability/Visual Observations
I.P.	Potting Compounds	Lap Shear

Table 4. Specification Tests Used for Materials Testing

Test	Specification/Document
Tensile/Elongation	D-1414 (Type I "O" Rings)/D-412 Type II
Compression Set	D-395 (Method B)
Hardness (Pencil)	D-2240
Volume Swell	D-471
Tear Resistance	D-624
Resistivity	D-257-O
Tape Adhesion	Fed. Std. 1418 (Method 6301)
Laminar Shear	D-79O
Peel Strength	ASTM D-413
Lap Shear	ASTM D-1002
Hardness	ASTM D-2240
Torque	MIL-S-22473
Pressure Rupture	MIL-S-85334
SCC	ASTM F-945
Weight loss/gain	ASTM F-483
Cleaning	ASTM G1
Pitting evaluation	ASTM G46

Table 5. Fuel Property Tests

Test	Specification/Document
Color	Visual Observation
Acid No.	ASTM D-3242 (Modified)
Gums	D-381
Hydroperoxides	D-3703
Conductivity	D-2624/D-4308
Graphite Furnace/ICP	Used equipment manufacturers measurement techniques
Fuel Additives	ASTM D-4054

Table 6. Reaction Mechanism for Chemical Kinetic Modeling

Reaction	Arrhenius A-Factor (moles, liters, and secs units)	Activation Energy (kcal/mole)	Reaction Number
$I \Rightarrow R\cdot$	1×10^{-3}	0.0	(1)
$R\cdot + O_2 \Rightarrow RO_2\cdot$	3×10^{9}	0.0	(2)
$RO_2\cdot + RH \Rightarrow RO_2H + R\cdot$	3×10^{9}	12.0	(3)
$RO_2\cdot + RO_2\cdot \Rightarrow$ termination	3×10^{9}	0.0	(4)
$RO_2\cdot + AH \Rightarrow RO_2H + A\cdot$	3×10^{9}	5.0	(5)
$AO_2\cdot + RH \Rightarrow AO_2H + R\cdot$	3×10^{5}	10.0	(6)
$A\cdot + O_2 \Rightarrow AO_2\cdot$	3×10^{9}	0.0	(7)
$AO_2\cdot + AH \Rightarrow AO_2H + A\cdot$	3×10^{9}	6.0	(8)
$AO_2\cdot + AO_2\cdot \Rightarrow$ products	3×10^{9}	0.0	(9)
$R\cdot + R\cdot \Rightarrow R_2$	3×10^{9}	0.0	(10)
$RO_2H \Rightarrow RO\cdot + \cdot OH$	1×10^{15}	42.0	(11)
$RO\cdot + RH \Rightarrow ROH + R\cdot$	3×10^{9}	10.0	(12)
$RO\cdot \Rightarrow R_{prime}\cdot +$ carbonyl	1×10^{16}	15.0	(13)
$\cdot OH + RH \Rightarrow H_2O + R\cdot$	3×10^{9}	10.0	(14)
$RO\cdot + RO\cdot \Rightarrow RO\cdot$ termination	3×10^{9}	0.0	(15)
$R_{prime}\cdot + RH \Rightarrow$ alkane $+ R\cdot$	3×10^{9}	10.0	(16)
$RO_2H + SH \Rightarrow$ products	3×10^{9}	0.0	(17)

Table 7. Integer Ranking of Fuels by Thermal Stability Tests.

Fuel	Average TS Scale	ICOT	MCRT	QCM 8 hrs	QCM 15 hrs	JFTOT BP	HLPS
A	1	1	1	1	1	1	1
B	2	2	2	2	2	2	2
C	3	3	3	3	4	3	9
D	4	9	5	4	3	8	3
E	5	8	6	6	5	7	4
F	6	4	10	7	7	4	5
G	7	7	11	5	6	6	6
H	8	5	4	8	11	8	8
I	9	6	9	9	10	4	7
J	10	10	7	9	8	10	10
K	11	11	7	11	9	12	12
L	12	12	12	12	12	10	11

Appendix A.

Oxidation of Jet Fuels and the Formation of Deposits

Shawn P. Heneghan
Steven Zabarnick
University of Dayton
300 College Park
Dayton, OH 45469-0140

Oxidation of jet fuels and the formation of deposits

Shawn P. Heneghan and Steven Zabarnick
University of Dayton, Dayton, OH 45469-0140, USA
(Received 18 June 1992; revised 14 December 1992)

Jet fuels and jet fuel surrogate were thermally stressed to simulate the time–temperature history of aircraft fuel-handling systems. The resulting fuels and soluble and insoluble products were analysed. The results are shown to be incompatible with previous mechanisms concerning the source of deposit precursors. In general, two important dependences on oxygen have been found: (1) in agreement with previous research, the amount of deposit formed decreases significantly if oxygen is removed from the fuel before thermal stressing; (2) fuels that oxidize easily are likely to be more stable (as measured by deposits). New evidence is presented to support the free-radical mechanisms of oxidation and deposit formation, in contrast to proposed ionic mechanisms of oxidation. A general theory of oxidation of hydrocarbons has been incorporated to account for the observed oxygen-dependences, involving a free-radical, autoxidation, chain mechanism. It is proposed that the presence of naturally occurring antioxidant molecules plays an important role in both inhibiting the oxidation of the fuel and forming deposit precursors. Some properties (concentration, reactivity) of these antioxidant molecules and the implications of the theory are discussed.

(Keywords: jet fuels; oxidation; deposits)

It has long been known that oxygen consumption is an important first step in the formation of deposits in jet fuels[1–7]. Many mechanisms have been proposed to account for deposit formation. Most start with the autoxidation chain cycle, and assume that the products of the oxidation initiate the formation of deposits.

Bol'shakov[1] stated that condensation reactions of peroxides and other oxidized products are responsible for solid formation. Clark and Smith[2] defined the initial stage of deposit formation as oxidation via a free-radical chain mechanism and the second stage as the reaction of trace compounds with the oxidation products. Hazlett[3] proposed that hydroperoxides are deposit precursors. He attributed the cause of deposits to the alkoxy free radical that forms from the decomposition of hydroperoxides.

The general consensus of knowledge about the chemistry and physics of jet fuel thermal-oxidative stability was summarized by Baker *et al.*[4] on the basis of the results of a NASA workshop[8]. The six key points are:

1. the initial process is a reaction involving both oxygen and fuel;
2. the chemistry involved is primarily free-radical;
3. deposit formation depends on temperature, fuel flow, dissolved metals, and dissolved oxygen;
4. deposits form in liquid and vapour phases, and simultaneous occurrence of both phases enhances deposit formation;
5. metals can have a significant effect on deposit formation;
6. the amount of dissolved oxygen is important; removal of oxygen generally reduces significantly the amount of deposit formed.

Since all the reported research has demonstrated the importance of oxygen to the deposition process, there is general agreement that peroxides, alcohols, ketones and acids are precursors to solids formation and that fuels oxidize to form gums, which in turn polymerize and condense to form solids. Although several researchers[5] have noted that there is no direct correlation between the oxidation of fuels and the formation of deposits, many groups have followed the deposition process by monitoring the appearance of oxidation products[9–15].

Recent reports on deposit formation in jet fuels (in both flowing and static tests), combined with oxidation measurements[9–12,16–23] have questioned the above time-honoured mechanisms. This paper reviews the current research. The first section of this review discusses stability measurements based on deposit formation (referred to as thermal stability), and the second section a measure of the ability to oxidize (referred to as oxidative stability). A theoretical analysis using standard chain reactions for autoxidation and radical trapping is then developed and the relation between reactivity and concentration of antioxidant molecules is calculated. The subsequent discussion also deals separately with the mechanism for deposit formation and the mechanism for oxidation. Concerning deposit formation, it is shown that previous models of deposit formation are inadequate, in that they do not predict the observed oxygen-dependence of both thermal and oxidative stability. Concerning oxygen consumption, it is shown how the antioxidant mechanism presented here can account for the observed oxygen-dependences in not only recent but also much previous work. Then, with one assumption concerning the source of the deposit molecules, it is shown how this mechanism can be used to account for the formation of deposits. Finally, the implications of the analysis are considered.

0016-2361/94/01/0035-09

Table 1 Properties of baseline jet fuels

	ASTM method	Fuel F-2799	Fuel F-2747	Fuel F-2827
JFTOT[a] breakpoint (°C)	D3241	399	332	266
Sulfur (wt%)	D4294	0.0	0.0	0.1
Aromatics (vol%)	D1319	9	19	19
Existent gum (mg/100 ml)	D381	0.4	0.0	0.0
Flash point (°C)	D93	49	59	50

[a] Jet fuel thermal oxidation tester

REVIEW OF RECENT EXPERIMENTS

Many different types of apparatus[9–12,17,18,21] have been used to evaluate the thermal stability of jet fuels, and several techniques have been used to measure their oxidative stability[9–12,19,20,22]. Only a brief compilation of the important results is presented here. Most of these recent results were obtained using three distinct fuels; some of their properties are listed in *Table 1*. Fuel F-2747 is a highly hydrotreated Jet A-1 fuel, while F-2799 is an Air Force specification fuel, jet propellant thermally stable (JPTS), which has good thermal stability characteristics. Fuel F-2827 is a non-hydrotreated Jet A fuel, with a broader boiling range and increased heteroatom concentration. It is expected that this fuel will exhibit lower thermal stability than F-2747 and F-2799.

In addition to the large number of experiments that used the three fuels in *Table 1*, two sets of experiments were conducted to study more diverse sets of fuels. Heneghan *et al.*[11] studied the base fuels plus three JP-8 fuels, a JP-7 fuel and a surrogate JP-8 fuel (JP-8S). Using a Fourier transform infrared (FT-i.r.) spectroscopic probe, they measured the concentration of alcohols and ketones to estimate the amount of oxidation, and also gravimetrically determined the amount of filterable solids. Hardy *et al.*[9] studied F-2747, F-2827 (D. L. Hardy, personal communication) and 13 additional JP-5 fuels. They measured the amount of deposit by weighing a metal strip from a flowing system, and separately measured the 'peroxide potential' (the sum of the peroxide numbers determined by titration after 24, 48, 72 and 96 h).

Thermal stability of base fuels

The expected order of relative thermal stability of the base fuels is F-2799 > F-2747 > F-2827. This expectation is based on the heteroatom concentration, boiling range, past experience with hydrotreated fuels and the fact that F-2799 is a special thermally stable fuel that includes a thermal-stability additive package (JFA-5). The order of thermal stability was verified by the JFTOT breakpoint (*Table 1*). JFTOT breakpoint values were verified by Biddle *et al.*[12]. The relative thermal stability of these three fuels has also been established in several flowing systems, including single-pass heat exchangers[10], multipass heat exchangers[17], hot liquid process simulators[12], a microthermal precipitation test[12], a gravimetric determination in a flowing system[9] and a vaporization deposition test at high temperatures[22]. Static tests, such as a microcarbon residue tester[23] and flask tests[11,18], have also been used to study the relative thermal stability of the three fuels. The flowing and static tests agree well with the JFTOT breakpoint in indicating that the thermal stability of the baseline fuels decreases in the expected order. A summary of these measurements is given in *Table 2*. Note that less deposit indicates greater thermal stability, as does a higher breakpoint temperature.

Oxidative stability of base fuels

Originally it was believed[13] that the more thermally stable fuels would oxidize less easily. The first indication that this supposition was not accurate came from the Phoenix rig[10]. With a dissolved oxygen analyser[19], a plot of bulk fuel temperature versus dissolved oxygen concentration showed that the order of oxidation resistance was the reverse of that of thermal stability (*Figure 1*). A lower temperature for the disappearance of dissolved oxygen indicates a more easily oxidized fuel. *Figure 1* also shows that methane appears at approximately the same temperature as oxygen disappears. As will be shown later, this lends strong support to the theory that free radicals are involved in the deposition–oxygen-consumption process.

The shape of the oxygen consumption curve was originally accounted for by assuming a first-order oxygen-dependence[10]. Jones *et al.*[20] have recently measured oxygen disappearance in F-2827 in an essentially isothermal flowing reactor. The data are consistent with a strongly terminated autoxidation with autoacceleration due to peroxide decomposition. The result is a good fit to zero-order oxygen-dependence and a first-order peroxide decomposition as the initiation step.

Table 2 Results of thermal stability tests on the baseline fuels

	F-2799	F-2747	F-2827
Phoenix rig (μg deposit)[10]	300	450	2800
Multipass heat exchanger (μg cm^2 h^{-1} deposit)[17]	56	348	2250
Hot liquid process simulator (mg cm^{-2} deposit)[12]	3	8	152
Microthermal precipitation (μg deposit/50 ml)[12]	2818	4438	7162
JFTOT breakpoint (°C)[13]	399	332	266
Total insolubles in gravimetric JFTOT (ppm)[9]	not measured	0.2	0.8
Microcarbon residue test (wt%)[23]	0.11	0.10	0.46
Flask test (mg)[11,18]	0	2	7
Vaporization deposition (μg)[22]	1183	875	4703

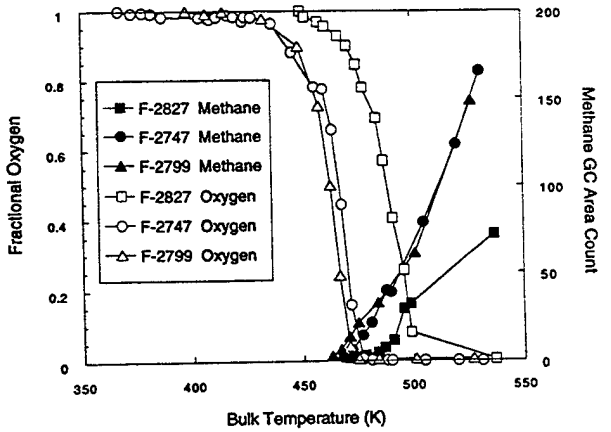

Figure 1 Dissolved oxygen and methane concentrations versus output bulk temperature from a single-tube heat exchanger. Input temperature 30°C; input oxygen concentration 50 ppm; residence time in heat exchanger 6.3 s (from Ref. 10)

Table 3 Results of oxidative stability tests on the baseline fuels

	F-2799	F-2747	F-2827
Peroxide potential (ppm)[9]	not measured	46	2
Onset of oxidation exotherm from d.s.c. (°C)[12]	189	198	206
Temperature (°C) for 50% oxygen depletion in Phoenix rig[10]	185	190	215
Total acid number[23]	3.54	2.27	0
Total concentration of alcohols, ketones and acids (mol l^{-1})[11]	0.6	1.8	0.03

The observation that the more thermally stable fuels (F-2799 and F-2747) were more easily oxidized was verified in flask tests at 180°C with bubbling oxygen. The relative amounts of oxidative products were measured using FT-i.r., gas chromatography with atomic emission and oxygen flame ionization detection, high-performance liquid chromatography with dielectric constant detection, and gravimetric techniques[11,13]. The availability of oxygen was found to increase significantly the amount of deposit from F-2747. However, most (>98%) of these deposits were soluble in acetone or methanol. If only those deposits insoluble in hexane and acetone or methanol were considered, the ranking of thermal stability was independent of oxygen availability. These additional deposit materials also proved to be rich in oxygen, whereas those deposits made in F-2827 showed almost no absorption in the carbonyl stretch region of the infrared[13]. This was taken as further evidence that the thermally stable fuels reacted easily with oxygen.

The amount of oxidation was also studied in three additional separate static tests. First, in a flask test, the fuels were heated (175°C) in a flask with bubbling oxygen for 2 h. The three test fuels were studied by FT-i.r.[11] to determine the concentration of ketones, alcohols and acids. Second, two of the baseline fuels were studied in an accelerated storage stability test at 100°C and 0.34 MPa oxygen[9], to measure the peroxide potential. Third, the total acid number[23] was determined after the fuels were heated with bubbling air at 180°C for 5 h. Since these techniques measure the appearance of oxidized products, larger values indicate more oxidation.

Differential scanning calorimetry (d.s.c.)[12] was used to determine the onset temperature for the oxidation exotherm. The Phoenix rig also measures the temperature at which these fuels consume oxygen, as shown in *Figure 1*. These two tests heat the fuels at different rates, so the temperatures should not be expected to agree. However, the trend for the baseline fuels should be the same: the d.s.c. technique and the Phoenix rig should give lower temperatures for fuels that are more easily oxidized. Finally, a cyclic voltammetry technique[21] was used to evaluate the appearance of oxidation products in flask tests.

These tests all showed that the hydrotreated fuels oxidized at lower temperatures or to a greater extent than the non-hydrotreated fuel (F-2827). Some discrepancies in the oxidation of F-2799 may be due to the relative effectiveness of antioxidants in JPTS and the hydrotreated F-2747. The quantitative results are summarized in *Table 3*.

These recent experiments clearly show that the order of thermal stability of the three baseline fuels is F-2799 > F-2747 > F-2827. This order has been established by seven quantitative techniques. Although two techniques show F-2747 slightly better than F-2799, all agree in showing that F-2827 is the least thermally stable. These same fuels show the reverse order of oxidative stability, as demonstrated by four quantitative techniques. Again, although one test shows F-2747 more easily oxidized than F-2799, all five techniques show that F-2827 is the most oxidatively stable.

Just as clearly, however, three fuels do not represent the entire range of fuels. Hardy *et al.*[9] measured the peroxide potential and the gravimetric JFTOT deposits for 13 JP-5 fuels as well as two of the baseline fuels. The results are shown in *Figure 2*. Heneghan *et al.*[11] studied seven fuels (including a JP-7, two JP-8s and JP-8S); their results are shown in *Figure 3*. Two fuels seem to deviate from the inverse relation: F-2799 (which gave the least deposit) and JP-8S (the most deposit). However, as noted previously, the discrepancies may be due to the relative effectiveness of antioxidants added to JPTS, JP-7 and F-2747, or to the dispersant and metal deactivator that are part of the thermal-stability additive package (JFA-5) in JPTS. Also, JP-8S is not really a fuel, so its inclusion may not be totally appropriate.

Despite some small discrepancies, the data show a clear trend. As expected, the hydrotreated fuels (F-2799 and F-2747) are significantly more thermally stable than F-2827 when deposition tendency is considered as the stability criterion. However, the trend is strong and unexpectedly reversed for oxidative stability. As shown in *Figures 2* and *3*, the inverse relation between oxidative and thermal stability holds for a large number of fuels.

THEORETICAL ANALYSIS

A detailed examination of the mechanism of chain-breaking antioxidants can provide an interesting view of

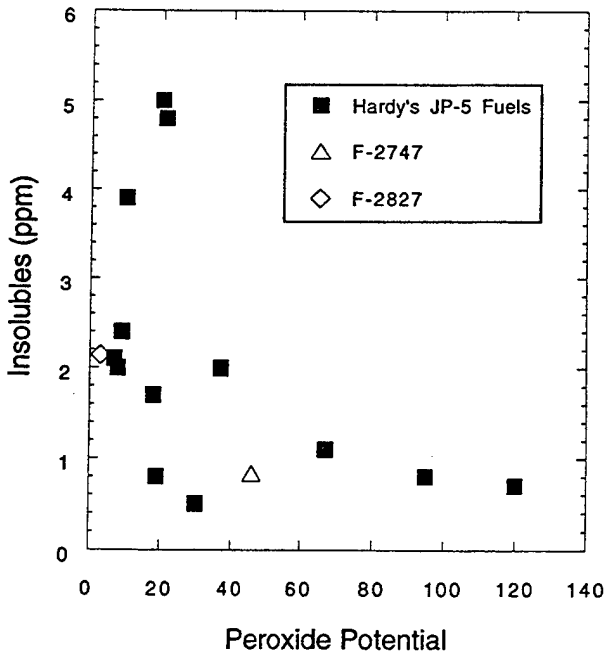

Figure 2 Peroxide potential versus gravimetric JFTOT of 15 fuels (from Ref. 9 and D. L. Hardy, personal communication)

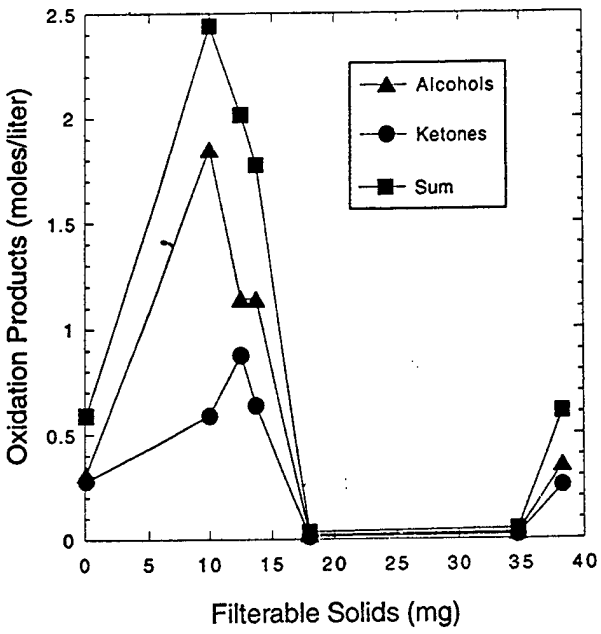

Figure 3 Concentration of alcohols and ketones versus filterable solids (from Ref. 11)

the structure of jet fuels. It also accounts for the apparent anomaly represented by the inverse relation between the stabilities as measured by oxidation and by deposit formation. A review of the theory of oxidation and antioxidants will help to explain some previous kinetic data and present a new idea concerning the source of the deposit. The mechanism of oxidation has been kept as simple as possible in order to convey the concept of how some molecules could act as antioxidants. The actual mechanism of autoxidation, including possible initiation sources and back-reactions, is significantly more complicated.

Consider a chain-breaking mechanism, starting with the basic chemistry of the autoxidation chain reaction[24]. First, consider a single compound, RH:

initiation	Formation of $R^{\cdot}$	(A)
propagation	$R^{\cdot}+O_2 \rightarrow RO_2^{\cdot}$	(B)
	$RO_2^{\cdot}+RH \rightarrow RO_2H+R^{\cdot}$	(C)
termination	$RO_2^{\cdot}+RO_2^{\cdot} \rightarrow$ products	(D)

Reaction (D), termination, has been written as the recombination of $RO_2^{\cdot}$ rather than the $R^{\cdot}$ because reaction (B) proceeds with no activation energy, whereas reaction (C) has a significant activation energy for most hydrocarbons[25]. Therefore reaction (C) is the slow step and $RO_2^{\cdot}$ is the major radical species. A hydrocarbon is easily oxidized if reaction (C) proceeds with a small activation energy. This requires a weak carbon–hydrogen bond[25].

The concentration of radicals can then be calculated by Equations (1)–(3) on the assumption that the concentrations of $R^{\cdot}$ and $RO_2^{\cdot}$ radicals are constant in time; R_i is the rate of formation of radicals in the initiation reaction (A). This is known as the stationary-state hypothesis (SSH)[26].

$$d[R^{\cdot}]/dt = R_i - k_B[R^{\cdot}][O_2] + k_C[RO_2^{\cdot}][RH] = 0 \quad (1)$$

$$d[RO_2^{\cdot}]/dt = k_B[R^{\cdot}][O_2] - k_C[RO_2^{\cdot}][RH] - 2k_D[RO_2^{\cdot}]^2 = 0 \quad (2)$$

$$[RO_2^{\cdot}] = (R_i/2k_D)^{0.5} \quad (3)$$

Using the concentration of $RO_2^{\cdot}$ from Equation (3) and the steady-state Equation (1), the rate of oxygen consumption can be written

$$-\frac{d[O_2]}{dt} = k_B[R^{\cdot}][O_2] = R_i + k_C[RO_2^{\cdot}][RH]$$
$$= R_i + k_C(R_i/2k_D)^{0.5}[RH]$$
$$\approx k_C(R_i/2k_D)^{0.5}[RH] \quad (4)$$

Therefore the peroxidation of hydrocarbons by the chain mechanism proceeds without any dependence on the oxygen concentration. This of course can be true only for situations in which sufficient oxygen is available. In flowing tests, the amount of oxygen available is limited to that dissolved in the fuel at the beginning of the transit past the heated section (~75 ppmw)[27]. Consequently it should not be surprising to find an oxygen-dependence in these cases. Further, as the oxygen is removed, $RO_2^{\cdot}$ can no longer be the major radical. As will be seen later, the buildup of $R^{\cdot}$ radicals is responsible for the appearance of methane in the Phoenix rig at the same time or temperature as the oxygen is consumed.

Now a chain-breaking antioxidant, AH, can be added to this chain mechanism. The antioxidant operates by the transfer reaction (Ct), thus removing the chain-carrying radical $RO_2^{\cdot}$, from the autoxidation process:

$$RO_2^{\cdot}+AH \rightarrow RO_2H+A^{\cdot} \quad (Ct)$$

To be effective, the new radical formed, $A^{\cdot}$, must not propagate the chain. This is easily accomplished if reaction (Ct) is significantly exothermic, implying that the AH bond strength is weak compared with RH. This prevents $A^{\cdot}$ from regenerating the $R^{\cdot}$ radical and continuing the chain. However, it is also possible that some of the $A^{\cdot}$ radicals could combine with oxygen, producing $AO_2^{\cdot}$ peroxy radical as in reaction (B′). In this case, reaction (Ct′) must progress very slowly so that the chain propagation, reactions (B) and (C), is effectively terminated by (Ct):

$$A^{\cdot}+O_2 \rightarrow AO_2^{\cdot} \quad (B')$$

$$AO_2^{\cdot}+RH \rightarrow AO_2H+R^{\cdot} \quad (Ct')$$

It is generally argued that the activation energy for hydrogen atom abstraction by peroxy radicals, as in reaction (Ct′), depends on the carbon–hydrogen bond strength in RH, and not on the stability of the underlying radical of the peroxy radical, $A^{\cdot}$. This would seem to indicate that the activation energy of reaction (Ct′) is not significantly different from that of reaction (C), and therefore the radical formed in reaction (B′) would then be capable of regenerating the original chain.

There are three possible reasons for reaction (Ct′) to be significantly slower than reaction (B). The first is that there is steric hindrance, which would lower the pre-exponential factor for the reaction. The second, as postulated here, is that there is stabilization across the O–O bond for some radicals, and that the activation energy is increased. The third is that there may be a unimolecular rearrangement of the $AO_2^{\cdot}$ radical after formation. It is of course possible that the $A^{\cdot}$ radicals do not add oxygen.

The radicals formed in reactions (B') or (Ct) are then consumed in the major termination reaction (D'):

$$\left.\begin{array}{l} AO_2^{\cdot} + AO_2^{\cdot} \rightarrow \text{products} \\ \text{or} \\ A^{\cdot} + A^{\cdot} \rightarrow \text{products} \end{array}\right\} \quad (D')$$

It is reaction (D'), and in particular the $AO_2^{\cdot}$ termination product that is proposed as the major oxidative pathway to the formation of insoluble products. The rationale for the selection of this reaction, and its implications, are discussed later.

For reaction (Ct) to terminate the chain reaction effectively, it must compete with reaction (C) by being about as fast as or faster than the latter, i.e.

$$k_C[RH][RO_2^{\cdot}] < k_{Ct}[AH][RO_2^{\cdot}] \quad (5)$$

To maintain this inequality, k_{Ct}/k_C must exceed the ratio [RH]/[AH]. Assuming Arrhenius behaviour of the rate constants, and ignoring possible differences in the pre-exponential factor, the concentration of AH required to act as an antioxidant for the compound RH can be determined from the difference in the activation energies for reactions (C) and (Ct), Equation (6). For example, if the difference in E_a is $\sim 23\ kJ\ mol^{-1}$ at room temperature, AH must be added at ~ 100 ppm (at room temperature). Obviously if the hydrogen atom in AH is more easily abstracted in (Ct), an even smaller concentration of AH can be effective.

$$10^{(E_{aCt}-E_{aC})/\Theta} < \frac{[AH]}{[RH]} \quad (6)$$

where $\Theta = 2.3RT$

One additional consideration is that AH may oxidize in its own chain to consume oxygen, as shown in reactions (B') and (C'):

$$AO_2^{\cdot} + AH \rightarrow AO_2H + A^{\cdot} \quad (C')$$

However, in analogy to Equation (4), Equation (7) shows that the rate of oxygen consumption will decrease with ever-decreasing concentrations of AH:

$$-d[O_2]/dt = -d[AH]/dt = k_{C'}[AO_2^{\cdot}][AH]$$
$$= k_{C'}(R_i/2k_{D'})^{0.5}[AH] \quad (7)$$

Further, in a fully quenched system (one in which reaction (Ct) dominates (C)), the concentration of $RO_2^{\cdot}$ can be found from Equation (8). This equation assumes that reaction (Ct) is the only consumption path for the $RO_2^{\cdot}$ radical, that is, both k_C and k_D are zero. The consumption of oxygen is shown in Equation (9).

$$\frac{d[RO_2^{\cdot}]}{dt} = k_B[R^{\cdot}][O_2] - k_{Ct}[AH][RO_2^{\cdot}]$$
$$= R_i - k_{Ct}[AH][RO_2^{\cdot}] = 0 \quad (8)$$

$$-d[O_2]/dt = R_i + k_C[RO_2][RH] = R_i + \frac{k_C[RH]}{k_{Ct}[AH]}R_i \quad (9)$$

The importance of the relative rates of reactions (C) and (Ct) can be more easily appreciated in a more generalized view of the rate-law solution. A general solution for the autoxidation mechanism with inhibition by AH can be derived by using only reactions (A), initiation, (B) and (C), chain propagation, (Ct), chain termination by transfer to A', and (D), chain termination by radical recombination. Again assuming the SSH, ($d[RO_2^{\cdot}]/dt$ and $d[R^{\cdot}]/dt$ equal 0), Equations (10) and (11) can be derived for the steady state $[R^{\cdot}]$ and $[RO_2^{\cdot}]$. The solution to these equations for $[RO_2^{\cdot}]$ involves a quadratic equation. The general solution is shown in Equation (12).

$$d[RO_2^{\cdot}]/dt = k_B[R^{\cdot}][O_2] - k_C[RO_2^{\cdot}][RH]$$
$$- k_{Ct}[RO_2^{\cdot}][AH] - 2k_D[RO_2^{\cdot}]^2 \quad (10)$$

$$d[R^{\cdot}]/dt = R_i - k_B[R^{\cdot}][O_2] + k_C[RO_2^{\cdot}][RH] \quad (11)$$

$$[RO_2^{\cdot}] = \frac{k_{Ct}[AH] \pm \sqrt{\{k_{Ct}^2[AH]^2 + 8k_DR_i\}}}{-4k_D} \quad (12)$$

There are two interesting limits to this problem: $k_{Ct}[AH] = 0$, and $k_{Ct}^2[AH]^2 \gg k_DR_i$. The first implies that the termination step of the $RO_2^{\cdot}$ radical is reaction (D). The second implies that $k_{Ct}[AH] \gg k_D[RO_2^{\cdot}]$ (since $R_i > k_D[RO_2^{\cdot}]^2$; R_i must be greater than the rate of any individual termination step), and that the termination of the $RO_2^{\cdot}$ radical is significantly quicker through the transfer reaction (Ct) thus diminishing $[RO_2^{\cdot}]$.

The limiting solutions for the first case ($k_{Ct}[AH] = 0$) can be simply determined. Note that it is the negative square root that yields a real result for $[RO_2^{\cdot}]$ in Equation (12). This case simplifies to the uninhibited autoxidation as shown in Equation (13) (which is identical to Equation (4):

$$-\frac{d[O_2]}{dt} = k_B[R^{\cdot}][O_2] = R_i + k_C[RO_2^{\cdot}][RH]$$
$$= R_i + k_C\frac{\sqrt{(8k_DR_i)}}{4k_D}[RH]$$
$$= R_i + k_C\sqrt{(R_i/2k_D)}[RH] \quad (13)$$

The second case, $k_{Ct}^2[AH]^2 \gg k_DR_i$, is more complicated. However, a first-order binomial expansion solution ($\sqrt{(a^2+b)} \approx a + b/2a$) to Equation (10) yields $[RO_2^{\cdot}]$ in Equation (14). Note that, as in the first case, the negative square root is used. Upon inserting $[RO_2^{\cdot}]$ into $d[O_2]/dt$ and using Equation (11), the result, Equation (15), corresponding to Equation (9) is obtained:

$$[RO_2^{\cdot}] = \frac{k_{Ct}[AH] - \sqrt{(k_{Ct}^2[AH]^2 + 8k_DR_i)}}{-4k_D}$$
$$= \frac{4k_DR_i/k_{Ct}[AH]}{4k_D} = \frac{R_i}{k_{Ct}[AH]} \quad (14)$$

$$-\frac{d[O_2]}{dt} = k_B[R^{\cdot}][O_2] = k_C[RO_2^{\cdot}][RH] + R_i$$
$$= \frac{k_C[RH]}{k_{Ct}[AH]}R_i + R_i \quad (15)$$

The increasing value of $k_{Ct}[AH]$ results in an apparent change in the mechanism from a chain autoxidation to an inhibited oxidation. The apparent order-dependence varies from half-order in the initiation rate to first-order. The overall dependence on oxygen then depends on the initiation-rate-dependence on oxygen. The initiation rate in the preliminary stages depends on both oxygen and hydrocarbon[28]. Therefore in the early stages it is likely to have either a half-order or a first-order oxygen-dependence. In the later stages it is possible to observe zero-, half- or even first-order oxygen-dependence. The

observed order for oxygen depends on $k_{Ct}[AH]$ relative to $k_D[RO_2^{\cdot}]$ and the order of the initiation reactions.

This analysis shows that the addition of a small amount of an easily oxidized material can interfere with the major chain autoxidation mechanism, transferring the radical to a chain which may have faster rate constants but significantly lower concentration. The result is that the rate of oxidation decreases, despite the addition of easily oxidized compounds.

It can be concluded that if the assumptions concerning the rate of reaction (C') are true, then any molecule with a labile (easily removed) hydrogen can act like an antioxidant, if it has sufficient concentration so that reaction (Ct) competes with reaction (C), yet its concentration is small enough for the autoxidation rate from Equation (7) to be less than that from Equation (4). Interestingly, molecules with labile hydrogens typically have less activation energy for reaction (C) or (C'); thus they are more easily oxidized. This leads to the conclusion that adding a small amount of easily oxidized material to alkanes will decrease the rate of oxygen consumption, not increase it.

It is also important to note that the oxidation of a hydrocarbon system can proceed through a free-radical mechanism and yield a rate law which has zero-, half- or first-order dependence on the oxygen concentration. The exact dependence will depend on the nature of the initiation reactions (whether these reactions depend on oxygen), on the reactivity and quantity of antioxidants, and on the availability of oxygen. Other proposed radical mechanisms also show fractional-order dependences[29]. It is unwise to try to infer mechanisms from rate laws; however, rate laws can be derived from mechanisms, and an oxygen–hydrocarbon system with a good antioxidant could easily exhibit first-order dependence on the concentration of oxygen molecules for the formation of peroxides.

DISCUSSION

Mechanism of deposit formation

The present observations have not disagreed with any previous ones, but rather add to them. Hazlett[5] listed three key criteria for deposit formation that any proposed mechanism must meet:

1. dissolved oxygen initiates the process;
2. heteroatom-containing molecules should play an important role;
3. only a small amount of the fuel is involved in the deposit formation process.

The proposed mechanism meets these criteria. As a result of the authors' recent experiments, a fourth criterion is added:

4. the mechanism must account for the inverse relation between the ease of oxidation and the formation of deposits.

Clark and Smith[2] proposed a simplified two-step model. The first step is the production of peroxides and other oxidized intermediate materials. In the second step, these products react with sulfur- and nitrogen-containing compounds to form deposit materials. Taylor and Frankenfeld[6] proposed a mechanism in which the first step is the reaction of a sulfur- and nitrogen-containing compound with dissolved oxygen. These reaction products then oxidize further to form insoluble materials. These two schemes differ only in that the latter proposes oxidation in both steps. The former mechanism implies that fuels that form more oxidized product in the first step would form more deposit material in the second step. This clearly differs with the authors' observations (criterion 4). This is not necessarily the case in the Taylor–Frankenfeld mechanism, since other oxidation pathways are not ruled out. However, the inverse behaviour of oxidation with respect to deposit formation does not necessarily follow from that mechanism.

Oxygen consumption

The conclusion concerning the behaviour of easily oxidized materials added to alkanes can be used to explain many previous observations. In particular, it can be used to explain the rate-law behaviour of *n*-dodecane oxidations, the apparent antioxidant capability of dimethylpyrrole (DMP)[30], and several other previously measured oxidation rates for binary mixtures[14,15,30].

While studying DMP in *n*-dodecane, Beaver[30] noted that the deposit formed appeared to be oxidized DMP, while the rate law was first-order in oxygen. He proposed an electron transfer initiated oxidation (ETIO) mechanism to account for the observations[31]. In the ETIO mechanism, DMP reacts with oxygen molecules. The antioxidant capability observed by Reddy *et al.*[15] is explained by assuming the DMP is in competition with *n*-dodecane for the limited amount of oxygen available in the flowing JFTOT. Since the DMP is easily oxidized, it would preferentially acquire the oxygen, leave solution, and not be analysed (only soluble oxidation products were analysed)[15]. If this were the case, the addition of DMP to *n*-dodecane would (a) increase the rate of oxygen consumption and (b) lower the temperature at which the oxygen reacted in the JFTOT test section.

Neither of the last two effects has been studied, but several similar cases would indicate that neither is true. Hazlett[3] used a modified JFTOT to find the tube temperature at which half the dissolved oxygen would react. None of the compounds that he added to *n*-dodecane caused the oxygen to be consumed at a lower tube temperature, and several (e.g. fluorene, idene, triphenylmethane) increased the consumption temperature by $\geqslant 30$ K. Mayo and Lan[14] measured the amount of oxygen consumed versus time in *n*-dodecane oxidation. The addition of *N*-methylpyrrole resulted in a decrease in the amount of oxidation, not an increase. The test method used by Mayo and Lan would not have been deceived by oxidative deposit formation, since the disappearance of oxygen was measured, rather than the appearance of soluble oxidation products.

The free-radical mechanism can account for the appearance of oxidized DMP, the antioxidant characteristic of DMP, and the apparent first-order dependence on oxygen molecules. There seems to be little evidence that the mechanisms are not free-radical in nature. Further evidence that the oxidation reactions are free-radical is presented below, in the discussion of methane production.

The addition of a more easily oxidized compound to a less easily oxidized compound decreases the oxidation rate. This was seen by Russel[32] in a cumene–tetralin system, Mayo and Lan[14] in indene–*n*-dodecane and *N*-methylpyrrole–*n*-dodecane systems, and Reddy *et al.*[15]

Table 4 Types of molecule present in fuels, and bond dissociation energies (BDE)

Type	Bond	BDE (kJ mol^{-1})[a]
Alkenes	R=R-R—H	365
Substituted benzenes	Φ-C—H	335–355
Thiols	R-S—H	355
Pyrroles	Φ_N-R—H	335–355
Alkanes	R—H	410

[a] Estimated by the methods of Ref. 33

in DMP–*n*-dodecane. Further, Mayo and Lan[14] noted that the continuing increase in concentration of the easily oxidized compounds resulted in steadily increasing oxidation rates, until these compounds finally surpassed the original alkane in concentration. The theory of autoxidation presented here can account for each of these observations.

Examination of compounds likely to be present in a fuel reveals something about the origin of deposit materials. *Table 4* shows possible molecules and the strengths of the weakest bonds. The bond strength of a normal alkane is also shown for comparison. Recall that the ease of oxidation of a compound is inversely related to the bond strength of the most weakly bound hydrogen. In the proposed oxidation scheme, each type of molecule listed could act as an antioxidant if present in the correct quantity. Each is present in fuels—in only small quantities—and, interestingly, each has been implicated in the formation of deposits. If the precursor to deposits is considered to be the $AO_2^{\cdot}$ radical, this mechanism explains the observation that easily oxidized materials are inherently stable whereas unstable materials are difficult to oxidize. Further, the molecules are also rich in heteroatoms; this indicates that deposits should be rich in hereroatoms. Finally, the removal of oxygen would limit the formation of $AO_2^{\cdot}$ and thus the amount of deposit formed.

It is proposed that natural occurring molecules with weakly bound hydrogens in fuels are responsible for the formation of deposits. However, while they are oxidizing to form deposits, they are also acting as chain-breaking antioxidants, thus slowing the overall rate of oxygen consumption. This dual action of these antioxidant compounds is the reason for the seemingly conflicting result that although oxygen is necessary for the formation of deposits, the easier it is to oxidize a fuel, the more stable it is likely to be.

The proposed mechanism accounts for each of Hazlett's[5] three key criteria:

1. if oxygen is removed from the system, reaction (B′) cannot proceed and the precursors ($AO_2^{\cdot}$) to the formation of deposits are eliminated;
2. since A$^{\cdot}$ is formed from a molecule with a labile hydrogen (see *Table 4*), it is likely to be rich in heteroatoms, as is the $AO_2^{\cdot}$ radical and the resulting insoluble products;
3. only a small fraction of the fuel molecules is oxidized, and in only a small fraction of those oxidized is the process terminated by reactions leading to insoluble products.

This proposed mechanism, together with an understanding of the makeup of fuels, accounts for the observed fourth key criterion:

4. the observed inverse behaviour of oxidation with respect to deposit formation should be expected, if not required.

It should be noted that the formation of insolubles depends not only on the chemical nature of the trace molecules involved in the oxidation process but also on the solubility of the resulting products. This may account for the observation that some fuels do not oxidize easily, yet do not form solid deposits.

Deposit formation does not follow oxidation; this has been observed and commented on previously[5,7] and, in fact, several of the concepts described herein have already been recognized. It has been noted that the presence of some heteroatoms is responsible for increased deposit formation and that their removal increases both the thermal stability[6] and susceptibility to oxidation[5,34] of jet fuels. As early as 1963 it was recognized that hydrotreating removed some of the natural antioxidants from jet fuels. Consequently, antioxidant additives have been specified in UK and US military specifications DERD-2494 (1963) and MIL-T-5624 (modified 1976) for addition to hydrotreated fuels.

Mechanism of methane formation

The free-radical nature of the chemical reactions is supported further by the appearance of methane in the Phoenix rig. Methane was produced in the Phoenix rig at temperatures near 500 K (see *Figure 1*), and only when the oxygen was largely removed. It is reasonable to expect that methane is the result of methyl radical production arising from the unimolecular fission of larger alkyl radicals to form methyl and alkenes:

$$R^{\cdot} \rightarrow R'{=}CH_2 + CH_3^{\cdot} \qquad (E)$$

where $R'{=}CH_2$ is the resulting alkene, containing one less carbon than the original R$^{\cdot}$ radical. This process is normally associated with short hydrocarbons. Although there is a dearth of these compounds in jet fuels, there is usually a significant quantity of compounds with short active hydrocarbons. The simplest source would be ethyl- or propylbenzene.

The appearance of methane only after significant diminution of the oxygen concentration is consistent with a free-radical mechanism, as shown by the competing reactions, (F) and (G), and their respective rate equations, (16) and (17). Reaction (F) has the advantage of no activation energy and high pre-exponential factor. However, it suffers from a small and decreasing concentration of oxygen. As the concentration of oxygen decreases, reaction (G) will dominate, and methane will appear.

$$CH_3^{\cdot} + O_2 \rightarrow CH_3O_2^{\cdot} \qquad (F)$$

$$R_F = -d[CH_3^{\cdot}]/dt = A_F \exp(-E_F/RT)[CH_3^{\cdot}][O_2] \qquad (16)$$

$$CH_3^{\cdot} + RH \rightarrow CH_4 + R^{\cdot} \qquad (G)$$

$$R_G = -d[CH_3^{\cdot}]/dt = A_G \exp(-E_G/RT)[CH_3^{\cdot}][RH] \qquad (17)$$

If we assume that the pre-exponential factors A_F and A_G are nearly equal, and reaction (F) competes evenly with (G) (i.e. $R_F = R_G$) at an oxygen concentration of 25 ppmw and a temperature of 500 K, E_G can be expressed as

$$E_G = -RT \ln([O_2]/[RH]) = 44.4 \text{ kJ mol}^{-1} \qquad (18)$$

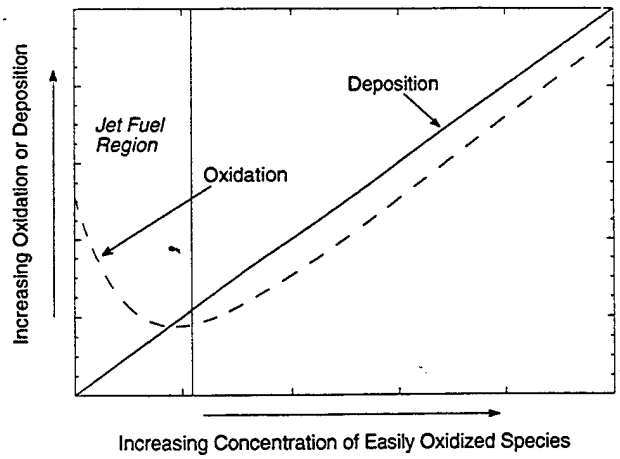

Figure 4 Qualitative behaviour of fuel oxidative and thermal stability with increasing concentration of easily oxidized species

This global activation energy is very reasonable for this type of reaction. For comparison, if RH is ethane, the activation energy is expected[33] to be 45.2 kJ mol^{-1} and larger alkanes would not be expected to show a significant change in activation energy. This does not prove that methane is the result of free-radical reactions; however, it shows that the assumption of a free-radical mechanism is a reasonable and self-consistent explanation which yields expected kinetic parameters.

IMPLICATIONS

Jet fuel oxidation results in the build-up of peroxides, ketones, aldehydes, alcohols and acids from the autoxidation cycle, sulfates, sulfones and nitrous compounds from the inhibitors originally present, and alkenes from the decomposition of radicals. Many of these oxidized compounds can, if present in sufficient quantity, inhibit fuel oxidation. That is, fuels will exhibit self-inhibition towards oxidation over time. However, the inability to oxidize is closely linked to the tendency to form deposits. Therefore, evaluation of jet fuel performance under accelerated conditions with excess oxygen may yield results that are not indicative of fuel quality.

The oxidative stability of a fuel is related to the availability of easily oxidized compounds. Interestingly, the addition of a small amount of easily oxidized compound will have an inhibiting effect on the overall oxidation rate. However, if sufficient quantities of the easily oxidized compound are available, the compound will help stimulate oxidation. The production of solids is strongly and positively affected by the presence of easily oxidized materials. A qualitative picture of the behaviour of both oxidizability and deposit formation is shown in *Figure 4* for increasing amounts of easily oxidized material in the fuel. Ease of oxidation decreases as concentration increases; however, it must eventually increase, causing a minimum in the oxidation curve. The deposit formation rate should steadily increase with increasing concentration. Note that the region for jet fuels is shown, where these two measures of stability move inverse to each other. Identification of this region is empirical. Other types of fuel may not behave in this manner because they may lie in a different region of the graph. Also, a jet fuel may yet be tested which does not fall in the indicated region.

The above implies that there is an ideal amount of antioxidant that should be present in a jet fuel. Less than the ideal amount does not prevent oxidation, whereas too much can induce deposit formation. The formulation of antioxidants for addition to fuels should be based not only on their ability to act as antioxidants but also to ensure that the termination products of the antioxidant radical are soluble rather than insoluble.

A fuel is not a single compound but comprises a large variety of compounds and chemical structures. It is the variety of chemical structures, and the resulting range of hydrogen bond dissociation energies, not the range of boiling point, which are of interest, because different structures will have H atoms that are more or less accessible to the metathesis reactions (C) and (Ct) important in the autoxidation chain propagation. In general, regardless of the initiation step, the chain oxidation of RH will be terminated by reaction (Ct) if there are molecules with H atoms that can be easily abstracted in sufficient quantity (based on Equation (4)). However, the AH chain oxidation will continue unless the AH concentration is insufficient to maintain a separate autoxidation cycle.

CONCLUSIONS

Classification of fuel stability into thermal stability (based on deposit-forming tendency) and oxidative stability (based on ability to oxidize and form peroxides, ketones, alcohols and acids) leads to the seemingly anomalous statement that, fuels that oxidize easily are likely to be thermally stable, whereas fuels that are not thermally stable are not easily oxidized. This is found to hold, regardless of the fact that oxygen reaction with fuel is a necessary first step for the production of solid deposits.

A theoretical analysis of the autoxidation mechanism of hydrocarbons can account for the observed oxygen-dependences as well as all the other criteria needed for the deposit mechanism[5], if the peroxy radicals of the antioxidant molecules are the precursors to deposit formation. Analysis of the reactions also accounts for the appearance of methane in the Phoenix rig[10], the previously surprising result that addition of small amounts of easily oxidized compounds to alkanes causes a decrease in the oxidation rate rather than an increase[14,15,30], and the observed first-order rate dependence of oxygen uptake in doped-hydrocarbon systems[30]. All the data are consistent with a free-radical-inhibited autoxidation mechanism.

The number of key criteria listed by Hazlett[5], for which a deposit formation mechanism must account, should be increased from three to four, to include the inverse relation between oxidative stability and thermal stability.

The autoxidation mechanism is summarized as follows.

Autoxidation chain mechanism of alkanes

initiation	Formation of R$^\cdot$	(A)
propagation	$R^\cdot + O_2 \rightarrow RO_2^\cdot$	(B)
	$RO_2^\cdot + RH \rightarrow RO_2H + R^\cdot$	(C)
termination	$RO_2^\cdot + RO_2^\cdot \rightarrow$ products	(D)

Chain transfer reactions

	$RO_2^\cdot + AH \rightarrow RO_2H + A^\cdot$	(Ct)
	$AO_2^\cdot + RH \rightarrow AO_2H + R^\cdot$	(Ct')

Autoxidation of antioxidants

propagation $A^{\cdot} + O_2 \rightarrow AO_2^{\cdot}$ (B')

$AO_2^{\cdot} + AH \rightarrow AO_2H + A^{\cdot}$ (C')

termination $AO_2^{\cdot} + AO_2^{\cdot} \rightarrow$ products (D')

It is proposed that reaction (D') is the major production pathway for solids.

ACKNOWLEDGEMENT

This work was supported by the US Air Force Wright Laboratories, Wright–Patterson Air Force Base, Ohio, under Contract No. F33615-87-C-2767, with W. M. Roquemore serving as technical monitor.

REFERENCES

1 Bol'shakov, G. F. 'The Physico-Chemical Principles of the Formation of Deposits in Jet Fuels', US Air Force Translation FTD-MT-24-416-74, 1970

2 Clark, R. H. and Smith, L. in Proceedings of the 3rd International Conference on the Stability and Handling of Liquid Fuels, Institute of Petroleum, London, 1988, p. 268

3 Hazlett, R. N. in 'Frontiers of Free Radical Chemistry' (Ed. W. Pryor), Academic Press, New York, 1980, p. 195

4 Baker, C. E., Bittker, D. A., Cohen, S. M. and Seng, G. T. NASA Technical Memorandum TM-83420, 1983

5 Hazlett, R. N. 'Thermal Oxidation Stability of Aviation Turbine Fuels', ASTM, Philadelphia, PA, 1991

6 Taylor, W. F. and Frankenfeld, J. W. in Proceedings of the 2nd International Conference on Long-Term Storage Stabilities of Liquid Fuels, Southwest Research Institute, San Antonio, TX, 1986, p. 496

7 Hazlett, R. N. in 'Fouling of Heat Transfer Equipment' (Eds E. F. C. Somerseald and J. G. Knudsen), Hemisphere, Washington, DC, 1981, p. 501

8 Taylor, W. F. 'Jet Fuel Thermal Stability', NASA Technical Memorandum TM-79231, 1979

9 Hardy, D. R., Beal, E. J. and Burnett, J. C. in Proceedings of the 4th International Conference on Stability and Handling of Liquid Fuels, US Department of Energy, Washington, DC, 1991, p. 260

10 Heneghan, S. P., Williams, T. F., Martel, C. R. and Ballal, D. R. *J. Eng. Gas Turbines Power* in press

11 Heneghan, S. P., Locklear, S. L., Geiger, D. E., Anderson, S. D. and Schulz, W. D. *AIAA J. Propulsion Power* 1993, **9**, 5

12 Biddle, T. B., Hamilton, E. H. and Edwards, W. H. United Technologies Corporation R&D Status Report No. 13 to WL/POSF, Wright–Patterson Air Force Base, OH, 1991

13 Anderson, S. D., Edwards, J. T., Byrd, R. J., Biddle, T. B., Edwards, W. H., Martel, C. R., Williams, T. F., Pearce, J. A., Harrison, W. E. and Heneghan, S. P. ASTM Annual Meeting, Toronto, 1991

14 Mayo, F. R. and Lan, B. Y. *Ind. Eng. Chem. Prod. Res. Dev.* 1986, **25**, 333

15 Reddy, K. T., Cernansky, N. P. and Cohen, R. S. *J. Propulsion* 1989, **5**, 6

16 Heneghan, S. P. and Harrison, W. E. Paper no. PETR404 to Symposium: 'Structure of Jet Fuels III', American Chemical Society, San Francisco, 1992

17 Lefebvre, A. H., Chin, J. and Sun, F. Paper no. AIAA 92-0685 to 30th Aerospace Sciences Meeting, American Institute of Aeronautics and Astronautics, Reno, NV, 1992

18 Jones, E. G. and Balster, W. J. Paper no. 92-GT-122, International Gas Turbine Institute, Köln, 1992

19 Rubey, W. A., Striebich, R. C., Anderson, S. A., Tissandier, M. D. and Tirey, D. A. Paper no. PETR371 to Symposium: 'Structure of Jet Fuels III', Americal Chemical Society, San Francisco, 1992

20 Jones, E. G., Balster, W. J. and Post, M. E. Paper submitted to International Gas Turbine and Aeroengine Congress and Exposition, May 1993

21 Kauffman, R. E. and Tirey, D. A. Paper no. PETR412 to Symposium: 'Structure of Jet Fuels III', American Chemical Society, San Francisco, 1992

22 Edwards, J. T. Paper no. AIAA 92-0687 to 30th Aerospace Sciences Meeting, American Institute of Aeronautics and Astronautics, Reno, NV, 1992

23 University of Dayton. Final Report for Contract F-33615-C-2767 to WL/POSF, Wright–Patterson Air Force Base, OH, 1992

24 Nixon, A. C. in 'Autoxidation and Antioxidants' (Ed. W. O. Lundberg), Wiley, New York, 1962, p. 724

25 Benson, S. W. and Nangia, P. S. *Accts Chem. Res.* 1979, **12**, 223

26 Benson, S. W. 'The Foundation of Chemical Kinetics', McGraw-Hill, New York, 1960

27 Coordinating Research Council. CRC Report no. 530, Atlanta, GA, 1983

28 Emanuel, N. M. 'The Oxidation of Hydrocarbons in the Liquid Phase', Pergamon, Oxford, 1965

29 Baird, J. K. Paper no. PETR420 to Symposium: 'Structure of Jet Fuels III', American Chemical Society, San Francisco, 1992

30 Beaver, B. D., Hazlett, R. N., Cooney, J. V. and Watkins, J. M. *Fuel Sci. Technol. Int.* 1988, **6**, 131

31 Beaver, B. D. and Gilmore, C. *Fuel Sci. Technol. Int.* 1991, **9**, 811

32 Russel, G. A. *J. Am. Chem. Soc.* 1956, **78**, 1035

33 Benson, S. W. 'Thermochemical Kinetics', Wiley, New York, 1976

34 Coordinating Research Council. CRC Report no. 559, Atlanta, GA, 1988

Appendix B.

Chemical Kinetic Modeling of Jet Fuel Autoxidation and Antioxidant Chemistry

Steven Zabarnick
University of Dayton
300 College Park
Dayton, OH 45469-0140

Reprinted from I&EC RESEARCH, 1993, 32.

Chemical Kinetic Modeling of Jet Fuel Autoxidation and Antioxidant Chemistry

Steven Zabarnick†

Applied Physics Division, KL-463, University of Dayton Research Institute, 300 College Park, Dayton, Ohio 45469-0140

Chemical kinetic modeling has been performed in order to simulate the chemical processes that occur during the autoxidation of jet fuels at temperatures near 200 °C. Rate parameters are estimated for the elementary reactions that comprise the mechanism. The mechanism used treats the fuel and antioxidant species as single compounds. The model is able to reproduce the autoxidation chain mechanism that is responsible for oxygen removal in the fuel. The inhibition of oxygen removal by antioxidants is reproduced successfully by the model. Also, the model predicts that the thermal decomposition of alkyl hydroperoxides, even at very small conversions, can play a crucial role in the oxidation mechanism.

Introduction

Aircraft jet fuels are derived from a relatively high boiling range (e.g., 205–300 °C for JP-8) distillation of crude oil often referred to as the kerosene fraction (Martel, 1987). These fuels are composed primarily of alkanes and cycloalkanes, with aromatics limited to 25% by volume (for JP-8). Autoxidation chemistry occurs both upon fuel storage at ambient temperatures and upon exposure to high temperatures in fuel lines during flight time. This exposure to high temperatures or "thermal stressing" results in the formation of oxidized soluble and insoluble products. The build-up of insolubles in aircraft fuel systems is of great concern because of the resulting possibility of fuel system failure. Fuels which tend not to form these insolubles are often referred to as "thermally stable" fuels. As present and future military aircraft will be subject to greater heat loads due to higher air speeds, the thermal stability problem is receiving a great deal of study. The thermal stability of a fuel differs from its "oxidative stability"—oxidative stability refers to the rate at which oxygen is consumed and oxidative products are formed, while thermal stability refers only to the formation of solid deposits. Recent work has demonstrated an apparent inverse relationship between oxidative and thermal stability for a variety of jet fuels (Heneghan and Harrison, 1992; Heneghan et al., 1992; Heneghan and Zabarnick, 1993). Recently, Heneghan and Zabarnick (1993) have proposed a chemical kinetic mechanism that attempts to account for this inverse behavior and yields interesting conclusions about the mechanism of antioxidant chemistry. In this work we have attempted a more quantitative study of these chemical kinetic mechanisms. Rate constant parameters are estimated and numerical modeling of the mechanism is performed in order to better understand the role that autoxidation and antioxidants play in fuel chemistry and thermal stability.

Methodology

The chemical kinetics modeling was performed using the modeling package REACT (Whitbeck, 1990). REACT is a relatively simple code that integrates the multiple differential equations that result from a chemical kinetics mechanism and yields the species concentration profiles versus time. It does not solve the energy equation, and therefore does not include energy production or removal due to chemical reaction. The code was run on an HP 9000/730 Unix RISC workstation. The following is input to the code: reaction mechanism with rate constants, initial concentrations for each species present in the mechanism, reaction time and time intervals for output, and various tolerances for the precision of the computation. The code outputs the individual species concentrations at each time interval. The version of REACT used here did not have the ability to read in reaction Arrhenius parameters (i.e., *A*-factors and activation energies), so a Unix "awk" code was written that converts a text file with Arrhenius parameters to the proper format required for REACT at the supplied reaction temperature.

Jet fuels are composed of hundreds of compounds, with alkanes comprising a large fraction. Thus, it is impractical to attempt to model the chemical changes of all components of the mixture. In order to perform this study we have chosen to model the bulk fuel as a single compound, RH, which has the chemical properties of a straight-chain alkane, such as *n*-dodecane. This single compound "fuel" can also contain dissolved oxygen (O_2) and an antioxidant species (AH). Using the same formalism, Heneghan and Zabarnick (1993) have proposed the following mechanism for the autoxidation and antioxidant chemistry of jet fuels.

$$\text{formation of } R^{\bullet} \qquad \text{(a)}$$

$$R^{\bullet} + O_2 \Rightarrow RO_2^{\bullet} \qquad \text{(b)}$$

$$RO_2^{\bullet} + RH \Rightarrow RO_2H + R^{\bullet} \qquad \text{(c)}$$

$$RO_2^{\bullet} + RO_2^{\bullet} \Rightarrow \text{termination products} \qquad \text{(d)}$$

$$RO_2^{\bullet} + AH \Rightarrow RO_2H + A^{\bullet} \qquad \text{(e)}$$

$$AO_2^{\bullet} + RH \Rightarrow AO_2H + R^{\bullet} \qquad \text{(f)}$$

$$A^{\bullet} + O_2 \Rightarrow AO_2^{\bullet} \qquad \text{(g)}$$

$$AO_2^{\bullet} + AH \Rightarrow AO_2H + A^{\bullet} \qquad \text{(h)}$$

$$AO_2^{\bullet} + AO_2^{\bullet} \Rightarrow \text{products} \qquad \text{(i)}$$

$R^{\bullet}$ is a hydrocarbon alkyl radical species, RH represents the bulk fuel as a single hydrocarbon compound, AH is an antioxidant species (i.e., a species with an easily abstractable hydrogen atom, also referred to in the literature

† E-mail: zabarnic@udavxb.oca.udayton.edu.

0888-5885/93/2632-1012$04.00/

as an inhibitor (Nixon, 1962; Waters, 1964)), and O_2 represents the dissolved oxygen present in the liquid fuel. The alkyl radicals required to begin the mechanism are produced by an initiation step, reaction a. At present the reactions responsible for the initiation process in hydrocarbon oxidation are unknown. Emanuel et al. (1967) have concluded that the termolecular reaction,

$$2RH + O_2 \Rightarrow 2R^\bullet + H_2O_2$$

is primarily responsible for R• radical initiation in the low-temperature liquid-phase oxidation of hydrocarbons. A bimolecular reaction has also been proposed,

$$RH + O_2 \Rightarrow R^\bullet + HO_2^\bullet$$

Benson and Nangia (1979) have pointed out that both of these reactions are too slow to account for initiation at temperatures less than 450 °C (with the former reaction being even slower than the latter), and have instead proposed an ion-pair mechanism that may play a role in the initiation process.

Reaction b converts the R• radicals to $RO_2^\bullet$ radicals; this addition reaction is expected to have a near zero activation energy, and thus proceeds very rapidly. In reaction c, $RO_2^\bullet$ abstracts a hydrogen atom from a fuel molecule, generating a hydroperoxide, RO_2H, and another R• radical, thus propagating the chain. At sufficiently high temperatures, the hydroperoxide will decompose to yield the additional radicals, RO• + OH; we have included this pathway in the more complete mechanism discussed later. If the concentration of $RO_2^\bullet$ radicals is sufficient, the termination reaction, reaction d, can occur; this reaction can produce aldehydes, alcohols, and ketones, and regenerate oxygen by a disproportionation pathway. For ethylperoxy radicals, the reaction produces ethanol and acetaldehyde,

$$2C_2H_5O_2^\bullet \Rightarrow C_2H_5OH + C_2H_4O + O_2$$

These first four reactions (reactions a–d) constitute a simplified autoxidation mechanism for hydrocarbons in the liquid phase. We will demonstrate later through modeling that this mechanism displays the characteristics of a chain autoxidation.

The remaining reactions (e–i) include the chemistry of an antioxidant molecule. The antioxidant species, AH, acts primarily by competing with RH (see reaction e), the fuel molecules, for $RO_2^\bullet$, thus preventing the reformation of R• radicals, which propagate the chain after forming $RO_2^\bullet$. Reaction e generates a hydroperoxide and an antioxidant radical, A•. This antioxidant radical may react with oxygen (reaction g), in a similar manner to reaction b, generating a peroxy radical. This antioxidant peroxy radical can react with the fuel (reaction f), an antioxidant molecule (reaction h), or with another antioxidant peroxy radical (reaction i). Reaction f regenerates an R• radical; we will show that this is very undesirable for antioxidant chemistry. Reaction h produces another antioxidant radical. Reaction i produces products that have been proposed to be precursors to deposit formation in fuels (Heneghan and Zabarnick, 1993).

Table I lists the expanded reaction mechanism used for the modeling study of this paper. Reactions a–i above correspond directly to reactions 1–9 in Table I. We have added additional reactions to the above mechanism to take into account the thermal decomposition of alkyl hydroperoxides and the chemistry that occurs in the absence of oxygen. At the highest temperatures of this study (220 °C), thermal decomposition of the alkyl hydroperoxides are expected to contribute to the mechanism due to the weakness of the RO–OH bond, which is

Table I. Reaction Mechanism for Chemical Kinetic Modeling

reaction	Arrhenius *A*-factor (mol, L, and s)	activation energy (kcal/mol)	reaction no.
$I \Rightarrow R^\bullet$	1×10^{-1}	0.0	1
$R^\bullet + O_2 \Rightarrow RO_2^\bullet$	3×10^9	0.0	2
$RO_2^\bullet + RH \Rightarrow RO_2H + R^\bullet$	3×10^9	10.0	3
$RO_2^\bullet + RO_2^\bullet \Rightarrow$ termination	3×10^9	0.0	4
$RO_2^\bullet + AH \Rightarrow RO_2H + A^\bullet$	3×10^9	5.0	5
$AO_2^\bullet + RH \Rightarrow AO_2H + R^\bullet$	3×10^5	10.0	6
$A^\bullet + O_2 \Rightarrow AO_2^\bullet$	3×10^9	0.0	7
$AO_2^\bullet + AH \Rightarrow AO_2H + A^\bullet$	3×10^9	5.0	8
$AO_2^\bullet + AO_2^\bullet \Rightarrow$ products	3×10^9	0.0	9
$R^\bullet + R^\bullet \Rightarrow R_2$	3×10^9	0.0	10
$RO_2H \Rightarrow RO^\bullet + {}^\bullet OH$	1×10^{15}	42.0	11
$RO^\bullet + RH \Rightarrow ROH + R^\bullet$	3×10^9	10.0	12
$RO^\bullet \Rightarrow R_{prime}^\bullet$ + carbonyl	1×10^{16}	15.0	13
${}^\bullet OH + RH \Rightarrow H_2O + R^\bullet$	3×10^9	10.0	14
$RO^\bullet + RO^\bullet \Rightarrow RO^\bullet$ termination	3×10^9	0.0	15
$R_{prime}^\bullet + RH \Rightarrow$ alkane + $R^\bullet$	3×10^9	10.0	16

≈40 kcal/mol (Gray et al., 1967). We also wish to model the chemistry that occurs after the dissolved oxygen is consumed. Thus we need to include pathways that take into account reactions in the absence of dissolved oxygen.

Reaction 10 in Table I is necessary for conditions where oxygen has been consumed; the alkyl radicals can no longer react with oxygen to form peroxy radicals (reaction 2), but they now can recombine producing the dimeric species, R_2. These dimers have been observed in the autoxidation of octane and dodecane (Edwards and Zabarnick, 1992; Reddy et al., 1988). The cross-termination reaction, $R^\bullet + RO_2^\bullet \rightarrow$ ROOR, may also play a role in the regime where oxygen is beginning to become depleted. We have chosen to leave out this reaction, as we are not concentrating on this regime. Alkyl hydroperoxide decomposition occurs via reaction 11, which forms alkoxy and hydroxyl radicals. These alkoxy and hydroxyl radicals can abstract H-atoms from the fuel to yield an alcohol and water, respectively (reactions 12 and 14). The alkoxy radicals can also decompose unimolecularly via reaction 13, yielding a smaller alkyl radical, R_{prime}, and a carbonyl compound, i.e., a ketone or aldehyde. These alkoxy radicals can also self-terminate via reaction 15. The small alkyl radicals generated in reaction 13 can abstract H-atoms from the fuel to yield an alkane and another R• radical via reaction 16. R_{prime} has been included to differentiate these smaller alkyl radicals from those that are part of the primary autoxidation chain.

The chemical kinetics modeling code, REACT, requires that rate constants be input for each reaction in the mechanism. We have estimated these rate constants using a combination of techniques: comparison with measured rate constants and Benson style (Benson, 1976) "thermochemical kinetics" type of analysis. For some reactions the rate parameters were adjusted, and the effects of these adjustments were observed in the output. The rate constants, k, were estimated in Arrhenius form, i.e., $k = A \exp(E_a/RT)$; thus, an activation energy, E_a, and an Arrhenius "A-factor" were estimated for each reaction. The rate constant parameters used for each reaction are also shown in Table I. We have assumed that the bimolecular reactions have Arrhenius A-factors of 3×10^9 M^{-1} s^{-1}. This A-factor is close to the value ($10^{9.5}$ M^{-1} s^{-1}) recommended by Benson (1976) for $R^\bullet + O_2$ and is similar to the average value of 2.2×10^9 M^{-1} s^{-1} calculated by Moelwyn-Hughes (1947) for the average collision frequency of solution-phase bimolecular reactions. For the present purpose, it is reasonable to assume that the A-factors of these reactions are similar and "fast", as these are all simple bimolecular type reactions. For radical recombination

reactions, it is reasonable to assume that the activation energies are close to zero; therefore a zero activation energy was assigned to reactions 2, 4, 7, 9, 10, and 15. The activation energy of 10.0 kcal/mol chosen for reaction 3 was based on an average of similar H-atom abstraction reactions in the literature (Benson, 1976). In addition, as will be discussed later, in the presence of oxygen the chain carrier in autoxidation will be $RO_2^\bullet$; a lower value for the activation energy of reaction 3 results in this reaction being fast enough for the R$^\bullet$ radical concentration to be greater than the $RO_2^\bullet$ radical concentration.

In order for an antioxidant molecule to compete with the fuel molecules for reaction with $RO_2^\bullet$, reaction 5 must have a smaller activation energy than reaction 3. As antioxidants are usually added to fuels in very small amounts (<100 ppm), the activation energy of reaction 5 must be much smaller than reaction 3. If we equate the rate of reactions 3 and 5, we get

$$\exp\left(\frac{E_{a5}-E_{a3}}{RT}\right)=\frac{[RH]}{[AH]} \qquad \text{(eq 1)}$$

Thus an AH concentration of 7.4×10^{-4} M at 25 °C (100 ppm), yields an activation energy difference ($E_{a5}-E_{a3}$) of 5 kcal/mol (assuming an antioxidant molecular weight of 100 amu and RH with properties of *n*-dodecane). Thus 5.0 kcal/mol was chosen as a reasonable estimate of the activation energy of reaction 5. The activation energy for reaction 8 was chosen to be the same as that of reaction 5, as the energetics of H-atom abstraction by $AO_2^\bullet$ or $RO_2^\bullet$ from AH are expected to be very similar. The activation energies of each of the reactions where an H-atom is abstracted from the fuel by a radical (i.e., reactions 12, 14, and 16) have been assumed to be 10.0 kcal/mol by analogy to reaction 3. The small *A*-factor chosen for reaction 6 was found to be required for proper antioxidant behavior, and will be discussed in detail later in this paper.

For simplicity, we have assumed that the initiation step, reaction 1, involves the unimolecular decomposition of an initiator species, I, into R$^\bullet$ radicals. This is an obvious oversimplification of the poorly understood initiation process, but its inclusion is required to begin the chain with a very small production rate of R$^\bullet$ radicals. An activation energy of zero was chosen for simplicity, although it is most likely that the real initiation rate increases strongly with temperature. The *A*-factor was chosen along with the initial I concentration to produce an initial R$^\bullet$ radical production rate that is large enough to start the autoxidation chain, yet small enough to remain an insignificant source of radicals once the chain has begun.

The rate parameters chosen for the unimolecular decomposition of the alkyl hydroperoxide, reaction 11, are from average values in the literature (Benson, 1964; Gray et al., 1967). It was found that the modeling results are very sensitive to the rate parameters of this reaction. The final unimolecular reaction in the mechanism is the decomposition of the alkoxy radical, RO, via reaction 13. The rate parameters of this reaction were estimated by comparison with measured rate parameters of alkoxy radical decompositions (Batt, 1979).

The initial concentrations of each of the species present in the mechanism are also required input to the modeling code. These initial concentrations are listed in Table II. The RH concentration was estimated from the room temperature molarity of *n*-dodecane liquid (molecular weight of 170 amu and density of 0.752 g/cm^3). The dissolved oxygen concentration was estimated from the review of oxygen solubility by Battino et al. (1983) and from a compilation of jet fuel properties (Coordinating Research Council, 1983). From these papers we estimate the dissolved oxygen concentration at room temperature and 1 atm air in jet fuels and hydrocarbons as ≈79 ppm (by weight); therefore we have used 1.8×10^{-3} M for the oxygen concentration. The antioxidant concentration, AH, was varied over a wide range in the calculation, so a typical value of 2.0×10^{-4} M was listed in the table. A very small concentration (1.0×10^{-7} M) of the initiator species, I, was included for the initial production of R$^\bullet$ radicals required to get the chain mechanism started.

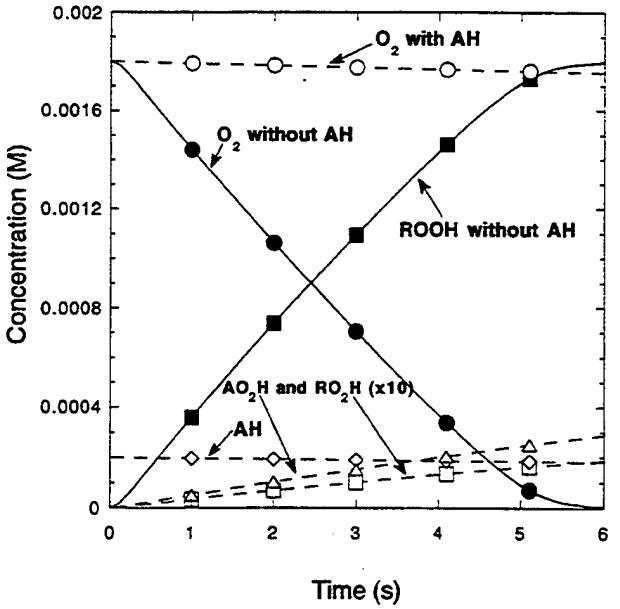

Figure 1. Plots of concentration vs time for runs with and without antioxidant at 200 °C: without antioxidant, (●) O_2 and (■) RO_2H; with 2.0×10^{-4} M of antioxidant, (○) O_2, (□) RO_2H, (△) AO_2H, and (◇) AH. The concentrations of AO_2H and RO_2H (□ and △) for the antioxidant case have been multiplied by a factor of 10. The symbols are drawn to mark the individual plots.

Table II. Initial Concentrations of Species

species	init concn (M)	species	init concn (M)
I	1.0×10^{-7}	AH	2.0×10^{-4}
O_2	1.8×10^{-3}	all other species	0.0
RH	4.4		

Autoxidation and Antioxidant Behavior in the Absence of Alkyl Hydroperoxide Decomposition

In order to confirm that the model demonstrates the autoxidation chain of reactions 2 and 3, we first ran the model without alkyl hydroperoxide decomposition. Thus, in this section we set the rate constant for reaction 11 to zero, thus preventing reactions 11–16 from occurring. In Figure 1 are plotted the results from two modeling runs performed for a temperature of 200 °C, the first without antioxidant present and the second with antioxidant present at a concentration of 2.0×10^{-4} M. In the absence of antioxidant, the oxygen decays to zero within 6 s and RO_2H is rapidly formed. Over the course of the reaction, essentially all of the O_2 is converted to RO_2H; 1.8×10^{-3} M of RO_2H is produced in 6 s with an initiation rate of (reaction 1) 1×10^{-8} M/s. Thus it is apparent that reaction 1, the initiation step, occurs very slowly in comparison with the production of RO_2H, and that chain propagation occurs via reactions 2 and 3. The chain length can be computed from the ratio of the rate of chain propagation (R_3) to initiation (R_1),

$$\text{chain length} = R_3/R_1 = (3.0 \times 10^{-4}\ \text{M s}^{-1})/(1 \times 10^{-8}\ \text{M s}^{-1}) = 3.0 \times 10^4 \qquad \text{(eq 2)}$$

Chain lengths of the order of tens of thousands are

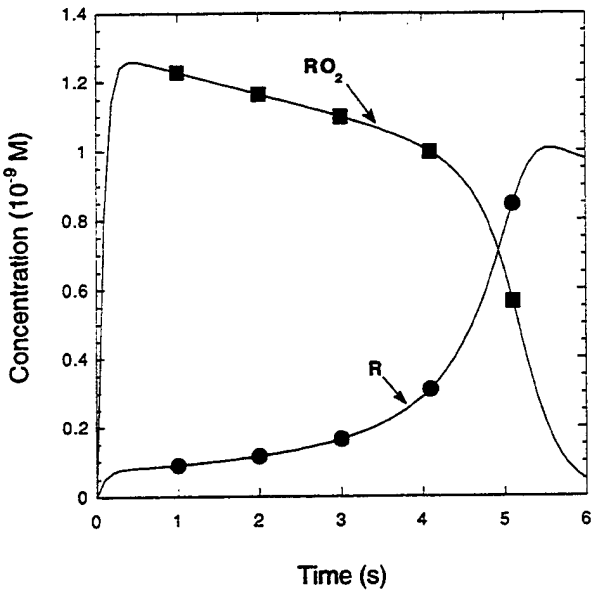

Figure 2. Plots of radical concentrations vs time at 200 °C: (●) R• and (■) RO_2• without antioxidant present. The symbols are drawn to mark the individual plots.

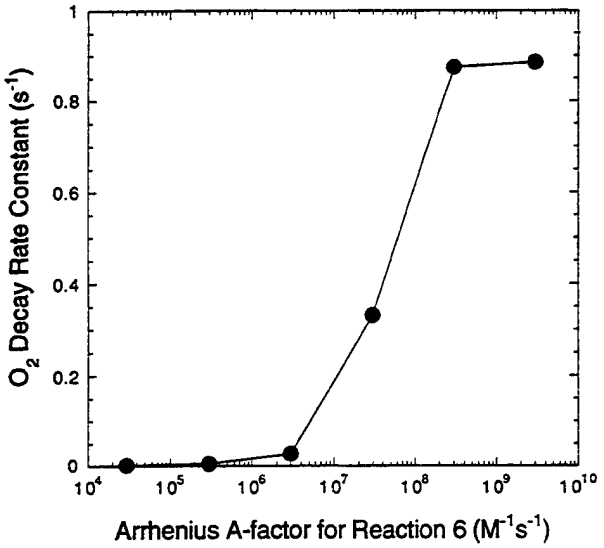

Figure 3. Semilog plot of oxygen decay rate constant vs Arrhenius *A*-factor of reaction 6, AO_2• + RH ⇒ AO_2H + R•, for 200 °C and 2.0 × 10^{-4} M antioxidant concentration. The symbols represent actual data points, and lines are drawn between the points to demonstrate the trend.

reasonable for such a linear chain (i.e., nonbranching chain) (Walling, 1957).

In the absence of antioxidant, AH, if reaction 3 is slow relative to reaction 2, RO_2• becomes the primary chain carrier, and it can be shown that the rate of consumption of oxygen will be zero order with respect to oxygen (Heneghan and Zabarnick, 1993). It is apparent from Figure 1 that the oxygen decay is indeed linear with respect to time, except at very short and long times. Early in the reaction there is a short induction period of ≈0.1 s in the oxygen profile; this induction period is a result of the slow build-up of radicals in the initiation step (reaction 1). Induction periods are commonly observed in autoxidation experiments (Jones and Balster, 1992). From the oxygen decay in Figure 1, it is also apparent that as the oxygen concentration gets small at long times (>4.5 s), its removal rate slows. This change from zero-order kinetics is expected, as at low oxygen concentrations reaction 2 becomes slow enough that RO_2• can no longer be the chain carrier. The chain carrier then becomes R•, and the rate of oxygen removal is equal to the rate of reaction 2, i.e., $k_2[R^\bullet][O_2]$. In Figure 2 are plotted the concentrations of R• and RO_2• versus time. The plot demonstrates that RO_2• is indeed the chain carrier during most of the reaction period. Only after 5 s, when the oxygen concentration gets relatively low, does the R• concentration approach and then surpass that of RO_2.

Also shown in Figure 1 are the results when 2.0 × 10^{-4} M of antioxidant is present. With the added antioxidant, oxygen is observed to decay much more slowly: only 3% is consumed after 6 s of reaction time. The presence of the antioxidant is also seen to substantially decrease the formation of RO_2H. Also plotted for the added antioxidant case are the concentration profiles for AH and AO_2H. The figure shows that the antioxidant is not significantly depleted (<10%) and that AO_2H is formed in only small concentrations. The results shown in Figure 1 display the type of behavior that is expected for autoxidation and its inhibition by antioxidants and thus gives us confidence that the mechanism and estimated rate parameters are reasonable (Mayo and Lan, 1986).

It was mentioned earlier that the *A*-factor for reaction 6 needed to be adjusted to obtain correct antioxidant behavior. In initial modeling studies it was found that if the *A*-factor for this reaction was set equal to 3 × 10^9 M^{-1} s^{-1}, antioxidant behavior (i.e., a slowing of the oxygen consumption rate as shown in Figure 1) did not occur for any concentration of AH. If Reaction 6 is fast, R• radicals are regenerated and the chain is not inhibited. In Figure 3 is plotted the oxygen decay rate constant versus the Arrhenius *A*-factor for reaction 6. These oxygen decay rate constants were derived from fits of the oxygen concentration profile data (as in Figure 1) by the equation $x\exp(-yt)$, where x and y are parameters calculated from the fits (y is the resulting oxygen decay rate constant) and t is the reaction time. This equation did a very good job of fitting the faster oxygen decays (as in the case without antioxidant of Figure 1), but the slower decays (as in the case with antioxidant of Figure 1) did not fit the function well because the data did not appear to be approaching zero oxygen concentration at infinite time, as in the fitted equation. Nonetheless, the fitted equation provides a good way of comparing the oxygen decays at different antioxidant concentrations. *A*-factors greater than 1 × 10^7 M^{-1} s^{-1} yield rapid oxygen decays. The figure shows that the *A*-factor of reaction 6 needs to be less than 1 × 10^6 M^{-1} s^{-1} in order for the antioxidant to inhibit the removal of oxygen. It is apparent from the figure that for an antioxidant to inhibit oxygen removal it needs to avoid regenerating R• radicals through H-atom abstractions from fuel molecules, such as in reaction 6. Thus, reaction 6 needs to be slow through its having either a large activation energy or a small *A*-factor. It is expected that the activation energy for the abstraction of a H-atom from RH by a peroxy radical should not be a strong function of the molecular structure of the peroxy radical, as the identity of the R or A group in RO_2• or AO_2• should not significantly affect the reactivity of the radical site. Thus it does not seem reasonable that reactions 3 and 6 would have very different activation energies. For this reason we have chosen to vary the Arrhenius *A*-factor rather than the activation energy. A possible explanation for such a large lowering of the *A*-factor is that antioxidant molecules are often severely sterically hindered, as in BHT (butylated hydroxytoluene). This steric hindrance will cause reactions like reaction 6 to proceed very slowly; the kinetic effect due to steric hindrance usually appears as a decrease in the Arrhenius *A*-factor rather than an increase in the

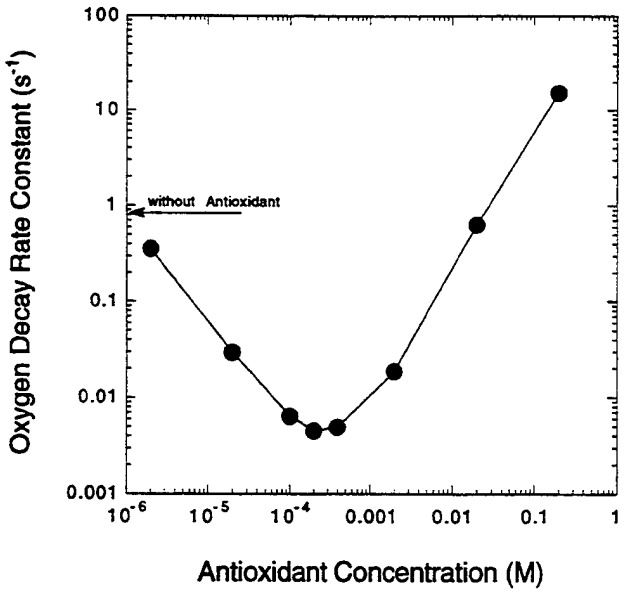

Figure 4. Log–log plot of oxygen decay rate constant vs antioxidant concentration at 200 °C. The oxygen decay rate constant obtained without added antioxidant is indicated with the arrow.

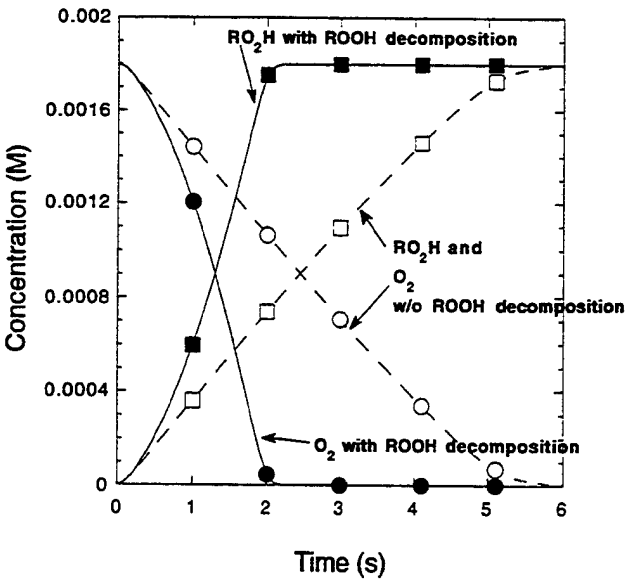

Figure 5. Plots of concentration vs time at 200 °C comparing modeling performed with and without inclusion of alkyl hydroperoxide decomposition: without alkyl hydroperoxide decomposition, (○) O_2 and (□) RO_2H; with alkyl hydroperoxide decomposition, (●) O_2 and (■) RO_2H. The symbols are drawn to mark the individual plots.

activation energy (Gardiner, 1969). We have chosen to decrease the *A*-factor by 4 orders of magnitude in order to decrease the rate of reaction 6, and allow expected antioxidant behavior. A decrease in Arrhenius *A*-factor of this magnitude is not unreasonable for this type of steric hindrance effect (Gardiner, 1969). Another justification for using a slow rate for reaction 6 is that some antioxidants may not even produce the $AO_2^\bullet$ radical, and thus reaction 6 may not need to be considered for these antioxidants.

For the same reasons one can argue that reaction 8 should have also have a reduced *A*-factor, since this reaction is also an H-atom abstraction by an $AO_2^\bullet$ radical. We have compared the oxygen decay rate constants before and after reducing the *A*-factor of reaction 8 to 3×10^5 M^{-1} s^{-1}. The measured oxygen decay rate constant for the smaller *A*-factor case was reduced by only 10%. Thus we have chosen to perform the modeling with the larger *A*-factor for reaction 8.

The amount of antioxidant required in a real fuel sample is usually found by trial and error, an expensive and time-consuming process. To address this issue, in the calculations we have varied the initial antioxidant concentration over a wide range in order to determine the optimum antioxidant concentration for the model conditions. In Figure 4 is plotted the oxygen decay rate constant vs antioxidant concentration for antioxidant concentrations over the range 1.0×10^{-6} to 1.0×10^{-1} M at 200 °C. Figure 4 demonstrates that the mechanism predicts antioxidant behavior is a strong function of the initial antioxidant concentration. As antioxidant is added to the fuel, the plot shows the oxygen decay rate constant decreases sharply; as more antioxidant is added the oxygen decay rate constant goes through a minimum and then increases with additional antioxidant concentration. The minimum of the plot, where the antioxidant is performing the best, is near an antioxidant concentration of 2×10^{-4} M. Of course, the location of this minimum is a function of the rate parameters chosen for the two reactions that compete for $RO_2^\bullet$ radicals, reactions 3 and 5. It appears that adding antioxidant above 0.02 M results in oxygen decay rate constants equal to or greater than those without antioxidant. This type of behavior, where large concentrations of antioxidant actually decrease the oxidative stability, has been observed in fuel systems (Mayo and Lan, 1986; Nixon, 1962).

Autoxidation and Antioxidant Behavior in the Presence of Alkyl Hydroperoxide Decomposition

This study concentrates on the chemistry that occurs in the region near 200 °C. At these temperatures it is expected that the alkyl hydroperoxides generated in reaction 3 may decompose by a thermal unimolecular path producing alkoxy radicals, RO, and hydroxyl radicals, OH, via reaction 11. Thus, in this section we have changed the rate of reaction 11 to be nonzero, and therefore reactions 11–16 may now proceed and affect the overall chemistry. In Figure 5 are compared the oxygen and alkyl hydroperoxide concentration profiles with and without inclusion of alkyl hydroperoxide decomposition. It is apparent that including hydroperoxide decomposition strongly increases the rate of oxygen removal. Additionally, the shape of the oxygen removal profile has changed. The rate of oxygen removal starts off slowly (at less than 0.5 s) and rapidly increases to when the oxygen is nearly completely removed at ≈2 s. This increase in rate with time is sometimes referred to as "autocatalysis". Interestingly, this strong increase in the oxygen decay rate occurs without significant decomposition of the alkyl hydroperoxide, RO_2H (only 0.02% of the hydroperoxide is decomposed). This increase in the oxygen removal rate is due to the increased initiation of radical formation from reaction 11. For the case where 1×10^{-3} M of hydroperoxide is formed, 0.02% decomposition over 6 s yields an increase in the initiation rate of $\approx 7 \times 10^{-8}$ M/s. This is significantly greater than the initiation rate used for the initial production of R• radicals, 1×10^{-8} M/s. Thus, the alkyl hydroperoxide decomposition can play a very important role in controlling oxygen removal even though it decomposes to only extremely small extents.

Oxygen decay profiles have been obtained for various concentrations of added antioxidant, as shown in Figure 4 for the case without hydroperoxide decomposition. The oxygen decay profiles in this case do not fit exponential profiles very well (see Figure 5), and therefore decay rates were not determined. It was found that the qualitative behavior of the oxygen decay profiles as a function of the antioxidant concentration was very similar to that shown in Figure 4; the slowest oxygen decays were obtained near 2×10^{-4} M antioxidant concentration.

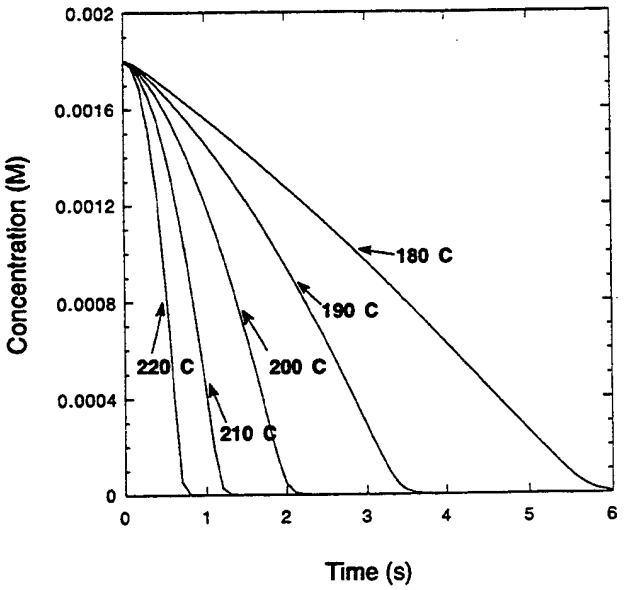

Figure 6. Plots of oxygen concentration vs time at various temperatures when alkyl hydroperoxide decomposition is included (reaction 11).

In Figure 6 are plotted the oxygen profiles vs time for the temperature range 180–220 °C. In these runs the antioxidant concentration is zero. The increase in oxygen removal rate is mostly a function of the temperature dependencies of reactions 3 and 11. The temperature dependence of reaction 3 will cause an increase in the rate with temperature, but not a change in the curvature of the plot. Reaction 11, the decomposition of the alkyl hydroperoxide, will cause the curvature of these plots to change with temperature. At low temperatures the oxygen should decay nearly linearly, because of the high activation energy of reaction 11. At higher temperatures the hydroperoxide will begin to decompose, and the curvature is due to this increase in the initiation of radicals. Thus, the 180 °C plot of Figure 6 is nearly linear, and the nonlinearity increases with temperature. Walling (1957) has cited a bimolecular decomposition of alkyl hydroperoxides to explain this type of increase in oxygen removal rate with time:

$$2RO_2H \Rightarrow RO_2^{\bullet} + RO^{\bullet} + H_2O$$

Bateman et al. (1953) have shown that this bimolecular pathway for hydroperoxide decomposition only occurs at hydroperoxide concentrations greater than 0.02 M. The maximum hydroperoxide concentration that can be formed in the present system is limited by the dissolved oxygen concentration to 1.8×10^{-3} M; thus the hydroperoxide decomposition must occur by a unimolecular pathway. The present data demonstrate that the unimolecular decomposition of alkyl hydroperoxides is adequate to explain the curvature in oxygen profiles without the inclusion of a bimolecular pathway for peroxide decomposition. This is despite the fact that only a very small fraction of the alkyl hydroperoxide is decomposing (even at 220 °C, only 0.1% decomposition is predicted).

Conclusions

Chemical kinetic modeling has been performed in order to simulate the chemical processes that occur during the autoxidation of jet fuels. The model demonstrates that the $RO_2^{\bullet}$ radical is the chain carrier while oxygen is present in the fuel. The model is also able to correctly duplicate the behavior that results upon the addition of antioxidants to the fuel. The addition of antioxidants is seen to drastically lower the oxidation rate at low concentrations and increase the rate at higher concentrations. The model demonstrates that molecules with easily abstractable H-atoms may act as oxidation inhibitors. The model also demonstrates the important role that the thermal decomposition of alkyl hydroperoxides can play in the autoxidation process. Unimolecular decomposition of these hydroperoxides, even at very small conversions, can play a crucial role in the oxidation process.

Literature Cited

Bateman, L.; Hughes, H.; Morris, A. L. Hydroperoxide Decomposition in Relation to the Initiation of Radical Chain Reactions. *Discuss. Faraday Soc.* **1953**, *14*, 190.

Batt, L. The Gas-Phase Decomposition of Alkoxy Radicals. *Int. J. Chem. Kinet.* **1979**, *11*, 977.

Battino, R.; Rettich, T. R.; Tominaga, T. The Solubility of Oxygen and Ozone in Liquids. *J. Phys. Chem. Ref. Data* **1983**, *12*, 163.

Benson, S. W. Kinetics of Pyrolysis of Alkyl Hydroperoxides and Their O-O Bond Dissociations Energies. *J. Chem. Phys.* **1964**, *40*, 1007.

Benson, S. W. *Thermochemical Kinetics*; Wiley: New York, 1976.

Benson, S. W.; Nangia, P. S. Some Unresolved Problems in Oxidation and Combustion. *Acc. Chem. Res.* **1979**, *12*, 223.

Coordinating Research Council. *Handbook of Aviation Fuel Properties*; Coordinating Research Council: Atlanta, GA, 1983.

Edwards, T.; Zabarnick, S. Supercritical Fuel Deposition Mechanisms. Presented at the 1992 AIChE National Meeting, Miami Beach, FL, 1992; paper 58d.

Emanuel, N. M.; Denisov, E. T.; Maizus, Z. K. *Liquid Phase Oxidation of Hydrocarbons*; Plenum Press: New York, 1967.

Gardiner, W. C. *Rates and Mechanisms of Chemical Reactions*; W. A. Benjamin: Menlo Park, 1969.

Gray, P.; Shaw, R.; Thynne, J. C. J. In *Progress in Reaction Kinetics*; Porter, G., Ed.; Pergamon Press: Oxford, 1967; Vol. 4, p 63.

Heneghan, S. P.; Harrison, W. E. Anti-Oxidants in Jet Fuels: A New Look. Presented at the 203rd National Meeting of the American Chemical Society, Division of Petroleum Chemistry, San Francisco, CA, 1992.

Heneghan, S. P.; Zabarnick, S. Oxidation of Jet Fuels and the Formation of Deposits. *Fuel.* **1993**, in press.

Heneghan, S. P.; Martel, C. R.; Williams, T. F.; Ballal, D. R. Studies of Jet Fuel Thermal Stability in a Flowing System. Presented at the Transactions of the ASME, Cologne, Germany, 1992.

Jones, E. G.; Balster, W. J. Application of a Sulphur-Doped Alkane System to the Study of Thermal Oxidation of Jet Fuels. Presented at the International Gas Turbine Institute, Cologne, Germany, 1992.

Martel, C. R. "Military Jet Fuels, 1944–1987"; Air Force Wright Aeronautical Laboratories, 1987.

Mayo, F. R.; Lan, B. Y. Gum and Deposit Formation from Jet Turbine Diesel Fuels at 130 °C. *Ind. Eng. Chem. Prod. Res. Dev.* **1986**, *25*, 333.

Moelwyn-Hughes, E. A. *The Kinetics of Reactions in Solution*; Clarendon Press: Oxford, 1947.

Nixon, A. C. In *Autoxidation and Antioxidants*; Lundberg, W. O., Ed.; Wiley: New York, 1962; Vol. II, p 695.

Reddy, K. T.; Cernansky, N. P.; Cohen, R. S. Modified Reaction Mechanism of Aerated n-Dodecane Liquid Flowing over Heated Metal Tubes. *Energy Fuels.* **1988**, *2*, 205.

Walling, C. *Free Radicals in Solution*; Wiley: New York, 1957.

Waters, W. A. *Mechanisms of Oxidation of Organic Compounds*; Methuen: London, 1964.

Whitbeck, M. Numerical Modeling of Chemical Reaction Mechanisms. *Tetrahedron Comput. Methodol.* **1990**, *3* (6B), 497–505.

Received for review November 16, 1992
Accepted March 22, 1993

Appendix C.

Studies of Jet Fuel Thermal Stability and Oxidation Using a Quartz Crystal Microbalance and Pressure Measurements

Steven Zabarnick
University of Dayton
300 College Park
Dayton, OH 45469-0140

Reprinted from I&EC RESEARCH, 1994, 33.

Studies of Jet Fuel Thermal Stability and Oxidation Using a Quartz Crystal Microbalance and Pressure Measurements

Steven Zabarnick†

Aerospace Mechanics Division/KL-463, University of Dayton Research Institute, Dayton, Ohio 45469-0140

The thermal stability of aircraft jet fuels was measured in real time with a quartz crystal microbalance (QCM) at 140 °C. Qualitative data on the oxidation of these fuels was also obtained by monitoring the system pressure during thermal stressing. The system was operated at relatively low oxygen availability (1 atm air) which more closely approximates the oxygen availability of flowing fuel tests and real fuel systems than previous work. The high sensitivity and good reproducibility of the QCM permitted deposition measurements under unaccelerated conditions (i.e., relatively low temperature and oxygen availability). Correlation of oxidation and deposition behavior provided insight into the deposition and oxidation processes.

Introduction

Jet fuel is presently used as a coolant in military aircraft, in addition to its primary use as a propellant. It is used to cool the lubrication systems, avionics, electrical systems, and environmental control systems, and is also used as a hydraulic fluid. The trend of advanced aircraft toward increasing performance results in ever-increasing heat loads. Exposure of fuels to high temperatures results in the formation of oxidized soluble and insoluble products (thermal stability refers to the deposit-forming tendency of the fuel). The buildup of insolubles in aircraft fuel systems is of great concern because of the resulting possibility of fuel system failure. Many test devices have been developed to measure the deposition characteristics of jet fuel under the varied time–temperature histories to which a fuel is subjected during flight (Hazlett, 1991). Unfortunately, the difficulty in measuring small amounts of deposits has resulted in the development of accelerated tests. These are conducted at temperatures that exceed those expected under real fuel system conditions, or are run under elevated oxygen concentration or availability. One concern is that the chemical mechanisms of oxidation and deposition significantly differ at these higher temperatures and/or greater extents of oxidation.

Two types of accelerated tests are most common: flowing and static. In the flowing tests, air-saturated fuel flows through a heated tube. At the end of the test the tube is cut into sections and carbon burn-off or gravimetric analysis of the tube is performed. This type of test most closely approximates the conditions of oxygen availability that exist under real fuel system conditions; that is, the oxygen availability is limited to the oxygen dissolved in the fuel. Relatively high temperatures are used to generate measurable amounts of deposits. In the static tests, fuel is heated in a flask or reactor and oxygen is bubbled through the fuel during the test. Usually, deposits are measured gravimetrically. Under bubbling oxygen conditions, the fuel can be oxidized to a great extent. Thus the extent of reaction or oxidation may not reasonably approximate real fuel system conditions. Relatively high temperatures are also usually used; the large extents of oxidation and high temperatures are required to generate measurable deposits. Additionally, both the carbon burn-off and gravimetric deposition measurements are performed off-line, subsequent to the test run, and therefore do not readily yield time-dependent information.

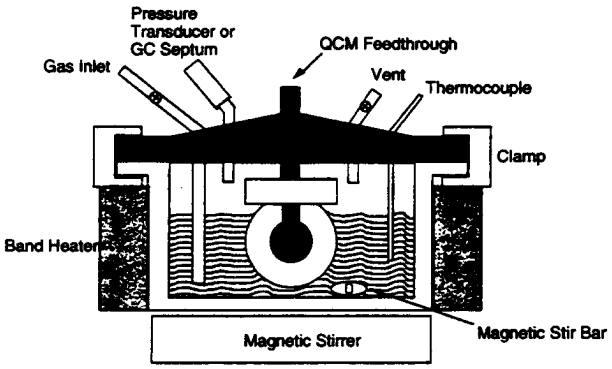

Figure 1. Drawing of the Parr bomb/QCM assembly.

The quartz crystal microbalance (QCM) has the ability to perform real-time, *in situ* measurements of deposition at temperatures that closely approximate real fuel system conditions (Klavetter et al., 1993). The QCM has extremely high sensitivity for the measurement of surface deposition; it is able to readily resolve ≈0.1–0.2 $\mu g/cm^2$. Thus, the device can follow the real-time deposition at low temperatures. In the present work, we use a QCM device in a static-type test, but we limit the oxygen availability to that present in the air-saturated fuel and the small air headspace. Limiting the oxygen availability to that of the air-saturated fuel more closely approximates the oxygen availability of flowing tests and real fuel system conditions (previous work concentrated on the high oxygen availability regime (Klavetter et al., 1993)). We have also modified the QCM system for the present study by adding a pressure transducer. This allows us to follow the oxidation of the fuel in real time by measuring oxygen consumption.

Experimental Section

Jet fuels were thermally stressed in a Parr bomb/QCM system that has been described in detail previously (Klavetter et al., 1993). A drawing of the reactor is shown in Figure 1. The reactor is supplied with a gas inlet line (below the liquid level) for sparging the liquid fuel and with a vent (above the liquid level). A magnetic stir bar and stirrer are used to minimize spatial temperature gradients. The QCM crystal is suspended vertically in the jet fuel in order to minimize gravitational effects on deposition.

The quartz crystals used were 5-MHz, 2.54-cm-diameter, 0.33-mm-thick, AT-cut wafers. These crystals, obtained from Maxtek Inc., were manufactured with gold electrodes

† E-mail: zabarnic@udavxb.oca.udayton.edu.

0888-5885/94/2633-1348$04.50/0

and overtone polished. The quartz crystal resonator is driven at 5 MHz by an oscillator circuit that was developed at Sandia National Laboratories (Klavetter et al., 1993). This circuit tracks the impedance variations of the crystal in order to determine the resonant frequency of the device. The oscillator frequency output is read by a frequency counter (HP Model 5384A). The change in frequency of the device at constant temperature is related to surface mass deposition on the crystal. The oscillator circuit also provides an amplitude output that indicates crystal damping. The amplitude output is read by a digital multimeter (HP Model 3478A).

The Parr bomb is a 100-mL stainless steel vessel that was modified with an rf feedthrough to allow attachment of the QCM. It is heated with a clamp-on band heater which is controlled by a PID temperature controller (Parr Model 4842). A thermocouple is immersed in the liquid fuel to monitor the fuel temperature. The temperature can be readily maintained ±0.4 °C at 140 °C over a 15-h run. The vessel is filled with 60 mL of jet fuel, sealed, and the fuel sparged for 1 h with the appropriate gas (usually air), to ensure that the fuel is saturated with the gas. When sparging is complete, the sparge gas is turned off, and the reactor is sealed at ambient pressure. At this point, the heater is turned on and computer data acquisition begins. The crystal frequency, reactor temperature, and reactor pressure or crystal damping amplitude are monitored and recorded at 1-min intervals by a personal computer. Most runs are conducted for 15 h. At the end of this time the heater is turned off, but the computer continues to record data for much of the cool-down period (3 or 4 h to return to room temperature). The heat-up time of the reactor is ≈45 min to 140 °C. Between runs the reactor and all surfaces that contact the fuel are cleaned repeatedly with an equivolume mixture of toluene, acetone, and methanol, and subsequently allowed to dry. The crystal is replaced with an unused crystal prior to each run.

For many runs the reactor was fitted with a Sensotec absolute pressure transducer. This pressure measurement could also be read by the digital multimeter and recorded by the computer. Thus the pressure in the headspace of the reactor was recorded at 1-min intervals, in addition to the frequency and temperature. This pressure measurement was used to monitor oxidation of the fuel; this technique is explained and verified later in the paper.

The presence of air in the headspace of the reactor results in additional oxygen that is available for reaction, beyond the oxygen that is dissolved in the fuel. For a typical fuel with a dissolved oxygen concentration of 1.8×10^{-3} M (Hazlett et al., 1977), 60 mL of this fuel contains 1.08×10^{-4} mol of oxygen. The 40 mL of air headspace contains 3.42×10^{-4} mol of oxygen at 25 °C. Thus, this system has an oxygen availability that is ≈4 times greater than that of a flowing system, which has no headspace air. As 60 mL of fuel contains ≈0.26 mol of fuel molecules (using the molarity of *n*-dodecane), the total oxygen availability of 4.5×10^{-4} mol can be used to calculate that only 0.17% of the fuel molecules can be oxidized (assuming that each O_2 molecule is able to oxidize one fuel molecule). This is a relatively small extent of oxidation relative to studies with bubbling air or oxygen, where there is the possibility of oxidizing most of the fuel molecules (Blaine and Savage, 1991).

In general, the reproducibility of the mass deposition measurements on fuels is limited to ±20% for the QCM technique. This estimate of the precision of the technique was derived from multiple runs of the same fuel, performed for various fuels.

Theory

The theory that relates the measured frequency changes to surface mass has been presented in detail elsewhere (Martin et al., 1991) and will only be discussed briefly. When a crystal is excited at its resonant frequency, it undergoes a shear deformation with displacement maxima at the crystal faces. Mass accumulation on the crystal surface moves synchronously with the surface, resulting in a decrease in the resonant frequency. Also, a thin layer of liquid can be entrained by the surface, also resulting in a decrease in the resonant frequency. The decrease in resonant frequency is described by

$$\Delta f_0 \approx -\frac{2f_0^2}{N(\mu_q \rho_q)^{1/2}}\left[\rho_s + \left(\frac{\rho\eta}{4\pi f_0}\right)^{1/2}\right] \qquad (1)$$

where f_0 is the unperturbed resonant frequency, N is the harmonic number, μ_q is the quartz shear stiffness, ρ_q is the quartz mass density, ρ_s is the surface mass density (mass/area), and ρ and η are the liquid density and viscosity, respectively. Thus the frequency change is due to two terms: the first results from changes in surface mass density (the quantity we wish to measure); the second is due to changes in liquid properties (density and viscosity). If the liquid properties are constant, then changes in frequency can be used to determine surface mass accumulation. The liquid properties, density and viscosity, will remain relatively constant under conditions where temperature is held constant and the chemistry of the fuel is restricted to small extents of reaction. Under these conditions the surface deposition can be related to the frequency as

$$\rho_s = -(2.21 \times 10^5 \text{ g/(cm}^2 \text{ s)})\frac{\Delta f}{f_0^2} \qquad (2)$$

for the fundamental resonance. The surface deposition measurements reported here occur for fuel oxidation at constant temperature (±0.4 °C) and under limited oxygen conditions, where only a small fraction of the fuel molecules undergo chemical change. Thus, the fuel density and viscosity remain constant during our measurements, and the above equation can be used to measure surface deposition.

Under conditions where the liquid properties are changing, the amplitude output of the oscillator circuit can be used to determine the motional resistance of the crystal (Klavetter et al., 1993). The motional resistance can then be related to these changes in liquid properties, and thus the changes in liquid properties can be resolved from the surface mass accumulation. For each of the runs where the amplitude was monitored, we detected no change in the motional resistance during the constant-temperature period. Thus, consideration of changes in liquid properties was not needed.

Results and Discussion

Table 1 lists the properties of the fuels used in this study. In Figure 2 are shown the QCM frequency and temperature profiles for a typical experimental run. This particular run is for fuel F-2922 at 140 °C for 15 h. In this plot, time zero is defined by the moment the heater and temperature controller are turned on. The temperature rapidly rises to slightly higher than the set point (140 °C) and then stabilizes at the set point in the first 45 min. The temperature than stays constant within ±0.4 °C for the 15-h test period. At 15 h the heater is turned off and the

Table 1. Properties of Fuels Studied

fuel number	hydro-treated?	JFTOT break-point (°C)	oxygen concn in air-satd fuel at 25 °C (ppm w/w)[a]	sulfur (mass %)
F-2747 (Jet A-1)	yes	332	73	<0.001
F-2827 (Jet A)	no	266	65	0.1
F-2922 (Jet A)	yes	277	not measured	0.02

[a] As measured by Striebich and Rubey (1993).

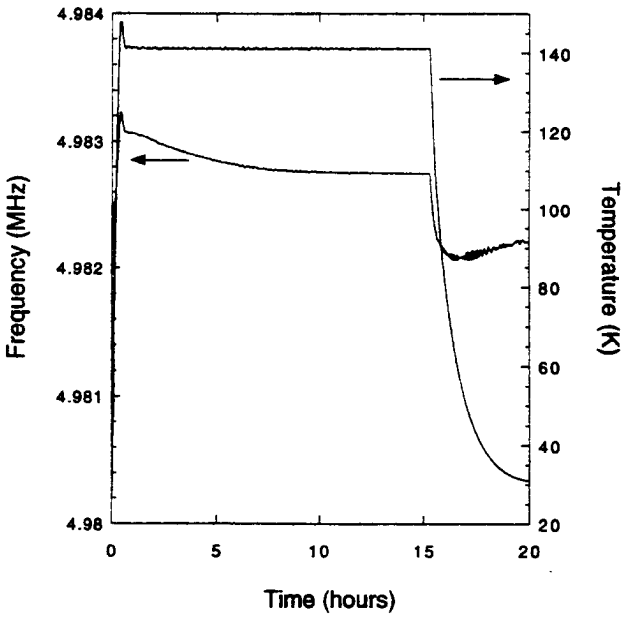

Figure 2. Plots of QCM frequency and temperature vs time for fuel F-2922.

temperature slowly returns to ambient. The measured QCM frequency closely follows the temperature profile as the QCM is extremely sensitive to small changes in temperature. The QCM frequency rises during the initial temperature rise and peaks during the temperature overshoot. During the constant-temperature period the QCM frequency decreases a relatively small amount, and when the heater is turned off the frequency drops along with the temperature. It is the relatively small decrease in frequency during the constant-temperature period that we use here to determine the surface mass deposition. In addition, for most runs either the damping voltage or headspace pressure were also measured. The damping voltage follows the temperature inversely, i.e., decreasing as the temperature increases, due to the decrease in viscosity of the liquid fuel with temperature. In every case the damping voltage remained constant during the constant-temperature period of the run. The headspace pressure also closely follows the temperature profile. The headspace pressure increases with increasing temperature due to the increasing vapor pressure of the fuel and the ideal-gas behavior of the headspace air. During the constant-temperature period of the run, the headspace pressure was observed to decrease for many fuels; this is due to oxygen removal via oxidation in the liquid phase as discussed below.

For each of the data plots to follow we have presented the deposition and pressure measurements for the constant-temperature period of the experimental run only. In Figure 3 are shown mass accumulation and pressure plots for the fuel F-2747 at 140 °C. This fuel deposits 0.5 $\mu g/cm^2$ in the first 4 h with little deposition after this time. The system pressure increases from 1 atm during the 45-min heat-up time to ≈1.5 atm (not shown). During

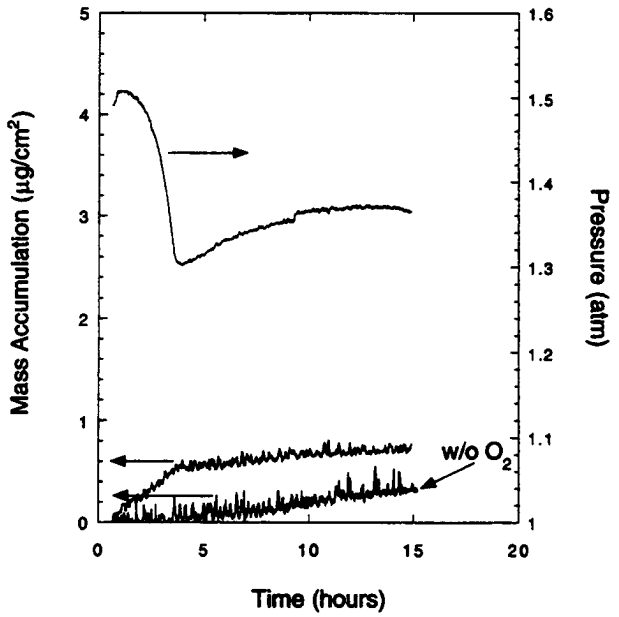

Figure 3. Plots of mass accumulation and pressure for fuel F-2747 at 140 °C.

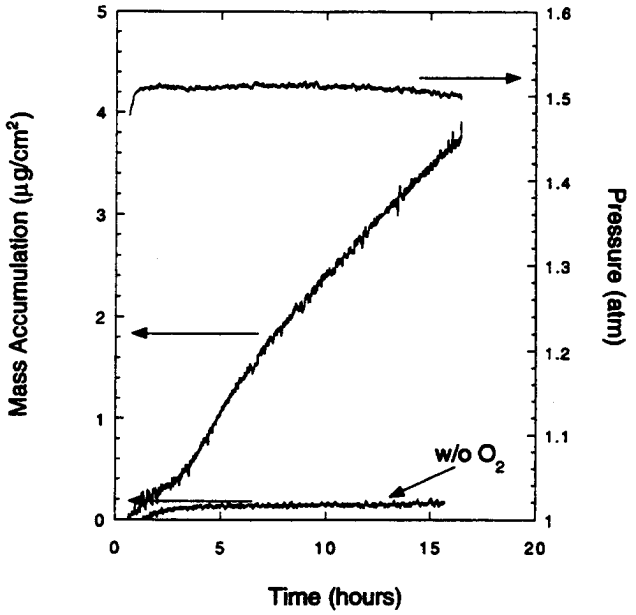

Figure 4. Plots of mass accumulation and pressure for fuel F-2827 at 140 °C.

the first 4 h the pressure rapidly decreases, and there is a more moderate pressure increase between 4 and 10 h. We attribute the pressure decay during the first 4 h to the reaction of oxygen in the liquid fuel and the diffusion of oxygen from the headspace into the liquid. This interpretation is supported by the gas chromatography data shown below. We must keep in mind that the pressure measurements follow the oxygen present in the headspace which, as will be presented, lags the liquid phase oxygen level. Interestingly, the figure shows that nearly all of the deposition occurs during the oxidation period. The deposition levels off close to the same time as the oxygen is depleted. We attribute the pressure rise observed after 4 h to the production of volatile compounds, such as methane, as previously observed in the autoxidation of jet fuels (Heneghan et al., 1993; Heneghan and Zabarnick, 1994).

In Figure 4 are shown plots of mass accumulation and pressure for fuel F-2827. This fuel exhibits much greater

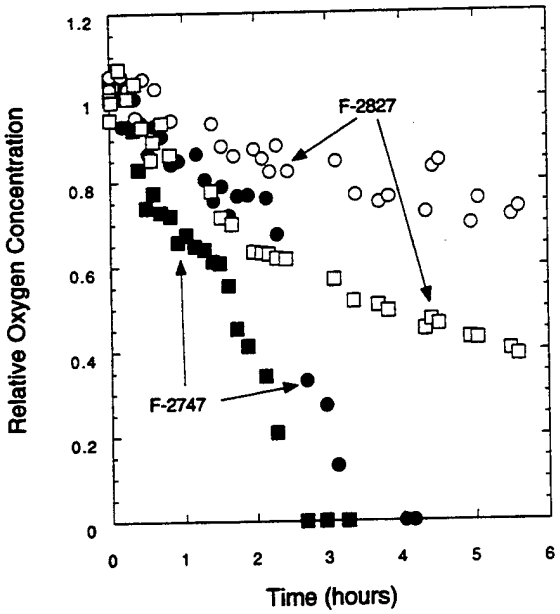

Figure 5. Plots of relative oxygen concentration vs run time obtained by GC–MS sampling of the liquid fuels and reactor headspace. Symbols represent □, liquid F-2827; ○, headspace F-2827; ■, liquid F-2747; and ●, headspace F-2747.

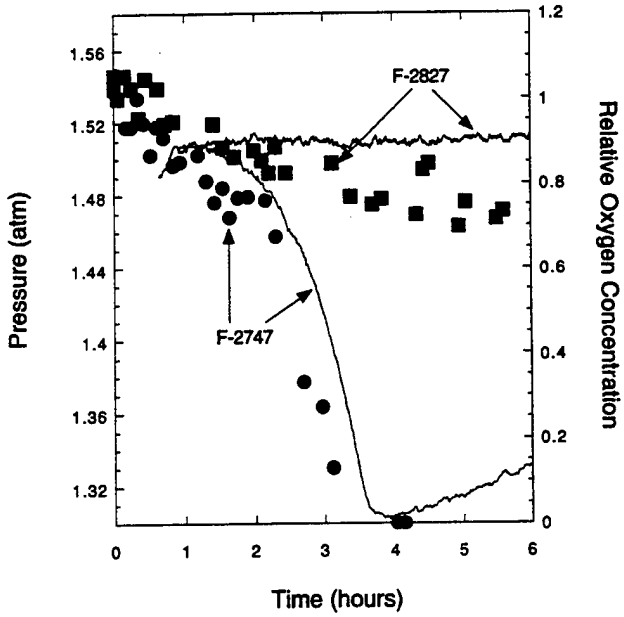

Figure 6. Plots of pressure and oxygen GC measurements of headspace during the runs with F-2747 and F-2827 at 140 °C. Lines represent pressure measurements, and the symbols are the GC relative oxygen measurements.

deposition than F-2747, producing 3.6 $\mu g/cm^2$ after 15 h. Furthermore, the deposition does not level off, even after 15 h. The pressure plot shows almost no decrease over the course of the run. The deposition does show a small change in slope at 3 h. The increased deposition and decreased oxidation of this fuel relative to F-2747 is in accord with previous data on these fuels (Heneghan and Zabarnick, 1994). Also, the presence of a significant concentration of sulfur-containing molecules (see Table 1) is known to increase deposition (Hazlett, 1991). Also included in both Figures 3 and 4 are deposition results after sparging the liquid fuels with nitrogen gas to remove dissolved oxygen. The well-known effect of a reduction of deposits in the absence of oxygen is readily observed.

In order to determine the usefulness of headspace pressure measurements as a technique for monitoring the extent of oxidation, we have performed oxygen concentration measurements by gas chromatography–mass spectrometry (GC–MS) (Striebich and Rubey, 1993). During a run 1.0-μL liquid fuel samples and 0.3-μL gas samples were extracted by standard GC syringe techniques. For these measurements the Parr bomb was equipped with a GC septum port which allowed both gas and liquid samples to be withdrawn during a run. The mass spectrometer detector of the GC was operated in single-ion monitoring (SIM) mode; the detector monitors only the 32 amu mass for detection of oxygen. Thus, the nonretained chromatographic air peak is, in effect, separated into its component constituents by mass detection. Calibration is readily accomplished by injection of varying volumes of room air. The fuel is held on the column and/or injector by holding these at relatively low temperatures.

The results of oxygen measurements for the fuels F-2747 and F-2827 at 140 °C are shown in Figure 5. Samples were taken of both the headspace air and the liquid fuel during the course of these two runs. It is apparent that oxygen is removed more rapidly in fuel F-2747, and for both fuels the oxygen removal is more rapid in the liquid phase. The fact that the headspace oxygen removal lags that of the liquid phase demonstrates that oxygen removal occurs primarily in the liquid phase (as expected) and that the oxygen that is consumed in the liquid is replenished by diffusion from the headspace more slowly than it is consumed. That is, the oxygen concentration is not in equilibrium between the two phases during the oxidation period. For fuel F-2747, the liquid-phase oxygen is completely depleted after 3–4 h. Fuel F-2827 still contains 40% of the original liquid-phase oxygen after the end of the run at 6 h. These trends are in substantial agreement with those observed by independent experiments (Heneghan and Zabarnick, 1994). Striebich and Rubey (1993) have measured the room temperature absolute concentrations of oxygen in these air-saturated fuels by this GC–MS technique, and these results are listed in Table 1. The downward curvature of the F-2747 oxygen profiles in the first 4 h is indicative of the type of behavior generally called "autocatalytic" or "autoaccelerative".

As we now have pressure and GC sampled oxygen measurements for both of these fuels, we can compare the measurements to interpret the pressure monitoring technique. For plotting purposes, we have normalized the GC oxygen and pressure data so that the data overlap at 45 min into the run and so the minimum in the F-2747 data represents zero oxygen remaining. These results are plotted for comparison in Figure 6. It is apparent that the GC oxygen and pressure data agree quite well. For fuel F-2827, the pressure plot shows a smaller extent of oxygen consumption, but the production of small amounts of volatile compounds can result in this difference. For fuel F-2747, the GC oxygen and pressure plots exhibit very similar shapes, both reaching a minimum between 3 and 4 h. The pressure plot exhibits a slightly slower oxygen decay and a pressure rise after 4 h. The production of volatile compounds would cause both of these effects. This figure demonstrates that the pressure technique is very promising as a simple method to monitor the oxidation of a fuel under the present conditions. The technique does tend to underestimate the extent of oxidation, and this needs to be taken into consideration. This underestimation of the extent of oxidation results from the diffusion of oxygen between the headspace and the liquid fuel, in addition to the production of volatile compounds. In this work we use this method to provide a *qualitative* measure of the extent of oxidation vs time.

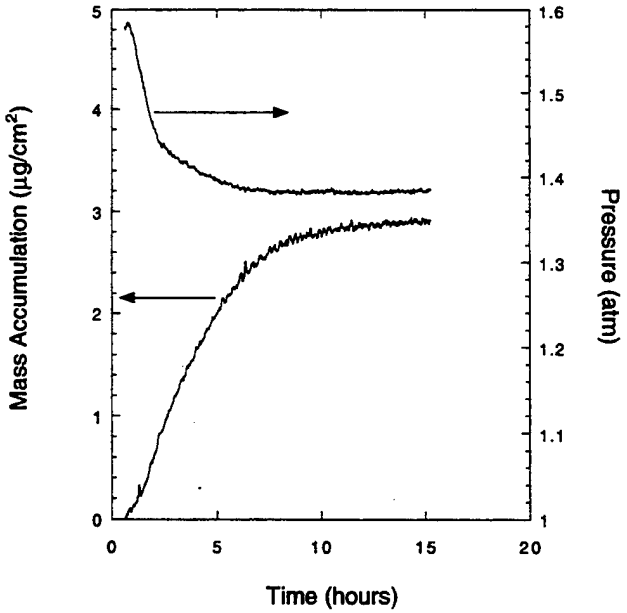

Figure 7. Plots of mass accumulation and pressure for fuel F-2922 at 140 °C.

Figure 7 demonstrates the results for a hydrotreated fuel which produces a moderate amount of deposits and shows an interesting correspondence between oxidation and deposition. This fuel, F-2922, shows oxidation that can be well fit to an exponential decay rather than the downward-curving "autocatalytic" profiles observed for fuel F-2747. Exponential oxygen profiles can be interpreted as occurring in a process that is first-order in oxygen; the complexity of oxygen diffusion from the headspace to the liquid fuel prevents us from drawing conclusions on the reaction order. The deposition is quite substantial during the oxidation period of the first 8 h, and then levels off as the oxygen is completely consumed. This correspondence between deposition and oxidation is strong evidence that oxidation reactions result in deposition, and that the deposition reactions quickly "turn off" when oxygen is no longer present. This fuel is particularly interesting to study because both oxidation and deposition occur fairly rapidly and to a large enough extent that they can be measured readily. Thus, this fuel is a prime candidate for studies of the mechanism of antioxidant and detergent/dispersant additives.

Solid-phase extraction (SPE) techniques have proven to be extremely valuable for the analysis of oxidation products and additives in jet fuels (Schulz, 1992). These techniques allow one to concentrate and remove the polar and oxygenated compounds from the fuel. We have used SPE techniques in an attempt to improve the thermal stability of a fuel and to concentrate the compounds that play a role in degrading the thermal stability. We have added this extract to a thermally stable fuel to determine if the thermal stability is significantly degraded. Briefly, 60–70 mL of unstressed fuel was passed through a 6-mL Bakerbond Silica Gel SPE cartridge (J.T. Baker). The cartridge was back extracted with 2–3 mL of methanol. The methanol back extract was roto-evaporated at 65–70 °C to remove most of the methanol. The results of this study are shown in Figure 8. Plotted in the figure is the fuel F-2827 before and after SPE treatment. The treatment appears to improve the thermal stability greatly. We have also observed significant improvement in the thermal stability of F-2922 by a clay-treating process. The polar compounds extracted from unstressed F-2827 were then back-extracted from the cartridge by elution with

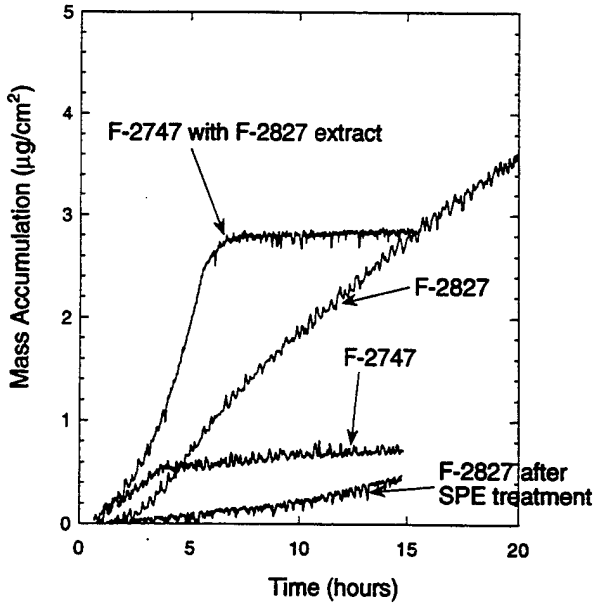

Figure 8. Plots of solid-phase extraction experiments.

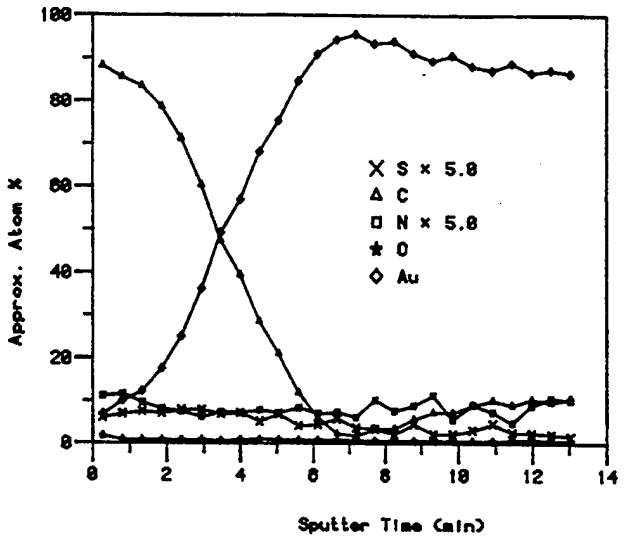

Figure 9. Auger spectroscopy on gold electrode of quartz crystal for fuel F-2747.

methanol. This back extract was added to F-2747, a fuel with a high thermal stability. These results are also shown in Figure 8. It is apparent that the addition of the F-2827 extract to F-2747 decreases the thermal stability of the fuel. Also note that the deposition occurs during the first 5–6 h of the run and then levels off. Thus this fuel still appears to consume oxygen readily (no pressure measurements were performed), but now forms significantly more deposits. We are in the process of attempting to identify the compounds responsible for this behavior, but at the present time it appears as if phenol-containing and sulfur-containing compounds play a key role in the inhibition of oxygen consumption and the formation of deposits.

We have used Auger and X-ray photoelectron (XPS) spectroscopies to study the gold electrode surfaces onto which the fuel deposits in the QCM test. The results for Auger spectroscopy are shown in Figures 9 and 10 for the fuels F-2747 and F-2827, respectively. The plots show both surfaces have carbon deposited with the F-2827 deposit being much thicker than F-2747. The gold surface occurs approximately where the carbon and gold plots cross. The sputtering rate used was 20 Å/min, which corresponds to a deposit thickness of 70 and 200 Å for

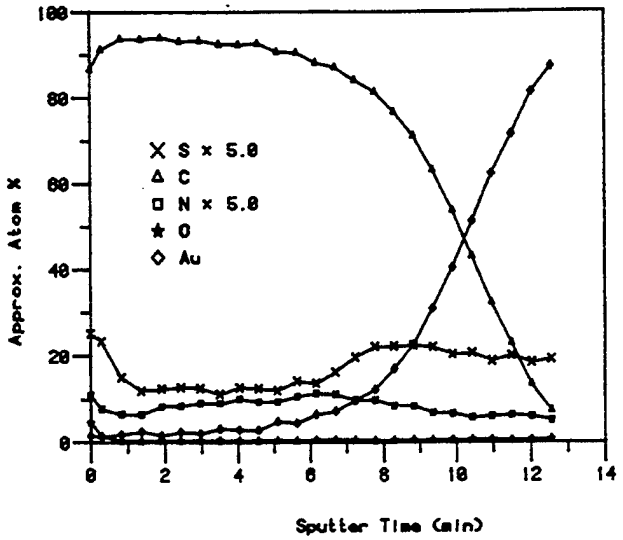

Figure 10. Auger spectroscopy on gold electrode of quartz crystal for fuel F-2827.

Table 2. X-ray Photoelectron Spectroscopy Analysis of Surface of Gold Electrode of Quartz Crystal for Two Fuels Stressed at 140 °C for 15 h

fuel	atom	type of bonding	approx atomic %
F-2747	C	C=O, C–O	6.5
	C	C–N, C–C=N	8.2
	C	CH, C	60.3
	O		17.5
	N		3.6
	S	S–O	2.1
	Au		1.7
F-2827	C	C=O, C–O	7.9
	C	C–N, C–C=N, C–S	9.3
	C	CH, C	56.1
	O		18.9
	N		2.7
	S	S–O	2.5
	S	S–C	1.2
	Si		2.5

F-2747 and F-2827, respectively. For these runs, the QCM measures a final surface mass of 0.6 and 4.0 $\mu g/cm^2$ for F-2747 and F-2827, respectively. Also, measured by Auger spectroscopy were sulfur, nitrogen, and oxygen atoms. The plots show that more sulfur is incorporated into the F-2827 deposit, a result that is not surprising since we know that F-2827 contains a greater concentration of sulfur. The two fuels show similar amounts of nitrogen in the deposits. Very little oxygen is observed due to the low sensitivity this technique has for oxygen.

The results for XPS analysis are shown in Table 2. The major surface species is carbon, with approximately 18% oxygen for both fuels. The F-2827 deposit exhibits a higher concentration of sulfur, in agreement with the Auger data. For F-2827 the sulfur is found bonded to both oxygen and carbon atoms, while only the oxygen form is found in F-2747. The nitrogen concentration is slightly higher for F-2747. Gold is observed on the F-2747 surface demonstrating that the deposit is relatively thin and/or does not entirely cover the surface. Silicon is also observed on the surface of the F-2827 deposit; the source is unknown.

We have studied the temperature dependence of deposition for fuel F-2827 over the range 140–180 °C. The deposition rate increases with increasing temperature. Figure 11 shows data taken for the fuel F-2827 at three temperatures 140, 160, and 180 °C. It is apparent that the deposition rate increases upon moving from 140 to 160 °C. The 160 °C deposition appears to begin to level off near 8 h. At first glance the 180 °C plot appears to show

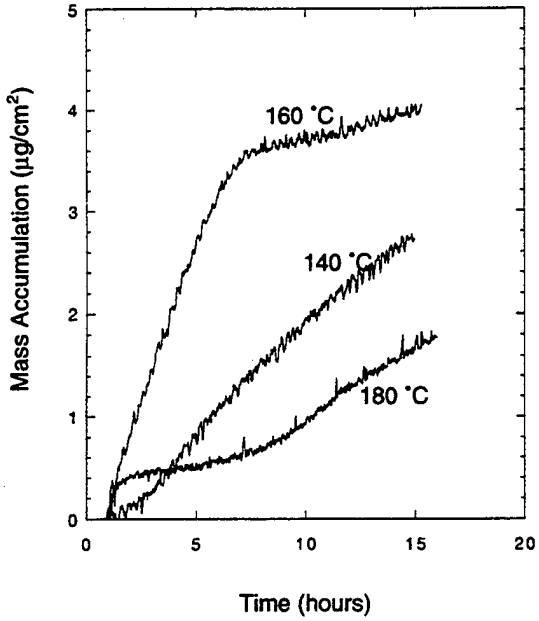

Figure 11. Plots of mass accumulation vs time for fuel F-2827 at three temperatures: 140, 160, and 180 °C.

lower deposit formation. This is due to the fact the deposition rate is so rapid that most of the deposition occurs within the 30–45 min heat-up time of the Parr bomb. As the QCM only measures a relative mass, the deposition needs to be minimal during this period in order to correctly measure deposition under the oxygen limited conditions employed here. One possible technique to circumvent this limitation is to purge the fuel of oxygen for the heat-up period and only add air/oxygen after the temperature has stabilized. This technique may be attempted in the future. Also, Klavetter and Martin (1993) have recently developed an automatic temperature compensation technique for the QCM. The technique compensates for the viscosity changes with temperature of the liquid. Using this technique, mass deposition during the heat-up time may be able to be measured.

The three fuels studied here represent three classes of fuels that have been encountered during this study. It is difficult to generalize about properties of fuels, as the variety of fuels is great. However, the data taken during the study of over 20 different fuels has resulted in the separation of these three classes by their thermal stability characteristics, as measured by the QCM, and oxygen consumption characteristics, as measured by pressure measurements. The classification of these three fuel types is summarized in Table 3. The first class of fuel, as represented by fuel F-2747, exhibits very good thermal stability and consumes oxygen readily. This class of fuel includes pure hydrocarbon species such as *n*-dodecane, and high thermal stability fuels such as JP-7. Some hydrotreated fuels appear in this class. These fuels tend to lack easily oxidized compounds that can act as antioxidants, and thus tend to oxidize rapidly. The lack of these compounds, which may include sulfur compounds that are removed by hydrotreatment, results in fuels that exhibit good thermal stability characteristics. The second class of fuels is represented by fuel F-2827; these fuels exhibit poor thermal stability and consume oxygen relatively slowly. These fuels contain easily oxidized species that act as antioxidants, reducing the oxygen consumption rate. Some of these easily oxidized species, such as certain sulfur compounds, may cause the fuel to have poor thermal stability characteristics. These fuels tend to be unhydrotreated. These two classes of fuels characterize the

Appendix D.

Studies of Jet Fuel Additives Using the Quartz Crystal Microbalance and Pressure Monitoring at 140° C

Steven Zabarnick
Rebecca R. Grinstead
University of Dayton
300 College Park
Dayton, OH 45469-0140

Reprinted from I&EC RESEARCH, 1994, 33.

Studies of Jet Fuel Additives Using the Quartz Crystal Microbalance and Pressure Monitoring at 140 °C

Steven Zabarnick* and Rebecca R. Grinstead

Aerospace Mechanics Division / KL-463, University of Dayton Research Institute, 300 College Park, Dayton, Ohio 45469-0140

The quartz crystal microbalance (QCM) and pressure monitoring are used for the evaluation of jet fuel additives for the improvement of jet fuel thermal stability. The mechanisms of additive behavior are determined by measuring the time-dependent deposition with the QCM and oxidation by pressure measurements. Studies at various additive concentrations permits the determination of optimum additive concentrations. Additive packages made of mixtures of antioxidants, detergent/dispersants, and metal deactivators are shown to yield good improvements in thermal stability over a wide range of jet fuel types.

Introduction

Recent advances in jet aircraft and engine technology have placed an ever increasing heat load on the aircraft. The bulk of this excess heat is absorbed by the aircraft fuel, as jet fuel is used as the primary coolant for the numerous heat sources. This hot fuel reacts with dissolved oxygen to form oxidized products and deposits. The formation of deposits results in the fouling of fuel lines, valves, actuators, nozzles, and various other aircraft components with the potential to result in catastrophic failure. Jet fuel additives are added to fuel in small quantities to improve its oxidation and deposition characteristics.

In this paper we present results on the study of four classes of jet fuel additives: antioxidants, dispersants, detergents, and metal deactivators. Other additives used in jet fuels are lubricity enhancers, static dissipaters, and corrosion inhibitors. Antioxidants interfere with the fuel autoxidation chain mechanism by intercepting peroxy radicals, which are the primary radicals responsible for continuing the chain (Zabarnick, 1993). These antioxidant molecules have an easily abstractable hydrogen atom which encourages reaction with peroxy radicals. Dispersants and detergents usually consist of molecules with a polar "head" attached to a long nonpolar hydrocarbon chain. In a nonpolar fuel the hydrocarbon chain is attracted to the bulk fuel, and the polar head is attracted to any polar compounds or groups of compounds present in the fuel. Dispersants work by surrounding these polar compounds forming a micelle-like structure around the polar compound. Thus, the polar compounds present are not able to aggregate and form larger groups of polar compounds that would result in formation of insoluble deposits and gums. Detergents act in a similar manner, but the polar head actually binds to the surface while the hydrocarbon chain extends into the fuel. Detergents are able to remove polar species from surfaces. Metal deactivators are species that can bind to metal atoms that may be present as atomic or molecular species in the bulk fuel or can also bind to metal surfaces. The interaction of these metal deactivator species with the bulk and/or surface metal atoms discourages the well-known catalysis of chemical reactions by metals.

The present work is part of the Air Force JP-8 + 100 program, in which an additive package is being developed to extend the thermal stability of JP-8 jet fuel by 100 °F ("thermal stability" refers to the deposit-forming tendency of a fuel). This program involves the evaluation of proprietary and nonproprietary additives from many manufacturers. Table 1 lists the additives studied in this work, their additive classification (as stated by the manufacturer), and the type of compound, if known. In this work, a quartz crystal microbalance (QCM) is used for the real-time, *in situ* monitoring of the surface deposition. Also, a pressure transducer is used to monitor the pressure decay in the reactor that results from oxygen reaction. The combination of a very sensitive technique for monitoring deposition (QCM), along with a method for directly monitoring oxidation (pressure measurements) allows us to not only evaluate additives but also to study and classify additives based upon their deposition/oxidation characteristics.

Experimental Section

The experimental apparatus has been described in detail previously, and will only be discussed briefly here (Klavetter et al., 1993; Zabarnick, 1994). The fuel is stressed in a 100 mL Parr bomb reactor which has been modified with an rf feedthrough for the quartz crystal microbalance. It is heated with a clamp-on band heater which is controlled by a PID temperature controller via a thermocouple which is immersed in the fuel. The reactor is filled with 60 mL of fuel and thus contains a ≈40 mL headspace. The fuel and headspace are sparged with air for 1 h at room temperature prior to each run. At the end of the sparge period the reactor is sealed at atmospheric pressure and the heater is turned on. At this point the computer data acquisition is initiated. The computer monitors the quartz crystal frequency, the crystal damping voltage, the temperature, and the headspace pressure at 1 min intervals. A typical run is performed for 15 h at a temperature of 140 °C. QCM

* To whom correspondence should be addressed. E-mail: zabarnic@udavxb.oca.udayton.edu.

0888-5885/94/2633-2771$04.50/0

Table 1. Properties of Additives Studied

additive name and supplier	additive classification	type of compound	concn (mg/L)	% active ingredient
Betz SPEC-AID 8Q405	dispersant	proprietary	100	proprietary
DuPont JFA-5	high-temperature thermal stability package	mixture of antioxidant, dispersant, and metal deactivator	12	proprietary
BHT	antioxidant	2,6 di-*tert*-butyl-4-methylphenol	25	100
MDA	metal deactivator	*N,N'*-disalicylidene-1,2-propanediamine	10	73–75
Mobil MCP-477	detergent	proprietary	300	100

Table 2. Properties of Fuels Studied

fuel no. and designation	hydrotreated?	JFTOT breakpoint (°C)	sulfur mass %	other notes
F-2747 (Jet A-1)	yes	332	<0.05	light depositor
F-2827 (Jet A)	no	282	0.10	heavy depositor
F-2922 (Jet A)	yes	277	0.02	fast oxidizer
F-2963 (JP-5)	not known	232	0.04	high copper fuel
F-2799 (JPTS)	yes	398	<0.05	high thermal stability
F-2926 (Jet A)	not known	288	0.10	
F-2980 (Jet A)	no	288	0.10	Merox treated
F-2936 (JP-5)	not known	277	0.10	
F-2934 (Jet A-1)	not known	266	0.10	high acid number
F-2985 (JP-5)	not known	266	not measured	high in nitrogen compds

deposition data are only valid during the relatively constant (±0.3 °C) period of the run after the ≈45 min heat-up time. The Parr reactor is cleaned thoroughly between runs and a new quartz crystal is used for each run.

The change in the quartz crystal frequency in time at constant temperature is used to monitor the deposition. The quartz crystals used were 5 MHz, 2.54 cm diameter, 0.33 mm thick, AT-cut wafers. These crystals, obtained from Maxtek Inc., were manufactured with gold electrodes and overtone polished. The quartz crystal resonator is driven at 5 MHz by an oscillator circuit that was developed at Sandia National Laboratories (Klavetter et al., 1993). This circuit tracks the impedance variations of the crystal in order to determine the resonant frequency of the device. The oscillator circuit also provides an amplitude output that indicates crystal damping. The reactor was also fitted with a Sensotec 0-50 psia absolute pressure transducer.

The theory that relates the measured frequency changes to surface mass has been presented in detail elsewhere (Martin et al., 1991), and will only be discussed briefly. When a crystal is excited at its resonant frequency, it undergoes a shear deformation with displacement maxima at the crystal faces. Mass accumulation on the crystal surface moves synchronously with the surface, resulting in a decrease in the resonant frequency. Also, a thin layer of liquid can be entrained by the surface, also resulting in a decrease in the resonant frequency. The decrease in resonant frequency is described by

$$\Delta f_0 \approx -\frac{2f_0^2}{N(\mu_q \varrho_q)^{1/2}}\left[\varrho_s + \left(\frac{\varrho\eta}{4\pi f_0}\right)^{1/2}\right] \qquad (1)$$

where f_0 is the unperturbed resonant frequency, N is the harmonic number, μ_q is the quartz shear stiffness, ϱ_q is the quartz mass density, ϱ_s is the surface mass density (mass/area), and ϱ and η are the liquid density and viscosity, respectively. Thus the frequency change is due to two terms: the first results from changes in surface mass density (the quantity we wish to measure); the second is due to changes in liquid properties (density and viscosity). If the liquid properties are constant, then changes in frequency can be used to determine surface mass accumulation. The liquid properties, density and viscosity, should remain relatively constant under conditions where temperature is held constant and the chemistry of the fuel is restricted to small extents of reaction. Under these conditions the surface deposition can be related to the frequency as

$$\varrho_s = -(2.21 \times 10^5 \text{ g/(cm}^2 \text{ s)})\frac{\Delta f}{f_0^2} \qquad (2)$$

for the fundamental resonance. The surface deposition measurements reported here occur for fuel oxidation at constant temperature (±0.4 °C) and under limited oxygen conditions, where only a small fraction of the fuel molecules undergo chemical change (Zabarnick, 1994). Thus, the fuel density and viscosity remain constant during our measurements, and the above equation can be used to measure surface deposition.

Under conditions where the liquid properties are changing, the amplitude output of the oscillator circuit can be used to determine the motional resistance of the crystal (Klavetter et al., 1993). The motional resistance can then be related to these changes in liquid properties, and thus the changes in liquid properties can be resolved from the surface mass accumulation. We have observed changes in crystal damping for some of the additives studied in this work, despite observing no changes in liquid fuel properties. No changes in crystal damping were observed for any of the neat (unadditized) fuels during a run. The implications of these changes in crystal damping will be discussed below.

In general, the reproducibility of the mass deposition measurements on fuels is limited to ±20% for the QCM technique. This estimate of the precision of the technique was derived from multiple runs of the same fuel, performed for various fuels.

Results and Discussion

In Table 2 are listed the fuels studied here and their properties. We have chosen to perform additive testing using a wide variety of different fuels to ensure that the additive evaluation is not biased by the study of a single fuel type. Thus this work involves the study of both hydrotreated and unhydrotreated fuels. In this paper we report on a representative sample of fuel types. The first fuel is a non-hydrotreated Jet A fuel that is a moderate to heavy depositor, called fuel F-2827. This fuel exhibits a relatively low JFTOT (jet fuel thermal oxidation test) breakpoint and contains a measurable

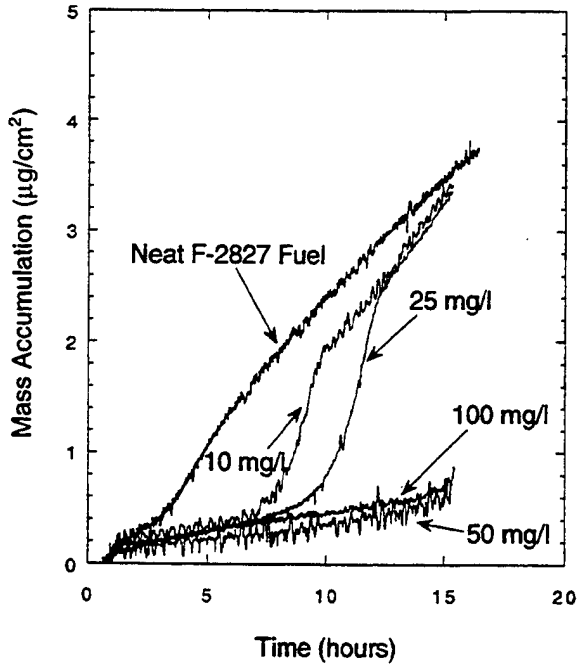

Figure 1. Plots of mass accumulation vs time for fuel F-2827 with varying concentrations of SPEC-AID 8Q405.

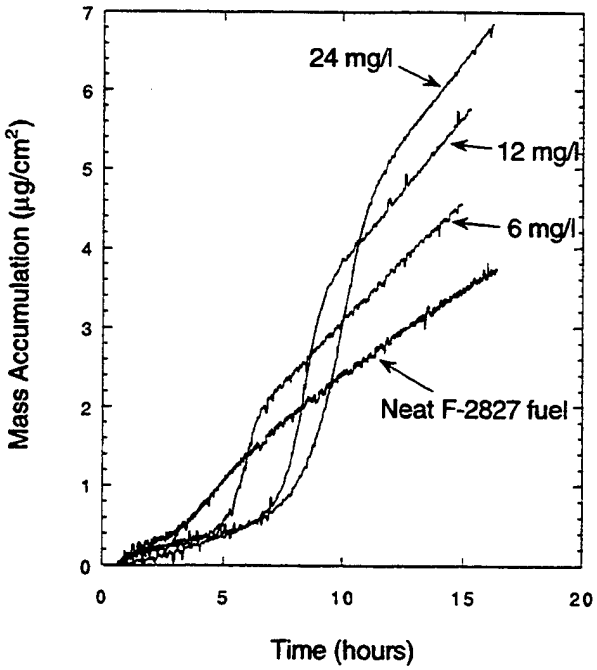

Figure 2. Plots of mass accumulation vs time for fuel F-2827 with varying concentrations of JFA-5.

amount of sulfur. In Figure 1 are shown the deposition results from the QCM for fuel F-2827 at 140 °C for 15 h with varying concentrations of Betz SPEC-AID 8Q405. This additive is classified as a dispersant by the manufacturer (see Table 1). The additive concentration was varied from 0 to 100 mg/L. The figure demonstrates that at all concentrations tested the additive significantly improves the thermal stability of this fuel at short times. At 10 mg/L SPEC-AID 8Q405 shows a large improvement in thermal stability until ≈7 h, at which time the deposition rate increases. At long times the deposition begins to approach that of the unadditized fuel. Similar behavior is exhibited for the 25 mg/L run, except here the low deposition region is extended out to ≈9 h. Also shown in the figure are runs with 50 and 100 mg/L of SPEC-AID 8Q405. These two runs exhibit low deposition during the entire 15 h experiment. Within the experimental uncertainty the deposition at 50 and 100 mg/L are the same. We will show below that though SPEC-AID 8Q405 has limited antioxidant characteristics it works primarily as a dispersant. The concentration dependence demonstrated in Figure 1 implies that at low concentrations the dispersant capability of this additive is overwhelmed by the relatively high concentration of polar species and/or aggregate particles generated in this fuel. At 50 mg/L and above there exists a high enough concentration of the additive to disperse the polar species created by the autoxidation process over the entire 15 h run time of the experiment. These results show how an additive concentration can be optimized for a given fuel and stressing conditions using the QCM. It is important to understand that this concentration dependence is only valid for the temperature, time, and oxygen availability conditions of this experiment. At higher temperatures, it is expected that the oxidation rate will increase, thus deposit rate increases will occur, shortening the time to the sudden deposition rate change in this fuel/additive combination. The final amount of deposition after oxygen consumption is completed is mainly controlled by the oxygen availability in the system and thus should not be greatly affected by relatively small changes in temperature. With relatively large changes in temperature, mechanistic changes will occur in the autoxidation process, resulting in changes in both oxidation and deposition (Zabarnick, 1993).

In Figure 2 are shown the deposition data for DuPont JFA-5 in fuel F-2827 over the concentration range 0−24 mg/L. The figure demonstrates that JFA-5 improves the thermal stability of F-2827 early in the run, but at all concentrations the deposition increases above that of the neat fuel later in the run. The 6 mg/L run shows improved deposition until 5 h into the run, after which the deposition is ≈0.5 $\mu g/cm^2$ above the neat fuel. The 12 mg/L run shows low deposition until ≈7 h, after which the deposition is 1-2 $\mu g/cm^2$ above the neat fuel. In the 24 mg/L run, the deposition remains low for ≈8 h, after which deposition is 2-3 $\mu g/cm^2$ above the neat fuel. It appears that JFA-5 actually decreases the fuel thermal stability for extended stressing times. An added complication in interpreting these data is the observation that for these runs with JFA-5 the crystal damping voltage did not remain constant during the course of the run. The damping voltage was observed to increase along with the apparent increase in deposition observed at long times. Changes in damping voltage are normally caused by changes in the fuel density and viscosity. These properties were measured after the completion of thermal stressing; under the conditions employed in this study no significant changes in viscosity and density were observed. As the liquid properties are not changing during the run, the change in damping voltage must be due to some other process that causes crystal damping. One possibility is the formation of a thin viscous film on the crystal electrode surface. The formation of such a film would result in a damping voltage change and an apparent increase in deposition due to the decrease in crystal frequency caused by the film formation. We have no other evidence to support this supposition, but at this time viscous film formation appears to be a reasonable hypothesis to explain the observations.

If the formation of viscous films result in anomalous increases in deposition for JFA-5, how do we evaluate

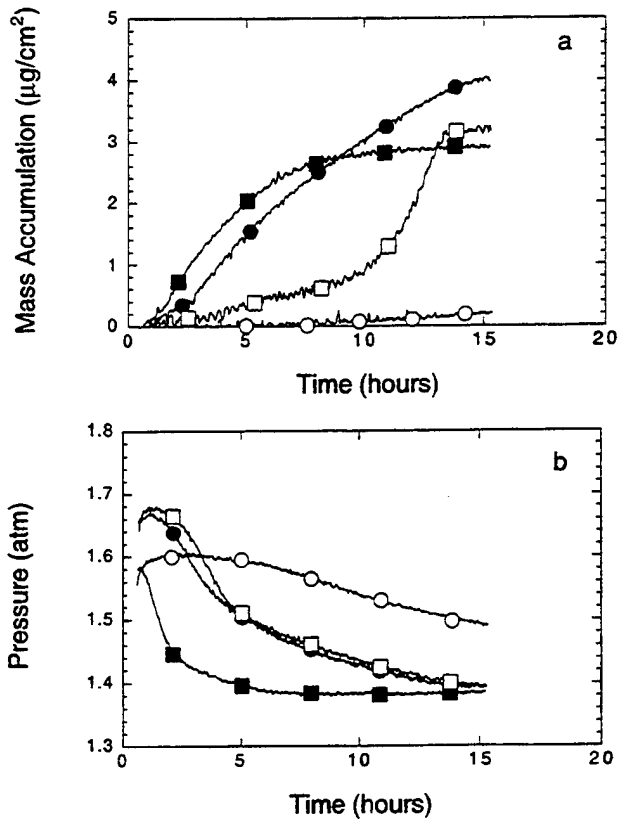

Figure 3. Plots of mass accumulation and pressure vs time for fuel F-2922: ■, neat fuel; ●, with 25 mg/L BHT; □, with 100 mg/L SPEC-AID 8Q405; ○, with both SPEC-AID 8Q405 and BHT.

this additive properly? As we have no data on the properties of this film, it is safer to assume that its formation is a negative characteristic of the additive. It is reasonable to expect that the formation of a viscous film would add to the fouling of fuel systems and therefore be a characteristic to be avoided in a potential additive. The formation of gums in fuels is detrimental to fuel systems, and a viscous film is likely to affect fuel negatively by a similar mechanism.

The effects of the addition of SPEC-AID 8Q405 and BHT in fuel F-2922 are shown in Figure 3. This fuel is hydrotreated and oxidizes quite rapidly as shown by the relatively rapid pressure decay observed for the unadditized fuel. BHT, which is an antioxidant, is added at 25 mg/L and causes a significant slowing of the oxidation. The unadditized fuel consumes oxygen over the first 7 h, at which time the pressure decay levels as the oxygen present is completely consumed. The additized fuel continues to consume oxygen even up to the end of the 15 h run. The additized fuel also appears to have a higher initial vapor pressure, perhaps due to the carrier oil in which the additive is dissolved. The effect of the additive on the fuel thermal stability is also shown in the figure. The additized fuel produces deposition to a smaller extent until 9 h, at which time the deposition increases above that of the unadditized fuel. The smaller deposition at short times appears to be due to the slower rate of oxidation that results from the presence of the antioxidant. However, when the oxygen is consumed, the additive actually results in increased deposition. This effect has been observed for a wide variety of antioxidants in fuel F-2922. Apparently, the polar nature of the antioxidant molecules result in their causing increased deposition upon their being oxidized. It is well-known that the presence of polar, easily oxidizable molecules has a detrimental effect on the thermal stability of fuels (Hazlett, 1991). We have found, as shown below, that the addition of a detergent/dispersant additive can prevent the antioxidant from causing a reduction in the thermal stability of the fuel. Thus one gets the positive effect of the antioxidant inhibition of the oxidation process without increased deposition.

Also shown in Figure 3 are results for the addition of 100 mg/L of SPEC-AID 8Q405 to F-2922. SPEC-AID 8Q405 is classified by the manufacturer as a dispersant. The figure shows that oxidation is slowed by the addition of this additive; this pressure decay is very similar to that observed for BHT. This additive also decreases the deposition significantly up to 10 h, when the deposition suddenly increases, leveling off at a mass accumulation similar to the unadditized fuel at 14 h. Thus, although this additive displays antioxidant properties, it also shows a significant effect on the deposition, as also observed for fuel F-2827 in Figure 1. Apparently, the sudden increase in deposition observed at 10 h is also due to this dispersant additive being overwhelmed by the large production of polar species in this fuel. Note that Figure 1 shows that the sudden increases in deposition in fuel F-2827 containing SPEC-AID 8Q405 occurs at much lower concentrations than for F-2922. We have observed previously that F-2827 consumes oxygen much more slowly than F-2922 (Zabarnick, 1994); thus the optimum concentration of a dispersant will be higher for the faster oxidizing fuel (F-2922), as seen here.

The effect due to the addition of both SPEC-AID 8Q405 and BHT to fuel F-2922 is also shown in Figure 3. The oxygen decay is very slow when the two additives are present; oxygen consumption is only partially complete at 15 h. At these concentrations the antioxidant properties of these two additives appears to be enhanced by the presence of the other. The deposition measured is extremely low during the entire run, reaching only 0.2 $\mu g/cm^2$ at the end of the run. In this hydrotreated fuel, a combination of antioxidant and detergent/dispersant appears to work quite well; the antioxidant slows the oxidation, while the dispersant keeps the polar compounds formed during oxidation in solution so that they cannot aggregate to form larger depositing species. Note that the slowly oxidizing, nonhydrotreated fuel F-2827 does not require the presence of the antioxidant additive to achieve low deposition with the addition of SPEC-AID 8Q405 (Figure 1).

We have found two requirements for a fuel to be useful in evaluating antioxidants at 140 °C for use in a thermal stability additive package. The fuel must oxidize relatively rapidly so that the oxidation is easily monitored, and the fuel must produce an easily measurable amount of deposits. Fuels that are slow oxidizers, such as F-2827, are not useful for evaluating antioxidants; such fuels tend to be heavy depositors. Fuels that oxidize rapidly, such as F-2747 (Zabarnick, 1994), have a tendency to be very light depositors, making it difficult to evaluate their effect on thermal stability. A fuel such as F-2922 which oxidizes rapidly and produces an easily measured amount of deposits, as shown in Figure 3, is ideal for evaluation of antioxidants.

JPTS is a special-purpose jet fuel developed for the U-2 aircraft. This fuel has excellent thermal stability characteristics and contains 12 mg/L JFA-5 by specification. We have examined the oxidation and thermal stability of a JPTS fuel (F-2799) with and without JFA-

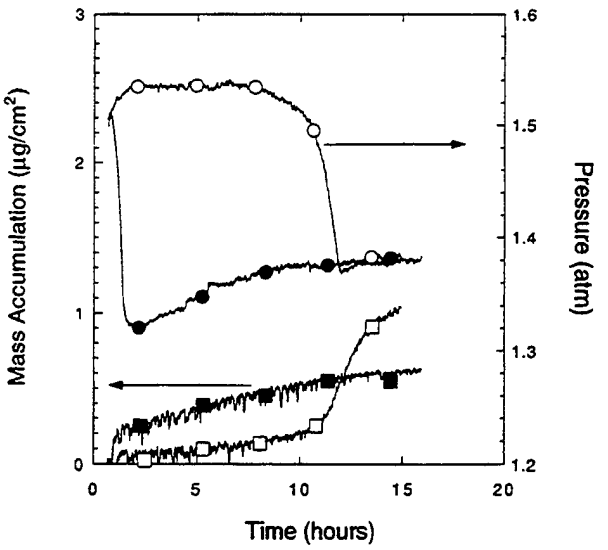

Figure 4. Plots of mass accumulation and pressure vs time for fuel F-2799: □, mass accumulation of fuel; ■, mass accumulation of fuel without JFA-5; ○, pressure of fuel; ●, pressure of fuel without JFA-5.

5; the data are shown in Figure 4. JFA-5 is an additive package which consists of an antioxidant, a dispersant, and a metal deactivator. Figure 4 shows that the presence of the additive greatly delays the oxidation process. The unadditized fuel oxidizes very rapidly, reaching a minimum pressure in less than 2 h. The additized fuel oxidizes very slowly over the first 7 h; oxidation then occurs rapidly, reaching a minimum pressure at 12 h. The additized fuel produces deposits slowly during the first 10 h, at which time there is a sudden increase in the deposition rate. This sudden increase corresponds to the time of pressure decrease that results from the oxidation of this fuel. The unadditized fuel produces deposits during the early, rapid oxidation, and then deposits more slowly after 2 h. It is possible that some of the deposition is missed in the unadditized fuel, as the oxidation process occurs rapidly and can occur during the 45 min heat-up time, when the deposition process cannot be monitored. It is apparent from the large delay in the oxidation and deposition of the additized fuel that JFA-5 acts as an antioxidant under these conditions. Presumably, the species responsible for this delay is the antioxidant present in the JFA-5 package.

The effect of additives on fuel F-2963 is shown in Figure 5. This is a JP-5 fuel which has been doped with ≈50 ppb copper. The presence of copper in fuel is known to result in decreased thermal stability; the U.S. Navy uses copper fuel lines in its aircraft carriers and therefore has problems with copper contamination of its fuels (Morris et al., 1988). Figure 5 shows that the neat fuel produces deposits quite heavily, leveling off at near 6 $\mu g/cm^2$ at 12 h. The pressure plot also shows that the neat fuel consumes oxygen over the first 9 h of the run. The addition of 100 mg/L of SPEC-AID 8Q405 results in much decreased deposition, although the deposition rate shows a rapid increase at 11 h before leveling off at 13 h. The addition of SPEC-AID 8Q405 also slows the oxidation of the fuel. Also shown in the figure is the combination of SPEC-AID 8Q405 and BHT. This combination further decreases the oxidation rate and also decreases the final amount of deposits measured. No sudden change in deposition rate is observed with this additive combination. Also shown in the figure is

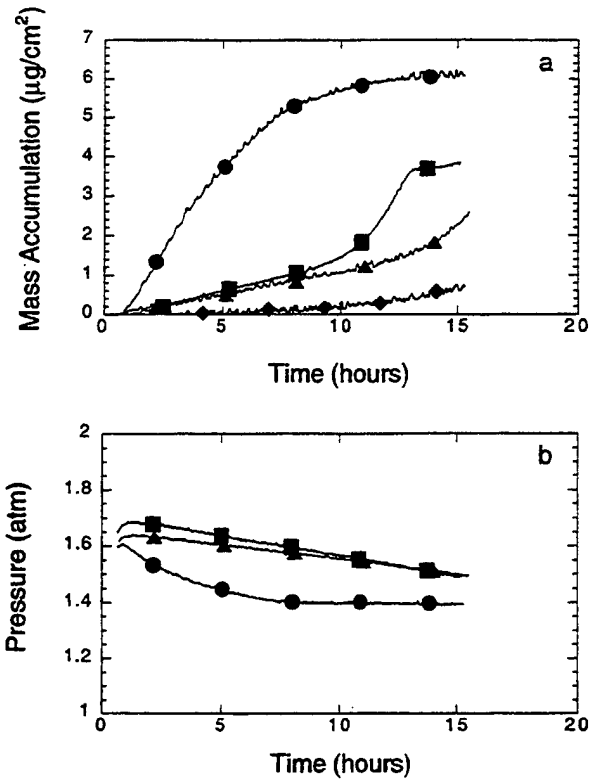

Figure 5. Plots of mass accumulation and pressure vs time for fuel F-2963: ●, neat fuel; ■, with 100 mg/L SPEC-AID 8Q405; ▲, with 100 mg/L SPEC-AID 8Q405 and 25 mg/L BHT; ◆, with SPEC-AID 8Q405 and BHT and 10 mg/L MDA.

the effect of adding SPEC-AID 8Q405, BHT, and 10 mg/L MDA. MDA is a metal deactivator which is thought to improve the thermal stability characteristics of fuels which contain an excess of dissolved metal species. This three additive combination further decreases the deposition observed in this fuel (no pressure measurements are available for this additive combination).

We have tested the effectiveness of a variety of additives and additive packages in a variety of different fuels. A comparison of four additive combinations in eight different fuels is shown in Figure 6. The mass accumulation plotted is the QCM measured final accumulation at the end of the 15 h run at 140 °C. The time chosen can affect the comparative results as some additized fuels show sudden increases in deposition following a period of relatively light deposition (e.g., see Figure 2). We have chosen the mass accumulation at 15 h for comparison purposes as it represents a worst case for fuels which display sudden deposition increases. Thus this comparison will be biased against such additives. The horizontal line near 1 $\mu g/cm^2$ represents the deposition of JPTS a fuel with very good thermal stability characteristics and whose mass accumulation is a goal of the additive program. The neat fuels shown in the figure display deposition over the range 2.9−10 $\mu g/cm^2$. The addition of SPEC-AID 8Q405 alone improves some fuels substantially (F-2980 and F-2827), some slightly (F-2985 and F-2963), and some not at all (F-2926 and F-2922). Fuels F-2926 and F-2922 are both fuels that oxidize readily (F-2922 is hydrotreated); it has been demonstrated in static tests with bubbling oxygen that these fuels produce copious deposits when given unlimited oxygen (Grinstead, 1993). Thus, an antioxidant, BHT, was added to these fuels in order to limit the rate of oxidation. The figure shows that the addition

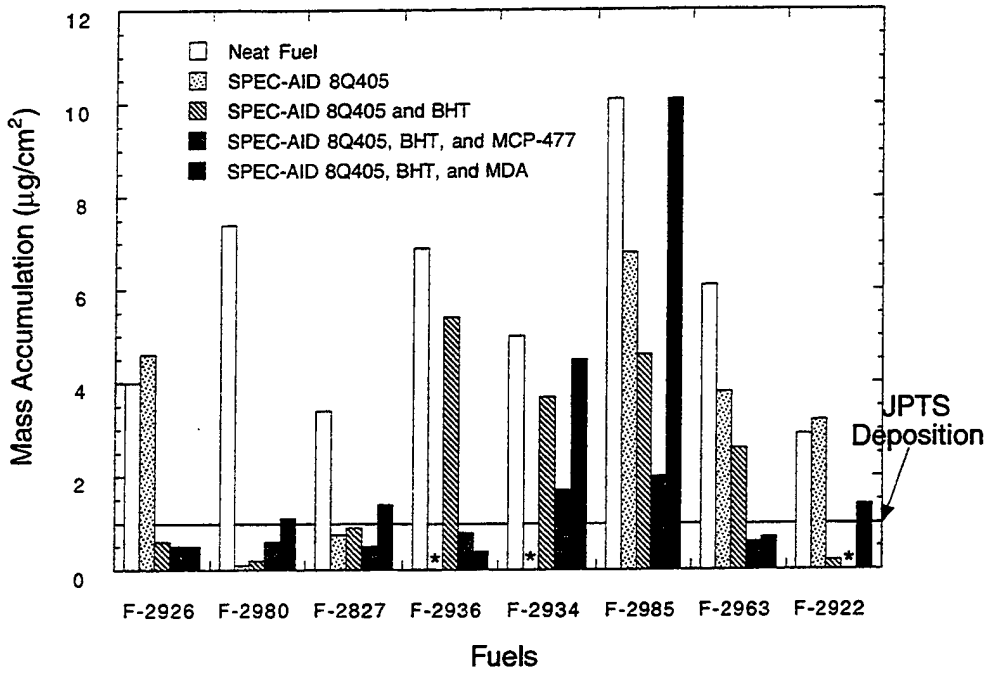

Figure 6. Comparison of QCM mass accumulation for six fuels with four additive packages. An asterisk indicates a fuel/additive combination test that was not performed.

of BHT greatly improves the behavior of F-2922 and F-2926 but only slightly improves the other fuels, all of which are slower oxidizers. The addition of BHT does not significantly worsen the thermal stability of fuels F-2827 and F-2980, which were strongly improved by SPEC-AID 8Q405. Thus the combination of SPEC-AID 8Q405 and BHT, a dispersant and antioxidant, significantly improves four of the eight fuels (this additive combination also improves a variety of other similar fuels). The other four fuels (F-2936, F-2934, F-2985, and F-2963) show only partial improvements with this additive package. These four relatively heavily depositing fuels have proven to be very difficult to improve with additives. It was found that the addition of a second detergent, Mobil MCP-477, to the package produced significant improvements, as shown in the figure. The addition of MCP-477 brings both F-2936 and F-2963 below the 1 $\mu g/cm^2$ goal, while F-2985 and F-2934 remain slightly above the goal. Unfortunately, it was found in flowing tests at higher temperatures that this three-additive package generally increased deposition above the neat fuel. This discrepancy between higher temperature flowing tests and the 140 °C QCM measurements only occurred for packages involving MCP-477. Apparently MCP-477 enhances deposition at higher temperatures; further work on the QCM at higher temperatures is being studied in order to determine the cause of this discrepancy. The fourth additive combination shown in the figure is for MDA, a metal deactivator, added to SPEC-AID 8Q405 and BHT. This gives surprisingly poor results for fuels F-2934 and F-2985, markedly increasing their deposition. The only fuel in which this package shows improvement over the SPEC-AID 8Q405 and BHT package is fuel F-2963. This result is not surprising considering that fuel F-2963 has been doped with 50 ppb of copper (see Table 2); a metal deactivator additive is designed to improve such a fuel. Other tests at higher temperatures have shown significant improvements for MDA (Grinstead, 1993); future QCM work at higher temperatures will attempt to study this behavior.

In the past, jet fuel additives have been evaluated in a wide variety of experimental devices. Various workers have used modified and unmodified versions of the JFTOT at various temperatures; see for example Morris et al. (1988). Flask oxidation tests have been performed to evaluate antioxidants, see for example Kendall and Mills (1986). Also, relatively large scale single tube heat exchangers have been used to measure the effects of additives, see for example Clark (1988). These various tests differ in the essential parameters for examining fuel thermal stability: temperature, stress duration, oxygen availability, and surface materials, among others. Most tests are conducted under accelerated conditions, where the temperature or oxygen availability is increased above real fuel systems conditions. The study of additives in this work was performed at 140 °C, a relatively low temperature compared with other thermal stability tests. The presence of an air headspace in our reactor yields a higher oxygen availability than a flowing test by a factor of ≈4 (Zabarnick, 1994). Also, the fact that our test is conducted in static mode at low temperatures dictates that the test time be relatively long (15 h). Aircraft fuel systems consist of extremely complex pathways for fuel flow with various residence times at various temperatures; these temperatures and residence times vary with flight conditions; e.g., higher fuel system temperatures may occur at flight idle descent. In the laboratory, it is impossible to test additives under the exact conditions of an aircraft. These QCM tests address one set of conditions that the fuel may encounter—low temperature and moderate oxygen availability—as might occur in the fuel tank or fuel recirculation line. Higher temperature flowing tests may do a better job of simulating high-temperature parts of the fuel system, such as the engine fuel nozzle. High oxygen availability tests, such as flask tests with bubbling oxygen, address a different regime. The Air Force JP-8 + 100 additive program is using a wide variety of tests in an attempt to simulate most conditions to which a fuel is subjected. A successful additive package must have the ability to prevent deposition over

Appendix E.

Dissolved Oxygen Concentration and Jet Fuel Deposition

Jamie S. Ervin
Theodore F. Williams
University of Dayton
300 College Park
Dayton, OH 45469-0140

Dissolved Oxygen Concentration and Jet Fuel Deposition

Jamie S. Ervin* and Theodore F. Williams

University of Dayton Research Institute, 300 College Park, Dayton, Ohio 45469-0210

The effects of low dissolved oxygen concentrations on fuel thermal stability are far from being understood; however, such an understanding is essential for aircraft fuel system design. Experiments were conducted using a flowing system in which the dissolved oxygen level at the entrance of the apparatus is varied. One of the most intriguing results of these experiments is the increase in deposits in heated sections for decreased oxygen consumption. This observation is seemingly contrary to nearly all previous observations concerning the relation between deposit formation and oxygen consumption. For a given system, there appears to be a least favorable dissolved oxygen concentration which produces the maximum amount of deposits. In addition, the deposition mechanisms in heated locations were quite different from those in cooled regions.

Introduction

Recent advances in jet aircraft technology have placed an ever-increasing heat load on aircraft cooling systems. Fuel is circulated through the airframe and engine components because it offers effective heat transfer without the increased complexity associated with other media, such as air. Unfortunately, upon heating, jet fuel reacts with dissolved oxygen gas to produce oxidized products and deposits that can block fuel lines, foul close-tolerance valves, and deteriorate sealing materials (Hazlett, 1991; Mushrush et al., 1994; Ervin et al., 1995). Additives can be added to fuels in small quantities to improve their oxidation and deposit-forming characteristics (Zabarnick and Grinstead, 1994). However, a more direct approach to inhibit fouling may be to reduce the dissolved oxygen concentration within the fuel before heating.

It has long been thought that reducing the dissolved oxygen would decrease the resulting deposition. This has been observed in the limiting case of zero oxygen concentration (Zabarnick and Grinstead, 1994; Heneghan et al., 1995; Edwards and Krieger, 1995). Surprisingly, relatively few studies have considered the effects of oxygen availability on deposition except in the case of complete oxidation. In previous works (Bradley et al., 1974; Taylor, 1974, 1976; Taylor and Frankenfeld, 1978; Frankenfeld and Taylor, 1980), the effects of intermediate levels of dissolved oxygen (5–40 ppm oxygen) on surface fouling were not studied in detail, and the flow conditions and temperature fields were not well-defined. More recent works (Heneghan et al., 1995; Jones et al., 1995) have studied the formation of jet fuel deposits under conditions of relatively high bulk fuel temperatures and complete consumption of the dissolved oxygen such that deposition and oxidation follow each other. However, in aircraft, the dissolved oxygen may be only partially consumed because of generally large fuel flow rates which necessarily result in lower residence times and bulk fuel temperatures than those available in most flow studies.

A fundamental understanding of the effect of low dissolved oxygen concentrations, partial oxidation conditions, and recirculation on thermal stability (thermal stability refers to the deposit-forming tendency of the fuel) is incomplete but essential in aircraft design for several reasons. On certain military jets, the fuel tanks are vented to the ambient air. At high altitudes, the ambient pressure is reduced significantly, resulting in a diminished concentration of dissolved oxygen. In addition, as a fire-preventative measure, an inert gas generating system may be used to reduce the oxygen level in the fuel tank ullage space and, ultimately, in the liquid fuel. Moreover, as fuel flows through intricate fuel system passages, only part of the oxygen may react as the thermal oxidation process occurs. Finally, fuel recirculation systems using ram air heat exchangers are likely to be part of future designs. The effect of these three characteristics on the formation of jet fuel deposits must be more fully understood. For this purpose, experiments were conducted using a flow system in which the dissolved oxygen level at the entrance of the apparatus is varied. High flow rates allowed for incomplete oxygen consumption, and a three-part heat exchanger simulated a complicated thermal and flow environment.

Table 1. Neat Fuel Properties

fuel (Jet A)	sulfur, mass %	aromatic s, vol %	JFTOT breakpoint (°C)
F-2980	0.1	17.0	288
F-2827	<0.05	19.0	282

Experimental Section

Table 1 lists characteristics of neat (Jet A) F-2980 and F-2827, the two base fuels used in this study. From extensive testing performed elsewhere (for example, Zabarnick and Grinstead, 1994) in a variety of test devices, these fuels are considered to be representative fuels. For all tests, both F-2980 and F-2827 were additized with JP-8 additives. Fuels which contain additives in the amounts (military specification MIL-T-83133) listed in Table 2 are referred to as JP-8 fuels.

In the experimental apparatus which is described in detail in Heneghan et al. (1993) (Figure 1), JP-8 fuel at ambient temperature passes from the preconditioning tank at a pressure of 2.48 MPa into the heated sections. At this pressure level, the fuel exists as a subcooled liquid. In the preconditioning tank, nitrogen and oxygen are bubbled through the fuel to control the amount of dissolved oxygen which enters the test section. Dissolved oxygen concentrations at the inlet were varied from 70 to 1 ppm (mass basis). (The nominal dissolved oxygen concentration for air-saturated fuel is 70 ppm.) Bulk dissolved oxygen levels were measured at the locations shown in Figure 1 by means of a Hewlett

* Author to whom correspondence is addressed. E-mail: ervin@udavxb.oca.udayton.edu.

0888-5885/96/2635-0899$12.00/0

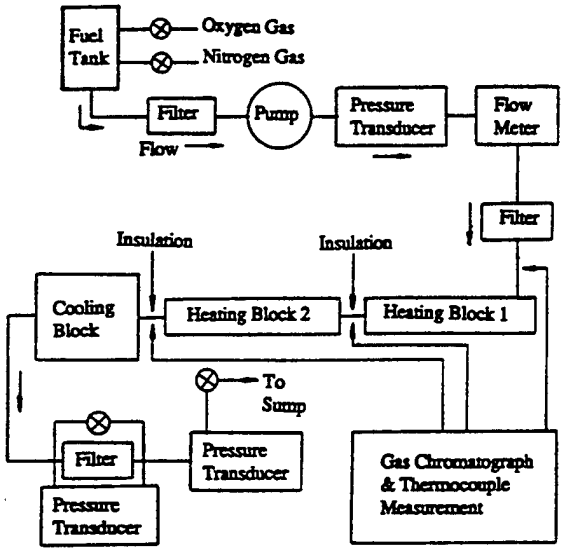

Figure 1. Experimental apparatus.

Packard 5890 Series II gas chromatograph (Rubey et al., 1992). After passing through two heated sections, the fuel flows into the cooled section and then is collected in a waste reservoir.

Two heated copper blocks envelope the 316 stainless steel tubing (180-cm long by 2.16-mm i.d. by 3.18-mm o.d.) through which the fuel passes. Each block (46-cm long with a 7.6-cm diameter) is heated in such a way that the tube wall temperature distribution remains steady (within ±2 °C). The tubing between the heated blocks is insulated. In the cooled section, the tubing is clamped within a copper block (46-cm long with a 7.6-cm diameter) which has internal passages through which chilled water flows. Calibrated thermocouples (20 gauge) are welded to the outer surface of the stainless steel tubing to provide the outer tube wall temperatures with an uncertainty of ±2 °C. The stainless steel tubes (ASTM-grade A269/A213) have a surface roughness (arithmetic average) of 8−15 μin. and are cleaned with a Blue Gold alkaline solution in an ultrasonic bath, rinsed with deionized water, and dried with flowing laboratory-grade nitrogen gas prior to use.

Fluid dynamics is an important but poorly understood element of fouling. An oxygen concentration distribution for a laminar velocity distribution is anticipated to be quite different from the concentration profile occurring with turbulent flow conditions for otherwise identical circumstances (Katta et al., 1995). Moreover, turbulent rather than laminar flow is more likely in actual aircraft. In the present experiments the volumetric flow rate, which was monitored by a positive displacement flow meter, was varied to examine the effects of flow velocity on the observed deposition. Two volumetric flow rates of 62 and 100 mL/min were used. For both flow rates, the flow was laminar at the entrance of the first heated block. At 62 mL/min, the Reynolds number based on the tube diameter (Re_D) was 1500 at the exit of the first heated section and 2500 at the exit of the second. At 100 mL/min, the Re_D was 2500 at the outlet of the first heated section and 3500 at the exit of the second.

The temperature profile within the tube is strongly influenced by the fluid dynamics. As a consequence, two different tube wall temperatures were imposed by the copper heating blocks. The heated tubing had wall temperatures near 563 K for the flow rate of 100 mL/min and nominally 543 K for the flow rate of 62 mL/min. Preliminary experiments showed that the wall temperature of 563 K imposed at 100 mL/min resulted in sufficiently measurable deposition and an oxygen consumption rate similar to that at the lower wall temperature and flow rate. In addition, the test duration was such that nearly the same total volume of fuel passed through the system. Thus, the experiments were conducted for periods of 24 h at 62 mL/min and 15 h at 100 mL/min.

At the termination of an experiment, the tubes were removed from the system, drained, and rinsed with hexane. They were then dried by flowing filtered, low-velocity nitrogen gas through them. Finally, they were sliced into 50-mm segments and heated in a vacuum oven at 120 °C for 1 h. A Leco (RC-412) multiphase carbon analyzer determined the mass of carbon on the segments. The reproducibility in the determination of the carbon deposit profile is on the order of ±5%, determined by sequential tests performed within 1 week using fuel from the same batch. Certain remaining segments, halved in the axial direction, were examined using scanning electron microscopy (SEM) to study the deposit microstructure and X-ray photoelectron spectroscopy (XPS) for chemical analysis. The XPS data were obtained with a modified AES ES-100 photoelectron spectrometer which is equipped with a magnesium X-ray source. Data reduction was performed using ESCA Tools Software (Surface/Interface Inc.). XPS determined the composition of the first three nanometers of the inner tube surface which was exposed to the thermally stressed fuel. Uncertainties in the absolute value of the composition are on the order of ±10% of the reported value.

Results and Discussion

In Figure 2, the mass of carbon obtained from carbon burnoff measurements is normalized by the inner surface area of the tube. The deposits were produced using F-2980 fuel under different inlet oxygen concentrations and a flow rate of 62 mL/min. In addition, the wall temperature distribution, given by polynomial fits of the measured values, and the computed bulk temperature distribution are provided for reference. In the experiments performed here, the deposits were extremely thin (on the order of microns) and, as a result, did not appreciably affect the heat transfer or fluid motion.

To compute the bulk temperature profile, the steady temperature and velocity distributions within the fuel were first obtained by the finite difference solution of the Navier−Stokes, turbulent energy, and enthalpy equations. The governing equations were discretized utilizing a hybrid scheme (Spalding, 1972) and solved sequentially using a uniform grid system of 30 nodes in the radial direction and 195 nodes in the axial direction. With this node distribution, the computed

Table 2. Properties of Additives

additive name and supplier	additive classification	type of compound	concn (mg/L)
DiEGME	icing inhibitor	diethylene glycol, monomethyl ether	25
DuPont Stadis 450	static dissipator	proprietary	2
DCI-4A	corrosion inhibitor/lubricity enhancer	proprietary	9

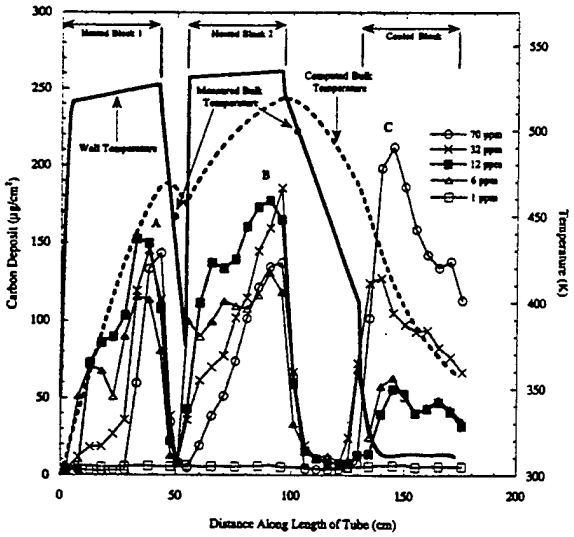

Figure 2. Carbon deposit profiles. F-2980 flowing at 62 mL/min for various O_2 levels.

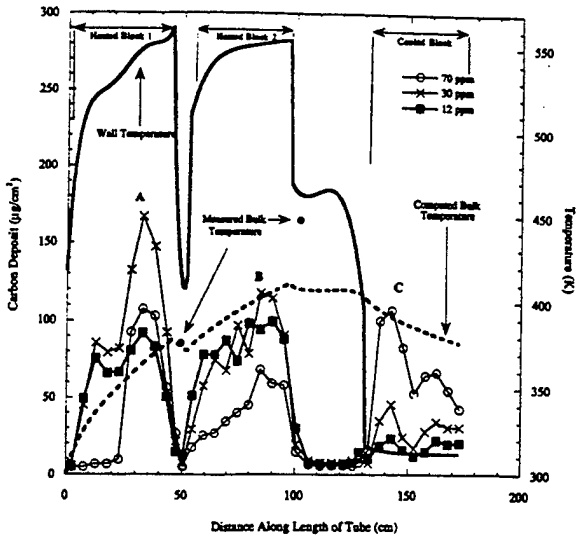

Figure 3. Carbon deposit profiles. F-2980 flowing at 100 mL/min for various O_2 levels.

results were fairly insensitive to additional grid refinement. Uniform velocity profiles were used at the tube entrance, and values of the flow variables at the tube exit were obtained by extrapolating the data at the interior nodes. Wall functions (Launder and Spalding, 1974) for the turbulent flow calculations were used to determine the gradients of the flow variables near the wall boundary. Fluid motion inside the tube was assumed to be axisymmetric, and a cylindrical coordinate system was used. The thermal conductivity, viscosity, enthalpy, density, and specific heat of the fuel at a given temperature are obtained from curve fits developed from available fuel data (Nixon et al., 1967). Further details of the computational method are given in Katta and Roquemore (1993). Turbulent simulations resulted in bulk temperatures which approximated the measured values at both 62 and 100 mL/min more accurately than did the laminar computations. The appearance of turbulence at low Re_D for horizontal fuel flow in a small-bore tube has been observed previously (Katta et al., 1995). It is believed that buoyancy forces normal to the forced-flow direction increase the heat and mass transport, rendering the flow turbulent.

Figure 2 shows three peaks, labeled A, B, and C, in the carbon deposit distribution. Between A and B, deposition abruptly declines as the wall temperature decreases and the bulk temperature has not yet begun to decrease. Deposition then increases near 51 cm as the wall temperature approaches 543 K. Between B and C, near 102 cm, another steep decline occurs in the deposition profile, which again coincides with a decrease in the wall temperature. Although the bulk temperature (522 K) at 102 cm is greater than that (461 K) at 49 cm, the deposition still falls to low levels, similar to those obtained with 1 ppm dissolved oxygen. Figure 2 shows that the deposition more closely follows the wall temperature than the bulk fuel temperature. The dependence of the deposition on wall temperature was also observed for experiments at 100 mL/min (Figure 3) and for fuel F-2827 (not shown).

In the heated sections, the dependence of deposition on wall temperature suggests preferential deposition at the stainless steel walls, the radial location in the tube of maximum temperature. In addition, it is known that the nature of the tube surface may influence the deposition rate (Kendall and Mills, 1985; Clark, 1988; Hazlett, 1991). Because of the greater temperatures existing at the wall together with the potential catalytic effects of the stainless steel, the fuel oxidation rate may be greatest there. Some theories (Hazlett, 1991) for the formation of deposits assume that particles nucleate, grow, and agglomerate within the liquid bulk and then adhere to heated surfaces. However, Figures 2 and 3 suggest that the adherence of bulk particles alone does not adequately describe deposit formation. If agglomerated particles form in the bulk fuel and then adhere to the wall, the sharp drop in deposition, such as that which occurs at 49 and 102 cm, might not be expected (assuming wall adherence is not very temperature dependent) because the bulk temperature at 102 cm is greater than that at 49 cm. In fact, more deposits might then be anticipated to form at 102 cm because of the higher bulk temperatures; however, this was not observed.

From the carbon deposit profiles of Figure 2, it is noticed that in the first heated section (between 0 and 49 cm) the profiles for dissolved oxygen concentrations less than 70 ppm rise above background levels near the tube entrance, well upstream of that for air-saturated conditions. In this region of the tube, as the initially thin thermal boundary layer develops near the heated wall, the radial temperature gradient is large at the wall but decreases with increasing axial distance. In the second heated section (between 55 and 99 cm) following the insulated tube, the thermal boundary layer again develops. The deposit profiles for initial dissolved oxygen concentrations below 70 ppm again rise at locations upstream of the point where the deposit profile for initially air-saturated fuel rises. In addition, this upstream rise in the deposit profiles for initial dissolved oxygen levels which are below 70 ppm was observed at the greater flow rate (Figure 3) and with F-2827 (not shown). In a flowing system, the oxygen consumption is controlled by both the kinetics of oxidation and the species transport. The fuel near the wall is heated at a faster rate (within a smaller volume) and for a greater residence time than fuel passing through the center of the tube. It is believed that the development of thermal and species boundary layers is connected in some, as yet, unknown way to the upstream rise in deposits of fuels with initial dissolved oxygen concentrations below 70 ppm.

At location C of Figures 2 and 3, the wall temperature is a minimum, yet the level of deposition is of the same

Table 3. XPS Analysis of Deposits in Heated and Cooled Sections for Various Inlet O_2 Levels (F-2827 at 62 mL/min)[a]

inlet oxygen (ppm)/ location (cm)	OC=O	C=O	CO	CH, CN, C	O	Fe	Cr	N	SO	SC	Si
70/60	6.8	2.3	11.5	50.0	23.5	1.5		2.4	1.1	0.9	
70/140	1.6	2.5	7.3	55.7	21.8	3.0		4	3.7	0.4	
30/60	4.8	3.5	7.0	56.9	21.9	<0.3		0.8	<0.4		4.3
30/140	1.5	2.8	8.8	54.1	22.2	0.6	1.6	3.5	1.7	0.9	2.4
12/60	2.8	3.2	7.0	44.8	24.2	<0.8		1.3	1.3		5.0
12/140	1.2	2.8	7.7	51.0	25.5	1.0		4.4	5.0		1.5
new tube	4.8	1.9	5.4	30.2	30.1	14.6	4.1	<0.7	0.9	<0.2	7.1

[a] OC=O, acids and esters; C=O, aldehydes and ketones; CO, alcohols and ethers; SO, sulfur oxides; N, nitrogen compounds.

Table 4. Carbon Deposits in Heated and Cooled Sections for Various Inlet O_2 Levels (F-2980 at 62 mL/min and 24 h)

	oxygen consumed				deposits	
inlet oxygen concentration (ppm)	heated block 1 (ppm)	heated block 2 (ppm)	total oxygen consumed (ppm)	fraction consumed	heated blocks (μg)	cooled block (μg)
70	5	11	16	0.23	4057	4774
30	4	6	10	0.33	5800	2976
12	3	5	8	0.67	7420	1253
6	1	3	4	0.67	6007	1400
1	0.7	0.3	1.0	1.0	482	183

Table 5. Carbon Deposits in Heated and Cooled Sections for Various Inlet O_2 Levels (F-2980 at 100 mL/min and 15 h)

	oxygen consumed				deposits	
inlet oxygen concentration (ppm)	heated block 1 (ppm)	heated block 2 (ppm)	total oxygen consumed (ppm)	fraction consumed	heated blocks (μg)	cooled block (μg)
70	3	10	13	0.19	2881	2018
30	1	7	8	0.27	5676	871
10	2	1	3	0.30	4853	542

Table 6. Carbon Deposits in Heated and Cooled Sections for Various Inlet O_2 Levels (F-2827 at 62 mL/min and 24 h)

	oxygen consumed				deposits	
inlet oxygen concentration (ppm)	heated block 1 (ppm)	heated block 2 (ppm)	total oxygen consumed (ppm)	fraction consumed	heated blocks (μg)	cooled block (μg)
70	4	7	11	0.16	2986	6179
32	1	5	6	0.19	5727	2407
16	4	6	10	0.63	4573	1201

order as that at A and B where the temperature is greater. Hence, Figures 2 and 3 show that deposition mechanisms in the heated locations are different from those within the cooled tube. Furthermore, the oxygen consumption within the cooled tube was immeasurably small, in contrast to that measured in the heated sections (Tables 4–6) which contain locations A and B. The deposits in the cooled section are not the same as those "mature" deposits typically found in the heated sections when oxidation is complete. This is confirmed by the presence of acetone-soluble material in the cold tube but not in the heated tube. In addition, the XPS measurements of Table 3 for F-2827 at the flow rate of 62 mL/min show chemical differences between the deposits formed at locations 60 (heated section) and 140 cm (cooled section) shown in Figure 2. The OC=O composition is lower at 140 cm, but the sulfur oxide and nitrogen compositions are greater there. Also, there are striking differences in the morphology of the deposits formed in the heated sections and those formed in the cooled section, as shown in the micrographs of Figure 4. In the heated section, the deposits form layers which have a microspheroid structure (Figure 4a, SEM, magnification 5000×) that has been observed previously (Schirmer, 1970). However, in the cooled tube (Figure 4b, SEM, magnification 1000×), the deposit is a film which has no perceptible small-scale structure and conforms to the microgeometry of the underlying stainless steel surface. (The new tube is shown for reference.) The formation of two types of deposits has particular importance to the development of recirculating fuel systems. Recirculation systems will use a ram air heat exchanger to cool the fuel to an appropriate temperature prior to returning it to the fuel tanks. These heat exchangers would then be likely collectors of the second type of deposits found here.

Deposits are believed to accumulate within the cooled section as a result of oxidized fuel products becoming less soluble at lower temperatures. In a preliminary study to investigate the effects of fouling within the cooled tube (Figure 1), two different means of cooling were used. With the first, the copper block was cooled by free convective heat exchange with the ambient air. With the second, chilled water was circulated through passages within the copper block. Greater deposition (an order of magnitude) was obtained with water cooling which produced lower temperatures (as much as 50 °C lower) than those realized with air cooling. Increased deposition in cooled regions downstream of heated sections has been seen previously in a few instances (Heneghan et al., 1995).

The deposition profiles of Figures 2 and 3 are influenced by the inlet dissolved oxygen concentration. In Figures 2 and 3 at locations A and B, the measured deposition is greater for dissolved oxygen concentrations near 30 and 12 ppm than for air-saturated fuel. The XPS measurements in Table 3 reveal chemical differences in the deposits formed at 60 cm under conditions of different inlet oxygen levels. The levels of OC=O, CO, and N in the deposit are lower for 30 and 12 ppm than for air-saturated conditions. At 12 ppm, there appears to be a significant decrease in the hydrocarbon

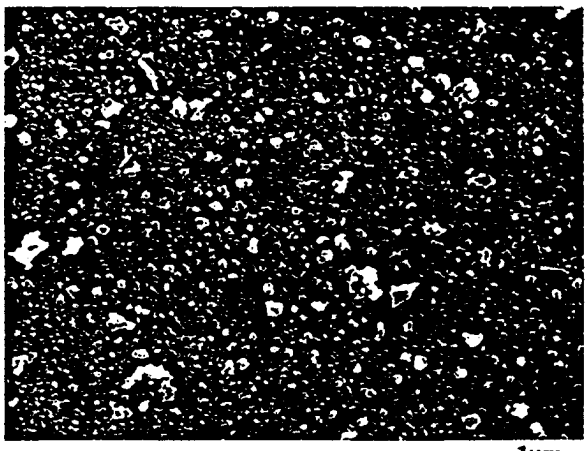

(a)

(b)

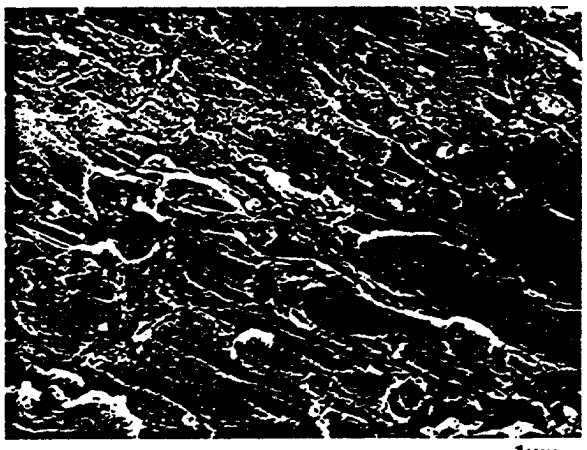

(c)

Figure 4. SEM micrographs F-2827 fuel: (a) 60 cm, 70 ppm (heated section, 5000×); (b) 140 cm, 12 ppm (cooled section, 1000×); (c) new tubing (5000×).

and carbon compositions. The microstructure of the deposits formed at 60 cm did not change as the oxygen concentration was varied from 70 to 16 ppm. For all oxygen levels, the microstructure consists of layers of spheroid particles (Figure 4), as described earlier.

At location C of Figure 2, deposition, presumably related to solubility phenomena, is greatest for the inlet oxygen concentration of 70 ppm. Lower inlet levels of dissolved oxygen resulted in lower levels of deposits in the cooled tube (between 95 cm and the exit). The relationship between inlet oxygen concentration and the mass of deposits formed in the cooled section is quite different from that in the heated sections; that is, the deposition in the cooled section declines with decreasing inlet oxygen concentrations. Similar trends in oxygen consumption and deposition are also observed at 100 mL/min (Table 5) and for F-2827 (Table 6). These observations suggest that oxygen is somehow effective at inhibiting deposit formation in the heated section as well as being responsible for deposit formation in the cooled section.

Table 4 shows that, with decreasing inlet oxygen concentrations for F-2980 flowing at 62 mL/min, the mass of deposits in the heated sections approaches a maximum for an inlet oxygen concentration of 12 ppm and then falls with lower oxygen concentrations. Moreover, the fraction of oxygen consumed in the heated section (ratio of the concentration of consumed oxygen to that available at the inlet) increases with decreasing inlet oxygen availability. This behavior is particularly important for aircraft fuel system design because most fuel systems do not stress the fuel at high enough temperatures and/or long enough times to allow the dissolved oxygen to react completely. Thus, only a fraction of the oxygen is likely to be consumed. Deposition is significantly reduced for the test in which the inlet dissolved oxygen concentration (1 ppm) is of the same order as the amount consumed. Except for oxygen levels at or below 10 ppm, Tables 4–6 show that oxygen consumption is greatest within the second heated block (between 55 and 95 cm of Figures 2 and 3) where the bulk temperature is highest. Thus, Tables 4–6 show, for a given fuel and system, that a least favorable dissolved oxygen content exists which produces the maximum mass of deposits.

One intriguing result is that increases in deposits in the heated sections coincide with decreased oxygen consumption. With static testing under conditions of partial oxygen consumption and reduced oxygen availability, Zabarnick et al. (1995) recently observed that deposition is not necessarily reduced. This observation is seemingly contrary to nearly all previous observations concerning the relation of deposit formation and oxygen consumption (Heneghan et al., 1995; Jones et al., 1995). Further, it is in conflict with theories concerning the formation of deposits (Heneghan and Zabarnick, 1994; Hazlett, 1991). Zabarnick et al. (1995) have hypothesized that production of antioxidant species at high oxygen levels can inhibit oxidation and deposition processes. They also propose that a change in chemical kinetic reaction order with dissolved oxygen level can play a role. To date, a complete understanding of the connection between oxidation and deposit formation is not available. Moreover, the relation is complicated by the fact that deposition under conditions of complete oxygen consumption is different from deposition under partial oxidation conditions and may be affected by the original oxygen concentration.

Conclusions

Jet fuel deposit formation involves complex chemical and physical processes. In air-saturated fuel at low temperatures, it is commonly accepted that deposits form from a series of free-radical chain reactions, but these reactions are not understood. The most obvious difference between previous investigations and the results found here is that only a fraction of the available oxygen was consumed in the current study. From

discussion of the results obtained in this work, the following conclusions may be drawn:

1. Fuel deoxygenation may sometimes increase surface fouling, an important finding for future fuel system design.

2. Deposits formed with deoxygenated fuel and partial oxygen consumption arise from reactions different from those with air-saturated fuel and complete oxygen consumption.

3. Global reaction mechanisms are used frequently in reactive fluid dynamics computational models for engineering design purposes, but the results of the present experiments suggest that the mechanisms currently assumed in some fouling models may be inadequate.

Acknowledgment

This work was supported by the U.S. Air Force, Aero Propulsion and Power, Fuels and Lubrication Division, Wright Laboratories, Wright-Patterson AFB, Dayton, OH, under Contract No. F33615-92-C-2207 (Technical monitor: C. W. Frayne). The authors also acknowledge the many helpful discussions with Dr. Shawn Heneghan and Dr. Steven Zabarnick of the University of Dayton Research Institute and Dr. V. R. Katta of Innovative Scientific Solutions, Inc.

Nomenclature

ASTM = American Society for Testing and Materials
D = tube diameter, m
F-2827 = Jet A neat fuel
F-2980 = Jet A neat fuel
JFTOT = jet fuel thermal oxidation test
JP-8 = F-2827 or F-2980 with additives given by MIL-T-83133
Re_D = Reynolds number, $\rho DU/\mu$, dimensionless
SEM = scanning electron microscopy
U = mean velocity, m/s
XPS = X-ray photoelectron spectroscopy
μ = dynamic viscosity, N s/m^2
ρ = density, kg/m^3

Literature Cited

Bradley, R.; Bankhead, R.; Bucher, W. High Temperature Hydrocarbon Fuels Research in an Advanced Aircraft Fuel System Simulator on Fuel AFFB-14−70 (AFAPL-TR-73-95). Air Force Aero Propulsion Laboratory, Wright-Patterson Air Force Base, Dayton, OH, 1974.

Clark, R. H. The Role of a Metal Deactivator in Improving the Thermal Stability of Aviation Kerosines. *Proceedings of the 3rd International Conference on Stability and Handling of Liquid Fuels*; London, U.K., 1988; U.S. Department of Energy: Washington, DC, 1988; p 283.

Edwards, T.; Krieger, J. The Thermal Stability of Fuels at 480 °C: Effects of Test Time, Flow Rate, and Additives. Presented at ASME Turbo Expo '95, Houston, TX, June 1995.

Ervin, J. S.; Heneghan, S. P.; Martel, C. R.; Williams, T. F. Effects of Surfaces on Deposits Resulting from Thermally Stressed Jet Fuels. *ASME J. Eng. Gas Turb. Power* **1995**, in press.

Frankenfeld, J.; Taylor, W. Deposit Formation from Deoxygenated Hydrocarbons. 4. Studies in Pure Compound Systems. *Ind. Eng. Chem. Prod. Res. Dev.* **1980**, *19*, 65.

Hazlett, R. N. *Thermal Oxidation Stability of Aviation Turbine Fuels*; ASTM: Philadelphia, 1991.

Heneghan, S. P.; Zabarnick, S. Oxidation of Jet Fuels and the Formation of Deposits. *Fuel* **1994**, *73*, 35.

Heneghan, S.; Williams, T.; Martel, C.; Ballal, D. Studies of Jet Fuel Thermal Stability in a Flowing System. *ASME J. Eng. Gas Turb. Power* **1993**, *115*, 480.

Heneghan, S.; Martel, C.; Williams, T.; Ballal, D. Effects of Oxygen and Additives on the Thermal Stability of Jet Fuels. *ASME J. Eng. Gas Turb. Power* **1995**, *117*, 120.

Jones, E. G.; Balster, W. J.; Post, M. E. Degradation of a Jet-A Fuel in a Single Pass Heat Exchanger. *ASME J. Eng. Gas Turb. Power* **1995**, *117*, 125.

Katta, V. R.; Roquemore, W. M. Numerical Method for Simulating Fluid Dynamic and Heat Transfer Changes in Jet Engine Injector Feed-Arm Due to Fouling. *J. Thermophys. Heat Transfer* **1993**, *7*, 651.

Katta, V. R.; Blust, J.; Williams, T. F.; Martel, C. R. Role of Buoyancy in Fuel−Thermal Stability Studies. *J. Thermophys. Heat Transfer* **1995**, *9*, 159.

Kendall, V. R.; Mills, J. S. The Influence of JFTOT Operating Parameters on the Assessment of Fuel Thermal Stability. Society of Automotive Engineers Meeting, Longbeach, CA, Oct 1985.

Launder, B. E.; Spalding, D. B. The Numerical Computation of Turbulent Flows. *Comput. Methods Appl. Mech. Eng.* **1974**, *3*, 269.

Mushrush, G. W.; Beal, E. J.; Pellenberg, R. E.; Hazlett, R. N.; Eaton, H. R.; Hardy, D. R. A Model Study of the Thermal Decomposition of Cumene Hydroperoxide and Fuel Instability Reactions. *Energy Fuels* **1994**, *8*, 851.

Nixon, A. C.; Ackerman, G. H.; Faith, L. E.; Henderson, H. T.; Ritchie, A. W.; Ryland, L. B.; Shryne, T. M. Vaporizing and Endothermic Fuels for Advanced Engine Application: Part III, Studies of Thermal and Catalytic Reactions, Thermal Stabilities, and Combustion Properties of Hydrocarbon Fuels (AFAPL-TR-67−114). Air Force Aero Propulsion Laboratory, Wright-Patterson Air Force Base, Dayton, OH, 1967.

Rubey, W.; Striebich, R.; Anderson, S.; Tissandier, M.; Tirey, D. In Line Gas Chromatographic Measurement of Trace Oxygen and Other Dissolved Gases in Flowing High Pressure Thermally Stressed Jet Fuel. *Prepr.—Am. Chem. Soc. Div. Petrol. Chem.* **1992**, *37*, 371.

Schirmer, R. Morphology of Deposits in Aircraft and Engine Fuel Systems. Society of Automotive Engineers National Air Transportation Meeting, New York, April 1970.

Spalding, D. B. A Novel Finite Difference Formulation for Difference Expressions Involving Both First and Second Derivatives. *Int. J. Numer. Methods Eng.* **1972**, *4*, 551.

Taylor, W. Deposit Formation from Deoxygenated Hydrocarbons. I. General Features. *Ind. Eng. Chem. Prod. Res. Dev.* **1974**, *13*, 133.

Taylor, W. Deposit Formation from Deoxygenated Hydrocarbons. II. Effect of Trace Sulfur Compounds. *Ind. Eng. Chem. Prod. Res. Dev.* **1976**, *15*, 64.

Taylor, W.; Frankenfeld, J. Deposit Formation from Deoxygenated Hydrocarbons. 3. Effects of Trace Nitrogen and Oxygen Compounds. *Ind. Eng. Chem. Prod. Res. Dev.* **1978**, *17*, 87.

Zabarnick, S.; Grinstead, R. Studies of Jet Fuel Additives Using the Quartz Crystal Microbalance and Pressure Monitoring at 140 °C. *Ind. Eng. Chem. Res.* **1994**, *33*, 2771.

Zabarnick, S.; Zelesnik, P.; Grinstead, R. Jet Fuel Deposition and Oxidation: Dilution, Materials, Oxygen, and Temperature Effects. *ASME J. Eng. Gas Turb. Power* **1995**, in press.

Received for review June 20, 1995
Revised manuscript received November 27, 1995
Accepted December 6, 1995[⊗]

IE950378J

[⊗] Abstract published in *Advance ACS Abstracts,* February 1, 1996.

Appendix F.

Silver Corrosion and Sulfur Detection Using a Quartz Crystal Microbalance with Silver Electrode Surfaces

Steven Zabarnick
Paula Zelesnik
Shawn D. Whitacre
University of Dayton
300 College Park
Dayton, OH 45469-0140

Silver Corrosion and Sulfur Detection Using a Quartz Crystal Microbalance with Silver Electrode Surfaces

Steven Zabarnick, Paula Zelesnik, and Shawn D. Whitacre

Aerospace Mechanics Division,
University of Dayton Research Institute,
300 College Park/KL-463,
Dayton, Ohio 45469-0140

INDUSTRIAL & ENGINEERING CHEMISTRY **RESEARCH®**

Reprinted from
Volume 35, Number 8, Pages 2576–2580

MATERIALS AND INTERFACES

Silver Corrosion and Sulfur Detection Using a Quartz Crystal Microbalance with Silver Electrode Surfaces

Steven Zabarnick,* Paula Zelesnik, and Shawn D. Whitacre

Aerospace Mechanics Division, University of Dayton Research Institute, 300 College Park/KL-463, Dayton, Ohio 45469-0140

A quartz crystal microbalance (QCM) with silver electrodes is used for detection of sulfur and measurement of silver corrosion by sulfur in jet fuels. It is found that the device responds very sensitively to elemental sulfur by reaction at the silver surface, resulting in the formation of surface silver sulfide. It is also expected that the device will respond to hydrogen sulfide. The response of the QCM is found to depend on the fuel matrix. The presence of oxygen inhibits the surface reaction, resulting in a lower mass accumulation. It is also found that the sulfur compounds which produce a response in this test are not players in the formation of autoxidative surface deposition. It is shown that the QCM response (surface mass per unit time) is proportional to the concentration of elemental sulfur present in the fuel.

Introduction

In the early days of gas turbine aviation engines it was thought that these engines could run on almost any type of fuel. Over the intervening years jet fuel specifications have become increasingly more complicated and numerous due to the increased complexity of the turbine engine and its control. Increasing demands for improved performance, overhaul life, and economy will continue this trend, despite the necessary compromise between fuel quality and availability (Bishop and Henry, 1993). Of the chemical property specifications, some of the most important are the limits placed on concentrations of various sulfur compounds. The military specification for JP-8 fuel limits the total sulfur content to 0.3 mass % and mercaptan sulfur to 0.002 mass %. Sulfur content is strictly limited in jet fuel because high sulfur content can adversely affect deposition in combustion chambers and sulfur oxides in combustion gases can lead to corrosion problems. Also, sulfur compounds have been implicated in liquid-phase corrosion (Schreifels et al., 1989; Tripathi et al., 1973). Mercaptan sulfur is limited because of objectionable odor, elastomer degradation, and corrosiveness toward certain metals. For JP-8 fuel, direct corrosion due to sulfur is tested by ASTM Method D130, the copper strip corrosion test. In addition, service experience with corrosion of silver components has led to the British military Silver Corrosion Test, IP 227.

Previous work in our laboratory has demonstrated the usefulness of the quartz crystal microbalance (QCM) with an oxidation monitoring technique for studying the deposition and oxidation of jet fuels (Zabarnick, 1994). The QCM, and piezoelectric transducers in general, have proven to have multitudinous applications as detectors of interfacial chemical processes (Ward and Buttry, 1990). We have noted unusual behavior of the QCM in tests conducted with high sulfur fuels using silver crystal electrode surfaces (Zabarnick et al., 1995, 1996). This behavior was attributed to reaction of sulfur compounds in the fuel with the silver surface. In the current work we investigate the details of this interaction of fuel sulfur with silver surfaces in the QCM. This interaction provides the possibility of using the QCM as a silver corrosion test for jet fuel and/or a very sensitive test for fuel sulfur. This study reports on work which addresses the following questions as they pertain to using the QCM with a silver electrode as a silver corrosion test and/or sulfur detection test. What type of sulfur compounds in fuel are responsible for the QCM response? What is the sensitivity and selectivity of the test to these compounds? What is the effect of oxygen on this interaction? What is the effect of the fuel matrix on the response? Are these sulfur compounds responsible for autoxidative deposition?

Experimental Section

The QCM/Parr bomb system has been described in detail previously and will only be outlined briefly here (Zabarnick, 1994; Zabarnick and Grinstead, 1994). The Parr bomb is a 100 mL stainless steel reactor. It is heated with a clamp-on band heater and its temperature is controlled by a PID controller through a thermocouple immersed in the fuel. The reactor contains an RF feedthrough, through which the connection for the quartz crystal resonator is attached. The crystals are 2.54 cm in diameter and 0.33 mm thick and have a nominal resonant frequency of 5 MHz. The crystals were acquired from Maxtek Inc. and are available in crystal electrode surfaces of gold, silver, platinum, and aluminum. The QCM measures deposition (i.e., an increase in mass) which occurs on overlapping sections of the two-sided electrodes. Thus, the device responds to deposition which occurs on the metal surface and does not respond to deposition on the exposed quartz.

The device is also equipped with a pressure transducer to measure the absolute headspace pressure and a polarographic oxygen sensor to measure the headspace oxygen concentration. Previous studies have demonstrated the value of these detectors for determining the

* To whom correspondence should be addressed. E-mail: steve@snake.appl.wpafb.af.mil.

S0888-5885(96)00063-2 CCC: $12.00

Table 1. Properties of Fuels Studied

fuel no. and type	total sulfur (ppm)
2827 (jet A)	763
2747 (jet A-1)	37
2980 (jet A)	614

oxidation characteristics of fuels and fuels with additives, although in the present study most runs were conducted in the absence of oxygen. A personal computer is used to acquire data at 1 min intervals during the experimental run. The following data are recorded during a run: temperature, crystal frequency, headspace pressure, headspace oxygen concentration, and crystal damping voltage.

The reactor is charged with 60 mL of fuel, which is sparged with the appropriate gas for 1 h before each test. The reactor is then sealed, and the heater is started. All runs in this study were performed at 140 °C; heat-up time to this temperature is 40 ± 5 min. Most runs are conducted for 15 h, after which the heater is turned off and the reactor allowed to cool. Surface mass measurements can only be determined during the constant temperature (±0.5 deg) portion of an experimental run. The crystal frequency is converted to a surface mass measurement using the process described below.

The theory that relates the measured frequency changes to surface mass has been presented in detail elsewhere (Martin et al., 1991). The frequency change of a crystal immersed in a liquid fuel can be due to two effects: the first results from changes in the surface mass density, the second is due to changes in the liquid density and viscosity. At constant temperature and relatively small extents of chemical conversion the liquid properties remain constant and the frequency change can be related to surface deposition via the equation

$$\rho_s = -(2.21 \times 10^5 \text{ g/(cm}^2 \text{ s)})\frac{\Delta f}{f_0^2} \qquad (1)$$

where f_0 is the unperturbed resonant frequency, Δf is the change in resonant frequency, and ρ_s is the surface mass density (mass/area). In general, the reproducibility of the mass deposition measurements on fuels is limited to ±20% for the QCM technique. The fuels studied and some of their properties are listed in Table 1. The fuels were acquired from the Fuels and Lubricants Division of Wright Laboratory, Wright-Patterson AFB, Dayton, OH, and are referred to by the Wright Lab assigned ascension number.

Results and Discussion

When jet fuel is heated in an oxygen-containing environment, autoxidation chemistry occurs, which ultimately leads to formation of deposits on surfaces. Elemental analyses have shown that these deposits consist primarily of carbon and oxygen with smaller amounts of sulfur, nitrogen, and hydrogen (Hazlett, 1991). Removal of oxygen results in a significant reduction in deposit formation (Zabarnick, 1994). In a previous QCM paper, we studied the effect of surface metal on jet fuel deposition (Zabarnick et al., 1995, 1996). We found that gold and aluminum produced similar deposition, while platinum surfaces yielded increased deposition for some fuels. The most startling observation was extremely high deposition observed for silver crystal electrode surfaces. These data are shown in Figure 1. The "normal" deposition of ≈4 μg/cm^2 after

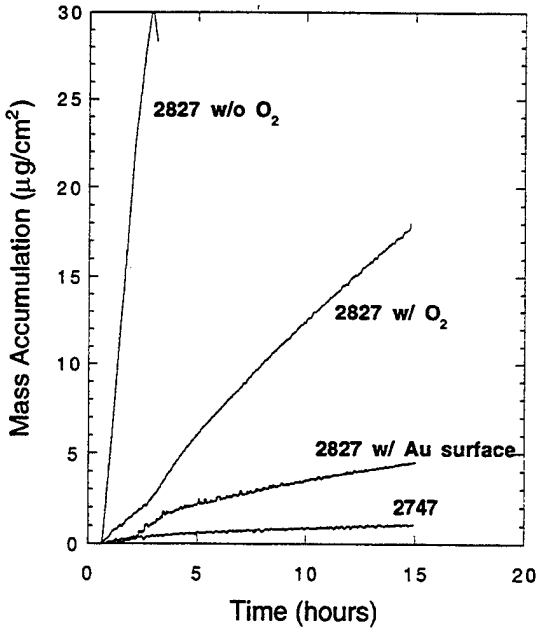

Figure 1. Plots of mass accumulation vs time for two jet fuels on silver and gold crystal electrode surfaces.

15 h at 140 °C for fuel 2827 on gold surfaces is shown. When a silver crystal is substituted, the resulting deposition approaches 17 μg/cm^2 at 15 h. Visually, the silver surface appeared to be discolored with a blue/black film in contrast to the usual "yellowing" or brownish color which results from autoxidative deposits. In order to confirm that this blue/black film was not due to an autoxidative deposit the test was run in the absence of oxygen by sparging the fuel with nitrogen. Figure 1 shows that the removal of oxygen results in a substantial increase in the deposition rate to ≈30 μg/cm^2 after only 3 h. Possible reasons for this increase in deposition in the absence of oxygen will be discussed later. Also shown in the figure is deposition for a second fuel, fuel 2747, on a silver electrode in the absence of oxygen. This deposition is similar to that normally observed on gold electrodes, and a blue/black film was not observed.

Table 1 shows that one major difference in these two fuels is their sulfur level; fuel 2827 is a relativity high sulfur fuel at 763 ppm, while fuel 2747 has a low sulfur level of 37 ppm. The difference in sulfur level of these fuels and the well-known tarnishing of silver surfaces by atmospheric sulfur compounds led us to suspect sulfur as the cause of this behavior. In order to substantiate this hypothesis, Auger electron spectroscopy (AES) analyses with argon-ion sputtering of the surfaces were performed. Figure 2 shows the AES depth profile of the surface film produced from a 15 h run with fuel 2827 in an oxygen-free environment. The elemental composition at the surface (at 0 Å sputter depth) consists primarily of silver (70%) and sulfur (25%) with smaller amounts of carbon. The well-known tarnishing of silver by atmospheric hydrogen sulfide results in the formation of silver sulfide, Ag_2S. It is apparent that the surface consists of silver sulfide almost exclusively; the small amount of carbon at the surface may be due to residual fuel. As one sputters through the film, there is an increasing amount of carbon and oxygen, most likely due to a small autoxidative deposit. It is believed that the formation of silver sulfide tarnish on silver surfaces occurs by the reaction of sulfur with surface silver atoms, and subsequent migration of subsurface silver atoms to the surface

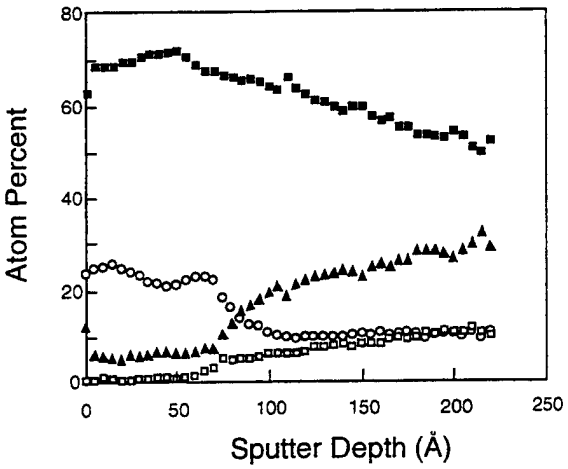

Figure 2. Auger electron spectroscopy depth profile of silver electrode for fuel 2827: (■) silver; (○) sulfur; (▲) carbon; (□) oxygen.

Table 2. Sulfur Compounds Tested in *n*-Dodecane

sulfur compd	concn (mg/L)	surface mass (μg/cm^2) after 15 h at 140 °C
3-methylthiophene	81	0.9
diphenyl sulfide	81	0.9
diphenyl disulfide	100	0.8
1-hexanethiol	67	0.4
1-hexanethiol	337	0.6
3,4 dimethylthiophenol	82	0.5
elemental sulfur	0.11	1.1
elemental sulfur	1.1	15.1
elemental sulfur	10.0	16.0

(Ricciardiello and Riotti, 1972). This behavior would account for the fact that although sulfur is observed to a depth of at least 230 Å, silver is still the major atomic species at the surface. In the case of fuel 2747, the AES analysis demonstrated (not shown here) that the surface consists almost entirely of silver (95%). A third fuel, 2980, which has a relatively high sulfur content (see Table 1), was also tested. This fuel, despite having 614 ppm sulfur, produced only 0.8 μg/cm^2. These results suggest that the device responds selectively to a particular type or types of sulfur compounds rather than universally to all sulfur-containing species.

Petroleum fuels can contain a wide variety of sulfur compounds. Some of these come from the original crude and are not removed during the refining process. Sulfur compounds can also result from sweetening processes to which some fuels are subjected. The corrosivity of a given sulfur compound is a function of its chemical structure; some sulfur compounds have even been shown to act as corrosion inhibitors (Garcia-Anton et al., 1995; Tripathi et al., 1973). In order to determine the types of sulfur compounds to which the silver electrode QCM responds, we spiked *n*-dodecane with various sulfur compounds. These compounds are listed in Table 2. The compounds tested represent the major sulfur compound types normally found in fuel: mercaptans, sulfides, disulfides, thiophenes, thiophenols, and elemental sulfur. Although the compounds were chosen to represent the classes of sulfur compounds in fuel, they may not be representative of specific individual compounds that have actually been identified in fuel. The table shows that none of the organosulfur compounds produced significant deposition (i.e., <1 μg/cm^2), but elemental sulfur produced extremely high levels of deposition at concentrations above 1 mg/L. Previous workers have observed similar behavior in studies of copper and silver corrosion by turbine fuels; they noted significant corrosion from elemental sulfur and hydrogen sulfide, in contrast to the lack of corrosion from organosulfur compounds (Tripathi et al., 1973). Mercaptans, sulfides, disulfides, thiophenes, and other naturally occurring sulfur compounds have been shown to act as inhibitors of elemental sulfur corrosion on silver and copper surfaces (Garcia-Anton et al., 1995; Tripathi et al., 1973). We have not tested hydrogen sulfide in this work, but we fully expect it to produce silver electrode QCM mass deposition (i.e., silver corrosion) because of its similar behavior to elemental sulfur (Tripathi et al., 1973).

The larger mass accumulation of sulfur in the absence of oxygen, as seen in Figure 1, can be due to a variety of effects. It is known that in the presence of oxygen a carbon-containing deposit readily forms in this fuel (Zabarnick, 1994). This surface carbon deposit may obstruct the surface and prevent the fuel sulfur from reacting with the surface silver atoms. In the absence of oxygen this carbon deposit is minimized, thus allowing maximum access to the silver surface. Another possible explanation involves the effect of oxygen on the chemistry of sulfur upon heating the fuel. The presence of oxygen will favor formation of oxidized sulfur species. Oxidized sulfur may be less likely to react with surface silver. It is well-known that sulfur in its reduced state, such as in elemental sulfur and hydrogen sulfide, is a much more effective tarnisher than oxides of sulfur, such as SO_2 (Ricciardiello and Riotti, 1972).

Sulfur compounds are thought to be important players in the deposit formation process when fuel is thermally oxidized in fuel systems. The different types of sulfur compounds have varied deposit-increasing tendencies. Previously, we have shown for one jet fuel that "polar sulfur compounds" (i.e., sulfur compounds that are retained by a silica gel solid-phase extraction (SPE) cartridge) are deposit-increasing species, while "nonpolar sulfur" compounds (those that are not retained by the SPE cartridge) are not deposit promoters (Zabarnick, 1994). In order to determine if the silver electrode QCM technique responds to deposit-promoting sulfur compounds, we have performed the following experiments. Fuel 2827 was passed through a silica gel SPE cartridge and then tested in the silver electrode QCM. The compounds which were retained on the cartridge were extracted from the cartridge with 2–3 mL of methanol. The methanol was evaporated from this extract, and the extract was added to a sample of fuel 2747. The results are shown in Figure 3. The figure shows that the silver electrode deposition characteristics of fuel 2827 do not change significantly after being subjected to the SPE process. Also, fuel 2747 does not produce increased mass deposition on a silver electrode after being spiked with the extract from fuel 2827. These results imply that the silver electrode QCM technique is responding to sulfur compounds that we classify as "nonpolar." Also, the sulfur compounds to which the silver QCM technique responds are not the types of sulfur compounds responsible for deleteriously affecting jet fuel thermal stability, as we have previously shown that these compounds are preferentially retained by the SPE cartridge (Zabarnick, 1994).

In order to employ the silver electrode QCM for detection of fuel sulfur, one needs to determine the effect of concentration on the QCM response. Also, the possible use of the test for measuring the corrosivity of jet fuel requires an evaluation of its sensitivity. To

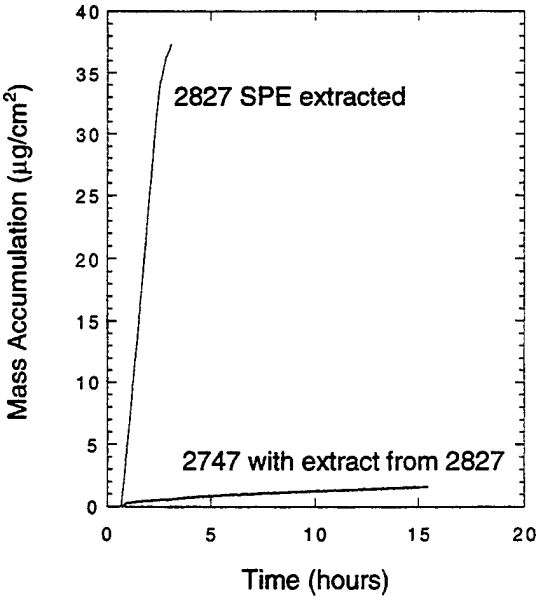

Figure 3. Plots of mass accumulation vs time for fuel 2827 after being subjected to solid-phase extraction of polar compounds and fuel 2747 after addition of extracts from fuel 2827.

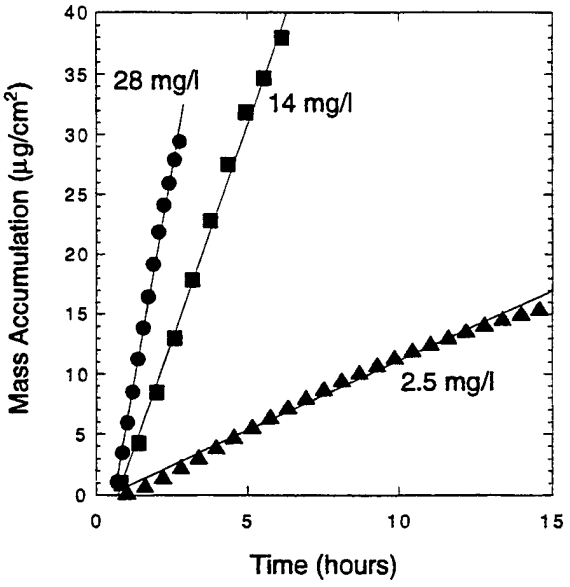

Figure 4. Plots of mass accumulation vs time for fuel 2827 at various levels of dilution resulting in elemental sulfur concentrations of (●) 28 mg/L, (■) 14 mg/L, (▲) 2.5 mg/L.

assess the concentration dependence of the silver electrode on sulfur, we tested fuel 2827 at various levels of dilution. The results are presented in Figure 4. Fuel 2827 was run neat and diluted 1:1 and 1:11 with Exxsol D80, a low sulfur (3 ppm) aliphatic solvent, yielding elemental sulfur concentrations of 28, 14, and 2.5 mg/L, respectively. The elemental sulfur concentration of fuel 2827 was determined by a reaction technique in which elemental sulfur is quantitatively converted to triphenylphosphine sulfide by reaction with triphenylphosphine and quantified by gas chromatography (Heneghan et al., 1996). As the fuel is nitrogen sparged for 1 h prior to the test, we do not expect the fuel to contain a significant concentration of hydrogen sulfide. Only the near linear portions of the deposition profiles are shown in Figure 4 for the two high sulfur concentration runs. At longer times problems are encountered with normal crystal oscillation. The plot shows that the slopes of the deposition vs time plots increase with the

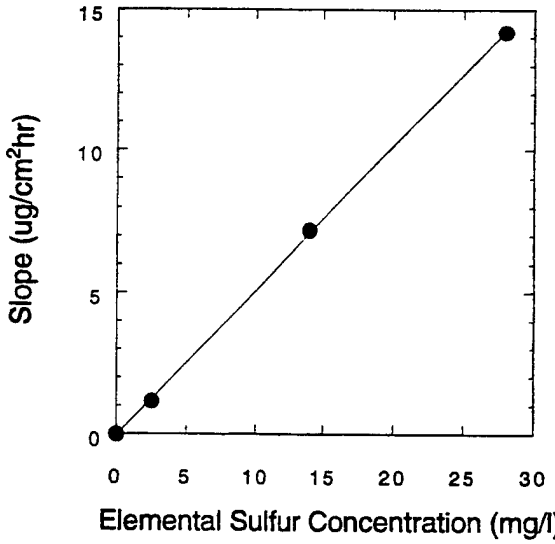

Figure 5. Plot of slope (from Figure 4) vs elemental sulfur concentration.

concentration of elemental sulfur. This result is expected, as the rate of deposition should be proportional to the rate of surface reaction, which in turn is proportional to the concentration of the reacting species, namely, elemental sulfur. In Figure 5, we have plotted the measured slopes of the deposition curves (from Figure 4) vs elemental sulfur concentration. The figure shows that there is a linear dependence of deposition rate vs elemental sulfur concentration over the range of 2.5−28 mg/L. It appears that the limit of detection for this technique is near 0.2 mg/L for this fuel by estimation from Figure 4. We have not undertaken a study to maximize this sensitivity. Running the test at a different (higher) temperature may provide a boost in the sensitivity and shorten the test time. It is important to realize that the sensitivity to elemental sulfur is a function of the fuel matrix due to the fact that fuel compounds may act as both inhibitors and promoters of the reaction of elemental sulfur with surface silver atoms. The response shown in Table 2, of 16.0 $\mu g/cm^2$ for 1.1 mg/L elemental sulfur doped into *n*-dodecane (for a 15 h run), shows that *n*-dodecane exhibits a somewhat higher sensitivity for elemental sulfur, indicating that fuel 2827 contains compounds which inhibit the surface reaction.

Conclusions

We have demonstrated the use of the silver electrode QCM technique for measurement of fuel corrosivity and detection of fuel sulfur. The results show that elemental sulfur is responsible for deposition on the silver electrode surface of the quartz crystal, resulting in formation of surface silver sulfide. The presence of oxygen inhibits the surface reaction, resulting in a lower mass accumulation. The sulfur compounds which produce a response in this test are not players in the formation of autoxidative surface deposition. We have shown that the QCM response (surface mass per unit time) is proportional to the concentration of elemental sulfur present in the fuel. The technique shows promise as a very sensitive method for detecting elemental sulfur in fuel. The effect of the fuel matrix on this response needs to be explored in further detail before the test can be used for detection of fuel sulfur.

Acknowledgment

This work was supported by the U.S. Air Force, Fuels and Lubrication Division, Wright Laboratories, Wright-Patterson AFB, under contract No. F33615-92-C-2207 with Mr. Charles Frayne as technical monitor.

Literature Cited

Bishop, G. J.; Henry, C. P., Jr. In *Manual on Significance of Tests for Petroleum Products*, 6th ed.; Dyroff, G. V., Ed.; ASTM: Philadelphia, 1993.

Garcia-Anton, J.; Monzo, J.; Gunon, J. L. Effect of Elemental Sulfur and Mercaptans on Copper Strip Corrosion and Use of the ASTM D 130 Test Method. *Corrosion* **1995**, *51*, 558.

Hazlett, R. N. *Thermal Oxidation Stability of Aviation Turbine Fuels*; ASTM: Philadelphia, 1991.

Heneghan, S. P.; Williams, T.; Whitacre, S. D. The Effects of Oxygen Scavenging on Jet Fuel Thermal Stability. *Prepr.—Am. Chem. Soc., Div. Pet. Chem.* **1996**, *41*, 469.

Martin, S. J.; Granstaff, V. E.; Frye, G. C. Characterization of a Quartz Crystal Microbalance with Simultaneous Mass and Liquid Loading. *Anal. Chem.* **1991**, *63*, 2272.

Ricciardiello, F.; Riotti, S. The Corrosion of Fe and Ag in S Liquid at Low Temperature. Effect of S Viscosity. *Corrosion Sci.* **1972**, *12*, 651.

Schreifels, J. A.; Bagwell, T.; Weers, J. J. Copper Corrosion Inhibition in Sour Hydrocarbon Fuels. *Corrosion* **1989**, *45*, 84.

Tripathi, R. P.; Gulati, I. B.; Pandey, S. S.; Rohatgi, H. S. Copper and Silver Corrosion by Aviation Turbine Fuels. *Ind. Eng. Chem. Prod. Res. Dev.* **1973**, *12*, 227.

Ward, M. D.; Buttry, D. A. In Situ Interfacial Mass Detection with Piezoelectric Transducers. *Science* **1990**, *249*, 1000.

Zabarnick, S. Studies of Jet Fuel Thermal Stability and Oxidation Using a Quartz Crystal Microbalance and Pressure Measurements. *Ind. Eng. Chem. Res.* **1994**, *33*, 1348.

Zabarnick, S.; Grinstead, R. R. Studies of Jet Fuel Additives Using the Quartz Crystal Microbalance and Pressure Monitoring at 140 °C. *Ind. Eng. Chem. Res.* **1994**, *33*, 2771.

Zabarnick, S.; Zelesnik, P.; Grinstead, R. R. Jet Fuel Deposition and Oxidation: Dilution, Materials, Oxygen, and Temperature Effects. ASME 95-GT-50, ASME: Fairfield, NJ, 1995.

Zabarnick, S.; Zelesnik, P.; Grinstead, R. R. Jet Fuel Deposition and Oxidation: Dilution, Materials, Oxygen, and Temperature Effects. *J. Eng. Gas Turbines Power* **1996**, *118*, 271.

Received for review February 6, 1996
Accepted May 20, 1996[⊗]

IE960063J

[⊗] Abstract published in *Advance ACS Abstracts,* July 1, 1996.

Appendix G.

Global Kinetic Modeling of Aviation Fuel Fouling in Cooled Regions in a Flowing System

Jamie S. Ervin
Theodore F. Williams
University of Dayton
300 College Park
Dayton, OH 45469-0140

Vishwanath R. Katta
Innovative Scientific Solutions, Inc.
Dayton, OH 45430-1658

Global Kinetic Modeling of Aviation Fuel Fouling in Cooled Regions in a Flowing System

Jamie S. Ervin* and Theodore F. Williams

University of Dayton Research Institute, Dayton, Ohio 45469-0210

Vishwanath R. Katta

Innovative Scientific Solutions, Inc., Dayton, Ohio 45430-1658

Jet fuel is used to cool military aircraft. Unfortunately, heated jet fuel reacts with dissolved oxygen to form products which foul fuel system components. Two categories of surface deposits which form in the autoxidative regime have been recently identified. The first forms in heated regions as the fuel is oxidized. The second accumulates in cooled regions as certain compounds within the reacted fuel become insoluble at reduced temperatures. This paper seeks to improve understanding of fouling at reduced temperatures and to develop a global chemistry model that can be used in computational fluid dynamics codes. Experiments were conducted in a flowing system using JP-8 fuel with different thermal stability additives. Some thermal stability additives reduced fouling in heated regions but were not as effective in cooled regions. The deposition and oxidation measurements obtained for specific flow conditions were used to calibrate a chemical kinetics model which uses global reactions to simulate deposition. The calibrated model yielded reasonable predictions within the thermal and flow regimes considered.

Introduction

Effective heat transfer is vital to the design of high-performance military aircraft. Ram air is used extensively for cooling, but as aircraft operate near and above the sonic velocity, the stagnation temperature of the air precludes its use as a coolant. As an alternative, fuel is circulated around airframe and engine components to provide heat transfer that is required to keep these components relatively cool. Unfortunately, heated fuel reacts with dissolved oxygen to form products which foul fuel passages and tubes contained within on-board heat exchangers. Fouling degrades the heat transfer effectiveness since the presence of the deposit on tube walls increases the thermal resistance between the heated tube wall and the flowing fuel. Moreover, accumulated deposits can potentially arrest or distort the flow in tubes of small diameter and in engine nozzles.

As autoxidation reactions proceed at elevated temperatures, bulk insolubles, bulk solubles, and surface-deposition precursors are produced (Ervin et al., 1995; Jones and Balster, 1993). With the cooling of thermally stressed straight-run jet fuel, once soluble species may become insoluble and form surface deposits. This is important for military aircraft which recirculate fuel. In those aircraft, a fraction of the thermally stressed fuel is cooled on return to the fuel tanks; the remainder is burned in the combustor. The thermal stability (thermal stability refers to the deposit-forming tendency of the fuel) of jet fuels is generally assessed (by the JFTOT, for example (Hazlett, 1991)) by the mass of surface deposits and bulk insolubles generated at elevated temperatures (Heneghan and Kauffman, 1995; Jones et al., 1995). Flowing and static tests for fuel thermal stability are often performed under isothermal conditions, and thus, deposits which could form under lower temperatures go undetected. Thus, surface deposits formed from soluble species which become insoluble upon cooling to lower temperatures have until now received little attention. Knowledge of deposits which accumulate in cooled regions downstream of heated regions is vitally important since catastrophic failure may result from decreased fuel recirculation due to blocked fuel tubes. The focus of the present work is to investigate the formation of surface deposits within cooled regions. To generalize the experimental results obtained using JP-8 jet fuel, surface deposition and bulk dissolved oxygen measurements are used for the calibration of a new computational fluid dynamics model which uses global reactions to simulate fouling not only in heated areas but also in cooled regions. Experiments are performed using a flowing system to investigate fouling in a complex thermal environment and to assess the ability of two candidate fuel additives to reduce fouling.

Table 1. Neat Fuel Properties[a]

fuel (Jet A)	total sulfur (ppm)	aromatics volume %	dissolved metals (ppb)	JFTOT break-point (°C)
F-2827, straight-run	790	19.0	Cu, <5; Fe, <8	266

[a] Metal concentrations measured for USAF using a graphite furnace Zeeman/5000 system atomic absorption spectrometer by United Technologies, Pratt and Whitney.

Experimental Description

Table 1 lists characteristics of the Jet-A fuel (Air Force designation F-2827) used in this work. The additives added to the Jet-A fuel such that it became classified as JP-8 fuel are given in Table 2, and the components of two different thermal stability additive packages (JP-8B or JP-8M) are given in Table 3. Currently, the U.S. Air Force is testing additive packages with the goal of increasing the thermal stability temperature limit of JP-8 jet fuel by 100 °F. These two additive packages were selected for study because they were found to reduce deposition in preliminary screening tests. Thus, the fuels used in the present experiments are JP-8, JP-8B, and JP-8M.

* E-mail: jervin@engr.udayton.edu.

Table 2. Properties of JP-8 Additives

additive name and supplier	additive classification	type of compound	concn
DiEGME	icing inhibitor	diethyleneglycol monomethyl ether	0.15% by volume
DuPont Stadis 450	static dissipator	proprietary	2 mg/L
DCI-4A	corrosion inhibitor/lubricity enhancer	proprietary	9 mg/L

Table 3. JP-8 Thermal Stability Additives

additive name and supplier	JP-8M ingred.?	JP-8B ingred.?	additive classification	type of compound	concn (mg/L)
BHT	yes	yes	antioxidant	2,6 di-*tert*-butyl-4-methylphenol	25
Betz 8Q406	no	yes	dispersant	proprietary	100
MDA	yes	yes	metal deactivator	*N,N'*-disalicylidene-1,2-propanediamine	2
Mobil MCP-1750	yes	no	detergent/dispersant	proprietary	300

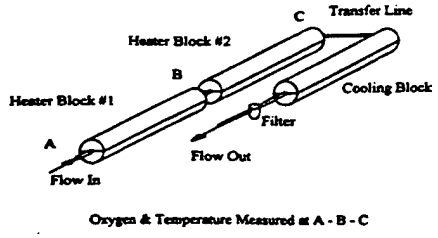

Figure 1. Fuel flow path.

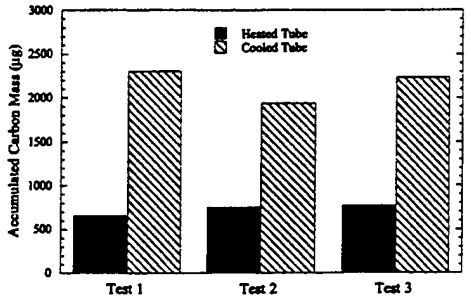

Figure 2. Demonstration of the repeatability of carbon mass measurements in sequential tests with a flow rate of 16 mL/min for a single heated block held at 270 °C and one cooled block.

The experimental apparatus is shown in Figure 1 (Heneghan et al., 1993). In a preconditioning tank, nitrogen and oxygen gases were bubbled through the fuel such that the dissolved oxygen concentration was nominally 70 ppm (by mass, normal air saturation level) as the fuel entered the first heated block. Bulk dissolved oxygen levels were measured at the locations shown in Figure 1 by means of a Hewlett Packard 5890 Series II gas chromatograph (Rubey et al., 1995). To produce the desired thermal flow environment, two heated copper blocks and a third cooled copper block envelope the 316 stainless steel tubing (180-cm long by 2.16-mm i.d. by 3.18-mm o.d.) through which the fuel passes. The electric power to each block (46-cm long with a 7.6-cm diameter) is controlled such that the tube wall temperature remains steady (within ±2 °C), and the tubing between the heated blocks is insulated. The cooled copper block has internal passages through which chilled water flows. Thermocouples are welded to the outer surface of the tubing to measure wall temperatures with an uncertainty of ±2 °C. The tubes (ASTM grade A269/A213) are cleaned in an ultrasonic bath, rinsed with deionized water, and dried with flowing laboratory-grade nitrogen gas prior to use.

Fluid dynamics is an important element of fouling; however, only a limited number of investigations on its role in fouling were conducted in the past due to the lack of good diagnostic tools for flow in narrow passages. In the present experiments, the volumetric flow rate was varied to show the effects of flow velocity on the observed deposition. Volumetric flow rates of 4 and 16 mL/min were used. For these flow rates, the flow was laminar at the entrance of the first heated block but became turbulent within the second block. Turbulence at these low flow rates results from large changes in the fuel density as the temperature varies, giving rise to considerable buoyancy force on the fuel near the tube wall. Buoyancy forces normal to the forced flow direction increase the heat and mass transport, and Taylor instabilities render the flow turbulent (Katta et al., 1995). Thus, turbulent simulations yielded bulk temperatures which followed the measured values more accurately than did the laminar computations. Most importantly, turbulent flow is normally encountered in the fuel systems of aircraft.

The extent of fuel oxidation depends on both the residence time and the temperature field. As the fuel passes through several heated components in an aircraft, not all of the dissolved oxygen may be consumed because of large flow rates. Since dissolved oxygen is more readily consumed under conditions of high temperature and long residence times, the rate of oxygen consumption may be increased by increasing the fuel temperature for a constant flow rate. In preliminary experiments with JP-8 at a flow rate of 16 mL/min and wall temperature of 240 °C, the dissolved oxygen was not fully consumed; with 270 °C, it was depleted within the first heated block. Thus, the experiments were performed with a wall temperature of either 240 or 270 °C and at a flow rate of 16 mL/min in order to obtain different levels of oxygen consumption. In addition, a flow rate of 4 mL/min, which is similar to the JFTOT (jet fuel thermal oxidation test) flow rate of 3 mL/min, was used with a tube wall temperature of 227 °C. The experiments with a flow rate of 16 mL/min were conducted in 6-h periods; those with a flow rate of 4 mL/min were performed in 12-h periods.

At the termination of an experiment, the tubes were rinsed with hexane, sliced into 50-mm segments, and heated in a vacuum oven at 120 °C for 1 h to remove fuel trapped in the deposits. A Leco (RC-412) multiphase carbon analyzer determined the mass of carbon on the tube segments; the repeatability of the carbon mass measurements was determined by sequential tests using one heated block and one cooled block. These 6-h tests were performed within the same week (as were the actual tests) using neat fuel from the same batch. The flow rate was 16 mL/min, and the heated block was held at 270 °C. Figure 2 gives an indication of the relatively good repeatability of the carbon mass measurements for sequential tests performed under nearly identical flow and thermal conditions. Some of the segments taken from locations within the second heated block and the cooled block were examined using scanning electron microscopy (SEM) for microstructural analysis and X-ray photoelectron spectroscopy (XPS) for

Table 4. Global–Kinetic Model of Katta et al. (1993)

	activation energy E (kcal/mol)	pre-exponential factor A	reaction number
bulk fuel reactions			
$F + O_2 \rightarrow ROO^{\bullet}$	32	2.5×10^{13} (mol m^{-3} s^{-1})	1
$ROO^{\bullet} + F \rightarrow$ solubles	10	1×10^{4} (s^{-1})	2
$ROO^{\bullet} + F_s \rightarrow P$	15	8×10^{9} (s^{-1})	3
$ROO^{\bullet} + F \rightarrow D_{bulk}$	10	200 (s^{-1})	4
$P + F \rightarrow$ solubles	30	3.2×10^{12} (s^{-1})	5
$D_{bulk} + F \rightarrow 2D_{bulk}$	0	1×10^{-3} (s^{-1})	6
wall reactions			
$O_2 + F \rightarrow P$	12	5.2×10^{-3} (ms^{-1})	7
$P \rightarrow D_{wall}$	17	260 (ms^{-1})	8
$D_{bulk} \rightarrow D_{wall}$	10	0.8 (ms^{-1})	9

chemical analysis. XPS determined the composition of the first three nanometers of the inner tube surface which was exposed to the thermally stressed fuel. The XPS measurements were obtained with a modified AES Es-100 photoelectron spectrometer which is equipped with a magnesium X-ray source. Uncertainties in the absolute value of the composition are on the order of 10%.

Numerical Model

To simulate fouling in a tube, the species, temperature, and velocity distributions were obtained by finite difference solution of the unsteady species conservation, enthalpy, Navier–Stokes, and turbulent energy equations. Following Katta and Roquemore (1993), the governing equations are solved sequentially using a uniform grid system of 11 nodes in the radial direction and 301 nodes in the axial direction. With this distribution of nodes, the computed results were only weakly sensitive to further grid refinement. The fluid motion bounded by the deposit was assumed to be axisymmetric, and a body-oriented coordinate system was used to track the shape of the surface deposit with time. The transport properties of the fuel at a given temperature are obtained from curve fits of fuel data (Nixon et al., 1967).

The development of computational fluid dynamics codes which include chemistry assist in the fundamental understanding and interpretation of experimental results. Since the chemical kinetics of the autoxidation of jet fuels and the subsequent surface deposition processes are extremely complex, global–kinetic models have been used in numerical simulations (Krazinski et al., 1992) to represent a series of elementary reactions. Katta et al. (1993) used the global kinetic model of Table 4 to simulate fouling in heated sections. In this model, calibrated parameters for Jet A fuel were found to be valid over a range of flow and temperature conditions. Here, F represents the fuel, F_s represents heteroatom-containing compounds within the fuel, P is deposit-forming precursor, D_{bulk} represents bulk insolubles, and D_{wall} is the wall deposit. The units for pre-exponentials in Table 4 do not correspond to bimolecular reactions because the concentrations of F and F_s are assumed constant and, consequently, are viewed as part of the Arrhenius expression for reaction rate. (The Arrhenius expressions used have the form $k = A \exp[-E/RT]$.) Reactions 1–6 are presumed to occur within the bulk fuel, and Reactions 7–9 are assumed to occur at the wall. Reactions 8 and 9 represent the conversion of particles D_{bulk} and P to wall deposit, D_{wall}.

The values of Arrhenius parameters come from a combination of theory, experiment, and trial-and-error. This model satisfactorily predicted surface deposition rates in both near-isothermal (Jones and Balster, 1993) and nonisothermal (Heneghan et al., 1995) flow rigs for a variety of flow rates and temperatures. To account for differences in fuel sources, the Arrhenius parameters of reaction 1 for a given fuel were obtained from the measurements of oxygen consumption obtained over a range of temperature and flow conditions. In addition, the reaction order was assumed to change from zero-order to first-order when the dissolved oxygen concentration falls below 10 ppm. In general, a two-parameter representation for reaction 1 is insufficient over a very wide temperature range (Heneghan and Chin, 1995). However within the temperature range of interest (25–270 °C) in the present experiments, a single set of Arrhenius parameters gave acceptable predictions of the measured oxidation. Since the emphasis of the present study is on surface deposit formation in cooled regions, the simpler representation of Katta et al. (1993) was used for reaction 1 of the new global-kinetic model.

Table 5. Global–Kinetic Model Including Insoluble Formation in Cooled Regions

	activation energy E (kcal/mol)	pre-exponential factor A	reaction number
bulk fuel reactions			
$F + O_2 \rightarrow ROO^{\bullet}$	32	4.2×10^{13} (mol m^{-3} s^{-1})	1a
$ROO^{\bullet} + F \rightarrow$ solubles	10	1×10^{4} (s^{-1})	2a
$ROO^{\bullet} + F_s \rightarrow P$	15	8×10^{9} (s^{-1})	3a
$ROO^{\bullet} + F \rightarrow D_{bulk}$	10	100 (s^{-1})	4a
$P + F \rightarrow P1$	15	1×10^{6} (s^{-1})	5a
$P1 + F \rightarrow D_{bulkc}$	0	0.3 (s^{-1})	6a
$P1 + F \rightarrow$ solubles	30	6.2×10^{11} (s^{-1})	7a
wall reactions			
$O_2 + F \rightarrow P$	12	5.2×10^{-3} (ms^{-1})	8a
$P \rightarrow D_{wall}$	17	260 (ms^{-1})	9a
$P1 \rightarrow D_{wallc}$	10	1.0 (ms^{-1})	10a
$D_{bulkc} \rightarrow D_{wallc}$	5	0.08 (ms^{-1})	11a

A deficiency of previous global computational models is that they do not predict the formation of deposits in cooled regions downstream of the autoxidation reactions. To compute the mass of species which accumulate in the cooled sections at sufficiently low temperatures, the global model of Table 5 is developed in the present work. In the new model three additional species are introduced namely, P1, D_{wallc}, and D_{bulkc}. P1 represents a precursor species which leads to the formation of deposits in the cold section. The wall deposit, D_{wallc}, is assumed to form only when the wall temperature falls below some critical temperature, T_{crit}. By taking T_{crit} to be 97 °C for this fuel, the predicted location of the maximum deposition rate within the cooled block most closely coincided with the observed location of the maximum deposition rate. As will be described later, D_{wallc} (surface deposits in the cold section) is both chemically and physically different from D_{wall} (surface deposits in the heated section). Bulk insolubles, D_{bulkc}, form when certain bulk solubles within the thermally stressed fuel become insoluble as the bulk temperature falls below T_{crit}.

The first four reactions in Table 5 are identical to those of Table 4. In the new model, reactions 5a, 6a, 7a, 10a, and 11a are introduced. Reaction 5a represents a pathway for the formation of soluble molecules (P1) which become the precursors for deposit formation under reduced temperatures. This reaction is presumed to occur at relatively low temperatures. Thus, the activation energy for reaction 5a was chosen to be similar to that of reaction 3a. Choice of a low activation energy for reactions similar to 3a appear in the literature. In a study of autoxidation kinetics, Zabarnick (1993) used an activation energy of 5 kcal/mol for

hydroperoxide formation resulting from hydrogen-atom abstraction reactions. Reaction 6a converts species P1 to D_{bulkc} when the bulk temperature of the thermally stressed fuel falls below T_{crit}. Reaction 6a is assumed to take place with zero activation energy when the temperature is sufficiently reduced. Reaction 7a has a relatively high activation energy which limits the concentration of P1 at high temperatures. Reaction 10a permits the conversion of soluble precursors (P1) produced by reaction 5a only when the wall temperature falls below T_{crit}. Reaction 11a represents adherence of D_{bulkc} to the wall, which is also assumed to take place at a temperature below T_{crit}. The activation energies for reactions 10a and 11a are anticipated to be low but were not taken as zero because the measured surface deposition in the cooled section exhibited a temperature dependence. The activation energies for reactions 10a and 11a were finally chosen by trial-and-error. Reactions 6 and 9 from the model of Table 4 have been eliminated from the new global scheme since the surface deposition resulting from them is insignificant in comparison to that resulting from the other wall reactions. Thus, reactions 1a–5a and 7a–9a represent reactions occurring in sufficiently warm regions, and reactions 6a, 10a, and 11a occur downstream of the warm regions in cooled sections where the temperature is less than T_{crit}.

As in the previous model, the global kinetics of the heated regions accommodates different fuels through the influence of the fuel-specific heteroatomic species, F_s, and the Arrhenius pre-exponential multipliers of the initial one-step oxidation reaction. The pre-exponential multiplier of reaction 1a, which was determined by a curve fit of the measured oxygen consumption over a variety of flow rates and block temperatures (Heneghan et al., 1993) is different from that of reaction 1 of the previous model in order to capture the different oxidation characteristics of this JP-8 fuel. Although not directly measurable, F_s for a specific fuel can be indirectly determined from metal coupon tests (Katta et al., 1993) or the multiplier A_{3a} can be calibrated by carbon burn-off measurements of heated tubes while assuming that all other constants are fixed for a given fuel. The magnitudes of the Arrhenius multipliers (A_{6a}, A_{10a}, and A_{11a}) for reactions at cooled surfaces have been determined by trial-and-error using experimental measurements of the mass of surface deposits formed there. In the present study, carbon deposition measurements obtained using a heated surface temperature of 270 °C and a flow rate of 16 mL/min provided values for A_{6a}, A_{7a}, A_{10a}, and A_{11a}. As will be shown later, the Arrhenius multipliers found for this condition satisfactorily predict surface deposition rates at a flow rate of 4 mL/min and at other heated block temperatures at 16 mL/min. The Arrhenius parameters for reactions 7 and 8 of the model of Table 4 are retained in reactions 8a and 9a.

In the heated sections, the strong dependence of deposition on wall temperature (Figure 4a and Ervin and Williams (1996)) suggests deposit initiation takes place at the stainless-steel surface, the location of maximum temperature in the radial direction. Because of the high temperatures existing at the heated wall together with the potential catalytic effects of the stainless steel, the fuel oxidation rate is greatest there. In contrast to deposition on heated surfaces, the efficiency of deposit accumulation at a cooled surface decreases with increasing temperature since the insoluble compounds may become soluble with increasing temperature and no longer adhere to the wall. This behavior is reflected in the new model since the sticking probability for the particles associated with cooled surfaces is assumed to be zero above T_{crit}. The sticking probability is defined as the probability that a particle reaching the wall will remain there and includes an Arrhenius-like dependence on the wall temperature (Epstein, 1986). The number of P, P1, and D_{bulkc} particles that attach to the wall and transform into either D_{wall} or D_{wallc} is dependent on the sticking probability and the concentration gradient of the respective species. Thus, the rate of deposition at the wall for $T_{wall} < T_{crit}$ is

$$\frac{dD_{wall}}{dt} = \frac{c}{\tau_{wall}^{0.7}}\{[P1]_{wall}A_{10_a}e^{-E_{10a}/(RT)} + [D_{bulkc}]_{wall}A_{11a}e^{-E_{11a}/(RT)}\} \quad (1)$$

and for $T_{wall} > T_{crit}$ is

$$\frac{dD_{wall}}{dt} = \frac{c}{\tau_{wall}^{0.7}}\{[P]_{wall}A_{9a}e^{-E_{9a}/(RT)}\} \quad (2)$$

In eqs 1 and 2, E represents an activation energy, and R is the universal gas constant. It is physically plausible that the sticking probability would vary inversely with the wall shear stress, τ_{wall}. Thus, τ_{wall} appears in the denominator of the right-hand sides of eqs 1 and 2. The constant 0.7 has been suggested by Katta et al. (1993).

Results and Discussion

In order to understand the formation of surface deposits along the fuel passage, it is important to visualize how dissolved oxygen is consumed along the tube. In Figure 3, dissolved oxygen concentration distributions computed using the single-step autoxidation reaction for JP-8 fuel are given along with those measured at three locations in the flow direction for flow rates of 16 mL/min (Figure 3a,b) and 4 mL/min (Figure 3c) for different imposed wall temperatures. Wall temperature distributions given by curve fits of the measured values, and the computed bulk temperature distribution are provided for reference. In these figures, the origin corresponds to the inlet of the first heated block. Figure 3a shows that at the high flow rate and the wall temperature of 270 °C, the dissolved oxygen is fully consumed within the first heated block. With an imposed heated wall temperature of 240 °C, Figure 3b shows that the dissolved oxygen is not consumed entirely in the heated sections. Thus, the residence time is insufficient at this temperature level to achieve complete oxygen depletion. The temperature of the fuel falls to sufficiently low temperatures within the cooled block such that very little further oxygen consumption is observed. Figure 3c (4 mL/min) is for an imposed wall temperature of 227 °C. In this case, the dissolved oxygen is fully consumed soon after the fuel enters the second heated block. Figure 3 shows that the computed dissolved oxygen concentration agrees with the measured concentration at the three indicated locations and that significant oxidation occurs in heated regions and in the insulated tube but not in the actively cooled tube.

In Figure 4, the mass of carbon measured on tube sections taken from along the flow path is normalized by both the inner surface area of the tube and the time

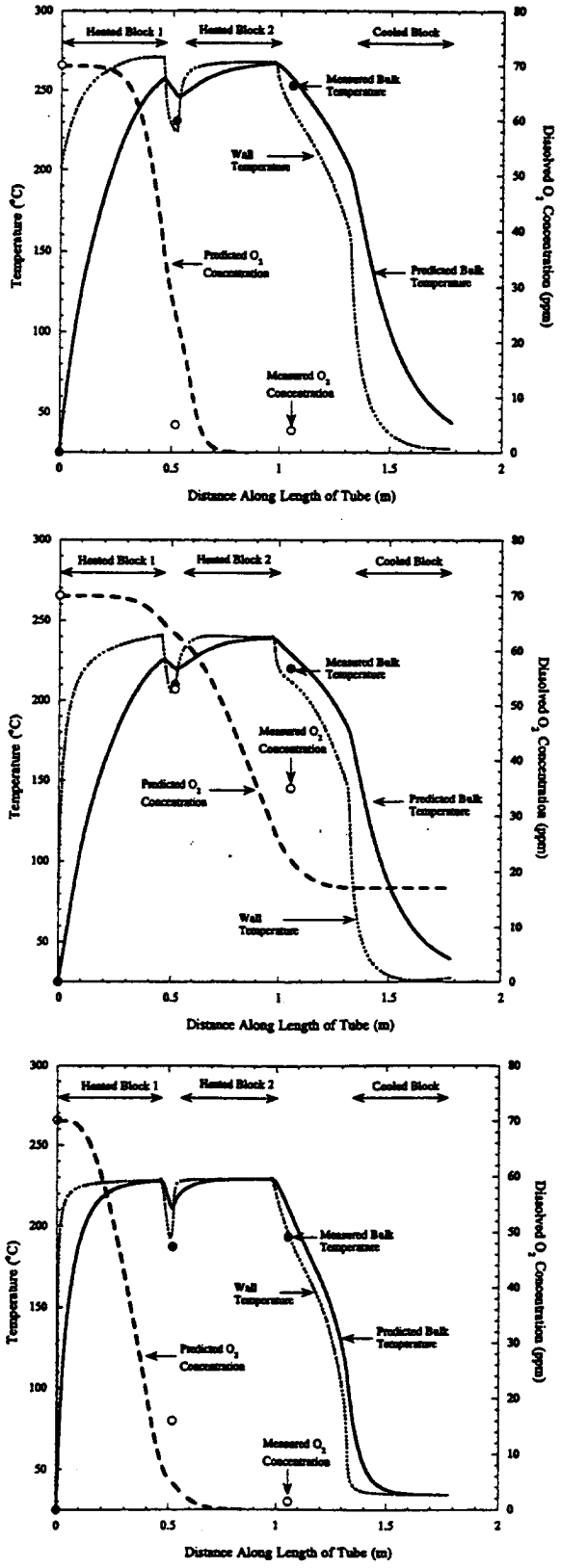

Figure 3. (a) Dissolved O_2 concentration and temperature profiles for JP-8. 270 °C heated block temperature and 16 mL/min flow rate. (b) Dissolved O_2 concentration and temperature profiles for JP-8. 240 °C heated block temperature and 16 mL/min flow rate. (c) Dissolved O_2 concentration and temperature profiles for JP-8. 227 °C heated block temperature and 4 mL/min flow rate.

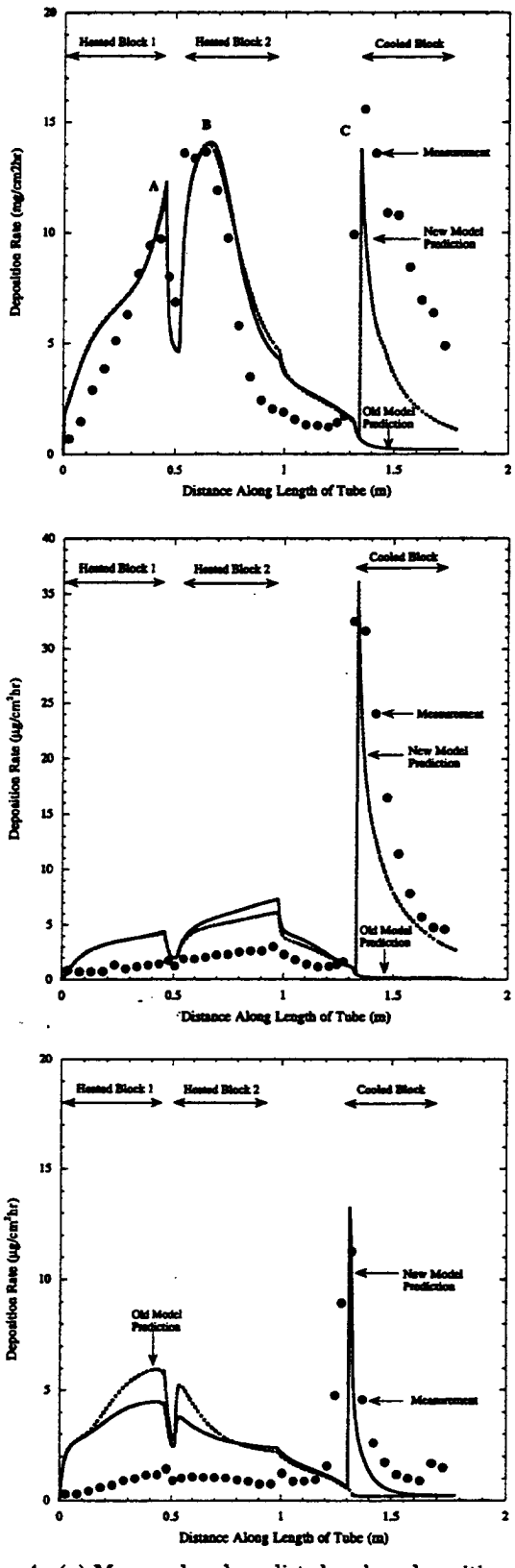

Figure 4. (a) Measured and predicted carbon deposition rates for JP-8. 270 °C heated block temperature and 16 mL/min flow rate. (b) Measured and predicted carbon deposition rates for JP-8. 240 °C heated block temperature and 16 mL/min flow rate. (c) Measured and predicted carbon deposition rates for JP-8. 227 °C heated block temperature and 4 mL/min flow rate.

period of testing to give an average deposition rate. Figure 4 shows computed and measured carbon deposition rate profiles for JP-8 fuel flowing at 16 mL/min (Figure 4a,b) or 4 mL/min (Figure 4c).

In Figure 4a, measured deposition rate profiles and those predicted by the models of Tables 4 and 5 are given for an imposed wall temperature of 270 °C. For calculations involving the old model, the value of the multiplier given for reaction 1a of Table 5 was used

rather than that given by reaction 1 of Table 4. The more recent value obtained by flowing tests for a variety of temperatures and applicable to either model was used because it represented the measured oxygen consumption more satisfactorily than the older value. Locations A, B, and C correspond to maxima in deposition. Between A and B, the measured deposition rate abruptly declines as the fuel enters the unheated tube segment between the first and second heated blocks, and the wall and bulk temperatures decrease. The deposition rate then increases near 50 cm as the wall temperature approaches 270 °C. Location B is in the region in which the dissolved oxygen is depleted, but the rate of deposition is relatively high. Similarly, large deposition rates in a flowing system have been observed near the location where oxygen depletion occurs (Heneghan et al., 1995). Immediately downstream of B, although the wall and bulk temperatures are nearly constant, the deposition rate declines in the absence of dissolved oxygen.

Within the heated or insulated tube, the deposition may fall to low levels for two reasons. The first is that the dissolved oxygen is fully consumed, and thus, there is no more fuel oxidation (Figure 4a, the region downstream of location B within the second heated block). In terms of the new model under conditions of oxygen depletion, the formation of peroxide radicals in the fuel bulk by reaction 1a and at the wall through reaction 8a ceases. Thus, the rates of production of P by reactions 3a and 8a and D_{wall} of reaction 9a all decline. The second reason is that the temperature (as shown in Figure 3a between locations A and B) is low. In terms of the model of Table 5, the rates of the bulk fuel reactions (1a−5a) and the wall reactions (8a and 9a) all decrease with decreasing wall and bulk fuel temperatures as found between locations A and B.

At location C the wall temperature is a minimum, yet the deposition rate is of the same order as that at locations A and B. Between 130 and 140 cm, (location C) the wall temperature sharply decreases by 200 °C. Moreover, since the dissolved oxygen is fully depleted beyond location B, it is believed that the local maximum in deposition at C is a consequence of compounds which were soluble at higher temperatures but are now insoluble at lower temperatures. A peak in the deposition rate in a cooled region in flowing tests has been observed previously (Heneghan et al., 1995; Ervin et al., 1995). Figure 4a shows that in the sections preceding the cooled block, the deposition rates predicted by both models generally follow the measured profiles. However, the global chemistry model proprosed by Katta et al. (1993) predicts zero deposition in the cooled block.

Figure 4b shows that for an imposed wall temperature of 240 °C the deposition rates in the heated sections are generally smaller than those observed at 270 °C. This is anticipated since less oxygen (Figure 3b) is consumed at the lower temperature. In addition in the heated sections, there is a gradual increase in the measured deposition rate rather than the well-defined peaks observed at 270 °C. The most striking differences in deposition rates between parts a and b of Figure 4 are the very large deposition rates near the entrance of the cooled section (130 cm) of Figure 4b but low deposition rates in the heated section of Figure 4b. Figures 3b and 4b show that at 240 °C less dissolved oxygen is consumed than at 270 °C, but the maximum measured deposition rates in the cooled tube for a heated block temperature of 240 °C are greater than those in the cooled tube for a heated block temperature of 270 °C. The new model predicts greater rates of deposition in the cooled section for the lower heated block temperature because the concentration of P1 required for the production of cold wall deposits (reaction 10a) is converted to soluble compounds (reaction 7a) at a significantly greater rate at the higher temperature. Thus, at the higher temperature, less precursor for cooled wall deposits is available. Figure 4b shows the ability of the new model in predicting the deposition in cooled regions where the deposition there is an order of magnitude greater than that in the heated sections.

Figure 4c shows measured and computed deposition rates along the length of tube at the flow rate of 4 mL/min and heated block temperature of 227 °C. As in Figure 4b, the deposition in the cooled section of Figure 4c is significantly greater than that in the heated regions. However under the heating and flow conditions of Figure 4c, the dissolved oxygen is now fully reacted within the second heated block. Clearly, in Figure 4b,c, the dominant form of surface deposition occurs in the cooled sections, and this is captured by the new model.

Parts a, b, and c of Figure 4 show a sharp rise in the measured deposition rate at the cooled block entrance followed by a decline in the deposition rate within the rest of the cooled tube. In terms of the new model, this is represented by a competition between reactions 6a within the fuel bulk and reaction 10a at the tube surface. As the warm fuel enters the cooled section, the location where the temperature initially falls below T_{crit} is at the cooled tube surface. There P1 is converted to D_{wallc} by reaction 10a alone. As the fuel passes through the cooled block, the thermal boundary layer produced by the cooled wall grows, and reaction 6a begins to occur within this fuel layer. As reaction 6a proceeds, less P1 is available for reaction 10a, and the deposition rate profile along the cooled section falls.

It has been observed (Ervin et al., 1995; Heneghan et al., 1995) that, as the heated block temperature is increased for a given flow rate, the production of wall deposit in the cooled tube section decreases while the mass of deposits formed in the heated tube increases. This observation can be explained in terms of the new model. As the temperature of the heated tube increases, the production of P increases by means of reactions 3a and 8a, and the concentration of D_{wall} increases. By way of reaction 5a, the conversion of P to P1 also increases with increasing temperature. Reaction 7a has a relatively high activation energy which limits the concentration of P1 at high temperatures and, consequently, the downstream production of deposits at a cooled surface. Thus with increased heated wall temperature, the new model has the ability to simulate increased deposition in heated regions but decreased fouling at cooled surfaces.

Chemical differences between fouling with JP-8 in the heated and cooled sections have been measured by means of XPS. Table 6 shows chemical differences between the deposits formed at locations 60 cm (heated section) and 140 cm (cooled section) for a fuel flow rate of 4 mL/min. As Table 6 shows, after 6 h of flowing fuel, the O−C=O and C=O percent atomic compositions are lower at 140 cm, but the sulfur oxide and nitrogen compositions are greater there. In a model proposed by Kauffman (1995), particles formed within the bulk of the fuel were assumed to play a role in the reactions

Table 6. XPS Analysis of Deposits in Heated and Cooled Sections (227 °C Heated Block Temperature)[a]

location (cm)	O−C=O	C=O	C−O	CH, C	O	Fe	Cr	N	S−O	S−C	Si	total
60 heated block 227 °C	4.5	4.6	7.3	51.0	26.2	2.5		1.8	1.1	0.37		99.4
140 cooled block	1.4	2.8	6.6	54.4	23.2	3.8		4	3.7	0.35		100.3
new tube	4.8	1.9	5.4	30.2	30.1	14.6	4.1	0.7	0.9	0.2	7.1	100.0

[a] O−C=O, acids and esters; C=O, aldehydes and ketones; C−O, alcohols nd ethers; S−O, sulfur oxides; N, nitrogen compounds.

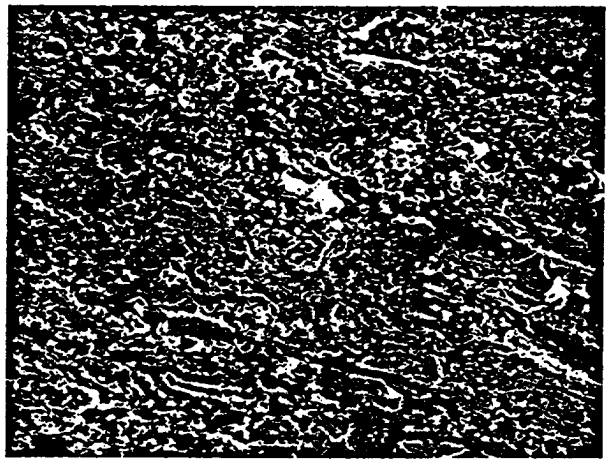

Figure 5. SEM micrographs of inner tube surfaces. Tube exposed to JP-8 fuel flowing at 4 mL/min: (A) within the second heated block (60 cm) (magnification 5000×) and (B) within the cooled block (130 cm) (magnification 4000×).

which form surface deposits. In flask tests using Jet-A fuel, Kauffman found by XPS analysis that filtered particles (with diameters > 0.4 μm) produced by oxidized sulfur compounds had significant nitrogen content. In addition, the deposits formed in the cold tube are acetone soluble, but those formed in the heated blocks are not. Thus, the deposits in the cooled section have different properities than those found in the heated sections.

Figures 3 and 4 show that oxidation and deposition mechanisms in the heated locations are different from those within the cooled tube; morphological differences in the two kinds of deposits become evident with SEM analysis. SEM micrographs (Figure 5) of JP-8 fuel deposits after 6 h of flow at 4 mL/min formed in the heated section (at 60 cm) reveal that the deposit appears to be composed of nearly spherical submicron particles, and this has been reported much earlier (Schirmer, 1970). At a location in the cooled tube near the maximum deposition rate (130 cm), the deposit micro-

Table 7. Measured Dissolved O_2 Consumption within Heated Blocks 1 and 2 for a Block Temperature of 270 °C and 16 mL/min Flow Rate

fuel	O_2 consumed heated block 1 (ppm)	O_2 consumed heated block 2 (ppm)	total O_2 consumed (ppm)
JP-8	70	0	70
JP-8B	65	4	69
JP-8M	70	0	70

Table 8. Measured Dissolved O_2 Consumption within Heated Blocks 1 and 2 for a Block Temperature of 240 °C and 16 mL/min Flow Rate

fuel	O_2 consumed heated block 1 (ppm)	O_2 consumed heated block 2 (ppm)	total O_2 consumed (ppm)
JP-8	22	17	39
JP-8B	14	16	30
JP-8M	25	22	47

structure conforms to the topography of the underlying tube surface and has a roughness length scale smaller than that of the original metal surface but larger than that of the microspheres.

The addition of thermal stability additives to JP-8 fuel complicates the understanding of the relation between deposition and oxidation because the thermal stability additives can change the chemical mechanisms of deposit formation. Tables 7 and 8 show that for the same flow rate but different imposed wall temperatures, JP-8B is oxidized at a slightly lower rate than the other fuels. In contrast, Zabarnick and Grinstead (1994) using a quartz crystal microbalance have demonstrated that the additive package added to JP-8 to make JP-8B can significantly delay the oxidation process. Figure 6 shows the variation in deposition rates along the length of the tube among JP-8, JP-8B, and JP-8M fuels. At 16 mL/min and a heated wall temperature of 270 °C (Figure 6a), JP-8M produces minimal deposits in the cooled section but moderate levels of deposits in the heated sections. Of the fuels with thermal stability additives, JP-8M produces the lowest total mass of deposits under the conditions of Figure 6a,b (16 mL/min and an imposed wall temperature of 240 °C). In Figure 6c for a flow rate of 4 mL/min and a heated tube wall temperature of 227 °C, JP-8B has the lowest deposition rate in the heated sections but a relatively high deposition rate in the cooled section. The thermal stability additives in JP-8B are effective in altering the deposition mechanisms which occur at high temperatures but are less effective in preventing deposition in cooled regions.

Generally, thermal stability experiments (Hazlett, 1991) do not study the flow of thermally stressed fuel through cooled sections. However, the results of Figure 6 show that thermal stability additives can be effective in heated regions but can also be less effective in downstream cooled regions. The implications of Figure 6 are significant for future thermal stability testing. Future thermal stability testing should incorporate deposition measurements in downstream cooled regions because the formation of two types of deposits is

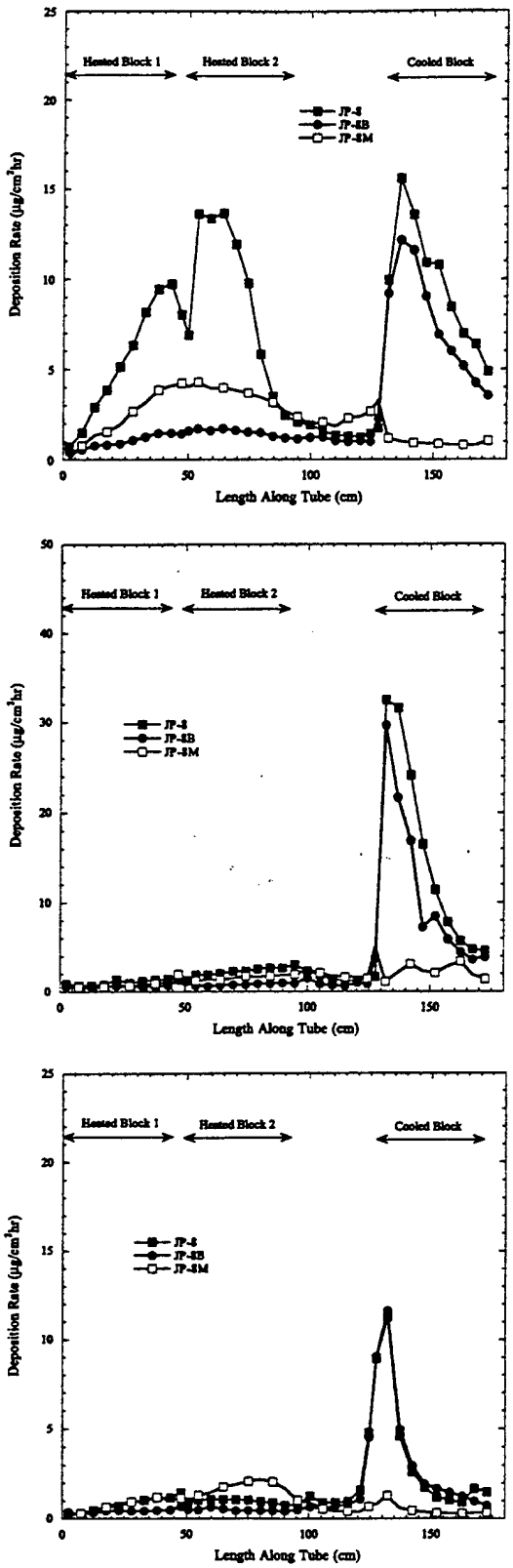

Figure 6. (a) Measured deposition rates: JP-8, JP-8B, and JP-8M. 16 mL/min, 270 °C. (b) Measured deposition rates: JP-8, JP-8B, and JP-8M. 16 mL/min, 240 °C. (c) Measured deposition rates: JP-8, JP-8B, and JP-8M. 4 mL/min, 227 °C.

important to the development of recirculating fuel systems. Recirculation systems will use heat exchangers to cool the fuel to an appropriate temperature prior to returning it to the fuel tanks. These heat exchangers would likely be collectors of the type of deposits found here in the cooled block.

Conclusions

With the cooling of thermally stressed straight-run jet fuel, once soluble species may form deposits. In previous work, this kind of deposit has received little attention because the thermal stability of aviation fuel is generally assessed by tests which consider deposition only in regions maintained at temperatures where the fuel is oxidized. In the current work, deposition in cooled regions was numerically simulated, and experiments were performed to examine the effects of two different thermal stability additives there. From examination of the results obtained in this investigation, the following conclusions may be drawn:

1. Numerical simulations of the global chemistry involved in surface deposition are valuable in interpreting experimental results obtained from different flow regimes.

2. The rate of fouling in cooled regions can be an order of magnitude greater than that occurring in heated regions. Hence, deposition at cooled surfaces may be a serious problem in aircraft which recirculate large volumes of fuel.

3. Thermal stability additives that are effective in heated regions may be less effective in cooled regions. Thus, the fouling of cooled surfaces should be studied in the assessment of candidate thermal stability additives.

Acknowledgment

This work was supported by the U.S. Air Force, Aero Propulsion and Power, Fuels and Lubrication Division, Wright Laboratories, Wright-Patterson AFB, OH, under Contract No. F33615-92-C-2207 (Technical monitor: C. W. Frayne). The authors also acknowledge the insightful comments of Dr. Steven Zabarnick and Dr. Shawn Heneghan of the University of Dayton Research Institute and Dr. Tim Edwards of Wright Laboratories.

Nomenclature

A_{1a} = exponential premultiplier corresponding to reaction 1a
ASTM = American Society for Testing and Materials
C = empirical constant in sticking probability expressions, $(m^2/N)^{0.7}$
D_{bulk} = particles formed from fuel oxidation
D_{bulkc} = insolubles formed below T_{crit} in bulk fuel
D_{wallc} = deposits formed at cooled tube surface
D_{wall} = deposits formed at heated tube surface
E_{1a} = activation energy for reaction 1a, kcal/mol
F = fuel
F-2827 = Jet-A neat fuel
F-2980 = Jet-A neat fuel
F_s = heteroatomic species within fuel
JFTOT = jet fuel thermal oxidation test
JP-8 = F-2827 with additives given by MIL-T-83133
k = reaction rate constant
P = precursor species for deposits formed in heated sections
P1 = precursor species for deposits formed in cooled sections
R = universal gas constant, kcal/mol K
SEM = scanning electron microscopy
T_{crit} = temperature at which soluble species become insoluble, K
τ_{wall} = wall shear stress, N/m^2
XPS = X-ray photoelectron spectroscopy

Literature Cited

Epstein, N. *Heat Exchanger Sourcebook*; Pale, J. W., Ed.; Hemisphere: Washington, DC, 1986.

Ervin, J. S.; Williams, T. F. Dissolved Oxygen Concentration and Jet Fuel Deposition. *Ind. Eng. Chem. Res.* **1996**, *35*, 899.

Ervin, J. S.; Heneghan, S. P.; Martel, C. R.; Williams, T. F. Surface Effects on Deposits from Jet Fuels. *J. Eng. Gas Turbines Power* **1996**, *118*, 278.

Hazlett, R. N. *Thermal Oxidation Stability of Aviation Turbine Fuels*; ASTM: Philadelphia, PA, 1991.

Heneghan, S.; Williams, T.; Martel, C.; Ballal, D. Studies of Jet Fuel Thermal Stability in a Flowing System. *J. Eng. Gas Turbines Power* **1993**, *115*, 480.

Heneghan, S. P.; Chin, L. P. Autoxidation of Jet Fuels; Implications for Modeling and Thermal Stability. In *Proceedings of the 5th International Conference on Stability and Handling of Liquid Fuels*; Giles, H. N., Ed.; U.S. Department of Energy: Washington DC, 1995; Vol. 1, pp. 91–102.

Heneghan, S. P.; Kauffman, R. E. Analytic Tests and Their Relation to Jet Fuel Thermal Stability. In *Proceedings of the 5th International Conference on Stability and Handling of Liquid Fuels*; Giles, H. N., Ed.; U.S. Department of Energy: Washington DC, 1995; Vol. 1, pp. 29–42.

Heneghan, S.; Martel, C.; Williams, T.; Ballal, D. Effects of Oxygen and Additives on the Thermal Stability of Jet Fuels. *J. Eng. Gas Turbines Power* **1995**, *117*, 120.

Jones, E. G.; Balster, W. J. Phenomenological Study of the Formation of Insolubles in a Jet-A Fuel. *Energy Fuels* **1993**, *7*, 968.

Jones, E. G.; Balster, W. J.; Post, M. E. Degradation of a Jet-A Fuel in a Single Pass Heat Exchanger. *J. Eng. Gas Turbines Power* **1995**, *117*, 125.

Katta, V. R.; Roquemore, W. M. Numerical Method for Simulating Fluid-Dynamic and Heat Transfer Changes in Jet Engine Injector Feed-Arm Due to Fouling. *J. Thermophys. Heat Transfer* **1993**, *7*, 651.

Katta, V. R.; Jones, E. G.; Roquemore, W. M. Development of Global-Chemistry Model for Jet-Fuel Thermal Stability Based on Observations from Static and Flowing Experiments. Presented at The 81st AGARD Symposium on Fuels and Combustion Technology for Advanced Aircraft Engines, Colliferro, Italy, May 1993.

Katta, V. R.; Blust, J.; Williams, T. F.; Martel, C. R. Role of Buoyancy in Fuel-Thermal Stability Studies. *J. Thermophys. Heat Transfer* **1995**, *9*, 159.

Kauffman, R. E. The Effects of Different Sulfur Compounds on the Oxidation and Deposition Mechanisms of Jet Fuel. Presented at IGTI Turbo Expo '95, Houston, TX, June 1995; ASME Paper 95-GT-222.

Krazinski, J. L.; Vanka, S. P.; Pearce, J. A.; Roquemore, W. M. A Computational Fluid Dynamics and Chemistry Model for Jet Fuel Thermal Stability. *J. Eng. Gas Turbines Power* **1992**, *114*, 104.

Nixon, A. C.; Ackerman, G. H.; Faith, L. E.; Henderson, H. T.; Ritchie, A. W.; Ryland, L. B.; Shryne, T. M. Vaporizing and Endothermic Fuels for Advanced Engine Application: Part III, Studies of Thermal and Catalytic Reactions, Thermal Stabilities, and Combustion Properties of Hydrocarbon Fuels (AFAPL-TR-67-114). Air Force Aero Propulsion Laboratory, Wright-Patterson Air Force Base, OH, 1967.

Rubey, W.; Striebich, R.; Tissandier, M.; Tirey, D.; Anderson, S. Gas Chromatographic Measurement of Trace Oxygen and Other Dissolved Gases in Thermally Stressed Jet Fuel. *J. Chromatogr. Sci.* **1995**, *33*, 433.

Schirmer, R. Morphology of Deposits in Aircraft and Engine Fuel Systems. Society of Automotive Engineers National Air Transportation Meeting, New York, April 1970; SAE Paper 700258.

Zabarnick, S. Chemical Kinetic Modeling of Jet Fuel Autoxidation and Antioxidant Chemistry, *Ind. Eng. Chem. Res.*, **1993**, *32*, 1012.

Zabarnick, S.; Grinstead, R. Studies of Jet Fuel Additives Using the Quartz Crystal Microbalance and Pressure Monitoring at 140 °C. *Ind. Eng. Chem. Res.* **1994**, *33*, 2771.

Received for review April 18, 1996
Revised manuscript received July 4, 1996
Accepted July 16, 1996[⊕]

IE960220E

[⊕] Abstract published in *Advance ACS Abstracts,* October 1, 1996.

Appendix H.

Surface Effects on Deposits from Jet Fuels

Jamie S. Ervin
Shawn P. Heneghan
Charles R. Martel
Theodore F. Williams
University of Dayton
300 College Park
Dayton, OH 45469-0140

Surface Effects on Deposits From Jet Fuels

J. S. Ervin

S. P. Heneghan

C. R. Martel

T. F. Williams

University of Dayton, Dayton, OH 45469

Flow experiments in a single-pass heat exchanger using JP-8 and certain additives were initiated under controlled conditions to explore the effects of a metal surface on deposition. The experimental apparatus permitted a unique viewing of the time evolution of deposits at different axial locations under conditions of limited oxygen availability somewhat similar to those in jet aircraft. Scanning electron microscopy was used to examine deposit microstructure. In addition, x-ray photoelectron spectroscopy and Auger electron spectroscopy determined the chemical composition of the deposits. Oxygen concentration measurements in the bulk flow were also performed, and the observed transient oxidation behavior was related to measured time-dependent changes in the deposit. Increasing dissolved oxygen levels and large changes in deposition were characteristic of the induction time. Mechanisms of fouling in the heated and cooled sections were different. Spectroscopic analysis indicated that deposits formed in the heated section had chemical compositions different from those formed in the cooled section. Scanning electron microscopy revealed differences in microstructure between the heated and cooled sections: More uniform deposits formed in the cooled section as a result of once-soluble species becoming insoluble at low temperatures. In addition, the JP-8 additives significantly reduced fouling in the heated section, but their effectiveness in the cooled section, especially after long periods, was unclear.

Introduction

In jet aircraft, fuel is employed as a heat transfer medium to cool the engine lubricant, hydraulic fluids, environmental system, and avionics. Further increases in fuel temperature occur with flow through the main fuel pump and the burner feed arm. Combined, the heat flux from these sources stimulates oxidation reactions, which ultimately result in deposits within fuel lines, on heat exchanger surfaces, and in fuel injectors (Hazlett, 1991). The gradual fouling of tubes within heat exchangers eventually leads to degradation of heat transfer effectiveness since the presence of the deposit increases the thermal resistance between the heated tube wall and the flowing fuel (Johnson et al., 1954; Bradley et al., 1974; Hazlett, 1981; Hazlett and Hall, 1985; Chin and Lefebvre, 1993). Ultimately, if unchecked, the fouling of valves and other close tolerance parts may result in failure of the fuel system. In addition, fouling of fuel nozzles can produce undesirable spray patterns, which cause severe thermal stressing and degradation of the combustor and turbine. Hence, knowledge of the physical structure and chemical properties of deposits, together with an understanding of accumulation mechanisms on metal surfaces, is of great value to jet aircraft designers.

The surface of a heated tube influences the deposition rate by both physical and chemical action, as has been demonstrated by experiment (Hazlett, 1991). The microgeometry of the surface affects the fluid motion near the wall, promoting turbulence and increased mass transport (Smith, 1969; Bradley et al., 1974). Also, the capillary mechanism and the increased surface area as a result of porosity changes are believed to have some role in the observed accelerated deposition rate during long-term testing (Giovanetti and Szetela, 1985; Kamin et al., 1988).

The chemical composition of the tube wall can also determine deposition reactions. For example, Kendall and Mills (1985) and have found that stainless-steel tubes tend to form more deposits than aluminum tubes, and that magnesium migration to the surface of an aluminum tube inhibits fouling. As part of a research program with the United States Air Force involving JP-8 fuels, Lefebvre (1992) found that the deposition rate depends on the metal surface pretreatment. In addition, Heneghan et al. (1985) proposed that a surface-catalyzed peroxide decomposition was responsible for some deposits formed at low temperatures.

Experiments were performed to study fuel deposition under controlled conditions in a forced-flow system in order to investigate effects of the wall and to obtain baseline data on the structure and chemical compositions of deposits after different time periods. Scanning electron microscopy (SEM) is used to examine deposit microstructure, and, in addition, x-ray photoelectron spectroscopy (XPS) and Auger electron spectroscopy (AES) are used to study the chemical composition of the deposits. The experimental arrangement described herein has the unique capability of permitting viewing of the time evolution of deposits under conditions of nonisothermal bulk flow with limited oxygen availability similar to that in jet aircraft.

Apparatus

In the experimental arrangement described in detail by Heneghan et al. (1993) (Fig. 1), fuel at ambient temperature passes from the preconditioning tank by means of a positive displacement diaphragm pump into the first heated block at a pressure of 2.48 MPa; then, eventually, it passes into a cooled block. The insoluble solids were produced by liquid-phase reactions alone since the high pressure maintained the fuel in the compressed liquid state. In the preconditioning tank, the fuel may be sparged with mixtures of nitrogen and oxygen to control the amount of dissolved oxygen and displace argon from the fuel in order to avoid misinterpretations of gas chromatograph measurements. In addition, a positive displacement flow meter monitors the volumetric flow rate of the fuel.

The two heated copper blocks are connected in series and envelope the 316 stainless-steel tubing (180 cm long by 2.16 mm ID by 3.18 mm OD) through which the fuel passes. Each block (46 cm long with a 7.6 cm diameter) can reach tempera-

Contributed by the International Gas Turbine Institute and presented at the 40th International Gas Turbine and Aeroengine Congress and Exhibition, Houston, Texas, June 5–8, 1995. Manuscript received by the International Gas Turbine Institute February 10, 1995. Paper No. 95-GT-103. Associate Technical Editor: C. J. Russo.

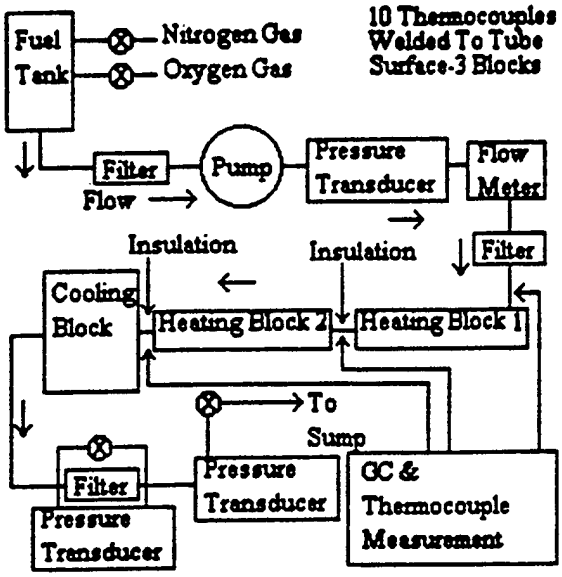

Fig. 1 Experimental apparatus

tures near 770 K and is controlled in such a way that the tube wall temperature distribution remains steady (within ± 2°C). The cooled section consists of an air-cooled copper block (46 cm long with a 7.6 cm diameter), which results in an exiting fuel bulk temperature near ambient. Calibrated type K thermocouples (20 gage) are welded to the outer surface of the stainless-steel tubing to provide the outer tube wall temperature with an uncertainty of ±1°C in both the heated and cooled sections. The stainless-steel tubes (ASTM grade A269/A213) have a surface roughness (arithmetic average) of 8 to 15 min. and are cleaned with Blue Gold alkaline solution in an ultrasonic bath, then rinsed with deionized water prior to use.

Two types of fuels were used: JP-8 and JP-8 with 25 mg/l of BHT (an antioxidant) and 100 mg/l of a dispersant (Betz Process Chemicals 8Q405). The mixture of JP-8 fuel, BHT, and 8Q405 is referred to below as JP-8A. The JP-8 fuel consisted of a Jet A fuel (POSF 2980) and the additives given by military specification MIL-T-83133. The chemical and physical properties of POSF 2980 are listed by Grinstead et al. (1994). Furthermore, Anderson et al. (1994) have identified BHT and 8Q405 as effective deposit-suppressing additives.

Oxygen is detected in-line by means of a Hewlett Packard 5890 Series II gas chromatograph with a microthermal conductivity detector; oxygen concentrations as low as 150 parts per billion can be detected. Oxygen concentrations are measured at the locations shown in Fig. 1: at the inlet of the first heated block, at the inlet of the second heated block, and at the inlet before the cooled block. Details of the installation, fabrication, and calibration of the oxygen analyzer are given by Rubey et al. (1992).

Procedure

In the current experiments, fuel flowed through the apparatus at a rate of 4 ml/min for periods of 0.5, 1.5, 3, 6, 12, or 24 hours. The heated section of the flow loop had bulk temperatures near 493 K for the JP-8 tests and 503 K for the JP-8A tests. A few preliminary tests demonstrated that a slightly higher bulk temperature of 503 K is required to have detectable deposition within the heated section when using JP-8A. The dissolved oxygen measured at the end of the first heated block for the tests involving JP-8A was nearly equal to that for tests with JP-8. In addition, increasing the bulk temperature for the JP-8A experiments resulted in maximum deposition at an axial location in the heated section coincident with that for tests performed with JP-8 alone. The temperature of the cooling block in all cases was held near 25°C.

At the termination of an experiment, the tubes are removed from the system, drained, and rinsed with hexane. They are then dried by flowing filtered, low-velocity nitrogen gas through them. Finally, they are sliced into 50-mm segments. The segments to be analyzed were halved in the axial direction, rinsed in hexane, and dried in a vacuum oven at 120°C for one hour. A Leco (RC-412) multiphase carbon analyzer determined the amount of carbon on half the segments from the carbon dioxide produced from complete combustion of the deposits. SEM determined the deposit microstructure and was used in conjunction with AES and XPS on the remaining segments.

XPS determined the composition of the first three nanometers of the inner tube surface, which was exposed to the thermally stressed fuel. With the AES measurements, a 100-μm-by-100-μm area was raster scanned and internal layers (up to a distance of 150 nm) within the deposit were probed. Uncertainties in the XPS measurements are on the order of 10 percent of the given value. Uncertainties in the absolute value of the composition, with regard to AES profiles of the deposits, are difficult to quantify because of preferential sputtering of certain species. Therefore, only qualitative comparisons can be made between XPS and AES measurements (Wittberg, 1994; Briggs and Seah, 1983).

Results

Axial Temperature and Oxygen Concentration Distributions. The outer tube wall and axial liquid bulk temperature distributions for the JP-8 fuel are given in Fig. 2; the origin corresponds to the inlet of the first heater block. The bulk temperature was steady, save for a moment as the experiment was initiated, indicating no detectable change in heat transfer from the heated blocks to the flowing fuel as the deposit accumulated. The fuel bulk temperature was calculated by finite difference solution of the coupled continuity, momentum, and energy equations using the outer tube wall temperature distribution and the thermal properties of the fuel and tube. The outer tube wall temperature distribution results from a least-squares fit of measured temperatures. The computational procedure, which permits the computation of the bulk temperature, is essentially the SIMPLE algorithm of Patankar (1980) and is described in more detail by Katta et al. (1994) and Krazinski et al. (1992). Turbulent flow conditions were assumed even though the Reynolds number in much of the tube was less than 2300. As described by Katta et al. (1994), buoyancy effects may induce

Nomenclature

AES = Auger electron spectroscopy
ASTM = American Society for Testing and Materials
BHT = butylated-hydroxy-toluene
JP-8A = JP-8 with BHT and 8Q405
JP-8 = POSF 2980 with icing inhibitor, static dissipator, and corrosion inhibitor
O(z) = oxygen composition distribution
POSF 2980 = jet A-neat fuel
SEM = scanning electron microscopy
t = time
XPS = x-ray photoelectron spectroscopy
z = coordinate direction normal to deposit surface
α = spatial mean value of oxygen composition
δ = deposit thickness, nm
δ' = average rate of change in deposit thickness, nm/h
8Q405 = Betz Corp. proprietary dispersant

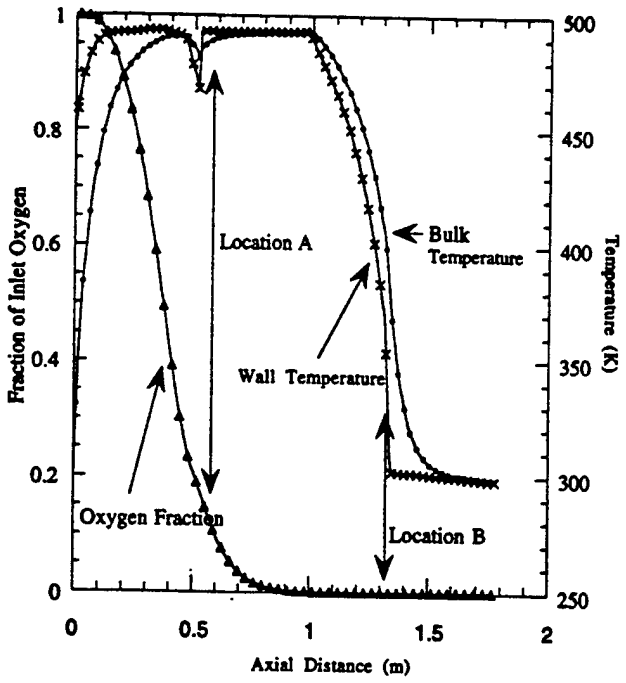

Fig. 2 Bulk oxygen and temperature distributions for JP-8 after 0.5 H

transition to turbulent flow. Furthermore, bulk fuel temperatures measured at different locations were in agreement with computed values (within 3 K). In Fig. 2 and subsequent figures, A and B correspond to local maxima in deposition as determined by carbon burnoff of tube segments, except for the period of 0.5 hours. At location A (near 55 cm), the temperature profile within the tube is essentially fully developed, and the bulk temperature is 493 K for the JP-8 tests and 503 K for the JP-8A tests. At B (near 130 cm), the bulk fuel temperature is 400 K for the JP-8 tests and 410 K for the JP-8A tests. The axial bulk temperature distribution for the JP-8A fuel was similar to that of the JP-8 fuel, except that it was 10°C greater in the heated section and in the entrance region of the cooled section.

Figure 2 shows computed transient oxygen concentrations (after 0.5 hours) ratioed by oxygen concentrations for JP-8 saturated with air. The oxygen concentration computations were performed using the same procedure as that for computation of the bulk temperatures. Measured values of the dissolved oxygen fraction compared well with the computed values. Oxygen distributions for other periods lie to the right of this curve, and oxygen distributions for JP-8A are similar to those of JP-8. In all instances at location A, the concentration of available dissolved oxygen is significantly reduced compared to the inlet conditions; at B, it is depleted.

To investigate the possibility of oxygen diffusion from the tubing or contamination from other sources, the fuel was first saturated with nitrogen gas, then pumped through the heated tubing. Since the oxygen concentration did not increase with time under nearly identical conditions (other than saturating the fuel with nitrogen gas), it was concluded that diffusion of oxygen from the walls was insignificant.

Carbon Mass Determination. In previous investigations such as Marteney (1989), deposit mass was described as a function of time, and the deposition rate increased after large times. Here, it is more physically meaningful to normalize the deposition by the total volume of fuel that has flowed for a given experiment. In Figure 3(a) for JP-8 and Fig. 3(b) for JP-8A, the deposition, determined by carbon-burnoff measurements, is scaled by the volume of fuel flowed for the tube in the first heated copper block. In addition, dissolved oxygen levels are given. The carbon deposition rate for the JP-8A mixture was an order of magnitude lower than that of JP-8.

In Figs. 4(a) and 4(b), the carbon mass, normalized by the inner surface area of the tube, is given for different axial locations, time durations, and fuels. In Fig. 4(a) for the JP-8, as might be intuitively expected, the carbon mass for the 24-hour test is greater than that for the shorter tests. However, the carbon accumulated along the tube after 0.5 hours and then after 1.5 hours is nearly the same; a similar comparison can be drawn between measurements at three and six hours. This seemingly inconsistent behavior is still reasonable since the reproducibility in the determination of the mass of carbon is on the order of ±25 percent. For all the times except 0.5 hours, there are two peak locations in the spatial distribution of the carbon deposit

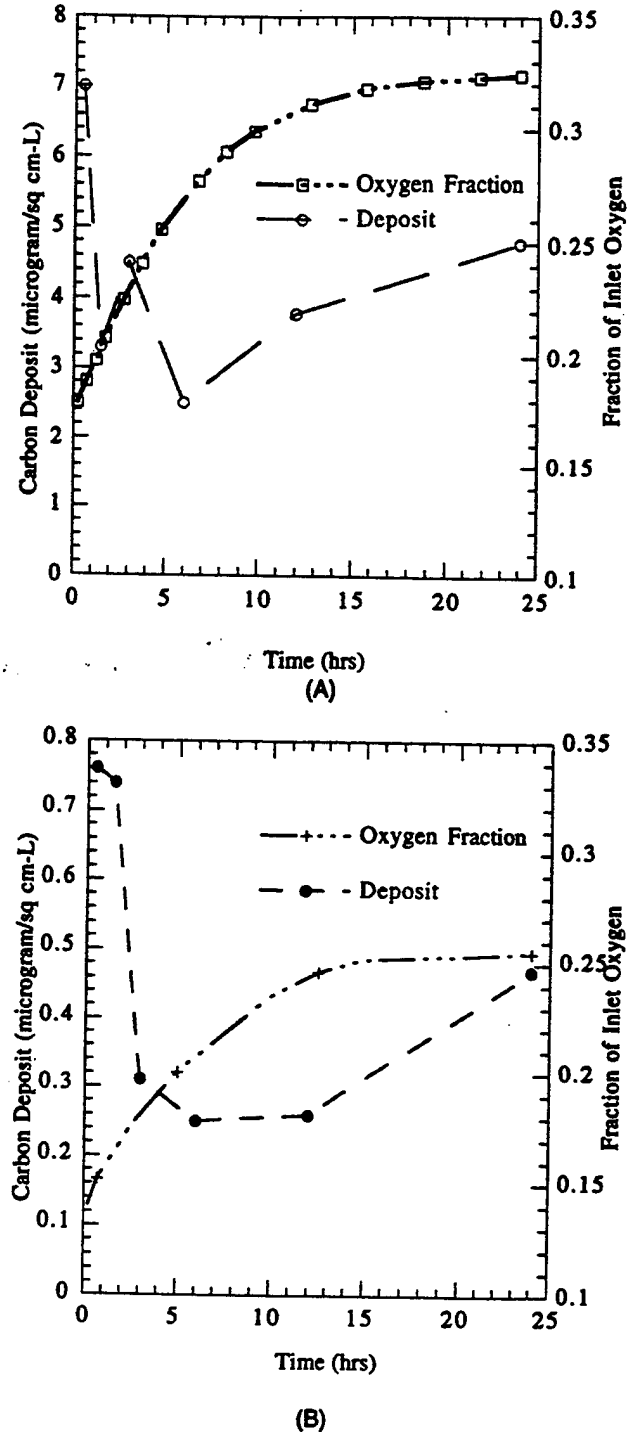

Fig. 3 Carbon deposition and fraction of inlet oxygen, heater block 1: (A) JP-8 fuel; (B) JP-8A fuel

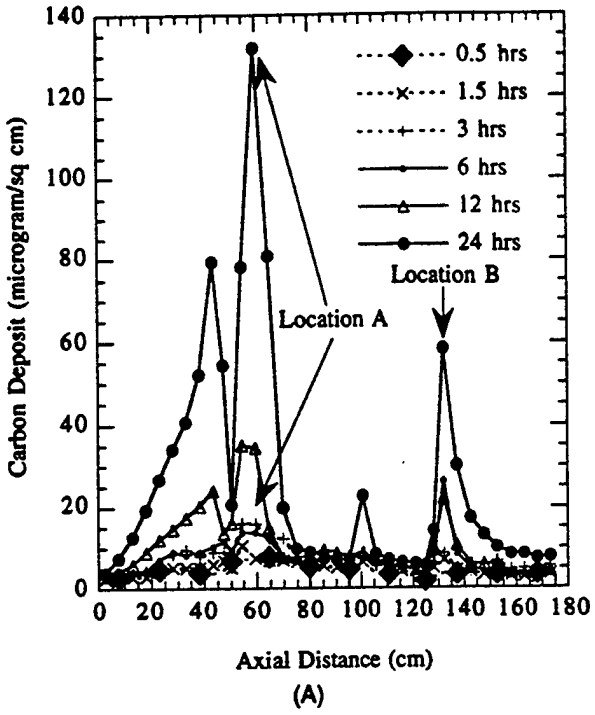

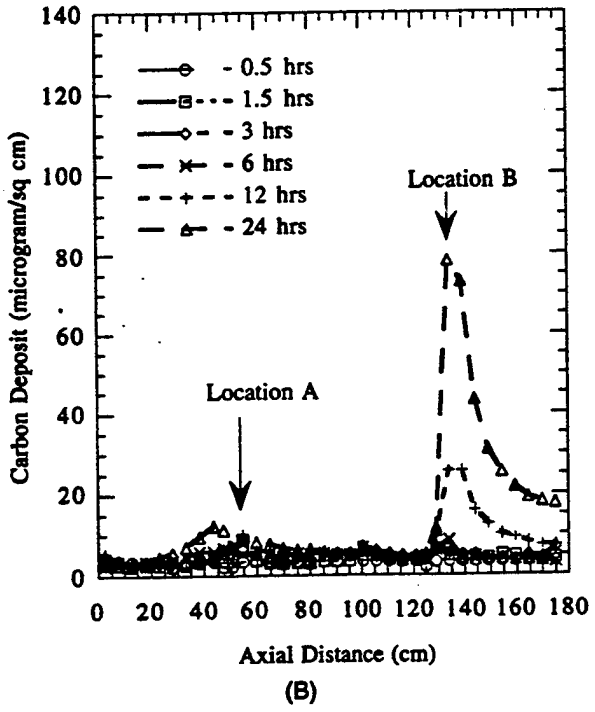

Fig. 4 Carbon deposition: (A) JP-8 fuel; (B) JP-8A fuel

as described above: locations A and B. In Fig. 4(*b*) for JP-8A with conditions somewhat similar to those in Fig. 4(*a*) except for the bulk temperature, locations A and B again correspond to the two maximal peaks in the spatial distribution of carbon.

Scanning Electron Microscopy

JP-8 Fuel. Figure 5(*a*) is a digitized image of the inner surface of a representative sample of the stainless-steel tube before exposure to thermally stressed JP-8 fuel. Asperities, pits, and grain boundaries are clearly visible. (For Figs. 5(*a*)–5(*c*), the magnification is 5000× and a scale of one micron is shown for reference.) Figure 5(*b*), a photograph of the interior of the tube corresponding to a bulk temperature of 220°C at location A, reveals very fine particles attached to the wall. The pits and microcrevices observed with the blank tube remain distinguishable after three hours of passing heated fuel through the tube. After 12 hours, the features of the underlying tube surface are no longer visible in Fig. 5(*c*), where the deposit appears to be porous and composed of fine submicron particles. The porosity would seem to be responsible for any accelerated deposit growth since the porous structure would trap fuel largely by capillary action. The trapped fuel would then remain at the higher temperature of the wall deposit for a longer residence time than otherwise might occur if it had not been trapped. Moreover, this porous microstructure has more surface area than that found with a nonporous, smooth deposit for the adhesion of insoluble bulk particles.

In Fig. 5(*d*), the magnified image (4000×) of location B after three hours shows a flakelike microstructure, which conforms to the topography of the underlying tube surface, and the deposit surface has a roughness length scale smaller than that of the original metal surface but larger than that of the deposits in Figs. 5(*b*) and 5(*c*). Similar microstructure is also observed after six-hour and twelve-hour periods.

SEM did not reveal any distinguishable structure on the tube surfaces at locations A and B for periods of 0.5 and 1.5 hours with JP-8.

JP-8A Fuel. For all the tests with JP-8A, the deposit thickness at A was in the range of 10 to 40 nm. As a consequence of this very thin layer, no deposit structure in the heated section was perceptible with SEM, and the magnified images resembled those of the unused tube surface. Figure 5(*e*) is a SEM image (magnification 3000×) following a 12-hour test from the cooled section at location B. The deposit micrograph, compared to the image of the unused tube of Fig. 5(*a*), is smooth, suggesting the uniform attachment of polymerized molecules as in the tests without the BHT and 8Q405. There are fissures in the deposit that are most likely the result of sectioning the tube. The large circles at the left side of the photo are cavities that have formed as pieces of the deposit have broken away; the metal surface below is visible within the confines of these circles. The structure of the deposit at B after six hours was similar in appearance to that after twelve hours; for times less than six hours, the microstructure was not discernible.

AES and XPS Analysis

Auger Electron Spectroscopy. AES elemental composition profiles were measured within the deposits for both the JP-8 and JP-8A experiments. In addition, the deposit thickness, δ, which changed only very gradually across the length of each piece of segmented tube, was obtained. As indicated in Figs. 6(*a*) and 6(*b*) (following a six-hour test), δ is defined as the distance from the surface exposed to the fuel to the point where the iron and carbon profiles intersect on an AES mapping. The sputter rate for the depth profiles was roughly 8 nm/min, and the maximum depth of profiling into the deposit with a reasonable certainty in the composition was 150 nm.

X-Ray Photoelectron Spectroscopy. Table 1 presents the XPS results for the JP-8 fuel at locations A and B for time durations of 0.5, 1.5, 3, and 6 hours, and an analysis of an unused tube is given for reference. The chemical composition of the deposit surface nearest the flowing fuel at either A or B essentially does not appear to change for periods greater than three hours. The organic acid, ester, aldehyde, and ketone compositions are nearly the same for a given period at A. However, upon comparison of the composition at A with that at B, we find that the organic acid, ester, aldehyde, and ketone composition is lower at B. The alcohol and ether compositions at A and B are similar. The deposit does not cover the tube wall at the end of a 1.5-h period for location B and, as a result, silicon and chromium are still detected.

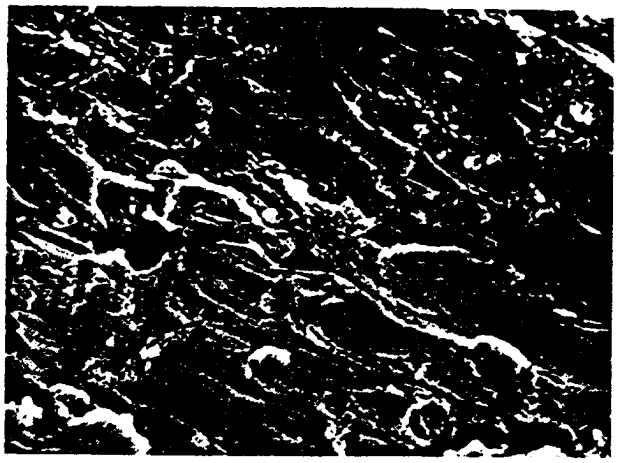

Fig. 5(A) Magnification 5000×; scale: 1 micron = ——

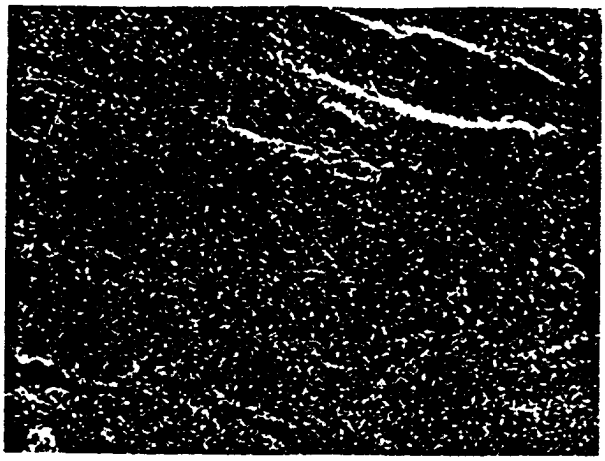

Fig. 5(B) Magnification 5000×; scale: 1 micron = ——

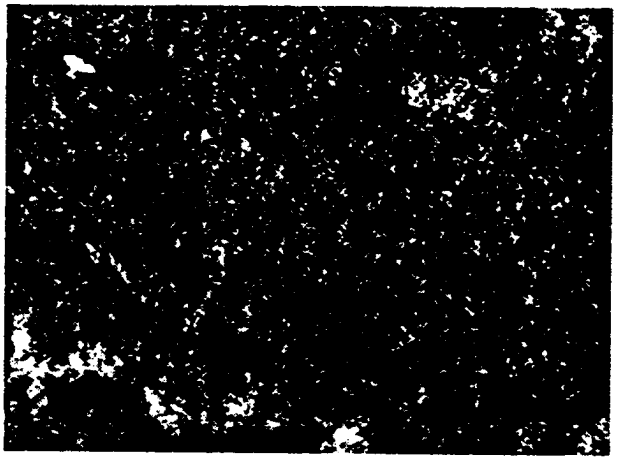

Fig. 5(C) Magnification 5000×; scale: 1 micron = ——

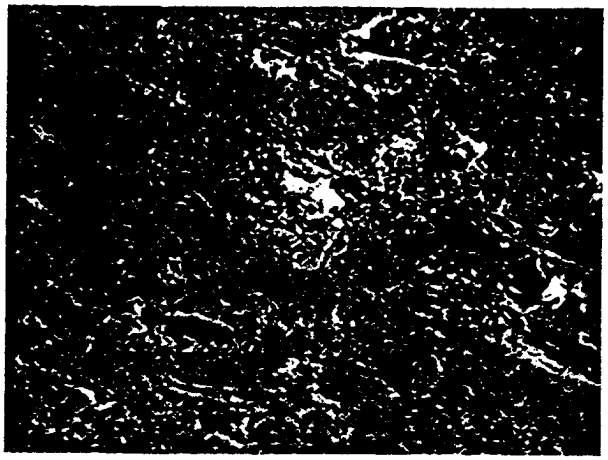

Fig. 5(D) Magnification 4000×; scale: 1 micron = ——

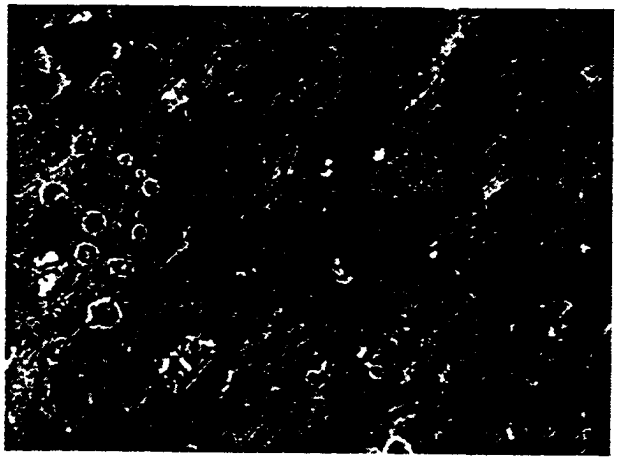

Fig. 5(E) Magnification 3000×; scale: 1 micron = ——

Fig. 5 SEM images of tube surfaces at locations A and B: (A) unused tube; (B) A after 3 h, JP-8 fuel; (C) A after 12 h, JP-8 fuel; (D) B after 3 h, JP-8 fuel; (E) B after 12 h, JP-8A fuel

In Table 2, there are differences in the surface composition between locations A and B, especially with regard to acids and esters, alcohols and ethers, hydrocarbons and elemental carbon, elemental oxygen, sulfur oxides, and sulfides. A comparison of Tables 1 and 2 reveals that the BHT and 8Q405 additives to the JP-8 have changed the chemical composition of the deposits at A with the following trends: CH, C, and C–S are greater with JP-8A, but O and S–O are lower with JP-8A. At B, the following trends are observed: aldehydes and ketones and C–S compounds are greater with JP-8A, but C–O and S–O compounds are lower with JP-8A. These results confirm prior reported measurements for jet fuels (Hazlett and Hall, 1981, 1985).

Discussion

Of particular interest in the AES measurements (Figs. 6(*a*) and 6(*b*)) was the elemental oxygen content of the deposit. Since the oxygen composition, O(z), varies spatially, it is convenient to examine the spatial mean value of the oxygen composition, a, as a function of time. Thus,

$$\alpha = \frac{\int_0^{\delta(t)} \mathrm{O}(z)\,dz}{\delta(t)} \qquad (1)$$

Hence, the total area beneath the oxygen profile as in Fig. 6(a) is scaled by δ (deposit thickness). Figure 7 presents α for JP-8 and JP-8A. At 0.5 h, the oxygen composition is greater at B than at A because the deposit thickness at B is very thin and the metal surface has an initial oxide layer. It is interesting that the mean oxygen content in the deposit of Fig. 7 decreases as the dissolved oxygen level of Fig. 3 increases during the initial three hours, suggesting that the dissolved oxygen somehow preferentially becomes a constituent of the tube deposits early in testing. (Moreover, this trend in α is further corroborated by

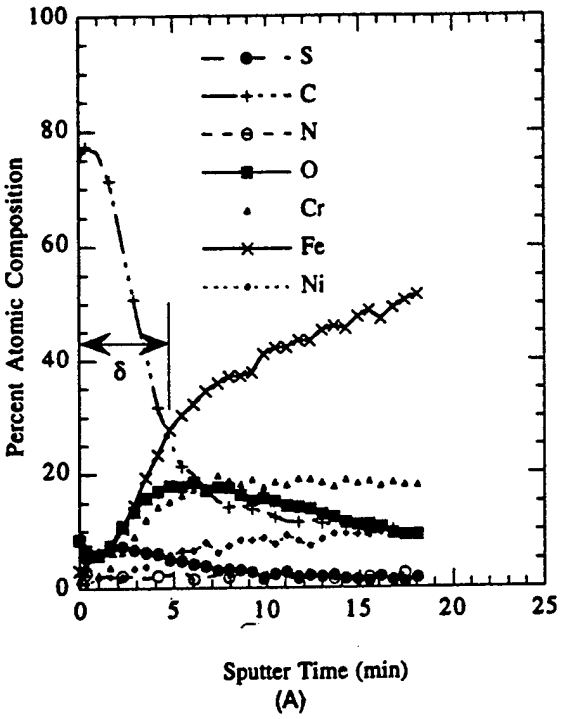

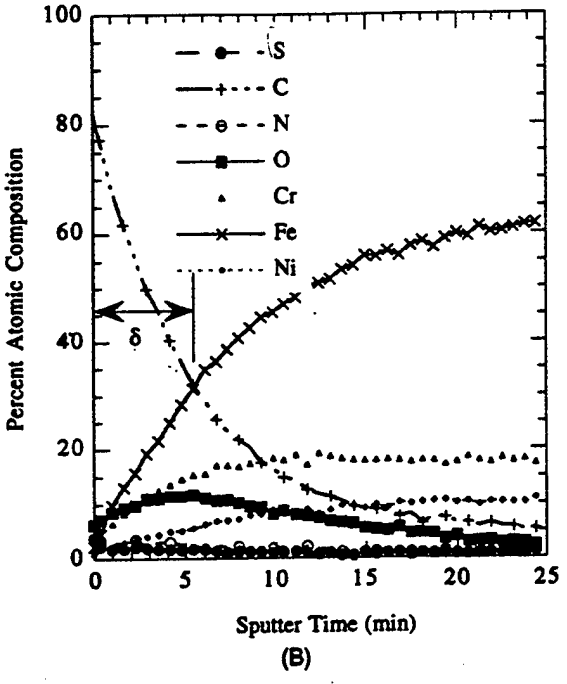

Fig. 6 AES profiles (after 6 hour test) for JP-8 fuel at location: (*A*) A; (*B*) B

the XPS deposit surface measurements in Tables 1 and 2 of O at both locations A and B for JP-8 and JP-8A.) In addition, as shown in Figs. 3(*a*) and 3(*b*), large changes in deposition per volume of fuel occur within the first three hours, are a minimum at the end of about six hours, then begin to increase gradually. These results may be contrasted by what is often ascribed to the induction period: small changes in deposition. The dissolved oxygen levels for both JP-8 and JP-8A increase with changes in the deposition for nearly ten hours, suggesting a relationship between disappearing active sites on the metal surface and the increasing oxygen levels. Similarly, Jones and Balster (1994) have observed changes in measured dissolved oxygen levels during the induction time in a flowing experiment.

JP-8 Fuel Deposits. Location A of Fig. 4 is in the region in which the dissolved oxygen is nearly depleted, but the rate of deposition is relatively high. Immediately downstream of A, the amount of deposition sharply declines. Heneghan et al. (1993a) have observed a similar peak in deposition simultaneously with dissolved oxygen depletion in flowing tests using the present experimental apparatus with certain other aviation fuels. At B, the bulk fuel temperature is nearly 100 K less than the bulk temperature at A. It is suspected that the deposition at B is a consequence of compounds that were soluble at higher temperatures but are now insoluble at lower temperatures. Hence, it might be anticipated that the physical mechanisms of deposition at A and B are very different; these differences will become more apparent with further consideration of the SEM, XPS, and AES measurements.

In the heated section at location A, a very thin (on the order of less than 50 nm) incipient polymolecular film that is detectable with AES forms on the metal surface before the appearance of detectable particles. In the AES measurements of Fig. 6(*a*), beginning with the surface of the deposit nearest the fuel, the local maxima and minima of the sulfur and oxygen distributions follow each other in cases of deposit formation at A, suggesting the presence of sulfur oxides. Their presence is further confirmed by XPS measurements and, perhaps, indicates the action of sulfonic acids. It is believed by many (Kendall et al., 1986; Mushrush et al., 1988; Heneghan and Kauffman, 1994; Kauffman, 1995; Schultz and Gillman, 1994) that sulfur-oxide compounds have some role in the initiation and subsequent growth of deposits under conditions of thermal stressing, as at location A. Furthermore, Kauffman (1995) has suggested a deposition mechanism for straight-run fuels involving phenols and sulfur compounds together with sulfur-oxide reactions at the metal surface. Deposits formed on heated steel wires were found to have sulfur and oxygen AES profiles similar to those measured here for location A.

At later periods at location A, particles formed on the incipient layer of deposit. It is important to note in the SEM image of Fig. 5(*b*) that there is not a continuous layer of particulate matter, but rather the particles are located at specific sites. This might be anticipated since grain boundaries, pits, and crevices all tend to trap impurities and are regions of higher free energy; thus, they are more likely to be nucleation sites. In addition, the observed site-specific formation is somewhat similar to that observed with the acid attack of metallic surfaces whereby the surface is affected at discrete locations, perhaps again suggesting the role of organic acids rather than a deposit film as might result from bulk particle migration to the walls. Similarly, Kendall et al. (1987) describe a layer of lacquer on a metal surface formed in the simulation of an injector feed arm. Microspheres (0.1 μm diameter) of deposit along with agglomerations of microspheres formed a "cauliflower" structure, which may have penetrated the lacquer surface.

The microstructure of the deposit (Fig. 5(*d*)), formed after three hours at location B with a lower bulk temperature of 400 K, is entirely different from that formed in the heated section of the tubing. The deposit is composed of layered lakes rather than fine particles, suggesting an entirely different mechanism for deposition. Moreover, the sulfur and oxygen distributions within the deposit, as determined by AES, appear unrelated. In fact, they move in opposite directions (Fig. 6). It is surmised that these solids are likely the result of polymerized molecules or agglomerates, which precipitate from solution at the lower temperature and eventually adhere to the wall. Schirmer (1970) found that deposits from a wide variety of fuel system simulators consistently were composed of microspheres and structures of randomly packed microspheres approximately 1000 Å in diameter. These microspheres sometimes fused to heated metal surfaces. A similar microsphere structure was observed for JP-8 fuel at location A. However, at location B for both JP-8 and JP-8A fuels, there was no microsphere structure but rather a

Table 1 XPS-determined percent atomic composition: JP-8 fuel

Hours	O-C=O	C=O	C-O	CH,C	O	Fe	N	S-O	C-S	Si	Cr	Total	Total	Total
A														
0	4.8	1.9	5.4	30.2	30.1	14.6	<0.7	0.9	<0.2	7.1	4.1	42.3	<1.1	99.1
0.5	3.7	4.4	5.7	45.1	30.6	5.5	2.4	2.2	0.46	-	-	58.9	2.7	100.1
1.5	4.1	4.6	7.8	49.9	26.1	3.4	1.8	1.6	0.53	-	-	66.4	2.1	99.8
3	4	4.8	6.8	50.4	27.2	2.8	2.1	1.5	0.34	-	-	66	1.8	99.9
6	4.5	4.6	7.3	51	26.2	2.5	1.8	1.7	0.37	-	-	67.4	2.1	100
B														
0	4.8	1.9	5.4	30.2	30.1	14.6	<0.7	0.90.	<0.2	7.1	4.1	42.3	<1.1	99.1
0.5	1.6	1.7	4.5	25.5	44.8	6.8	1.3	1.4	<0.2	8.3	3.9	33.3	<1.6	99.8
1.5	1.7	2.4	4.1	36.4	36.4	5.3	1.7	1.7	0.44	5.5	4.4	44.6	2.1	100
3	1.4	3.1	6.1	58.6	22.2	2.7	3	2.4	0.35	-	-	69.2	2.8	99.9
6	1.4	2.8	6.6	56.4	23.2	3.8	3.1	2.4	0.33	-	-	67.2	2.7	100

O—C=O, acids and esters; C=O, aldehydes and ketones; C—O, alcohols and ethers; CH and C, hydrocarbons and carbon; S—O, sulfur oxides; C—S, sulfides

continuous structure that somewhat resembled micrographs of asphalt formed at much higher temperatures.

JP-8A Fuel Deposits. As might be anticipated, the deposition at A using JP-8A (Fig. 4(*b*)) for periods greater than or equal to three hours is less than that at A for the experiments with JP-8 (Fig. 4(*a*). However, at B, following 12 hours of fuel flow, the amount of deposition was nearly the same as that formed with JP-8. After 24 hours of heating, the deposition at B with JP-8A was actually greater than that at B with JP-8 as in Fig. 4(*a*). Furthermore, the maximum deposition for longer times did not occur near A but rather at B in the cooled section. Hence, the BHT and 8Q405 additives are effective in altering the deposition mechanisms that occur at high temperatures but appear to be ineffective in preventing deposition at low temperatures for long periods under the conditions of the present experiments. The mechanisms of deposition in the cooled section seem to be related to the solubility of the oxidized products; as a result, an antioxidant such as BHT would not be expected necessarily to reduce deposition there.

In Fig. 8, the deposit thicknesses are given as a function of time. The thicknesses for time durations less than six hours are quite small—less than 50 nm. For JP-8, δ at locations A and B could well be represented by a linear relationship between 0.5 and 6 h, and the average rate of increase in the deposit thickness, δ', is roughly 8.3 nm/h for the initial six hours of testing. Following the initial six hours, δ' increases at both A and B, but is much greater in the heated section than in the cooled section. The larger δ' at A may be due to the capillary-trapping mechanism described above, while the lower δ' at B is likely related to the solubility of polymerized molecules. Transient deposit thicknesses are also given for locations A and B for JP-8A. The δ at A for the JP-8A fuel is less than that for the JP-8 fuel, and δ' is roughly 3.3 nm/h. The rate of increase of deposit thickness at B for JP-8A significantly increases after three hours to 50 nm/h, then decreases to 16.7 nm/h between 6 and 12 hours. The reasons for this are, as yet, open to speculation.

Conclusions

Experiments were performed in a forced-flow single-pass heat exchanger to obtain baseline data on the structure and chemical composition of deposits formed after different time periods and to investigate effects of the metal wall. The experimental arrangement permitted viewing of the time evolution of deposits under conditions of nonisothermal bulk flow with limited oxygen. SEM was used for examination of deposit microstructure, and, in addition, XPS and AES were used to study the chemical composition of the deposits. Dissolved oxygen concentration measurements of the bulk flow were performed, and carbon burnoff determined the axial distribution of deposits within the tubes.

This study found the following:

1 Induction time has not been well characterized previously and usually implies a waiting period for "sufficiently measurable" deposition. However, on the molecular scale, deposition is a continuous process regardless of a readily detectable deposit, and induction time may be speculated to be the period in which the catalytic action of the metal surface is dominant and incipient molecular layers form. Here, increasing dissolved oxygen levels and large deposition rates (per volume of fuel) within the tube were characteristic of the induction time.

2 Mechanisms of deposition in the heated and cooled sections were different. AES and XPS analyses indicated that deposits formed in the heated section had chemical compositions different from those formed in the cooled section. In addition, SEM revealed differences in microstructure between the heated and cooled sections: more uniform deposits formed in the cooled section as a result of once-soluble species becoming insoluble at low temperatures.

3 The microstructure of the deposits formed from JP-8A in the cooled section was different from that with JP-8. Moreover, the JP-8 additives significantly reduced fouling in the heated section, but their effectiveness in the cooled section, especially after long periods, is questionable.

Table 2 XPS-determined percent atomic composition: JP-8A fuel

Hours	O-C=O	C=O	C-O	CH,C	O	Fe	N	S-O	C-S	Si	Cr	Total	Total	Total
A														
0.5	3.2	3.7	5.7	45	28.6	6.6	1.9	0.62	0.59	3	1.2	58.2	1.2	100.1
1.5	3.4	3.7	5.3	48.7	26.2	7.2	1.3	0.55	0.58	1.8	1.2	61.7	1.1	99.9
3	3.6	4.8	4.8	52.6	24.1	5.8	2	0.79	0.56	1	-	66.4	1.4	100.1
6	3.9	3.8	6.6	53.4	22.9	4	1.9	1.46	0.51	1.5	-	68.2	2	100
12	3.6	3.7	6.3	54	22.7	4	1.9	1.2	1.2	<0.6	0.8	68.8	2.4	99.4
B														
0.5	2.5	2.9	4	34.8	36.7	7	1.7	0.34	<0.2	6.4	3.3	44.2	<0.5	99.6
1.5	2	3.3	3.5	42.6	31	6.1	1.3	0.63	0.69	5.4	3.6	52.1	1.3	100.1
3	1.5	3.1	3.9	44	30.2	5.7	1.4	1.21	0.42	5.1	3.5	52.9	1.6	100
6	1.4	3.7	4.1	56.4	23.5	4.8	1.9	2	<0.2	<0.6	1.3	65.6	<2.2	99.1
12	0.8	3.3	2.1	65.9	19	2.5	2.2	1.55	0.29	1	1.2	72.4	1.8	99.8

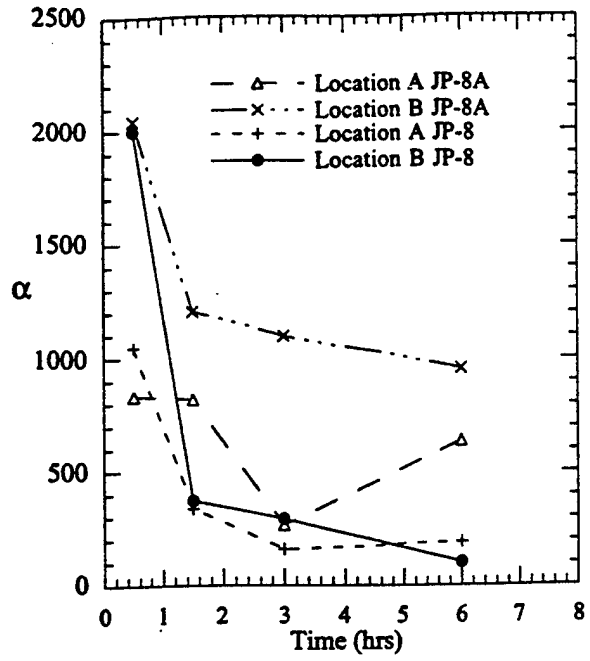

Fig. 7 Spatial mean oxygen content of deposits: JP-8 and JP-8A fuels

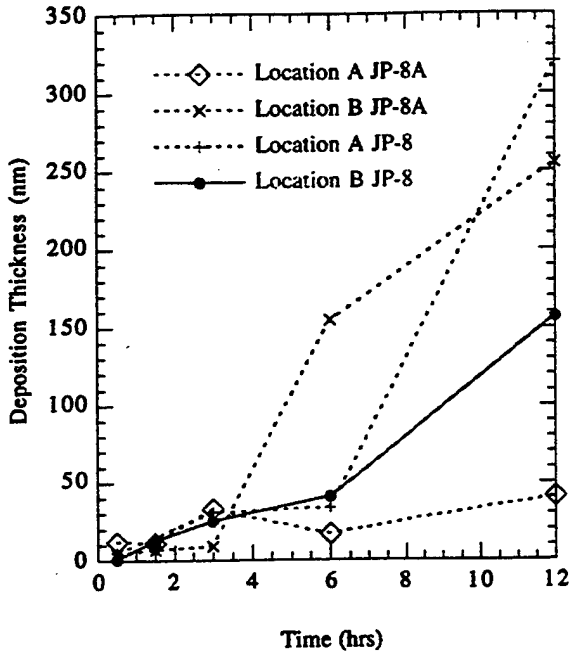

Fig. 8 Deposit thickness at different axial locations and times: JP-8 and JP-8A fuels

Acknowledgments

This work was supported by the U.S. Air Force under Contract No. F33615-92-C-2207 with Mr. C. W. Frayne serving as the technical monitor and Dr. D. R. Ballal as the principal investigator. The authors are grateful for stimulating discussions with Dr. E. G. Jones of Systems Research Laboratories, Dayton, Ohio.

References

Anderson, S., Harrison, W., III, and Roquemore, W., 1994, "Development of Thermal Stability Additive Package for JP-8," presented at the Fifth International Conference on the Handling and Stability of Liquid Fuels, Rotterdam, Netherlands.

Bradley, R., Bankhead, R., and Bucher, W., 1974, "High Temperature Hydrocarbon Fuels Research in an Advanced Aircraft Fuel System Simulator on Fuel AFFB-14-70," AFAPL-TR-73-95, Air Force Aero Propulsion Laboratory, Wright-Patterson Air Force Base, OH.

Briggs, D., and Seah, M., 1983, *Practical Surface Analysis by Auger and X-Ray Photoelectron Spectroscopy*, Wiley, New York.

Chin, J., and Lefebvre, A., 1993, "Influence of Flow Conditions on Deposits From Heated Hydrocarbon Fuels," ASME JOURNAL OF ENGINEERING FOR GAS TURBINES AND POWER, Vol. 115, p. 433.

Giovanetti, A., and Szetela, E., 1985, "Long-Term Deposit Formation in Aviation Turbine Fuel at Elevated Temperature," NASA Report CR-179579, United Technologies Research Center on contract with NASA, Cleveland, OH.

Grinstead, R., Heneghan, S., Striebich, R., and Zabarnick, S., 1994, "Jet Fuel Thermal Stability and Analytic Test Data," UDR-TR-94-20, University of Dayton, Dayton, OH.

Hazlett, R., and Hall, J., 1981, "Chemical Aspects of Jet Fuel Thermal Oxidation Stability," *Fouling of Heat Transfer Equipment*, E. Somerscales and J. Knudsen, eds., Hemisphere, New York.

Hazlett, R., and Hall, J., 1985, "Jet Aircraft Fuel System Deposits," *Chemistry of Engine Combustion Deposits*, L. Ebert, ed., Plenum Press, New York.

Hazlett, R., 1991, *Thermal Oxidation Stability of Aviation Turbine Fuels*, American Society for Testing and Materials, Philadelphia.

Heneghan, S., Martel, C., Williams, T., and Ballal, D., 1993, "Studies of Jet Fuel Thermal Stability in a Flowing System," ASME JOURNAL OF ENGINEERING FOR GAS TURBINES AND POWER, Vol. 115, p. 480.

Heneghan, S., Martel, C., Williams, T., and Ballal, D., 1995, "Effects of Oxygen and Additives on the Thermal Stability of Jet Fuels," ASME JOURNAL OF ENGINEERING FOR GAS TURBINES AND POWER, Vol. 117, pp. 120–124.

Heneghan, S., and Kauffman, R., 1994, "Analytic Tests and Their Relation to Jet Fuel Thermal Stability," presented at the Fifth International Conference on Stability and Handling of Liquid Fuels, Rotterdam, Netherlands.

Johnson, C., Fink, D., and Nixon, A., 1954, "Stability of Aircraft Turbine Fuels," *Ind. Eng. Chem.*, Vol. 46, p. 2166.

Jones, E., and Balster, W., 1994, "Surface Fouling: Short- Versus Long-Term Tests," presented at the Div. Petr. Chem., 208th American Chemical Society National Meeting, Washington, DC.

Kamin, R., Nowack, C., and Darrah, S., 1988, "Thermal Stability Measurements Using the Fiber Optic Modified Jet Fuel Thermal Oxidation Tester," *Proceedings of the 3rd International Conference on Stability and Handling of Liquid Fuels*, Inst. of Petroleum, London, United Kingdom.

Katta, V., Blust, J., Williams, T., and Martel, C., 1994, "Effects of Buoyancy on Heat Transfer and Oxygen Consumption in Fuel-Thermal-Stability Studies," ASME Paper No. 94-GT-346.

Kauffman, R., 1995, "Effects of Sulfur Compounds on the Oxidation of Jet Fuel," ASME Paper No. 95-GT-XX.

Kendall, D., and Mills, J., 1985, "The Influence of JFTOT Operating Parameters on the Assessment of Fuel Thermal Stability," SAE Paper No. 851871.

Kendall, D., Clark, R., and Stevenson, P., 1986, "The Influence of Polar Compounds on the Stability of Jet Fuel," *Proceedings of the 2nd International Conf. on Long-Term Storage Stabilities of Liquid Fuels*, San Antonio, TX.

Kendall, D., Houlbrook, G., Clark, R., Bullock, S., and Lewis, C., 1987, "The Thermal Degradation of Aviation Fuels in Jet Engine Injector Feed-Arms, Part 1—Results from a Full Scale Rig," presented at the Int. Gas Turbine and Aeroengine Congress and Exposition, Tokyo, Japan.

Krazinski, J., Vanka, S., Pearce, J., and Roquemore, W., 1992, "A Computational Fluid Dynamics Model for Jet Fuel Thermal Stability," ASME JOURNAL OF ENGINEERING FOR GAS TURBINES AND POWER, Vol. 114, p. 104.

Lefebvre, A., 1992, "Experimental Studies on Deposit Formation in JP Fuels at High Temperatures," Report No. WL-TR-92-2112, Air Force Aero Propulsion Laboratory, Wright-Patterson Air Force Base, OH.

Marteney, P., 1989, "Thermal Decomposition of JP-5 in Long Duration Tests," Report No. ADB148328, United Technologies Research Center, prepared for Naval Air Propulsion Center.

Mushrush, G., Watkins, J., Hazlett, R., Hardy, D., and Eaton, H., 1988, "Liquid Phase Oxidation of Thiophenol and Indene by *t*-Butyl Hydroperoxide and Oxygen," *Fuel Science and Technology International*, Vol. 6, p. 165.

Patankar, S., 1980, *Numerical Heat Transfer and Fluid Flow*, Hemisphere, Washington, DC.

Rubey, W., Striebich, R., Anderson, S., Tissandier, M., and Tirey, D., 1992, "In Line Gas Chromatographic Measurement of Trace Oxygen and Other Dissolved Gases in Flowing High Pressure Thermally Stressed Jet Fuel," presented at the Symposium on Structure of Jet Fuels III, American Chemical Society, Div. Petr. Chem., San Francisco, California.

Schirmer, R., 1970, "Morphology of Deposits in Aircraft and Engine Fuel Systems," SAE Paper No. 700258.

Schultz, W., and Gillman, A., 1994, "Effects of Sulfur Compounds on a JP-8 Surrogate Fuel," presented at the Div. Petr. Chem., 208th American Chemical Society National Meeting, Washington, DC.

Smith, J., 1969, "Fuel for the SST: Effects of Deposits on Heat Transfer to Aviation Kerosine," *Ind. and Eng. Chem. Process Design and Development*, Vol. 8, p. 299.

Wittberg, T., 1994, University of Dayton Research Institute, private communication.

Appendix I

Jet Fuel Deposition and Oxidation: Dilution, Materials, Oxygen and Temperature Effects

Steven Zabarnick
Paula Zelesnik
Rebecca R. Grinstead

University of Dayton
300 College Park
Dayton, OH 45469-0140

Jet Fuel Deposition and Oxidation: Dilution, Materials, Oxygen, and Temperature Effects

S. Zabarnick

P. Zelesnik

R. R. Grinstead

Aerospace Mechanics Division,
University of Dayton Research Institute,
Dayton, OH 45469

Quartz crystal microbalance (QCM) and pressure measurements are used for determination of jet fuel thermal stability in a batch reactor. The QCM is able to monitor extremely small amounts of deposition in situ, while the pressure measurements provide qualitative data on the oxidation process. The dependence of the deposition amount was monitored as a function of the oxygen availability for two fuels. Also, the effect of QCM electrode materials was investigated. Deposition and oxidation were compared for the following electrode materials: gold, aluminum, silver, and platinum. We also studied the effect of dilution on oxidation and deposition. Jet fuel was diluted with increasing amounts of hydrocarbon solvent. It was observed that this dilution procedure can help characterize a fuel's effective antioxidant concentration. Fuel dilution is also shown to be a good technique for improving thermal stability characteristics of poor fuels. Additionally we have studied the temperature effect on deposition for two fuels over the range 140 to 180°C.

Introduction

Recent advances in jet aircraft and engine technology have placed an ever-increasing heat load on the aircraft. The bulk of this excess heat is absorbed by the aircraft fuel, as jet fuel is used as the primary coolant for the numerous heat sources. This hot fuel reacts with dissolved oxygen to form oxidized products and deposits. The formation of deposits results in the fouling of fuel lines, valves, actuators, nozzles, and various other aircraft components with the potential to result in catastrophic failure. The recent development of the quartz crystal microbalance (QCM) technique provides an extremely sensitive technique for real-time, in situ measurements of jet fuel thermal oxidative deposition (Klavetter et al., 1993; Martin et al., 1991). The technique is sufficiently sensitive that deposition can be readily measured under realistic turbine engine thermal conditions, unlike the accelerated conditions of temperature and/or time under which most previous measurements have been made. The modification of the QCM system with addition of a pressure transducer has enabled simultaneous real-time, *in situ* measurements of both deposition and oxidation. Recent work has demonstrated the capabilities of the technique in evaluating both jet fuels and potential jet fuel additives (Zabarnick, 1994; Zabarnick and Grinstead, 1994). The ability to measure oxidation and deposition simultaneously provides an ideal environment in which to study the effect of oxygen concentration on the deposition process.

Many current and future military aircraft incorporate an onboard inert gas generating system (OBIGGS) to lower the oxygen level in the fuel tank ullage space. As this OBIGGS can lower the dissolved oxygen concentration present in the fuel, it is important to understand the effect this has on the deposit-forming process. In addition, during the thermal oxidation process in a flowing fuel system, the oxygen concentration in the fuel decreases as the oxidation process continues. Thus, a fundamental understanding of the effect of the oxygen concentration on thermal stability (thermal stability refers to the deposit-forming tendency of the fuel) is essential for designing jet fuel systems. For this purpose we have developed a technique to vary the oxygen level available to the fuel in the QCM system. In this work we will present results showing the effect of varying oxygen concentrations on fuel thermal stability.

On its trek through a complex military fuel system, jet fuel contacts a variety of materials. It is important to understand the effect these materials have on fuel thermal stability. Previous QCM jet fuel thermal stability work has exclusively studied crystal electrodes with gold surfaces (Klavetter et al., 1993; Zabarnick, 1994; Zabarnick and Grinstead, 1994). For the present work we have acquired quartz crystals with electrodes of the following materials: gold, platinum, aluminum, and silver. In this work we study the effect of the crystal electrode material on jet fuel thermal stability for a variety of jet fuel samples.

We have also investigated the technique of fuel dilution to study the effect of varying concentration of the antioxidant and deposit producing molecules naturally present in jet fuels. This technique provides a method for determining the relative effective antioxidant concentrations that are naturally present in various fuels. Fuel dilution also promises to provide a method for inexpensively improving the thermal stability of highly depositing jet fuels.

In modern military aircraft, jet fuel is recirculated through the aircraft fuel system and exposed to various temperatures for various residence times. These temperatures and residence times change constantly during a mission as the throttle is changed and the aircraft maneuvered. Thus, an understanding of the effect of temperature on jet fuel thermal stability is essential to the design of aircraft fuel systems and minimization of fuel system fouling phenomena. In this work we have varied fuel temperature over the range 140 to 180°C while monitoring deposition and oxidation for two different fuels.

Experimental

The QCM experimental apparatus has been described in detail previously and will be described only briefly here (Klavetter et al., 1993; Zabarnick, 1994). Jet fuels are thermally stressed

Contributed by the International Gas Turbine Institute and presented at the 40th International Gas Turbine and Aeroengine Congress and Exhibition, Houston, Texas, June 5–8, 1995. Manuscript received by the International Gas Turbine Institute February 10, 1995. Paper No. 95-GT-50. Associate Technical Editor: C. J. Russo.

Table 1 Properties of fuels studied

Fuel Number and Designation	Hydrotreated?	Total Sulfur (ppm)	JFTOT Breakpoint (C)	Other Notes
F-2747 (Jet A-1)	Yes	37	332	Light depositor, fast oxidizer
F-2827 (Jet A)	No	763	282	Heavy depositor, slow oxidizer
F-2980 (Jet A)	No	614	288	Merox treated, moderate oxidizer
Exxsol D80	-	3	-	Pure solvent, very fast oxidizer, very light depositor

in a 100 ml stainless steel Parr pressure reactor. The reactor is modified with an RF feedthrough for attachment of the QCM. The reactor is supplied with gas inlet (below the liquid level) and outlet (above the liquid level) lines. A magnetic stir bar and stirrer are used during the runs to minimize spatial inhomogeneities in species concentration and temperature. The reactor is heated with a clamp-on band heater, which is controlled with a PID temperature controller. A thermocouple is immersed in the fuel to monitor and control the temperature, which can be readily maintained ±0.4°C at 140°C over a 15 hour run. The reactor was also fitted with a Sensotec 0–50 psia pressure transducer for measurement of the reactor headspace pressure. The output of the pressure transducer is read by a digital multimeter (Keithley Model 199/1992).

The quartz crystals used were 5 MHz, 2.54 cm diameter, 0.33 mm thick, AT cut wafers. The QCM crystal is suspended vertically in the fuel in order to minimize gravitational effects on deposition. The crystals are obtained from Maxtek Inc. and are normally manufactured with overtone polished gold electrodes. For the materials work we acquired crystals with electrode surfaces of platinum, aluminum, and silver. The quartz crystal resonator is driven at 5 MHz by a oscillator circuit that was developed by Sandia National Laboratories (Klavetter et al., 1993). This circuit tracks the impedance variations of the crystal in order to determine the resonant frequency of the device. The oscillator frequency output is read by a frequency counter (HP Model 5384A). The change in frequency of the device at constant temperature is related to surface mass deposition on the crystal. The oscillator circuit also provides an amplitude output that indicates crystal damping. The output is read by the digital multimeter. The crystal frequency, reactor temperature, reactor pressure, and crystal damping voltage are monitored at 1 minute intervals over a GPIB bus via a personal computer.

A standard experimental run is conducted by filling the reactor with 60 ml of fuel, then sparging with air for one hour to air saturate the fuel. The reactor is then sealed at one atmosphere and heated to the test temperature. Typically the fuel reaches the test temperature after a 35 to 40 minute heat-up period. After the 15 hour run time, the heater is turned off and the reactor allowed to cool. For the oxygen and temperature effect studies, a slightly different method was used in order better to control the oxygen availability and/or to prevent significant oxygen consumption and deposition during the heat-up period. For these runs the fuel is sparged with nitrogen for one hour in order to purge the fuel of dissolved oxygen. The reactor is then sealed and heated to temperature. Once the fuel has reached temperature, air is added through the gas inlet line and the headspace pressure is monitored to determine the amount of air added. This technique provides a reproducible way of varying the oxygen availability of the reactor for the oxygen studies. It also prevents significant oxidation from occurring during the heat-up period for higher temperature runs.

The theory that relates the measured frequency changes to surface mass has been presented in detail elsewhere (Martin et al., 1991). The frequency change of a crystal immersed in a liquid fuel can be due to two effects: The first results from changes in the surface mass density; the second is due to changes in the liquid density and viscosity. At constant temperature and relatively small extents of chemical conversion, the liquid properties remain constant and the frequency change can be related to surface deposition via the equation

$$\rho_s = -(2.21 \times 10^5 \text{ g/(cm}^2 s)) \frac{\Delta f}{f_0^2} \qquad (1)$$

where f_0 is the unperturbed resonant frequency, Δf is the change in resonant frequency, and ρ_s is the surface mass density (mass/area). In general, the reproducibility of the mass deposition measurements on fuels is limited to ±20 percent for the QCM technique. The fuels studied and some of their properties are listed in Table 1.

Results and Discussion

Oxygen Dependence of Deposition. Here we present results of a study of the effect of oxygen availability on the deposition of a jet fuel. It is well known that the presence of oxygen is required for production of significant quantities of deposits (Hazlett, 1991). In most fuels the removal of oxygen results in a significant decrease in deposit formation. In flowing fuel systems, oxygen may be removed more readily near the hot tube walls; this results in oxygen concentration gradients in both axial and radial directions. Obviously, to understand the deposition process completely the oxygen dependence of deposition needs to be studied. To date, few studies have monitored jet fuel deposition as a function of oxygen availability.

Figure 1 shows the deposition measurements obtained when varying the oxygen availability for fuel F-2980. This fuel was chosen because of its moderate to slow oxygen consumption rate and its significant deposition. Thus both the deposition and oxidation processes could be readily monitored with the QCM and pressure monitoring techniques. Initially, the fuel was sparged with nitrogen to remove any dissolved oxygen. Then, the fuel was heated to 140°C at which time air was added via the gas inlet line at pressures ranging from 0 to 30 psi. The figure shows that the total deposition at the end of the 15 hour run increases with increased oxygen availability. The deposition varies from 0.3 μg/cm^2 for the zero oxygen run to 11.4

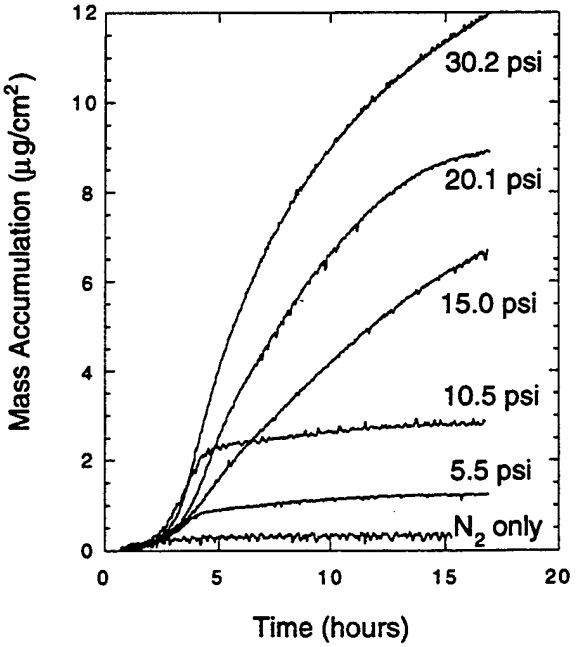

Fig. 1 Plots of mass accumulation versus time at various added air pressures in fuel F-2980

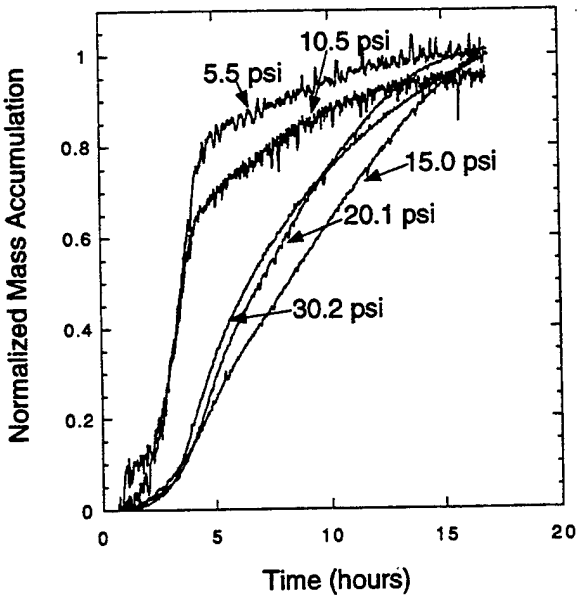

Fig. 2 Plots of normalized mass accumulation versus time at various added air pressures in fuel F-2980

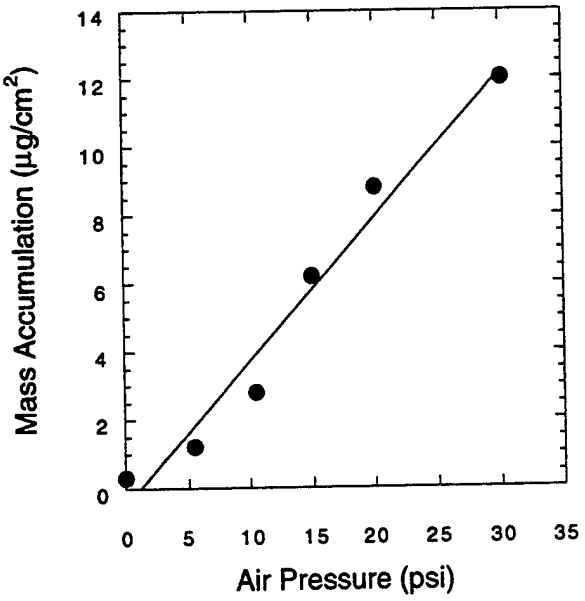

Fig. 3 Plot of final mass accumulation versus air pressure for fuel F-2980

$\mu g/cm^2$ for the 30.2 psi run. Each of the deposition curves shows an initial slow deposition rate up to 2 hours (induction period). The time at which the deposition levels off appears to occur at different times for the various oxygen levels plotted. To illustrate this dependence better, we have normalized each measured deposition by the maximum deposition at the end of each test and plotted the results in Fig. 2. It is apparent that the 5.5 and 10.5 psi runs have shorter early rise times and their depositions begin to level off much earlier than the higher oxygen runs. The 15.0 psi run has the slowest normalized deposit production rate. The corresponding pressure measurements for these runs (not shown) support the previous observation (Zabarnick, 1994) that the deposition production rate and leveling off times correspond well to the oxidation and oxygen consumption processes, respectively. Thus, these normalized deposition plots yield information about the oxidation process. The observed behavior of normalized deposition versus oxygen availability in Fig. 2 is complex but can be rationalized if one considers that the oxygen consumption process generates various product species, some of which may act as antioxidants, such as aldehydes. Thus the slower normalized deposition observed at 15 psi and above may be due to production of significant concentrations of antioxidant species at these higher oxygen conditions. Another possible explanation is that the chemical kinetic oxygen reaction order dependence may be changing as the oxygen availability is increased. That is, there may be a shift from near first-order oxygen consumption (where the oxygen consumption rate is proportional to oxygen concentration) to near zeroth-order (where the oxygen consumption rate is independent of oxygen concentration). The complex diffusion process of oxygen from the headspace of the reactor into the fuel during the test precludes a more exhaustive analysis of oxygen reaction orders.

The final deposition at 15 hours from Fig. 1 is plotted versus oxygen availability in Fig. 3. It appears that the deposition at 15 hours varies linearly with the oxygen availability in the reactor. The deposition varies from 0.3 $\mu g/cm^2$ for the zero oxygen run to 11.4 $\mu g/cm^2$ for the 30.2 psi run. This dependence is also approximately linear for deposition at 5 and 10 hours (not shown). The observed linear dependence of the measured deposition on the oxygen availability at various extents of reactions (reaction times) is a significant result for the fuel system design process if this linear response is universal for all jet fuels. In order to test this supposition, we have also performed these oxygen-dependent studies for a second fuel, F-2827. The final deposition at 15 hours versus oxygen availability for this fuel is shown in Fig. 4. The figure shows that the final deposition is linear over the range 0 to 20 psi added air, but above 20 psi the deposition appears to level. This leveling of the deposition may be due to incomplete oxygen consumption at these higher oxygen availabilities. Unfortunately, the slow oxidation of this fuel precludes use of the pressure measurement technique to confirm this supposition. These results point out that the level of oxygen consumption is an important parameter to monitor in studies of the oxygen dependence of deposition. It is apparent that the oxygen dependence of deposition cannot be represented as a simple linear dependence, especially when studying a varying array of different fuels. Also, under partial oxygen consumption conditions, lowering the oxygen availability does not necessarily result in reduced deposition (see Fig. 1).

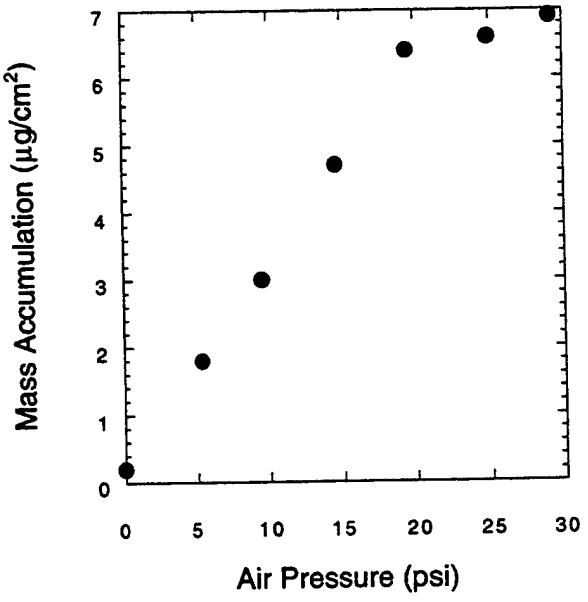

Fig. 4 Plot of final mass accumulation versus air pressure for fuel F-2827

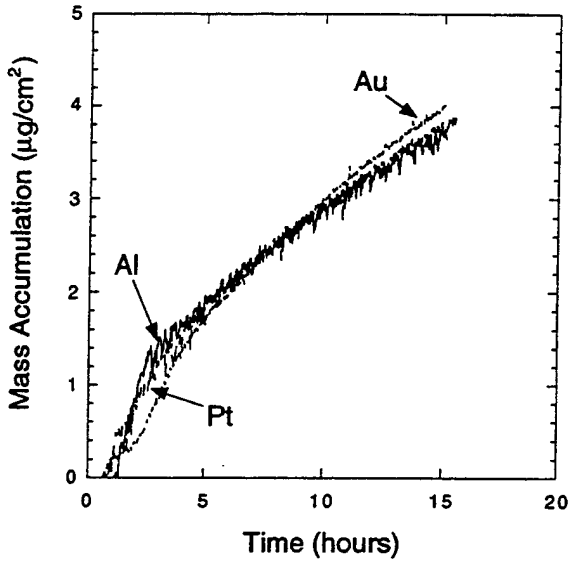

Fig. 5 Plots of mass accumulation versus time for aluminum, gold, and platinum electrode surfaces with fuel F-2827

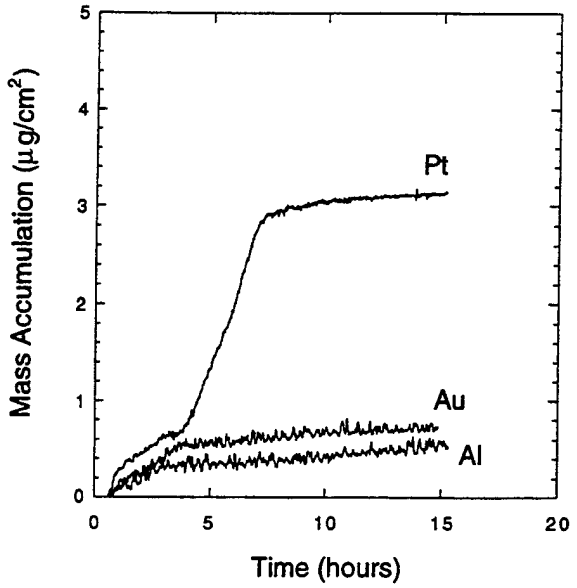

Fig. 6 Plots of mass accumulation versus time for aluminum, gold, and platinum electrode surfaces with fuel F-2747

Materials Effects on Deposition. Although the Parr reactor utilized for these QCM measurements is constructed of stainless steel, the deposition is measured on the surface of the quartz crystal electrode. To date, all QCM jet fuel deposition measurements have used crystals with gold electrodes. In general, gold is a rather unique metal that tends to be relatively unreactive. Also, gold is not used significantly in real jet fuel systems. Thus there is concern that measurements of deposition on gold surfaces do not adequately represent typical deposit processes in real fuel systems. In order to address this concern, we have acquired quartz crystals with electrode surfaces of the following materials: gold (Au), platinum (Pt), aluminum (Al), and silver (Ag). These materials do not necessarily represent common jet fuel system components, but these crystal types were readily available from the manufacturer.

We have studied deposition on crystal electrodes with gold, platinum, and aluminum surfaces for two different fuels (the silver electrode results are presented separately below). Deposition was monitored at 140°C and 1 atm air. The results are shown in Figs. 5 and 6 for fuels F-2827 and F-2747, respectively. Figure 5 demonstrates that in fuel F-2827 deposition is identical for each of the three electrode surface materials. Figure 6 shows that the gold and aluminum electrode show very similar deposition for fuel F-2747, while the platinum electrode experiences significantly higher deposition. Thus, the effect of materials appears to be fuel dependent. Gold and aluminum surfaces appear to yield identical results for both fuels studied. As aluminum is a material commonly found in fuel systems, this result reinforces the relevance of previous measurements of fuel thermal stability with gold electrodes. Platinum is a metal that is not commonly used in aircraft fuel systems. Platinum and platinum complexes are commonly used as catalysts in petroleum refining and other processes; thus, the increased deposition in Fig. 6 may be due to the catalytic activity of the platinum metal. Why does the platinum electrode show increased deposition in fuel F-2747 and not in F-2827? Fuel F-2747 is a rapidly oxidizing fuel (oxygen is consumed within 3 hours at 140°C) while F-2827 is a slowly oxidizing fuel (oxygen consumption takes >15 hours) (Zabarnick, 1994). Also, fuel F-2747 is known to produce significant quantities of hydroperoxides, while fuel F-2827 does not. The Pt surface may be able to catalyze the decomposition of hydroperoxides under these conditions. This would produce free radicals, which would further react with other substances, producing increased deposition. This hypothesis can be tested by monitoring the hydroperoxide concentration during these runs with and without the presence of Pt.

The results for deposition measurements on silver electrodes are shown in Fig. 7. We first tested fuel F-2827, which produced an extremely large surface deposition, 18.1 $\mu g/cm^2$, at the end of the 15 hour run. This is much larger than the deposition observed for the other materials (Fig. 5). Visually, the silver electrode surface did not appear to have a typical carbon deposit; instead, the surface of the electrode appeared to have a very thin blue/black film. To determine if the measured deposition was due to the normal thermal oxidative deposit, we reran the test with the fuel sparged with N_2 to remove O_2. The result is also shown in Fig. 7. Without O_2 present the deposition actually increased; the extremely large deposition actually prevented data from being acquired after 3 hours. It was quite apparent

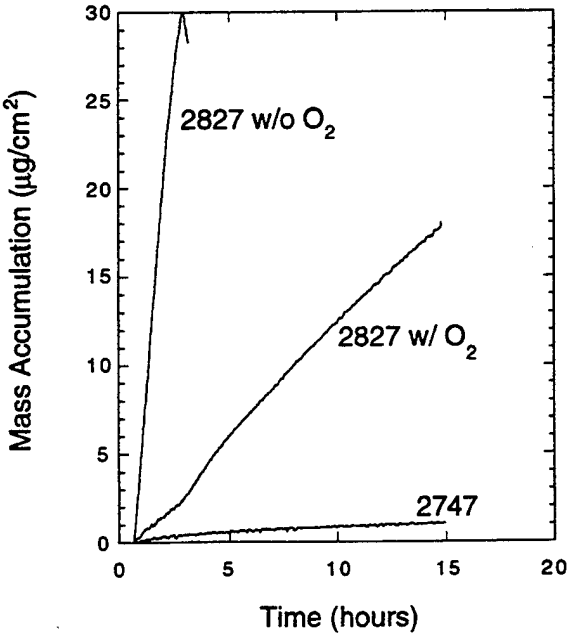

Fig. 7 Plots of mass accumulation versus time with a silver electrode surface

from the magnitude and appearance that this was not a "normal" carbon deposit. It is well known that silver reacts readily with sulfur compounds to form a thin film of silver sulfide (tarnish). In the atmosphere this is primarily caused by hydrogen sulfide, H_2S. Fuel F-2827 has a relatively high sulfur content (see Table 1). To test if sulfur might be responsible for this deposit, we sparged fuel F-2747, a low-sulfur fuel, with N_2 and measured the resulting deposition, as shown in the figure. This low-sulfur fuel yielded a significantly lower deposition of 1.1 $\mu g/cm^2$. In order to confirm that the measured deposition is due to sulfur, we have used Auger spectroscopy to measure the atomic constituents of the surface layer of the crystal electrode for the runs with F-2827 fuel. The analyses confirm the presence of silver sulfide, Ag_2S; the surfaces run with fuel F-2827 consist of 60–70 percent Ag and ≈30 percent S atoms. The surface of the F-2747 crystal was composed of silver almost exclusively (>95 percent). As the only source of sulfur in this system is from the fuel, this technique may provide a very sensitive measure of fuel sulfur.

For use as an analytical technique for sulfur, additional work needs to be done. The linearity of the test with fuel concentration and the effect of temperature need to be determined. Furthermore, the sensitivity of the test to various types of sulfur compounds needs to be measured. Also, the cause of the difference in measured profiles with and without the presence of oxygen, as seen in Fig. 7, needs to be determined. At present it is thought that formation of carbon deposits in the presence of oxygen may explain the lesser formation of deposits. It is believed that the formation of silver sulfide tarnish on silver surfaces occurs by the reaction of sulfur with the surface silver atoms, and subsequent migration of subsurface silver atoms to the surface (Ricciardiello and Riotti, 1972). We hypothesize that the deposition of carbonaceous fuel deposits may cover the surface enough to limit the reaction of sulfur with silver, thus explaining the lower deposition in the presence of oxygen. Another possible explanation is that the presence of oxygen may result in oxidation of these sulfur compounds, which may prevent their reaction with the surface. For maximum sensitivity as an analytical test for fuel sulfur the presence of oxygen should be limited.

Effect of Fuel Dilution. We have studied the effect of fuel dilution on oxidation and deposition by diluting fuel F-2827 with a hydrocarbon solvent, Exxsol D80. Fuel F-2827 is a moderately high depositing fuel and a very slow oxidizer, while Exxsol D80 is a narrow-cut, dearomatized, low-sulfur (3 ppm), aliphatic solvent. A jet fuel such as fuel F-2827 can be thought of as a hydrocarbon solvent, consisting of alkyl aromatics, naphthenes, and paraffins, with small concentrations of other species, such as phenols, sulfur compounds, and nitrogen compounds. These other species are thought to be major players in both the formation of deposits and the inhibition of oxidation (Heneghan and Zabarnick, 1994). Thus, the dilution of a jet fuel with a solvent such as Exxsol D80 in effect reduces the concentration of these species.

We have diluted F-2827 fuel with Exxsol D80 to create mixtures from 100 percent (by volume) Exxsol D80 (referred to here as 0 percent F-2827) to 100 percent F-2827. These air-saturated mixtures were run in the QCM system at the standard conditions of 140°C and 1 atm starting pressure. The results are shown in Fig. 8. The figure shows the very different deposition and oxidation characteristics of the neat fuels, F-2827 and Exxsol D80. After 15 hours Fuel F-2827 produces deposits of 3.6 $\mu g/cm^2$, while Exxsol D80 produces only 0.6 $\mu g/cm^2$. Fuel F-2827 exhibits a nearly constant pressure profile during the run, while Exxsol D80 oxidizes so rapidly (<1 hour) that only a portion of the pressure drop is observed during the constant-temperature run (a majority of the oxidation is thought to have occurred during the heat-up process). We have previously shown the relationship between the pressure decays and oxidation in this system (Zabarnick, 1994). Also in the figure are

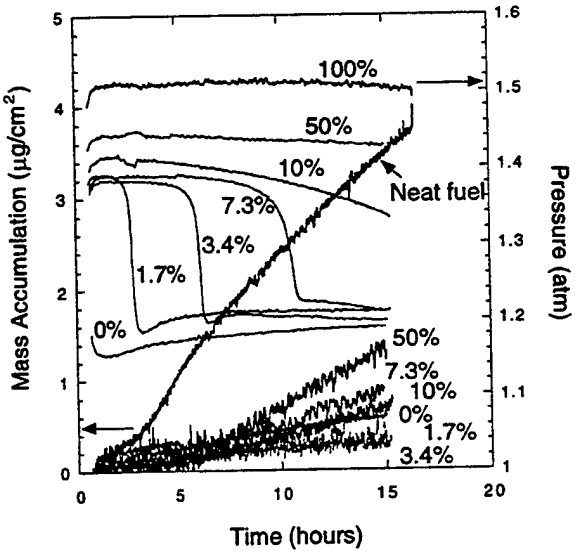

Fig. 8 Plots of mass accumulation versus time for dilution experiments at various percent fuel F-2827 concentrations

shown the results for mixtures composed of 1.7, 3.4, 7.3, 10, and 50 percent fuel F-2827. As the fuel is increasingly diluted, the oxygen removal begins to occur earlier in the run. The 50 percent run shows little pressure decay, while the 10 percent run begins to exhibit a small decay near the end of the run. The 7.3 percent run exhibits oxygen removal near 10 hours, the 3.4 percent run near 6 hours, and the 1.7 percent run near 3 hours. The corresponding deposition measurements show a reduction in deposition for the 50 percent run to 1.3 $\mu g/cm^2$, and at increasing dilutions the depositions scatter around that of the 0 percent run at 0.6 $\mu g/cm^2$. The data of Fig. 8 have implications in three areas: improving the thermal stability of a fuel by dilution, using a slow oxidizing fuel as an antioxidant, and characterizing the "effective" antioxidant concentration of fuels. We will address these individually below.

When we dilute fuel F-2827 to 50 percent we observe that the oxygen removal behavior does not change significantly, while the deposition measured is lower by a factor of ≈2.8. This demonstrates that the mixture of a moderately high depositing fuel with a low depositing fuel can yield a low depositing fuel with a slow oxidation rate. Thus, dilution with an inexpensive hydrotreated fuel may yield a simple and relatively inexpensive method of improving the thermal stability of a highly depositing fuel.

Exxsol D80 is a low depositor but it consumes oxygen quite rapidly. Rapid oxygen consumption is a negative characteristic of a fuel due to the resulting production of peroxides and acids under storage conditions. Mixing Exxsol D80 with relatively small amounts of fuel F-2827 results in a fuel with much delayed oxygen consumption, as seen in Fig. 8. Mixtures with 1.7 percent F-2827 delay oxidation for 2–3 hours, 3.4 percent delays oxidation for 7 hours, while 7.3 percent delays oxidation for 10–11 hours. From this point of view, the addition of small amounts of the slow oxidizing fuel F-2827 to the fast oxidizing "fuel" Exxsol D80 results in inhibition of oxygen consumption. Thus fuel F-2827 acts as an antioxidant when added in small quantities (<10 percent) to Exxsol D80 without significantly affecting deposition detrimentally. This demonstrates that a slow oxidizing fuel can be added to a fast oxidizing fuel to improve oxygen consumption characteristics and storage stability.

The dilution of a fuel with a solvent such as Exxsol D80 can also be used to determine the relative effective antioxidant concentration of the fuel. A characteristic of each individual fuel is the amount of fuel dilution required to bring the time

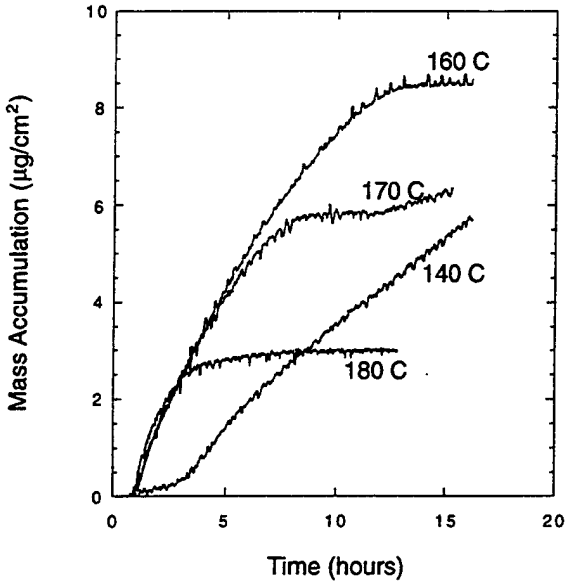

Fig. 9 Plots of mass accumulation versus time for fuel F-2827 over the temperature range 140 to 180°C at 20 psi added air

required for oxygen removal to a given value. Thus by performing this dilution procedure on various fuels and comparing the dilution amount, one can measure a relative effective antioxidant concentration, as the dilution required should be inversely proportional to the effective antioxidant concentration of the fuel. Of course such a relationship between dilution and effective antioxidant concentration is not necessarily linear, but an assumed linearity is sufficient for a relative measure of characterizing fuel antioxidant capabilities. With the current QCM/pressure measurement system this technique would only work on fuels that exhibit significantly delayed oxidation; it would not work on fast-oxidizing fuels. At this time we have not utilized this technique to compare various fuels, but it is a method that provides a way of comparing the relative antioxidant capabilities of fuels.

Effect of Temperature on Deposition. We have investigated the effect of temperature on the deposition of two jet fuels over the temperature range 140 to 180°C. The results are shown in Figs. 9 and 10. These runs were conducted in a similar manner to those described above for the oxygen dependence studies. The fuel was sparged with N_2 gas for one hour to remove the dissolved oxygen present in the fuel and headspace. As seen in the figures, the deposition rates at the higher temperatures are very rapid; the removal of oxygen minimizes deposition during the 45 minute heat-up period when QCM deposition measurements cannot be taken. After fuel heat-up, air is added to the reactor via the gas inlet until a given headspace pressure is reached. It is important to note that the headspace temperature is not measured or controlled, nor is its temperature uniformity known. Thus we do not know if the air bubbled through the fuel that resides in the headspace is at the fuel's temperature or lower. Thus it is difficult to control the oxygen availability of the fuel over a range of temperatures. The worst case situation is if the air actually reaches the fuel temperature; using the ideal gas law, this yields a decrease in oxygen availability of ≈9 percent in going from 140 to 180°C. As the reproducibility of the deposition measurements is greater than 9 percent, these concerns are minimized.

The data of Fig. 9 are for fuel F-2827 with 20 psi of added air. The data of Fig. 10 are for fuel F-2980 with 15 psi added air. Figure 9 shows that as the temperature is increased the rate of deposition appears to increase. This is especially apparent in going from 140 to 160°C. The figure also shows that the time at which the deposition levels off decreases with temperature. At 140°C the leveling has not occurred even at 15 hours, at 160°C leveling occurs near 13 hours, at 170°C leveling occurs near 9 hours, and at 180°C leveling occurs near 4 hours. The leveling off of deposition correlates quite well with the time at which oxygen consumption is complete for a wide variety of fuels (Zabarnick, 1994). Thus the data of Fig. 9 imply that oxygen consumption occurs more rapidly at higher temperatures, which is in agreement with previous observations (Hazlett, 1991). Interestingly, the final deposition at the end of the run displays complex temperature behavior. At 140°C the final deposition is 5.7 $\mu g/cm^2$, at 160°C the final deposition is 8.5 $\mu g/cm^2$, at 170°C the final deposition is 6.3 $\mu g/cm^2$, and at 180°C the final deposition is 3.0 $\mu g/cm^2$. Thus, there exists a temperature at which the deposition is a maximum, in this case 160°C; at both higher and lower temperatures the final deposition is lower. Figure 10 shows similar results for fuel F-2980, except that the peak temperature for final deposition for this fuel is 150°C.

The relationship between the final deposition and temperature is interesting because it appears to conflict with the conventional wisdom that deposition increases with temperature in the autoxidative temperature regime (Hazlett, 1991). This observation was based, for the most part, on devices operated in oxygen availability regimes that are different from the QCM system, as operated in the present work. Two such tests are static flask tests with bubbling oxygen/air and flowing heated tube tests. The flask tests have unlimited oxygen availability and thus the increase in deposits measured versus temperature results from the measurement reflecting the increase in deposition rate with temperature (i.e., the oxidation rate increases with temperature and therefore the deposition rate will reflect this behavior under unlimited oxygen conditions). Figures 9 and 10 show that the deposition *rate* does indeed increase with temperature in the QCM. The complex behavior observed here where the final deposition is lower at the highest temperatures measured is a result of the oxygen limited regime studied here. This behavior is a result of varying deposition with temperature for a given amount of oxygen consumed. The final deposition in an oxygen-limited system represents a measure of the efficiency of generating a given deposition level for a given amount of oxygen. This type of behavior is not monitored in bubbling flask experiments where the fuel has an unlimited oxygen availability.

Flowing heated tube experiments have yet a different regime of oxygen availability. Relatively high temperature and short

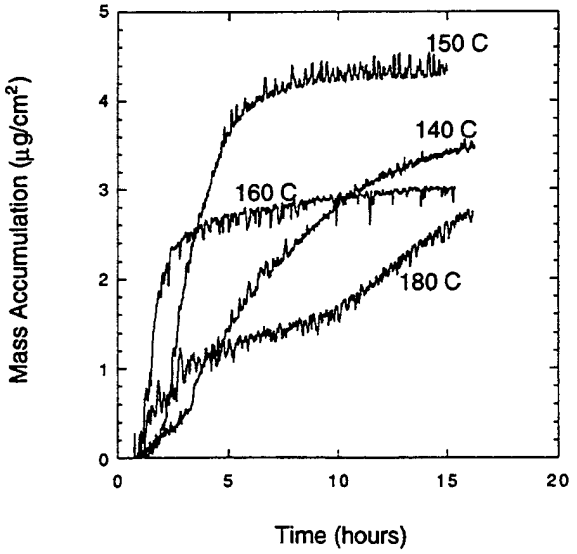

Fig. 10 Plots of mass accumulation versus time for fuel F-2980 over the temperature range 140 to 180°C at 15 psi added air

residence time tests such as the JFTOT (Hazlett, 1991) and the EDTST (Binns et al., 1994) often operate under conditions where oxygen consumption in the bulk fuel is not complete. The relatively short residence time and laminar flow conditions result in oxygen consumption occurring near the tube wall surface, while the bulk fuel does not show significant oxygen removal. The result is that the bulk fuel is able to supply essentially unlimited oxygen for reaction at the surface. Thus the apparent oxygen availability at the surface is unlimited. This results in the deposition versus temperature deposition rates as explained above for the bubbling air/oxygen flask experiments. Recently, other workers have observed a decrease in total deposition versus temperature above 185°C in a flowing heated tube (Jones et al., 1994). These experiments were conducted under very slow flow conditions, where complete oxygen consumption occurs within the tube. Thus the total deposition measured in these slow flow experiments is not dependent on the deposition rate but on the efficiency of deposit production for a given amount of oxygen, similar to the QCM system.

Conclusions

We have used the QCM/pressure measurement technique to study the thermal stability and oxidation characteristics of jet fuel. Both final deposit amounts and deposition rates were found to display complex dependencies on the oxygen availability; in addition, this behavior was observed to be fuel dependent. It was found that gold, aluminum, and platinum electrode surfaces yield similar deposition for fuel F-2827. Gold and aluminum electrodes yield similar results in fuel F-2747, but a platinum electrode gives significantly higher deposition for this fuel. Dilution of a moderate thermal stability fuel with a hydrocarbon solvent improves the thermal stability of the fuel without adversely effecting its oxidation characteristics. Addition of a slow oxidizing fuel to a hydrocarbon solvent can significantly delay oxidation of the solvent. The study of dilution of a slow oxidizing fuel with a hydrocarbon solvent can provide a measure of the relative effective antioxidant concentration of the fuel. Under limited oxygen conditions, we find that the final deposition increases and then decreases over the temperature range 140 to 180°C for two different fuels.

Acknowledgments

This work was supported by the US Air Force, Fuels and Lubrication Division, Wright Laboratories, Wright-Patterson AFB under contract No. F33615-92-C-2207 with Mr. Charles Frayne as technical monitor. We would like to thank Tom Wittberg (UDRI) for performing the Auger spectroscopy analyses.

References

Binns, K., Dieterle, G., Kalt, D., Martel, C., and Williams, T., 1994, "System Evaluation of Improved Thermal Stability Jet Fuels," presented at the 5th International Conference on Stability and Handling of Liquid Fuels, Rotterdam, the Netherlands.

Hazlett, R. N., 1991, "Thermal Oxidation Stability of Aviation Turbine Fuels," ASTM, Philadelphia.

Heneghan, S. P., and Zabarnick, S., 1994, "Oxidation of Jet Fuels and the Formation of Deposits," *Fuel*, Vol. 73, pp. 35–43.

Jones, E. G., Anderson, S. D., Goss, L. P., and Balster, W. J., 1994, "The Effect of Additives on the Formation of Insolubles in a Jet A Fuel," presented at the 5th International Conference on Stability and Handling of Liquid Fuels, Rotterdam, the Netherlands.

Klavetter, E. A., Martin, S. J., and Wessendorf, K. O., 1993, "Monitoring Jet Fuel Thermal Stability Using a Quartz Crystal Microbalance," *Energy and Fuels*, Vol. 7, pp. 582–588.

Martin, S. J., Granstaff, V. E., and Frye, G. C., 1991, "Characterization of a Quartz Crystal Microbalance With Simultaneous Mass and Liquid Loading," *Analytical Chemistry*, Vol. 63, pp. 2272–2281.

Ricciardiello, F., and Riotti, S., 1972, "The Corrosion of Fe and Ag in S Liquid at Low Temperature. Effect of S Viscosity," *Corrosion Science*, Vol. 12, pp. 651–659.

Zabarnick, S., 1994, "Studies of Jet Fuel Thermal Stability and Oxidation Using a Quartz Crystal Microbalance and Pressure Measurements," *Industrial and Engineering Chemistry Research*, Vol. 33, pp. 1348–1354.

Zabarnick, S., and Grinstead, R. R., 1994, "Studies of Jet Fuel Additives Using the Quartz Crystal Microbalance and Pressure Monitoring at 140°C," *Industrial and Engineering Chemistry Research*, Vol. 33, pp. 2771–2777.

Appendix J.

JP-8+100: Development of a Thermally Stable Jet Fuel

Shawn P. Heneghan
Steven Zabarnick
Dilip R. Ballal
University of Dayton
300 College Park
Dayton, OH 45469-0140

W. E. Harrison III
USAF Wright Laboratories
Wright Patterson AFB, OH 45433

JP-8+100: The Development of High-Thermal-Stability Jet Fuel

S. P. Heneghan

S. Zabarnick

D. R. Ballal

Aerospace Mechanics Division KL-463,
University of Dayton,
300 College Park,
Dayton, OH 45469-0140

W. E. Harrison III
USAF Wright Laboratories,
Wright Patterson AFB, OH 45433

Jet fuel requirements have evolved over the years as a balance of the demands placed by advanced aircraft performance (technological need), fuel cost (economic factors), and fuel availability (strategic factors). In a modern aircraft, the jet fuel not only provides the propulsive energy for flight, but also is the primary coolant for aircraft and engine subsystems. To meet the evolving challenge of improving the cooling potential of jet fuel while maintaining the current availability at a minimal price increase, the U.S. Air Force, industry, and academia have teamed to develop an additive package for JP-8 fuels. This paper describes the development of an additive package for JP-8, to produce "JP-8+100." This new fuel offers a 55°C (100°F) increase in the bulk maximum temperature (from 325°F to 425°F) and improves the heat sink capability by 50 percent. Major advances made during the development of JP-8+100 fuel include the development of several new quantitative fuel analysis tests, a free radical theory of autooxidation, adaptation of new chemistry models to computational fluid dynamics programs, and a nonparametric statistical analysis to evaluate thermal stability. Hundreds of additives were tested for effectiveness, and a package of additives was then formulated for JP-8 fuel. This package has been tested for fuel system materials compatibility and general fuel applicability. To date, the flight testing has shown an improvement in thermal stability of JP-8 fuel. This improvement has resulted in a significant reduction in fuel-related maintenance costs and a threefold increase in mean time between fuel-related failures. In this manner, a novel high-thermal-stability jet fuel for the 21st century has been successfully developed.

Introduction

Emerging environmental and technological demands of the 21st century imposed on the Air Force, the aircraft manufacturers, and the jet engine companies require the jet fuel to accomplish a variety of *noncombustion*-related tasks. In particular, jet fuel is the primary coolant for aircraft hydraulics, environmental control subsystems, and the engine. Future high-performance, high-thermal-efficiency engines will not only produce *more* excess heat, but also will have less fuel available with which to manage that heat. The end result is that jet fuel will be exposed to significantly higher temperatures for longer periods of time, causing the fuel to degrade and foul aircraft and engine components.

In 1990, an Aircraft Thermal Management Working Group of Wright Research and Development Center (WRDC) investigated the cooling requirements for current, next generation, and future aircraft (Harrison, 1990). Figure 1 illustrates the maximum estimated heat loads for various future aircraft and aircraft subsystems. These data show a threefold increase in the heat-loads for future aircraft as compared to the F4 aircraft. Also, Fig. 2 provides the worst case temperatures, pressures, and residence times experienced by fuel in typical modern engine and airframe components. After examining these and other projected requirements, the WRDC working group reached an alarming conclusion: "aircraft development in the near future will suffer performance penalties as tremendous quantities of ram air or excess fuel will be required to meet the heat sink requirements." To resolve the problem, the WRDC working group recommended the development of high thermal stability fuels, such as: (*i*) a high-temperature thermally stable "JP-8+100" fuel which provides a 50-percent improvement in heat sink capability over conventional JP-8 fuel, and (*ii*) a new JP-900 fuel that has a 482°C (900°F) thermal stability and could eliminate the need to recirculate fuel onboard an aircraft.

This paper presents a comprehensive study of the development of JP-8+100 jet fuel, from problem identification to current flight testing. Included are descriptions of the following:

(*i*) current and future heat load and temperature considerations that demand higher heat sink fuels;
(*ii*) challenges faced in the development of JP-8+100 thermally stable fuel including test development, theoretical advances, and modeling efforts; and
(*iii*) testing and selection process of an additive package from screening to flight tests.

Advanced Jet Fuel Requirements

Current aircraft can thermally stress the fuel to temperatures above its thermal stability causing the fuel to degrade and form varnishes, gums (oxidative instability products), and coke (thermal instability products). Fuel fouling and coking is an expensive maintenance burden. Fouling distorts fuel nozzle spray pattern which can lead to gas turbine combustor hot spots, poor combustor pattern factor, and excessive temperatures in the first-stage turbine blades. Fouling in augmentors can effect lightoff and can cause a low-frequency acoustic phenomenon called "rumble." Other more subtle problems found with fuel fouling include increased difficulty with engine cold starts, altitude relights, and fuel control anomalies. With an increase in engine performance and higher heat loading, engine component design (pumps, valves, manifolds, filters, controls, heat exchangers, fuel nozzles, augmentor parts) has become more difficult. Operating temperatures in main burner nozzles, fuel-powered actuators, fuel controls, and augmentor parts in many cases are above the thermal stability of the fuel and component designs to reduce fuel temperatures are complex, heavy, and costly. Improved thermal stability fuels, such as JP-8+100, offer

Contributed by the Fuels and Combustion Technologies Division for publication in the JOURNAL OF ENERGY RESOURCES TECHNOLOGY. Special solicited paper for the 75th FACT Anniversary received March 15, 1996; revised manuscript received May 22, 1996. Associate Technical Editor: C. Saltiel.

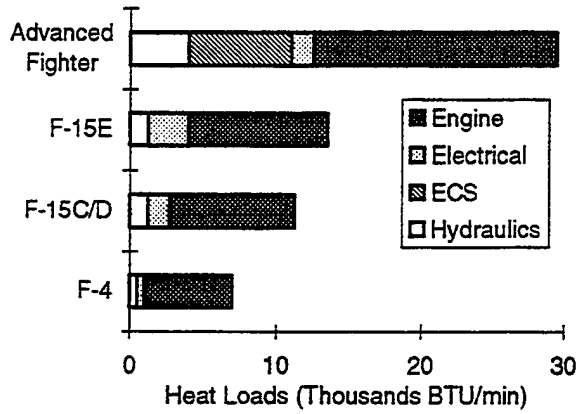

Fig. 1 Maximum estimated heat loads for various aircraft and aircraft subsystems

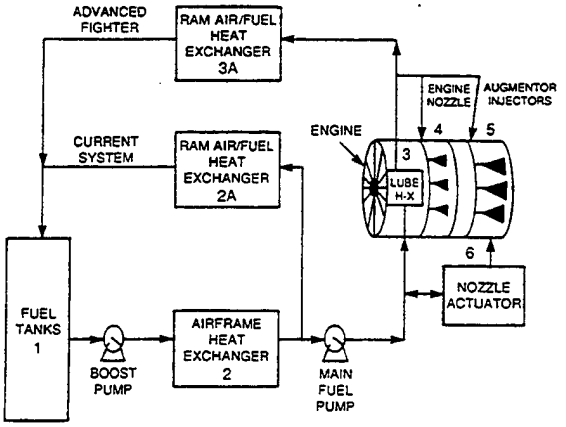

	1	2	2A	3	3A	4	5	6
T (F)	<160	<250	<250	300	<325	325+	500+	<350
P (psi)	<25	<80	<80	1200 to 2000	<80	<40#	<40#	1500 to 4000
Time	min to hrs	<15 sec	<2 sec	<3 sec	<2 sec	<2 sec*	min*	<20 min

*Time: <100 msec
#Pressure: 1200 - 2000 psi

Fig. 2 Worst case temperature, pressure, and residence time experienced by fuel in various airframe and engine components

significant benefits to the component designers, aircraft manufacturers, and maintenance personnel.

Jet Fuel Operating Temperatures

Twenty-first century high-performance engines will operate at much higher fuel and combustor inlet temperatures. If one uses current production technology fuel nozzles for these high-performance engines, for example, the F404 nozzle shown in Fig. 3, the estimated wetted wall temperature is 425°C (797°F) as compared to the acceptable wetted wall limit of 204°C (400°F) with JP-8. The corresponding desirable maximum bulk fuel temperature of 163°C (325°F) is lower than the inlet fuel temperature for this particular advanced application. Therefore, aviation fuels with thermal stability characteristics better than that of JP-8 are needed. Figure 4 shows the time variation of measured wall temperature of an engine fuel nozzle of an advanced fighter engine immediately following the engine pullback. For this situation, the measured outer wall transient temperatures are as high as 538°C (1000°F) and steady-state temperatures are close to 288°C (550°F). For the secondary circuit, wetted wall temperature increases from 149°C (300°F) to 204°C (400°F), and then asymptotically reaches 176°C (350°F) as described by Harrison et al. (1995). If the secondary fuel passage has no recirculation, and is not completely purged, the excessive stem wall temperature leads to unacceptable soak back coking/sticking problems, especially if the engine is shut down 15 s after the fuel chop.

Figure 5 shows a production engine combustor swirl cup, a fuel-air mixing device designed to decrease the sensitivity of the fuel injection system to fuel type. This device works free of carbon deposition as long as the fuel film temperature remains below or above certain critical metal temperatures. The carbon deposition tendency of a given swirl cup venturi surface can worsen or improve with the fuel switchover from JP-4 to JP-8. It is, therefore, important to understand the fundamentals of venturi carboning and how the operating temperature window changes as a function of engine operating conditions and the fuel properties. Further, a systematic analytical, component, and engine system test study is required to quantify potential toxic effects, hot-section hardware durability, high-temperature lubricity, and heat sink capability of high-thermal-stability jet fuels.

JP-8 and the JP-8+100 Program

JP-8, the current standard Air Force fuel, is a Jet A-1 fuel used by commercial airlines with a military additive package consisting of fuel system icing inhibitor, corrosion inhibitor/lubricity enhancer, and an antistatic additive. JP-8 fuel is a single battlefield fuel, since it can be used in all ground mobile diesel equipment (HUMMERs, trucks, tanks, etc.) as well as in all aircraft.

In 1989, the U.S. Air Force initiated a research program to increase the thermal stability of JP-8 while maintaining existing performance requirements, fuel cost, and fuel availability. The

Nomenclature

AFTS = aviation fuel thermal stability test unit
AH = antioxidant molecule
ARSFSS = advanced reduced scale fuel system simulator
BHT = butylated-hydroxy-toluene
CFDC = computational fluid dynamics with chemistry
EDTST = extended duration thermal stability test
HLPS = hot liquid process simulator
ICOT = isothermal corrosion oxidation test
JFTOT = jet fuel thermal oxidative tester
JP = jet fuels
k, k' = rate constants
mM = millimolar
MCRT = microcarbon residue test
MTBF = mean time between failure
NIFTER = near isothermal flowing test rig
pS = picosiemens
ppmW = parts per million by weight
QCM = quartz crystal microbalance
RH = fuel hydrocarbon molecule
R_i = rate of radical formation
TAC = total accumulated cycles
WRDC = Wright Research and Development Center
$X\cdot$ = free radicals (X = A, R, RO_2, RO, HO)
8Q405 = Betz proprietary additive

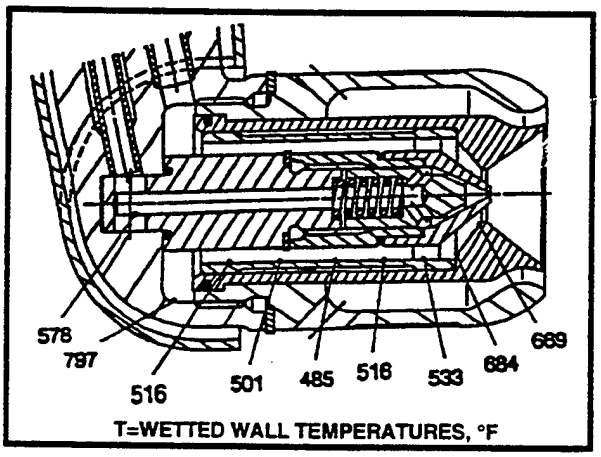

Fig. 3 Typical fuel nozzle wall temperatures measured in an advanced engine. Data are for cruise condition (T3 = 1260°F (682°C), fuel inlet temp. = 350°F (177°C)).

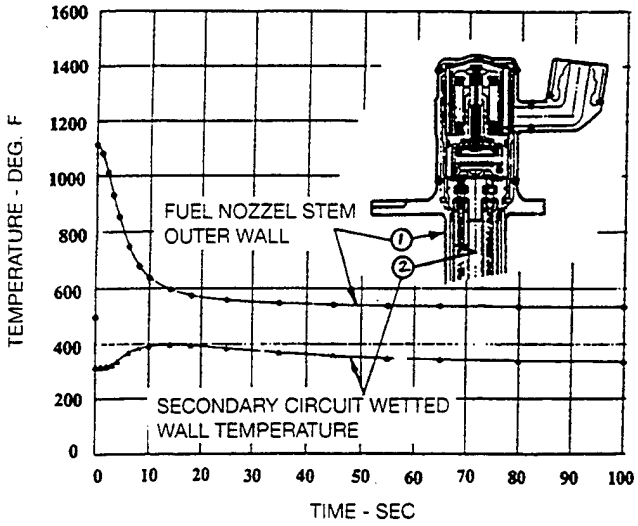

Fig. 4 Time variation of measured wall temperatures of an engine nozzle immediately following engine pullback

established goal of this program was to increase the heat sink capacity of current JP-8 fuel by 50 percent (i.e., a 55°C increase in fuel operating temperature from 163°C to 218°C) by developing additives to blend with the fuel at a cost of $1 per 1000 gal. This fuel will alleviate the need for using expensive specialty fuels, such as JP-7 and JP-TS, in future aircraft and decrease maintenance costs for existing aircraft. To meet this goal, the following five major research tasks were identified:

1 identify and develop new fuel thermal stability test techniques;
2 advance the fundamental understanding of fuel thermal stability;
3 develop global chemistry models and a thermal stability scale;
4 formulate effective thermal stability improving additive packages;
5 demonstrate, in actual aircraft flight time and maintenance records, the performance and cost savings produced by the use of new JP-8+100 fuel.

Test Technique Development

In an aircraft fuel system, appreciable deposits accumulate over thousands of hours of operation. The foremost problem in test development is that any laboratory testing must be accelerated to obtain measurable deposits in time scales and with fuel quantities appropriate to laboratory testing. This requirement necessitates that the test temperature be higher or oxygen availability increased. Since deposits are generally formed on the order of milligrams per kilogram of fuel, static tests must either use excess oxygen, or have high sensitivity to measure the deposits. Heneghan et al. (1993a) has discussed the test problems associated with the availability of excess oxygen. Flowing tests are limited in number due to their size and complexity, while the turnaround time for testing is limited by cleaning requirements. Lastly, long storage times can affect jet fuel performance, making baseline comparisons over time difficult.

Jet fuels undergo a variety of thermal stresses. The fuel absorbs heat as it moves toward the combustor, and may also spend significant times in hot fuel system sections either during or after the mission. Recirculation of jet fuels causes further complications in tracing the thermal history of the jet fuel. As a result, many different test environments are necessary to evaluate fuel thermal stability and additive effectiveness. Finally, there are several mechanisms and types of deposits formed under thermal/oxidative stressing. These have been referred to as gums, lacquers, bulk particulates, hard deposits, and soft deposits. Some of these deposits are found to be soluble in polar solvents, while others are not. Also, some deposits are found to occur in cooling sections of the fuel system, probably as a result of temperature-dependent solubility of the deposits in jet fuels, while others are formed generally in the heated sections.

As a result of the complications briefly described in the foregoing, old tests needed to be reevaluated, and new tests developed that expand the range of thermal stresses. Concurrently, we developed models that would aid in understanding the results of the individual test as well as assist in correlating the results of several tests.

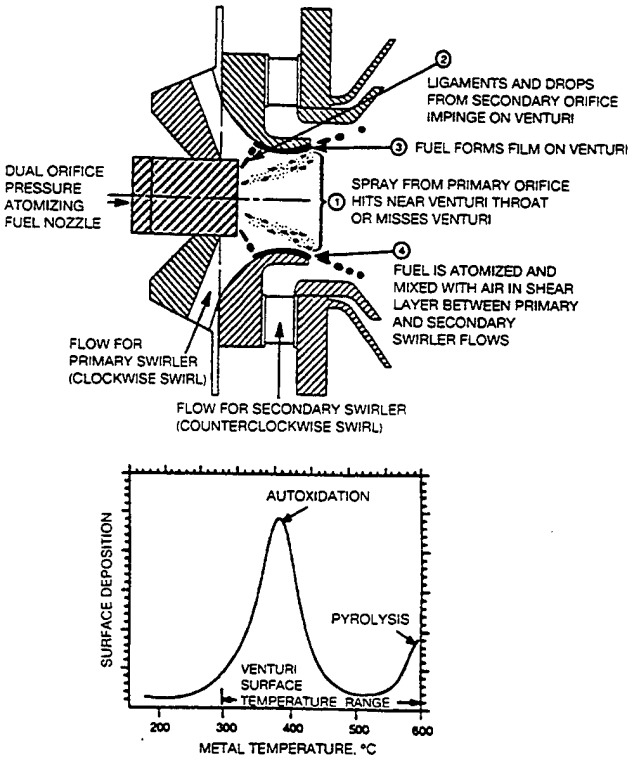

Fig. 5 Schematic of (a) production engine combustor swirl cup, and (b) surface deposition versus metal temperature relationship

Table 1 Summary of thermal stability test rigs and conditions

Test	Temperature Range (C)	Reference	Characteristics
Static Tests			
QCM	140	Zabarnick, 1994	Closed system - measures surface deposits
ICOT	180	Grinstead, 1994	Bubbling air - measures bulk deposits
MCRT	225	Grinstead, 1994	Distillation - measures residual deposits
Flask Test	180	Jones et al., 1992	Bubbling Air - measures bulk and surface deposits
Flowing Tests			
Gravimetric JFTOT	260	Beal et al., 1992	
	180 - 380	Marteney and Spadaccini, 1986	Constant heat flux system
Augmentor	up to 1000	Edwards, 1992	Vaporization flow system - simulates afterburner and nozzle soak back
	190 - 310	Chin and Lefebvre, 1992	Constant wall temperature, capable of recirculation studies
Phoenix	200-300	Heneghan et al., 1993b	Constant wall temperature with on-line dissolved O_2 measurement
NIFTER	140 - 210	Jones et al., 1995	Isothermal flow system with on-line dissolved O_2 measurement
HLPS	335	Biddle et al., 1994	JFTOT flow system
	140-200	Vilimpoc et al., 1995	In-Situ particle sizing, oxygen measurement and deposition
Engineering Tests			
AFTS*	180 - 230	Dagget and Veninger, 1994	
EDTST	160-200	Dieterle et al., 1995	Establishes fuel bulk and wetted wall temperatures
ARSFSS		Morris and Binns, 1994	Configured to simulate F-22
	230 - 400	Brandauer et al., 1995	Simulated turbine pre-vaporizers

Jet Fuel Thermal Oxidative Tester (JFTOT). Since 1973, the standard for evaluating thermal stability has been JFTOT and the test procedure as described in the American Society of Testing and Materials D3241. This test is only adequate for determining a go/no-go fuel rating and therefore does not provide any quantitative information whatsoever. Also, it is of a questionable value because JFTOT is based on a single high fuel operating temperature (260°C) and fuel quality is measured by a simple visual observation.

These limitations of JFTOT in defining thermal stability led to the development of several advanced research instrumentation and quantitative test techniques within the last five years. These test techniques, which are summarized in Table 1, are categorized into three classes; static tests, flowing tests, and large-scale engineering tests.

In all static and flowing tests (developed in the JP-8+100 program), the residence time and temperatures were sufficient to ensure the complete autoxidation of the dissolved oxygen within the test zone. This is not necessarily the case in the large-scale engineering tests. Understanding fuel oxidation characteristics is crucial to evaluating test results and the thermal stability mechanism (Hazlett, 1991). Table 1 provides a summary of all the new thermal stability tests developed (or used) in the present research.

Static Tests. Static tests use small quantities of fuel, involve reaction times from 2 to 20 h, and temperature ranges from 140°C to 250°C (284°F to 482°F). Oxygen is usually available in excess of that normally dissolved in jet fuel (1.6 mM or 65 ppmW or 50 mg/L), although the actual amount in some cases is limited. Static tests can be either "open" to ambient air (ICOT, MCRT, and flask tests) or "closed" (QCM). The "open" tests are the hardest to understand as the amount of reaction due to oxygen availability is difficult to determine, but they are among the easiest to set up. In typical open static tests, fuel (50–250 mL) is generally heated on a "hot plate," often with bubbling air/oxygen. The resultant fuel is filtered and the deposits measured gravimetrically (usually in mg quantities). The MCRT is a vaporization test, and the residue is determined by weighing a tared vial. Metal coupons can be inserted into the flask tests to measure surface deposits. The QCM test is probably the most useful of the static tests, and is, therefore, described in the forthcoming.

The QCM has the ability to perform real-time, in-situ measurements of extremely small levels of deposition (ca. 0.2 $\mu g/cm^2$). Thus, although small amounts of fuel (60 mL) are used, and small extents of oxidation occur, deposition (generally from 1 to 10 $\mu g/cm^2$) can be readily determined. Jet fuels are thermally stressed in The QCM/Parr bomb system, shown in Fig. 6. The reactor is equipped with a gas inlet line and vent for gas sparging. A magnetic stir bar is used to minimize spatial temperature gradients. The quartz crystal is a 5-MHz, 2.54-cm-dia, 0.33-mm-thick AT-cut wafer with gold electrodes. The Parr bomb is a 100-mL stainless steel vessel modified with an RF feedthrough. The temperature is monitored by thermocouple

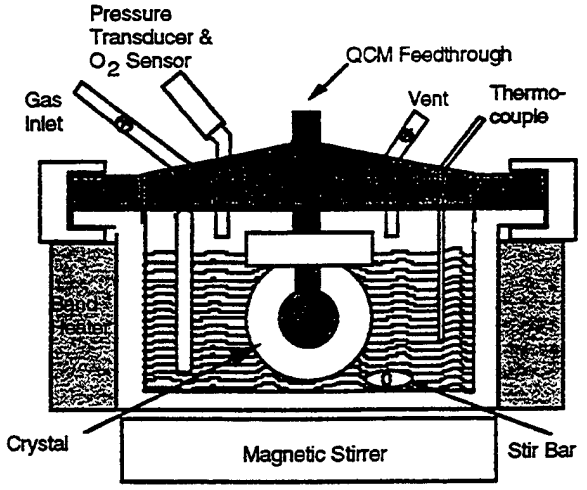

Fig. 6 Schematic diagram of quartz crystal microbalance/Parr bomb system

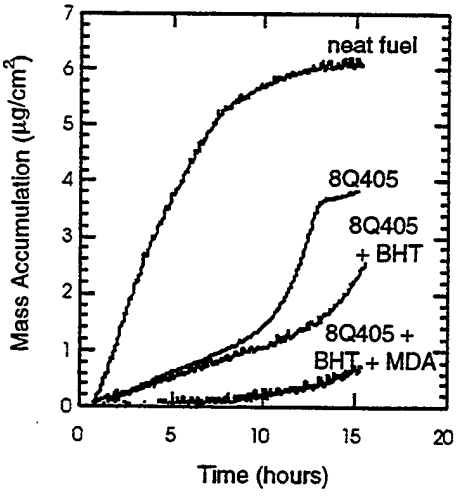

Fig. 7 Deposit formation versus time in QCM for various additives in a JP-5 fuel

and controlled by a PID temperature controller (typically at 140°C ± 0.4°C). Pressure is measured by an absolute pressure transducer. Tests are started at room temperature in a sealed, ambient-pressure vessel. A personal computer records the fuel temperature, pressure in the headspace, and resonant frequency of the crystal at one minute intervals over the 15-h test. The oxidation of the jet fuel is related to the pressure drop in the headspace and the deposition is related to the change in resonant frequency of the crystal. The device is capable of operating over a range of temperatures, pressures, and run times, although operating conditions of 140°C and near-ambient pressures for 15 h have proven to yield important information on both the fundamental behavior of fuel deposition and oxidation, and the behavior and evaluation of jet fuel additives. In particular, the simultaneous, real-time, in-situ monitoring of both deposition and oxidation yields important information on the details of fuel autoxidation. Figure 7 shows typical deposit versus time results for a JP-5 fuel blended with a series of additive combinations. These results will be discussed later.

Flowing Tests. Flowing tests generally use several gallons of fuel, have residence times of a few seconds, and test times of hours. The fuel is pretreated to establish a known dissolved oxygen level. Once the fuel enters the flow rig, no additional oxygen is available for reaction than that originally dissolved in the fuel. Pressures are generally established sufficiently high to prevent fuel boiling. Flows can be established in the laminar or transition to turbulent regime. Also, heating can be established (or at least approximated) as constant bulk temperature, constant wall temperature or constant heat flux. The temperature profiles can be complicated by the addition of cooling sections, reheat sections, or even recirculation. The temperature range of study can be extended from thermal oxidative temperatures up to the pyrolytic regime around 1000°C.

As shown in Fig. 8, typical of flowing rigs is the Phoenix rig which is a single-pass fuel-flow system that heats the fuel in a stainless steel tube. A preconditioning tank is equipped with a gas sparging system to control the concentration of dissolved oxygen. A diaphragm pump with a surge suppresser provides fuel flow in the range 1 to 100 mL/min at a pressure of 3.45 MPa and a pneumatic control valve maintains system pressure at 2.5 MPa. The test section is constructed of type 316 stainless steel tubing (560 mm long, 3.18 mm o.d., and 2.15 mm i.d.) heated by a copper block heater. It is designed to heat the test section up to 500°C and maintain a constant wall temperature throughout the test duration. The wall temperature profile is measured with welded thermocouples, and the bulk fuel temperature is calculated.

Fuel degradation is measured as the amount of carbon deposit formed on the tube. The deposits have been shown to be approximately 80 percent carbon and is independent of the fuel or the fuel quality. To determine the carbon, the test is shut down and the heated tubes are removed from the test setup, cleaned, sectioned, and analyzed by carbon burn-off. The surface of the tubes can also be studied by a variety of surface techniques to quantify the chemical character of the deposits.

Gas detection is accomplished using an on-line, but not in-situ dissolved gas analyzers to follow the consumption of oxygen and the production of other gases (principally methane). Figure 9 shows the consumption of oxygen as a function of the bulk fuel temperature for four fuels: a straight run jet fuel, a hydrotreated jet fuel, JP-TS (thermally stable jet fuel), and hexadecane. Differences in the ease of oxidation are easily measured, with the pure hydrocarbon being the most easily oxidized and the straight run jet fuel the most difficult.

Large-Scale Engineering Tests. Large-scale engineering tests range from more complex heat exchangers such as the extended duration thermal stability test (EDTST) to generic fuel system simulators such as the advanced reduced-scale fuel system simulators (ARSFSS) and aviation fuel thermal stability test unit (AFTS) that have actual fuel system components and heat fluxes. Brandauer et al. (1995) have set up simulators to study the formation of deposits in gas turbine prevaporizers. Test periods vary from days to weeks and can be set up to simulate specific missions. The test results may be evaluated as in the flowing systems by carbon burn-off or by using a boroscope or by measuring valve hysteresis.

The EDTST in particular uses established bulk fuel (325°F, 163°C) and wetted wall temperatures (400°F, 204°C) to determine JP-8 baseline data, and has established goals of bulk fuel (425°F, 218°C) and wetted wall temperatures (500°F, 259°C) to test JP-8+100. The system is not equipped with on-line oxygen analysis, although off-line analysis has shown that only a small fraction of the dissolved oxygen is generally consumed. The small amount of oxygen reaction is due to the short residence time and high flow rates used in the EDTST which is more representative of real fuel systems. As in the flowing tests, fuel degradation is determined by disassembling the heated sections, cleaning and sectioning the tube, and measuring deposits by carbon burnoff. Results for baseline JP-8 fuel, and two different additive packages are shown in Fig. 10 (Dieterle and Binns, 1995). These results, as is typical of most flowing tests, show that the deposits amounts tend to peak within the heated test sections. In this test (run for 96 h with recirculation), relatively large amounts deposits (1000 $\mu g/cm^2$) are formed. However, additives can reduce the deposits by two orders of magnitude.

Fundamental Advances

During the last few years, our research into the development of JP-8+100 has resulted in several significant fundamental advances in the understanding of jet fuel oxidative and thermal stability. Two important advances are: (*i*) relationship between thermal and oxidative stability, and (*ii*) understanding the free radical mechanism of oxidation. Each of these developments is in the following.

Thermal and Oxidative Stability. Figure 9 illustrates the oxidation behavior of four jet fuels as a function of bulk fuel temperature at a constant fuel flow in a Phoenix rig. These and other results on both the Phoenix rig and a nearly isothermal flowing test rig (NIFTER) showed that a more thermally stable hydrotreated fuel, such as JP-TS, oxidized at a lower temperature or in a shorter residence time than Jet A and Jet A-1 that have lower thermal stability. The trend towards oxidation at a lower threshold temperature continued for a pure hydrocarbon fuel, such as hexadecane. This inverse relationship between the thermal stability, as defined by deposits, and oxidative stability,

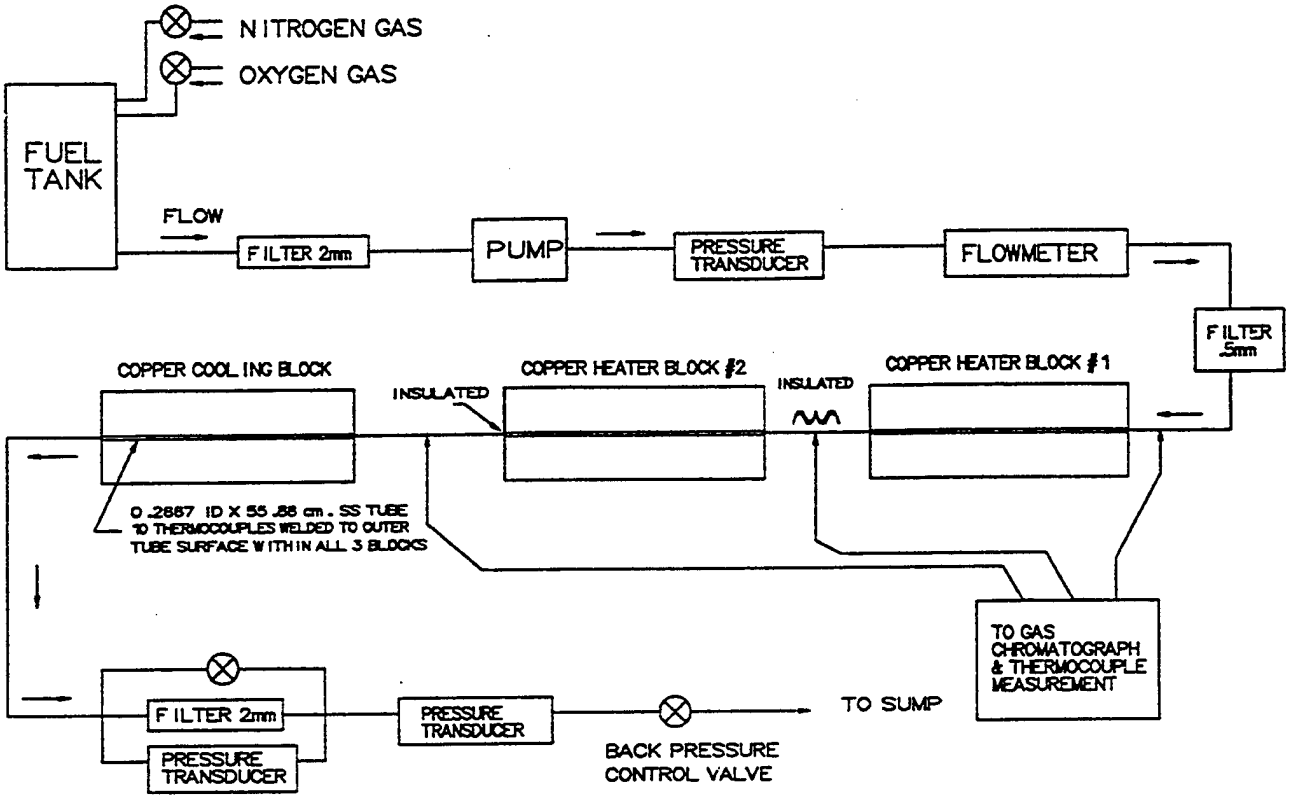

Fig. 8 Schematic diagram of the Phoenix rig flowing test

as defined by the production of oxidized products, has also been observed by Heneghan et al. (1993a) and Hardy et al. (1992). The generic behavior is shown plotted in Fig. 11.

Heneghan and Zabarnick (1994) showed that the observed inverse behavior was consistent with a known free radical autooxidation mechanism. They proposed that naturally occurring antioxidant molecules were necessary to the formation of deposits. The larger the concentration of antioxidant molecules, the slower the fuel would oxidize and the more deposits it would form. Several possible characteristics of proton donating antioxidant molecules were discussed. In particular, the necessary concentration was discussed in relation to the activation energy for proton metathesis. Interestingly, an easily oxidized molecule (one that has a weakly bonded proton) can act as an antioxidant molecule when present in sufficiently small quantities. They proposed aromatic amines, thiols, branched chain alkyl aromatics, or aldehydes, as possible molecules.

Autooxidation Mechanism. Figure 12 illustrates the complete free radical mechanism for solid carbon and gum formation. In these reactions, AH is the antioxidant molecule, RH is a fuel molecule, and the precursor to deposits is identified as A. The rate of oxidation for this system (for sufficient oxygen) is given as

$$-\frac{dO_2}{dt} = R_i + k_3[RO_2\cdot][RH] \qquad (1)$$

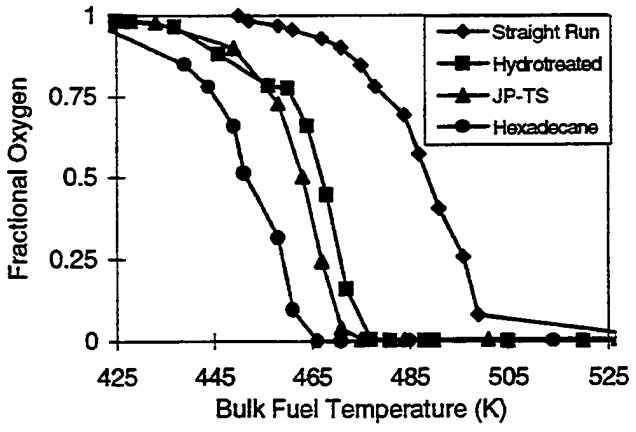

Fig. 9 Fractional oxygen remaining versus output bulk fuel temperature at constant flow conditions in Phoenix rig

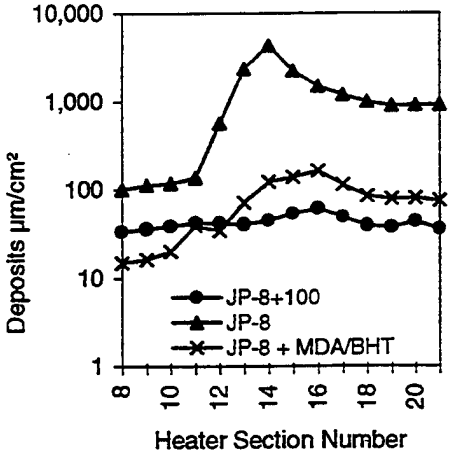

Fig. 10 EDTST showing improvement in thermal stability of a JP-8 by addition of proposed additive package. (350F bulk, 500F wetted wall, 96 h with active recirculation.)

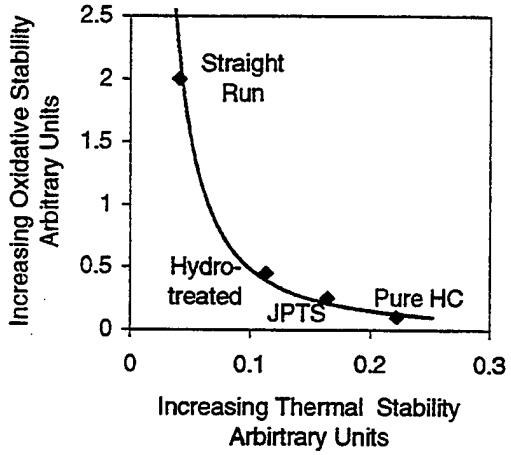

Fig. 11 Inverse relation between thermal stability and oxidative stability for various jet fuels and a pure hydrocarbon (HC)

where R_i is the rate of formation of R·, the subscripts refer to reactions shown in Fig. 12, and

$$[RO_2\cdot] = \frac{k_5[AH] - \sqrt{k_5^2[AH]^2 + 8k_6R_i}}{-4k_6} \quad (2)$$

This mechanism shows that the rate of oxygen consumption is independent of the oxygen concentration. It also reveals that at a low enough oxygen concentration, the rate-limiting step will switch from reaction 3 to reaction 2. At that time, the consumption of oxygen will be first order in oxygen. The increased lifetime of R· due to the decreased oxygen is responsible for the appearance of methane in the Phoenix rig experiments (Heneghan et al., 1993b) only after a complete depletion of the oxygen occurs. The rate of oxidation versus time at constant temperature was observed to increase proportionately to the amount of oxidation that had occurred up to that time (Jones et al., 1995) (i.e., $k_0(t) \propto ([O_2]_0 - [O_2]_t)$). Zabarnick (1993) demonstrated the proposed autooxidation/antioxidant mechanism and showed that the peroxide decomposition (reaction 7 in Fig. 12) can account for the observed acceleration. A bimolecular mechanism for the acceleration has also been proposed (Jones et al., 1995).

Thermal Stability Modeling

Global Chemistry Model. Modeling is an important tool in the development of thermal stability tests. It has long been known that temperature and oxygen concentration play important roles in deposit formation. Since all of the laboratory tests are accelerated, so as to acquire data in reasonable time periods, model development allows us to extrapolate from the accelerated laboratory tests and to make predictions concerning the effectiveness of an additive, or the stability of a fuel at long times under conditions of less oxygen, or higher temperatures.

Krazinski et al. (1992) developed a model of computational fluid dynamics with chemistry (CFDC) to predict jet fuel degradation. This CFDC model incorporates the process of jet fuel oxidation and requires a global reaction kinetics scheme to represent a series of elementary reaction steps. Typically, the global reaction rate parameters are assumed to be in Arrhenius form with parameters A and E that are independent of time and temperature. A third but usually unrecognized parameter in the system is the order of reaction (n)

$$-\frac{dO_2}{dt} = A\exp(-E/RT)[O_2]^n \quad (3)$$

Katta et al. (1993) used the Arrhenius assumption to predict the deposition profiles in an isothermal flowing system and observed that the activation energy changed with temperature. Heneghan (1994) studied the source of the global oxidation rate constant using the autoxidation mechanism with acceleration due to peroxide decomposition. He showed that the global rate constants for oxidation were neither constant in time nor Arrhenius in form. This autooxidation sequence was modeled by Zabarnick (1993) to account for the observation of acceleration by Jones et al. (1995). A time-dependent rate constant to account for the early oxygen consumption was derived as

$$-\frac{dO_2}{dt} = k\exp(k't) \quad (4)$$

where k and k' are ordinary Arrhenius rate constants.

Chin et al. (1994) developed this new oxidation model, including autoacceleration, and incorporated it into a CFDC code. Figure 13 shows that this model satisfactorily predicts the shape and amount of the deposition rate in the NIFTER flowing systems. Under high-temperature, high-flow-rate conditions typical of the real fuel systems, turbulent diffusion of the oxygen was found to be responsible for the increased oxygen consumption which results from a radially nonuniform temperature profile.

Thermal Stability Scale. As discussed earlier, several different tests were developed to help evaluate jet fuel thermal stability over a range of temperature and oxygen availability conditions. It was pointed out that due to the complexities of individual fuels and different mechanisms of deposit formation

initiation	$RH \xrightarrow{1} R\cdot + H\cdot$
propagation	$R\cdot + O_2 \xrightarrow{2} RO_2\cdot$
	$RO_2\cdot + RH \xrightarrow{3} RO_2H + R\cdot$
gum formation	$RO\cdot + RH \xrightarrow{4} ROH \rightarrow R{=}O + O_2$
	$\rightarrow$ Acids $\rightarrow$ Gums
Antioxidant	$RO_2\cdot + AH \xrightarrow{5} RO_2H + A\cdot$
	$A\cdot + O_2 \xrightarrow{5'} AO_2\cdot$
termination	$2\,RO_2\cdot(AO_2\cdot) \xrightarrow{6}$ products
acceleration	$RO_2H \xrightarrow{7} RO\cdot + OH\cdot$
solid formation	$A\cdot + O_2 +$ Heteroatoms $\rightarrow$ Solids

Fig. 12 Free radical autooxidation mechanism

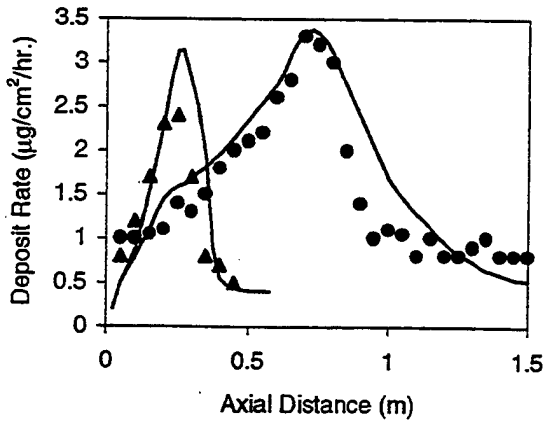

Fig. 13 Comparison of calculated versus experimental deposit formation in NIFTER using global oxidation parameters. (▲—0.125 cm³/min., ●—0.500 cm³/min., ———calculated fit.)

Table 2 Integer ranking of fuels by thermal stability tests

Fuel	Average TS Scale	ICOT	MCRT	QCM 8 hrs	QCM 15 hrs	JFTOT Breakpoint	HLPS
A	1	1	1	1	1	1	1
B	2	2	2	2	2	2	2
C	3	3	3	3	4	3	9
D	4	9	5	4	3	8	3
E	5	8	6	6	5	7	4
F	6	4	10	7	7	4	5
G	7	7	11	5	6	6	6
H	8	5	4	8	11	8	8
I	9	6	9	9	10	4	7
J	10	10	7	9	8	10	10
K	11	11	7	11	9	12	12
L	12	12	12	12	12	10	11

1 - Best Fuel (most thermal stability)
12 - Worst fuel (least thermal stability)

tests may not agree as to the thermal stability of jet fuels. Varying measurements (i.e., mg/cm^3 or mg/cm^2 or °C) make absolute comparison of fuel quality impossible. Further, there is no reason to believe that a 10-percent improvement in one scale corresponds to a 10-percent improvement in another (that is, linearity of scale is an assumption). Lastly, since the actual scale of thermal stability is not available for comparison, judging which if any of the tests is better or worse is difficult.

To account for the variety of tests and to determine if there is a general agreement among the tests used to evaluate JP-8+100 additives, Heneghan and Kauffman (1995) performed a nonparametric statistical analysis of the thermal stability test results for twelve fuels and six test techniques to develop an average thermal stability (TS) scale. The six tests were ICOT, MCRT, QCM (at two different times), JFTOT breakpoint, and HLPS. The twelve fuels included JP-TS, a high nitrogen fuel, hydrotreated fuels, stock run, and Merox-treated fuels. The nonparametric study assumed only that each of the tests was monotonic. That is, for example, if a JFTOT breakpoint temperature of 310°C is indicative of better thermal stability than a breakpoint temperature of 300°C, then 300°C is better than 290°C, which is better than 280°C, etc. However, no attempt to assess how much better is made. The fuels are merely ranked according to the breakpoint temperature. The result was an average thermal stability scale in which each fuel was ranked from 1 to 12.

Table 2 shows the ranking of these twelve fuels. It shows that most of the thermal stability tests can clearly delineate good and bad fuels. It is only in the undistinguished fuels that there is a significant difference. A carefully ordered statistics analysis of these ranks for each test versus the average shows that there is less than 5 percent probability that these tests are so ordered due to random processes. That is, it is clear that some underlying property of the fuels is responsible for establishing the order. This average order is then referred to as the thermal stability scale. The general agreement among the variety of tests and fuels gives confidence that each of the tests is well designed, and the results are understood.

Additive Testing and Formulation

The prime goal of the JP-8+100 development program was to find an additive or an additive combination that will improve the thermal stability of JP-8 fuel by 55°C. Additives were supplied by several additive manufacturers for testing. Many classes of additives were tested. These additive classes comprise antioxidants, detergents, dispersants, and metal deactivators. The QCM, ICOT, MCRT, HLPS, and JFTOT breakpoint tests were used for screening over 400 additives (see, for example, Anderson et al., 1995; Grinstead, 1994; and Zabarnick et al., 1995). To accommodate the large number of potential additives, a series of static and JFTOT-type tests were used to screen additives in a limited number of jet fuels. Tests were generally run at the manufacturer's recommended concentration. Those additives that performed "best" were selected for follow-on testing, including concentration optimization.

After selection of the candidate additive with the best likelihood of success, we verified that the additive package would work in most fuels by studying the effects in a world fuel survey. Then, the candidate was extensively tested in flowing tests (NIFTER and Phoenix rig) and large-scale engineering rigs (EDTST and ARSFSS). A series of materials compatibility tests were also run to identify/correct any adverse materials impact. Finally, an additive package was tested in ground engine and flight tests.

The original screening based on 4 fuels showed that a combination of Betz detergent/dispersant 8Q405 (100 mg/L) and butylated-hydroxy-toluene (BHT at 25 mg/L) effectively increased the thermal stability of the base jet fuels. Tests of 28 JP-8 and JP-5 fuels demonstrated significant thermal stability improvement with the JP-8+100 additive package in the QCM, ICOT, and HLPS. This study also showed that a further improvement in thermal stability could be expected when MDA (8 mg/L) was included in the additive package. The thermal stability improvement observed in a relatively large sampling of fuels gives a measure of confidence that the additive package will perform satisfactorily in the field.

Figure 7 shows deposit formation vs. test duration in a QCM for three different additive combinations and a neat JP-5 fuel sample. It can be readily observed that nearly an order of magnitude improvement in JP-5 fuel thermal stability is realized in this fuel by using the most effective additive package. The improvement resulting form each of the components (8Q405, BHT, and MDA) can be clearly seen. The final deposit level ($\sim$1 μg/cm^2) is about the same as that formed by JP-TS (not shown). A JP-5 sample was selected to show that the additive's effectiveness is not limited to strictly JP-8 samples. The proposed additive package was then tested in both flowing rigs (NIFTER and Phoenix) and in Engineering rigs such as the EDTST. Figure 10 shows the type of thermal stability enhancement achieved by the Betz 8Q405/BHT combination in a JP-8 fuel. In this test, which has been run with active recirculation the reduction is about two orders of magnitude. These and other tests have shown that the proposed additive package (100 mg/L 8Q405, 25 mg/L BHT, and 8 mg/L MDA) can achieve the original goal of thermal stability improvement as measured by deposit formation in thermal stability test rigs.

Fuel-materials compatibility tests were conducted with the proposed additive package. The purpose of this testing is to identify fuel system materials which may experience significant adverse interactions as a result of prolonged contact with the JP-8+100 jet fuel. This testing was performed in three distinct phases: identification of the possible materials and temperatures conditions, establishment of testing procedures, and finally, testing and comparison with baseline data. Details of the tests, materials tested and the test results are contained in Kalt (1996). To date, more than 120 materials have been tested with the proposed additive package without identifying any detrimental effects due to the additives.

Since the original identification of 8Q405/BHT as an additive, a second additive (Mobil MCP-147B) has been identified. Follow-on testing in engineering tests and materials compatibility tests have not progressed as far as the 8Q405/BHT/MDA combination. Other additive candidates are being evaluated in order to reduce additive cost through free market competition.

Engine and Flight Tests

Although extensive laboratory testing of JP-8+100 was conducted, the true validation of the fuel is obtained by testing in actual aircraft hardware. Initial combustion tests of JP-8+100 were conducted in a CFM-56 combustor rig at Wright Laboratory, WPAFB, OH. These tests showed excellent combustion behavior over a wide range of fuel to air ratios encompassing

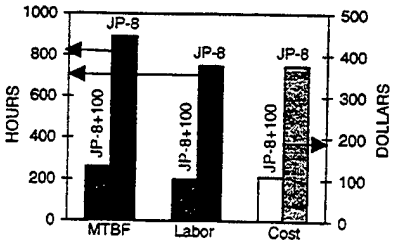

Fig. 14 Fuel system maintenance data (JP-8 versus JP-8+100) showing mean time between failure (MBTF), maintenance hours per thousand flight hours (labor), and cost per flight hour (cost)

the aircraft flight envelope. Also, the fuel was tested in a F100-PW-200 engine in a 50-h, 224 total accumulated cycles (TAC) test. The engine, prior to testing, was "dirty" with visible fouling typical of those found in the fleet. The JP-8+100 additive cleaned lightly fouled components, and improved overall engine operation by opening several small orifices such that the engine could operate at design conditions. Several other engines were tested (T63-A-700, F100-PW-200 (4000 TAC test), F100-PW-229, J69-T-25, J85-GE-5, T56-A-15, TF-34-GE-100A and in components of the F119-PW-100 engine) with similar improvements. Since these tests were successful, a flight test was conducted at Edwards AFB in Sept. 1994. An F-16 with a F100-PW-220E engine was flown for 4.4 h throughout the entire flight envelope including 28 engine restarts. This test found no problems, which cleared the fuel for use in other aircraft. Currently, field evaluations at Kingsley Field, OR and Sheppard AFB, TX are being conducted to quantify long-term benefits of JP-8+100.

An 18-mo field evaluation is being conducted with the 114FS (F-16A/B, F100-PW-200 engine) Air National Guard at Kingsley Fields, OR. The demonstration began in Nov. 1994, gradually converting 19 F-16s to JP-8+100 and continued two aircraft on JP-8 as a comparative baseline. Since dispersant/detergent additives disarm current generation filter coalescers (used to remove dirt and water from fuel), the additive was added to the fuel via a commercially available additive injector pump (after the fuel has passed through filter coalescence) as the fuel is loaded onto refueling trucks. The filter coalescers on the refueling trucks were replaced with a water-absorbing cartridge called a monitor to assure that any dirt and water that might infiltrate a truck is removed. This work can be used in any truck refueling situation, but new technology filter coalescers are required for full implementation of the additive by the Air Force. During the period Nov. 1994 to 1995, JP-8+100 increased the time between fuel-related augmentor anomalies by 340 percent, reduced fuel control change outs by 80 percent, and reduced fuel system maintenance by $268 (70 percent) per flight hour (see Fig. 14). These savings translated into a cost avoidance of over $825,000 for the guard unit.

A 1-yr field evaluation is being conducted by the 80th FTW (T-37B, J69-T-25 and T-38, J85-GE-5). Since the demonstration began in July 1995, cost reduction figures are still under evaluation; however, significant reduction in fuel nozzle (slinger) fouling in the J69 and reduction in augmentor spraybar fouling in the J85 have been observed. In addition, smoke/soot emission has been reduced. Additional 1-yr field evaluations are being conducted at Otis ANGB MA (F-15A/B, F100-PW-100), Westfield ANGB MA (OA-10, TF34-GE-100), Burlington ANGB VT (F-16C/D, F100-PW-220E), and Louisville ANGB KY (C-130H, T56-A-15). JP-8+100 is reducing fouling/coking in these aircraft.

JP-8+100 has been demonstrated to reduce fuel system fouling/coking and maintenance costs in ground support equipment. In tests of the A/M32A-60B ("Dash-60") startcarts with the 152nd RECCE Group (Air National Guard) in Reno, NV, JP-8+100 has significantly reduced fuel nozzle fouling and reduced combustor damage and burn-throughs. Savings of $1500 per startcart have been estimated. From the cost avoidance data collected so far, the Air Force could save approximately $80 million per year in reduced engine maintenance.

Summary

This paper has discussed the development of a high-thermal-stability JP-8+100 fuel which provides a 50-percent improvement in the heat sink capability over conventional JP-8 fuel. Some principle advances made during achieving this goal were:

1 New test techniques were developed that are superior to the established go/no-go JFTOT-type tests.

2 A free radical theory of thermal and oxidative stability was developed.

3 The free radical mechanism was incorporated into CFDC computer models to predict oxidation and deposition processes in jet fuels, and the new tests were validated using a thermal stability scale developed by nonparametric analysis.

4 An additive package comprising BHT (25 mg/L), MDA (8 mg/L), and Betz 8q405 (100 mg/L) was developed for JP-8 fuel. A combination of Betz 8Q405 BHT and MDA has been shown to increase the operating temperature of JP-8 jet fuels.

5 Flight testing of the proposed thermal stability additive package has successfully begun. Testing has been in progress for more than one year and shows significant maintenance cost savings. This increased operating capability has been estimated to result in a savings to the US Air Force of $80 million/yr.

In this manner, a novel high-thermal-stability jet fuel for the 21st century has been developed.

Acknowledgment

The University of Dayton's contribution to this research was supported by the US Air Force Wright Laboratories, Aero-Propulsion and Power Directorate, Fuels and Lubrications Division, Wright-Patterson Air Force Base, OH, under Contract No. F33615-92-C-2207 with Mr. Charles Frayne as the contract monitor. We recognize the large contribution of fellow researchers at the University of Dayton and Wright Laboratories as well as those at Innovative Scientific Solutions Incorporated and Pratt & Whitney. Finally, we acknowledge the support and encouragement of Dr. W. Mel Roquemore (WL/POSC) of Wright Laboratories, WPAFB, OH.

References

Anderson, S. D., Harrison III, W. E., and Roquemore, W. M., 1994, "Development of TS Additive Package for JP-8," *Proceedings of the 5th International Conference on Stability and Handling of Liquid Fuels*, Vol. 1, U.S. Department of Energy Washington DC, p. 255.

Beal, E. J., Hardy, D. R., and Burnett, J. C., 1992, "Results and Evaluation of a Jet Fuel TS Flow Rig which Employs Direct Gravimetric Analysis of both Surface and Fuel Insoluble Deposits," *Proceedings of the 4th International Conference on Stability and Handling of Liquid Fuels*, Vol. 1, U.S. Department of Energy Washington DC, pp. 245–259.

Biddle, T. B., Hamilton, E. H., and Edwards, W. H., 1994, "United Technologies Corporation R&D Status Reports to WL/POSF," Contract No. F-33615-90-C-2051, Wright Patterson Air Force Base, OH.

Brandauer, M., Schulz, A., and Wittig, S., 1995, "Mechanism of Coke Formation in Gas Turbine Combustion Chambers," ASME Paper No. 95-GT-49, accepted for publication in ASME *Journal of Engineering for Gas Turbines and Power*.

Chin, J., and Lefebvre, A. H., 1992, "Experimental Techniques for the Assessment of Fuel Thermal Stability," *Journal of Propulsion Power*, Vol. 8, pp. 3–4.

Chin, J., and Lefebvre, A. H., 1993, "Influence of Flow Conditions on Deposits from Heated Hydrocarbon Fuels," ASME *Journal of Engineering for Gas Turbines and Power*, Vol. 115, pp. 433–438.

Chin, L. P., Katta, V. R., and Heneghan, S. P., 1994, "Numerical Modeling of Jet Fuel Autoxidation in Flowing Systems," *ACS Petroleum Chemistry Preprints*, Vol. 39, pp. 19–25.

Dagget, D. L., and Veninger, A., 1994, "The Development of an Aviation Fuel Thermal Stability Test Unit," 39th International Gas Turbine and Aeroengine Congress, The Hague, The Netherlands, Paper No. 94-GT-217.

Dieterle, G. L., and Binns, K. E., 1995, "Extended Duration Thermal Stability Test of Improved Thermal Stability Jet Fuel," ASME Paper No. 95-GT-69, presented at the Turbo Expo, Houston, TX, June.

Dieterle, G. L., Binns, K. E., and Williams, T. F., 1995, "System Evaluation of Improved Thermal Stability Jet Fuels," *Proceedings of the 5th International Conference on Stability and Handling of Liquid Fuels*, Vol. 1, U.S. Department of Energy, Washington DC, p. 407.

Edwards, J. T., 1992, "Deposition During Vaporization of Jet Fuel in a Heated Tube," 30th Aerospace Sciences Meeting, Paper No. AIAA 92-0687, Reno, NV.

Grinstead, R. R., 1994, "Evaluation of JP-8+100 Additives by Isothermal Corrosion Oxidation Test and Microcarbon Residue Test," University of Dayton Technical Report, UDR-TR-94-85, Dayton, OH.

Hardy, D. R., Beal, E. J., and Burnett, J. C., 1992, "The Effect of Temperature on Jet Fuel Thermal Stability using a Flow Device which Employs Direct Gravimetric Analysis of both Surface and Fuel Insoluble Deposits," *Proceedings of the 4th International Conference on Stability and Handling of Liquid Fuels*, Vol. 1, U.S. Department of Energy Washington DC, pp. 260–271.

Harrison III, W. E., 1990, "Aircraft Thermal Management: Report of the Joint WRDC/ASD Aircraft Thermal Management Working Group," WRDC-TR-90-2021, Wright Patterson AFB OH.

Harrison III, W. E., Mongia, H. C., Heneghan, S. P., and Ballal, D. R., 1995, "Advanced Jet Fuels—JP-4 to JP-8 and Beyond," International ASME International Gas Turbine Institute Paper No. 95-GT-223.

Hazlett, R. N., 1991, *Thermal Oxidation Stability of Aviation Turbine Fuels*, American Society for Testing and Materials, Philadelphia, PA.

Heneghan, S. P., 1994, "Determining and Understanding the Global Oxidation Parameters of Jet Fuels," *ACS Petroleum Division Preprints*, Vol. 39, pp. 14–18.

Heneghan, S. P., and Kauffman, R. E., 1995, "Analytic Tests and Their Relation to Jet Fuel Thermal Stability," *Proceedings of the 5th International Conference on Stability and Handling of Liquid Fuels*, Vol. 1, U.S. Department of Energy, Washington DC, p. 29.

Heneghan, S. P., and Zabarnick, S., 1994, "Oxidation of Jet Fuels and the Formation of Deposits," *Fuel*, Vol. 73, pp. 35–43.

Heneghan, S. P., Locklear, S. L., Geiger, D. L., Anderson, S. D., and Schulz, W. D., 1993a, "Static Tests of Jet Fuel Thermal and Oxidative Stability," AIAA *Journal of Propulsion and Power*, Vol. 9, pp. 5–9.

Heneghan, S. P., Williams, T. F., Martel, C. R., and Ballal, D. R., 1993b, "Studies of Jet Fuel Thermal Stability in A Flowing System," ASME *Journal of Engineering for Gas Turbines and Power*, Vol. 115, pp. 480–484.

Jones, E. G., Balster, W. J., and Anderson, S. D., 1992, "Formation of Insolubles in Jet Fuels: Effects of Oxygen," *ACS Petroleum Chemistry Division Preprints*, Vol. 37(2), Apr., pp. 393–402.

Jones, E. G., Balster, W. J., and Post, M. E., 1995, "Degradation of a Jet-A Fuel in a Single Pass Heat Exchanger," ASME *Journal of Engineering for Gas Turbines and Power*, Vol. 117, p. 125.

Jones, E. G., Balster, W. J., and Goss, L. P., 1996a, "Application of JFA-5 as an Anti-Fouling Additive in a Jet-A Fuel," accepted for publication in *Industrial Engineering and Chemistry Research*.

Kalt, D., 1996, "Materials Compatibility Test Results," to be published as a three-volume set, University of Dayton Research Institute Tech Report.

Katta, V. R., Jones, E. G., and Roquemore, W. M., 1993, "Development of Global Chemistry Model for Jet-Fuel Thermal Stability Based on Observations from Static and Flowing Experiments," 81st AGARD Symposium on Fuels and Combustion Technology for Advanced Aircraft Engines, Collifero, Italy, AGARD-CP-536, Paper No. PEP-19.

Krazinski, J. L., Vanka, S. P., Pearce, J. A., and Roquemore, W. M., 1992, "A Computational Fluid Dynamics and Chemistry Model for Jet Fuel Thermal Stability," ASME *Journal of Engineering for Gas Turbines and Power*, Vol. 114, pp. 104–110.

Marteney, P. J., and Spadaccini, L. J., 1986, "Thermal Decomposition of Aircraft Fuel," ASME *Journal of Engineering for Gas Turbines and Power*, Vol. 108, pp. 648–654.

Morris, R. W., and Binns, K. E., "Evaluation of Improved Thermal Stability Jet Fuels in an Advanced Reduced Scale Fuel System Simulator," abstract to *5th International Conference on the Handling and Stability of Liquid Fuels*, Rotterdam, The Netherlands, p. 42.

Vilimpoc, V., Sarka, B., and Weaver, W. L., 1995, "Simultaneous Measurement Of Particle Size, Mass Rate of Deposition, and Oxygen Concentration in Thermally Stressed Jet Fuel," ASME International Mechanical Engineering Conference, San Francisco, CA.

Zabarnick, S., 1993, "Chemical Kinetic Modeling of Jet Fuel Autoxidation and Antioxidant Chemistry," *Industrial Engineering and Chemistry Research*, Vol. 115, pp. 1012–1017.

Zabarnick, S., 1994, "Studies of Jet Fuel Thermal Stability and Oxidation Using a Quartz Crystal Microbalance and Pressure Measurements," *Industrial Engineering and Chemistry Research*, Vol. 33, pp. 1348–1354.

Zabarnick, S., Zelesnik, P., and Whitacre, S. D., 1995, "Evaluation of Jet Fuel Additives Using the Quartz Crystal Microbalance and Pressure Measurements. Part II," University of Dayton Research Institute, UDR-TR-95-98.

Appendix K.

The Effects of Dissolved Oxygen Concentration, Fractional Oxygen Consumption, and Additives on JP-8 Thermal Stability

Jamie S. Ervin
Theodore F. Williams
Shawn P. Heneghan
Steven Zabarnick
University of Dayton
300 College Park
Dayton, OH 45469-0140

The Effects of Dissolved Oxygen Concentration, Fractional Oxygen Consumption, and Additives on JP-8 Thermal Stability

J. S. Ervin

T. F. Williams

S. P. Heneghan

S. Zabarnick

University of Dayton, Dayton, OH 45469-0210

Since dissolved oxygen participates in fuel deposit formation, knowledge of the effects of dissolved oxygen concentration on fuel thermal stability is critical for fuel system design. In this work, the combined effects of dissolved oxygen availability and additives on jet fuel thermal stability are studied. Experiments with JP-8 jet fuel were conducted in a three-part heat exchanger that simulated a complex thermal and flow environment. The dissolved oxygen content at the flow inlet was varied, and deposition was studied under conditions of either fractional or complete oxygen consumption. The effects of a thermal stability additive package were also studied. An intriguing result found with JP-8 fuels is an increase in deposits formed in heated regions for decreased oxygen consumption, but inverse behavior with the additive package.

Introduction

Most high-performance aircraft rely on jet fuel circulation for cooling. Unfortunately, heated fuel reacts with small concentrations of dissolved oxygen gas to form oxidized products and deposits that can block fuel lines, foul close-tolerance valves, and deteriorate sealing materials (Hazlett, 1991; Ervin et al., 1996). On certain military jets, the fuel tanks are vented to the ambient air. At high altitudes, the ambient pressure and temperature are reduced significantly, resulting in a diminished concentration of dissolved oxygen. In addition, as a fire-preventative measure, an on-board inert gas generating system (OBIGGS) may be used to reduce the oxygen level in the fuel tank ullage space and, ultimately, in the liquid fuel. A fundamental understanding of the effect of low dissolved oxygen concentration and oxygen consumption on thermal stability (thermal stability refers to the deposit forming tendency of the fuel) is essential for aircraft design.

There is a general concensus that reducing the dissolved oxygen decreases the resulting deposition (Baker et al., 1983; Taylor, 1979). This has been observed in the case of complete oxygen consumption (Zabarnick et al., 1996; Heneghan et al., 1995) for both static and flowing tests. Few studies have considered the effects of fractional oxygen consumption on deposition. In previous works (Bradley et al., 1974; Taylor, 1974, 1976; Taylor and Frankenfeld, 1978; Frankenfeld and Taylor, 1980), the effects of intermediate levels of dissolved oxygen (20 to 40 ppm, mass basis) on surface fouling were not studied in detail. This regime of available oxygen is particularly important for aircraft that make use of OBIGGS or have vented fuel tanks. Further, the flow conditions and temperature fields were not well defined. More recent works (Heneghan et al., 1995; Jones et al., 1995) have studied the formation of jet fuel deposits under conditions of complete consumption of the dissolved oxygen at relatively high temperatures. Under these conditions, the mass of deposits increased as the mass of oxygen consumed increased. In contrast, under conditions of incomplete consumption of the available oxygen, Ervin et al. (1996) in a flowing test and Zabarnick et al. (1996) in a static test have found that decreasing the oxygen availability does not necessarily result in reduced deposition. Moreover, in aircraft, high fuel flow rates often result in circumstances in which the dissolved oxygen is not completely consumed (Harrison et al., 1993).

Additives can sometimes be used in small quantities to improve the deposition characteristics of the jet fuel (Zabarnick and Grinstead, 1994). However, additives are not always effective in reducing fouling. The relationship between fuel oxidation and deposit formation is extremely complex, and the ways in which additives affect this relationship are unclear. Moreover, the effects of thermal stability additives on deposition for fuel oxygen concentrations below that of normal air saturation are unknown.

In this work, experiments were conducted using a three-part heat exchanger, which simulated a complex thermal and flow environment approaching that of an aircraft. Different dissolved oxygen concentrations at the flow inlet determined the amount of available dissolved oxygen within the bulk flow. The objectives of these experiments were:

1. To study fouling produced by JP-8 jet fuel under conditions of partial oxygen consumption.
2. To study the effect of a thermal stability additive package on deposition under conditions of partial oxygen consumption.
3. To study deposition produced by JP-8 fuel with different inlet dissolved oxygen concentrations under conditions in which the available bulk oxygen is entirely depleted.

Experimental

In the experimental apparatus described in detail in Heneghan et al. (1993) (Fig. 1), fuel at ambient temperature is pumped from a preconditioning tank into the heated sections, which are at a pressure of 2.48 MPa. At this pressure level, the fuel remains as a liquid everywhere within the system. In the preconditioning tank, nitrogen and oxygen are bubbled through the fuel to control the amount of dissolved oxygen which enters the test section. Dissolved oxygen concentrations at the inlet can be varied from the air-saturation concentration of 70 ppm to as

Contributed by the International Gas Turbine Institute and presented at the 41st International Gas Turbine and Aeroengine Congress and Exhibition, Birmingham, United Kingdom, June 10–13, 1996. Manuscript received at ASME Headquarters February 1996. Paper No. 96-GT-132. Associate Technical Editor: J. N. Shinn.

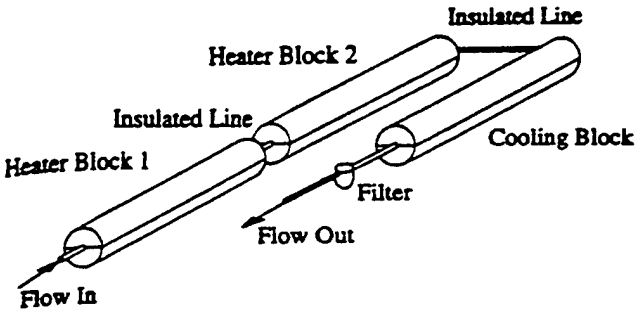

Fig. 1 Flow rig

low as 1 ppm. Bulk dissolved oxygen levels are measured online at the flow inlet and at a location within each insulated tube section by means of a Hewlett Packard 5890 Series II gas chromatograph (Rubey et al., 1992). After passing through two heated sections, the fuel flows into the cooled section, then is collected in a waste reservoir.

Two heated copper blocks (46 cm long with a 7.6 cm diameter) envelop the 316 stainless-steel tubing (180 cm long by 2.16 mm ID by 3.18 mm OD) through which the fuel passes. In the experiments performed here, the deposits remained thin (on the order of microns) and, as a result, did not appreciably affect the heat transfer or fluid motion. Thus, the temperatures were essentially steady. The tubing between the heated blocks is insulated. A third copper block (46 cm long with a 7.6 cm diameter), which has internal passages through which chilled water flows, provided cooling of the tube. Calibrated type K thermocouples (20 gage) are welded to the outer surface of the stainless-steel tubing to provide the outer tube wall temperatures with an uncertainty of ±2°C. The stainless-steel tubes (ASTM grade A269/A213) have a surface roughness (arithmetic average) of 8 to 15 μin. and are cleaned with Blue Gold alkaline solution in an ultrasonic bath, rinsed with deionized water, and dried with flowing laboratory-grade nitrogen gas prior to use.

Table 1 lists characteristics of neat F2980, F2827, and F3119, the straight-run base fuels used in this study. These Jet A fuels were acquired from different sources to avoid biasing the results. Jet A base fuels that contain compounds in the amounts (military specification MIL-T-83133) listed in Table 2 are referred to as JP-8 fuels. Table 3 lists additives that comprise the thermal stability additive package used, which is also being considered for use by the U.S. Air Force (Anderson et al., 1994). Here, JP-8 fuel containing the additive package is referred to as JP-8A.

In the present experiments, the volumetric flow rate was selected to be either 16 ml/min or 62 ml/min. The flow was laminar at the entrance of the first heated block for both flow rates, and Reynolds numbers (Re_D) based on the tube diameter and bulk temperature are listed in Table 4 for the exit of the second heated block. Steady temperature and velocity distributions within the fuel were obtained by the finite difference solution of the Navier–Stokes, turbulent energy, and enthalpy equations. Fluid motion inside the tube was assumed to be axisymmetric, and a cylindrical coordinate system was used (Katta and Roquemore, 1993). The density of the fuel changes significantly with temperature, which gives rise to considerable buoyancy force on the fuel near the tube wall. It is believed that the buoyancy forces normal to the forced flow direction increased the heat and mass transport, rendering the flow turbulent (Katta et al., 1995). Thus, turbulent simulations yielded bulk temperatures that approximated the measured values more accurately than did the laminar computations. Turbulent flow is normally encountered in the fuel systems of military aircraft.

The extent of oxidation depends on both the residence time and the temperature field. Dissolved oxygen is more readily consumed under conditions of high temperature and long residence times. Although the available dissolved oxygen is not completely consumed in aircraft fuel systems (Harrison et al., 1993), thermal stability studies of flowing jet fuel are generally performed under conditions of complete oxygen consumption (Heneghan et al., 1993; Jones et al., 1995). Thus, two categories of experiment were performed for purposes of comparison. In the first, the available dissolved oxygen was partially consumed. In the second, it was entirely depleted. For the first category, a block temperature of 270°C and a volumetric flow rate of 62 ml/min were used since these conditions resulted in little oxidation. The partial oxidation tests were conducted in 24 hour periods to obtain sufficient accumulation of deposits. In experiments performed with fractional oxygen consumption, both JP-8 and JP-8A fuel were used. In the experiments in which the dissolved oxygen was entirely consumed, the flow rate was 16 ml/min, the block temperature was either 300°C or 270°C, and the test period was six hours. In addition, JP-8 fuel alone was used. The dissolved oxygen concentrations provided at the flow rig inlet for all experiments are listed in Table 4. (The nominal dissolved oxygen concentration for air-saturated fuels here is 70 ppm; 30 ppm is representative of conditions that may be produced by an OBIGGS.)

At the termination of an experiment, the tubes were removed from the system, drained, and rinsed with hexane. They were then dried by flowing filtered nitrogen gas through them. Finally, they were sliced into 50 mm segments and heated in a vacuum oven at 120°C for one hour. Since the deposits are comprised largely of carbon, carbon measurements provide an indication of the axially distributed mass of deposits. A Leco (RC-412) multiphase carbon analyzer determined the mass of carbon in each tube segment; the reproducibility in the determination of the carbon mass is on the order of ±5 percent, determined by sequential tests performed within one week using fuel from the same batch.

Results and Discussion

In subsequent figures, the mass of carbon obtained from carbon burnoff measurements is ratioed by the inner surface area of the tube. The wall temperature distribution, given by polyno-

Nomenclature

$A^\cdot$ = antioxidant radical
AH = antioxidant species
$AO_2^\cdot$ = antioxidant peroxy radical
ASTM = American Society for Testing and Materials
BHT = butylated-hydroxy-toluene
D = tube diameter, m
FXXXX = U.S. Air Force naming scheme for neat Jet A fuels
JP-8A = JP-8 with BHT, MDA, and 8Q405
JP-8 = Jet A fuel with additives given by military specification MIL-T-83133
MDA = proprietary metal deactivator
OBIGGS = on-board inert gas generation system
O_2 = dissolved oxygen
PH = phenol molecule
$R^\cdot$ = hydrocarbon alkyl radical species
Re_D = Reynolds number = VD/ν
$RO_2^\cdot$ = peroxy radical
RH = hydrocarbon compound representing bulk fuel
RO_2H = hydroperoxide
V = mean velocity, m/s
8Q405 = Betz Corporation proprietary dispersant
ν = kinematic viscosity, m^2/s

Table 1 Neat fuel properties

fuel (Jet A)	sulfur mass %	aromatics volume %	JFTOT breakpoint (C)
F2980	0.1	17.0	288
F3119	0.1	18.0	285
F2827	<0.05	19.0	282

mial fits of the measured values, and the computed bulk temperature distribution are provided for reference. As the test section is horizontal, Taylor instabilities (Katta et al., 1995) yield an essentially turbulent flow at a flow rate of 16 ml/min. At 62 ml/min, the buoyancy force is less significant, and the flow undergoes a reverse transition to laminar flow (Katta et al., 1995). The complex dynamics of the flow at 62 ml/min are believed to be highly three dimensional and, hence, were not captured by the numerical simulation since the mathematical formulation was based on the assumption that the flow is axisymmetric. Thus, the bulk temperatures computed for 16 ml/min agree well with the measured values, but those computed for 62 ml/min lie above the measured temperatures within the heated sections and are used to show qualitative trends. As the fuel passes through the cooling block at 62 ml/min, the flow becomes more turbulent, and the computed and measured bulk temperatures become closer in agreement.

Partial Consumption of Dissolved Oxygen. In Fig. 2, the surface density of carbon deposited on the inner surface of the tube is expressed as a function of the axial distance through the two heated tube segments and the cooling block. Figure 2 shows three peaks, labeled A, B, and C, in the carbon deposit profiles obtained for both (F2980) JP-8 and JP-8A fuels under conditions of partial consumption of the bulk oxygen. Within the unheated segment between *A* and *B*, the deposition declines as the wall temperature decreases. Deposition then increases near 50 cm as the wall temperature approaches 270°C. Between *B* and *C*, near 100 cm, another decline occurs in the deposition profiles due to the fuel entering the unheated tube segment between the second heated block and the cooled block. Although the measured bulk temperature (200°C) at 100 cm is greater than that (160°C) at 50 cm, the deposition still falls to low levels. Figure 2 shows that the deposition in heated sections more closely follows the wall temperature than the bulk fuel temperature. The dependence of the deposition on wall temperature within heated sections was also observed in experiments with F2827 (Fig. 3) and F3119 (not shown). This dependence is plausible because in heated regions the stainless-steel wall is the location of maximum radial temperature and, thus, fuel oxidation rate. In addition, the wall is the location of minimum velocity and greater residence time than at the center of the tube. Further, the stainless-steel may be responsible for potential catalytic activity, such as the decomposition of hydroperoxides formed in the fuel autoxidation process.

At location C of Fig. 2, the wall temperature is a minimum, yet the level of deposition for JP-8 (and JP-8A) is of the same order as that at *A* and *B* where the temperature is greater. Increased deposition in cooled regions downstream of heated sections has been previously observed (Heneghan et al., 1995). The deposition mechanisms within the cooled tube are believed to be different from those in heated locations for several reasons. Chemical differences between fouling with JP-8 in the heated and cooled sections have been measured by means of X-ray photoelectron spectroscopy, and morphological differences have been detected by scanning electron microscopy (Ervin et al., 1996). Furthermore, the oxygen consumption within the cooled tube was immeasurably small, in contrast to that measured in the heated sections (Tables 5 and 6), which contain locations *A* and *B*. Lastly, experiments (Ervin et al., 1996) have shown that significantly more deposits are formed in the cooled section with higher cooling rates. Thus, deposits are believed to accumulate within the cooled section as a result of oxidized fuel products becoming less soluble at lower temperatures. The formation of deposits in cooled regions has particular import to the development of recirculating fuel systems. Recirculation systems will use ram air heat exchangers to cool the fuel prior to returning it to the fuel tanks. These heat exchangers would

Table 2 Properties of JP-8 additives

additive name	additive classification	type of compound	concn (mg/L)
DiEGME	icing inhibitor	diethylene-glycol -monomethyl-ether	25
DuPont Stadis 450	static dissipator	proprietary	2
DCI-4A	corrosion inhibitor/ lubricity enhancer	proprietary	9

Table 3 Properties of thermal stability additives

additive name	additive classification	type of compound	concn (mg/L)
BHT	antioxidant	butylated-hydroxy-toluene	25
8Q405	detergent-dispersant	proprietary	100
MDA	metal deactivator	N,N'-disalicylidene-1,2-propanediamine	2

Table 4 Experiments performed

JP-8 fuel	thermal stability additives	flow rate (ml/min)	testing period (hrs)	heated block temp. (C)	inlet O_2 concn. (ppm)	Re_D exit heated block 2
partial O_2 consumption						
F2980	no	62	24	270	70,30, 6.1	2500
F2980	yes	62	24	270	70,30	2500
F2827	no	62	24	270	70,30	2500
F2827	yes	62	24	270	70,30	2500
F3119	no	62	24	270	70,30	2500
F3119	yes	62	24	270	70,30	2500
complete O_2 consumption						
F3119	no	16	6	300	70,30, 19	950
F3119	no	16	6	270	70,30, 19	850

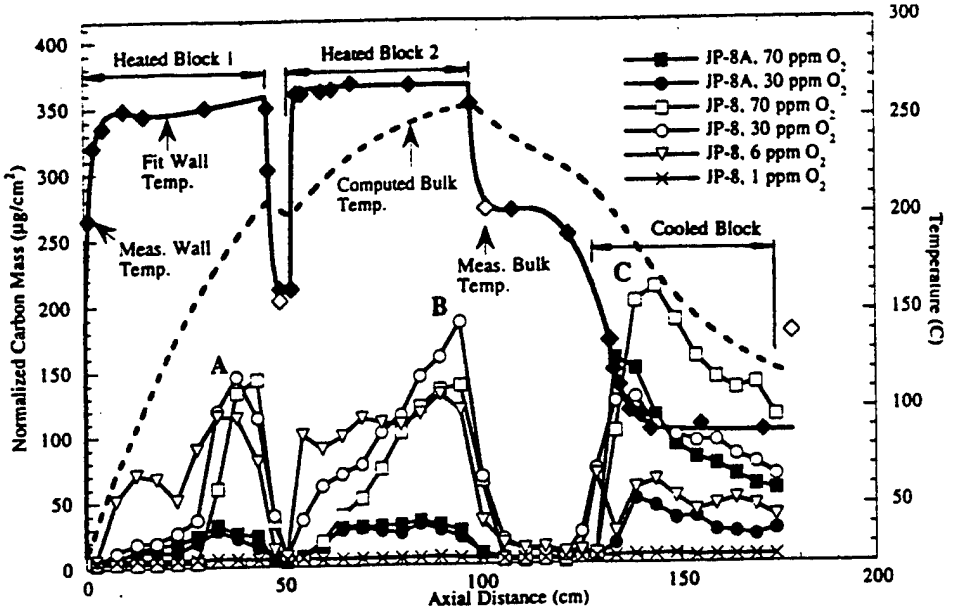

Fig. 2 Tube deposit and temperature profiles: partial O_2 consumption for fuel F2980, 62 ml/min, and 24 h

likely collect deposits similar to those found here in the cooled tube.

Figure 2 shows that the deposit profiles formed from JP-8 fuel are influenced by the inlet dissolved oxygen concentration. At locations *A* and *B*, the measured deposition for JP-8 fuel is greater for a dissolved oxygen concentration of 30 ppm than that obtained with air-saturated fuel. Similarly, greater deposition was observed with a dissolved oxygen concentration of 30 ppm rather than with 70 ppm for both F2827 (Fig. 3) and F3119 (not shown). Figure 2 shows that at a dissolved oxygen concentration of six ppm, the JP-8 fuel deposits at locations *A* and *B* are even greater than those that occur with higher dissolved oxygen concentrations and occur earlier in the tube. In Fig. 2, when the dissolved inlet oxygen is further lowered to 1 ppm, there is little deposition. Likewise, Tables 5 and 6 show that, with decreasing inlet oxygen concentrations for JP-8 (F2980 and F2827), the total mass of deposits formed in the heated sections approaches a maximum and then falls with lower oxygen concentrations.

The JP-8 deposit profiles of F2980 (Fig. 2), F2827 (Fig. 3), and F3119 (not shown) in the first heated section (between 0 and 49 cm) for dissolved oxygen concentrations less than 70 ppm rise above background levels near the tube entrance, well upstream of that for air-saturated conditions. In this region of the tube, as the initially thin thermal boundary layer develops near the heated wall, the radial temperature gradient is large at the wall but decreases with increasing axial distance. In the second heated section (between 55 and 99 cm) following the insulated tube, the thermal boundary layer again develops. The deposit profiles for initial dissolved oxygen concentrations below 70 ppm again rise at locations upstream of the point where the deposit profile for initially air-saturated fuel rises. In a flow-

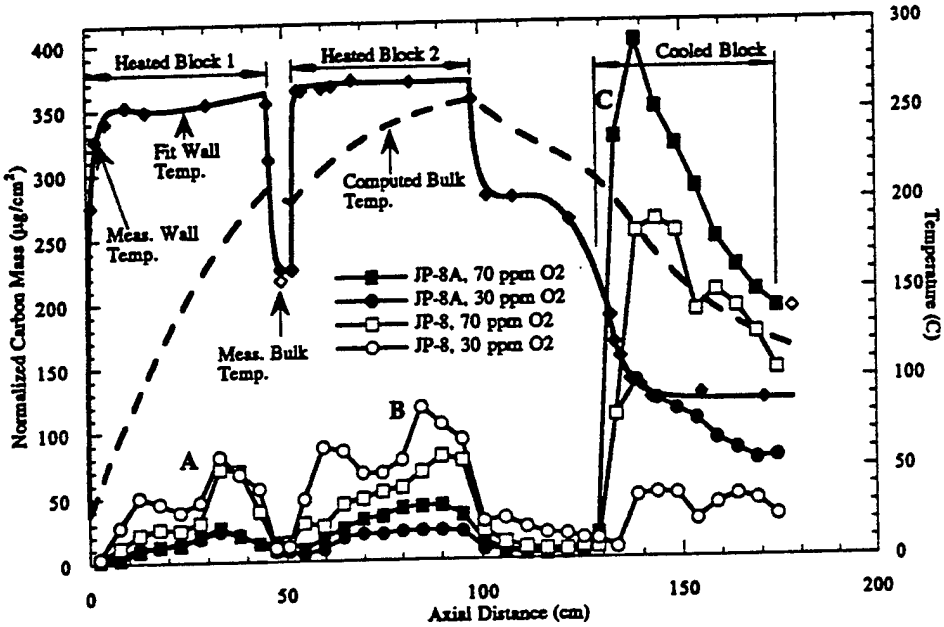

Fig. 3 Tube deposit and temperature profiles: partial O_2 consumption for fuel F2827, 62 ml/min, and 24 h

Table 5 Carbon deposits and consumed dissolved O_2 for partial consumption conditions and fuel F2980

inlet O_2 concn. (ppm)	O_2 consumed heated block 1 (ppm)	O_2 consumed heated block 2 (ppm)	total O_2 consumed (ppm)	deposits-heated blocks (μg)	deposits-cooled block (μg)
JP-8					
70	5	11	16	4057	4774
30	4	6	10	5800	2976
6	1	3	4	6007	1400
1	0.7	0.3	1	482	183
JP-8A					
70	5	6	11	1366	2909
30	5	6	11	1177	923

ing system, the oxygen consumption is controlled by both the kinetics of oxidation and the species transport. The fuel near the wall is heated at a faster rate and for a greater residence time than fuel passing through the center of the tube. In experiments using a quartz crystal microbalance, Zabarnick et al. (1996) observed an increasing fuel oxidation rate occurring at low dissolved oxygen concentrations. However, this observation is not consistent with the consumed oxygen values given in Tables 5 and 6.

At location *C* of Fig. 2, deposition for the JP-8 fuel is greatest for the inlet oxygen concentration of 70 ppm. Lower inlet levels of dissolved oxygen resulted in lower levels of deposits in the cooled tube (between 95 cm and the exit). The relationship between inlet oxygen concentration and the mass of deposits formed in the cooled section is quite different from that in the heated sections; that is, the deposition in the cooled section declines with decreasing inlet oxygen concentrations. Similar trends in deposition for JP-8 without additives are also observed for F-2827 (Fig. 3) and F-3119 (not shown). In addition, these observations support the previously described concept of a mechanism different from that of the heated sections, acting in the cooled section.

Additives and Partial Consumption of Dissolved Oxygen. Figure 2 shows deposit distributions resulting from stressed JP-8A (F-2980). Within the heated sections, the magnitude of deposit accumulation is significantly reduced in comparison to that formed from JP-8 for all inlet dissolved oxygen concentrations. Further, the level of deposition in the heated sections resulting from JP-8A now seems to follow the inlet oxygen concentration. Similar results were obtained with F2827 (Fig. 3) and F3119 (not shown). In addition as the inlet dissolved oxygen concentrations increased, Figs. 2 and 3 show that JP-8A, like JP-8, yielded more deposits in the cooled tube. In contrast to the deposition behavior of the JP-8 fuels described previously, Figs. 2 and 3 show that the deposit profiles of the JP-8A fuels rise above background levels at the entrance of the first and second heated blocks at nearly the same location, regardless of inlet dissolved oxygen concentration. Previous work (Zabarnick and Grinstead, 1994) has demonstrated that the additive package can significantly delay the oxidation process.

The addition of thermal stability additives complicates the understanding of the relation between deposition and oxidation for JP-8A because the thermal stability additives can change the chemical mechanisms of deposit formation. For example, Table 5 for fuel F2980 shows that for an inlet dissolved oxygen concentration of 30 ppm, JP-8 and JP-8A consumed similar amounts of oxygen. However, JP-8A formed significantly less deposits. These trends in oxidation and deposition were also found with F3119. Although (F2827) JP-8 and JP-8A consumed nearly the same mass of oxygen for each inlet dissolved oxygen concentration (Table 6), JP-8A formed more deposits in the cooled section than did JP-8. Thus, the thermal stability additive package affected deposition in the cooled tube with F2827 differently from that observed with F2890 and F3119.

Complete Consumption of Dissolved Oxygen. In military aircraft, jet fuel is recirculated through the fuel system and exposed to a variety of temperatures. These temperatures change continuously during a mission while the aircraft manuevers. Thus, an understanding of the effect of temperature on jet fuel thermal stability is essential to the design of jet fuels systems. In experiments performed under conditions of complete consumption of the bulk dissolved oxygen, the heated block temperature was varied while monitoring deposition and oxidation.

Figures 4(*a*) and 4(*b*) show deposition profiles for JP-8 fuel (F3119) resulting from different heated block temperatures, and the measured tube wall temperatures and computed bulk temperatures are given for reference. Within the heated or insulated tube, the deposition may fall to very low levels for two reasons. The first is that the dissolved oxygen is fully consumed and, thus, there is no more fuel oxidation. The second reason is that the temperature is low, and oxidation proceeds at a very slow rate (as shown in Figs. 2 and 3 between locations *A* and *B*). In Fig. 4(*a*), at a nominal block temperature of 300°C, the oxygen is fully consumed within the first heated block (Table 7). Thus, there is little deposition in the insulated tube and the second heated block. In the first heated block, deposition and oxidation follow each other except near the entrance of the first heated block (before 10 cm), where an inlet dissolved oxygen concentration of 19 ppm produces the greatest mass of deposits. In the cooled block there is little deposition. Figure 4(*b*) shows that a dissolved oxygen concentration of 19 ppm, the lowest level of dissolved oxygen, results in the greatest mass of deposits within the first heated section for block temperatures of 270°C. Interestingly, the dissolved oxygen is completely consumed within the first heated block for oxygen concentrations of 70 and 30 ppm. However, for an inlet dissolved oxygen concentration of 19 ppm, the bulk dissolved oxygen is not entirely consumed there (Table 7). Thus, Fig. 4 shows that even under conditions of partial oxygen consumption, greater deposition may occur with dissolved oxygen concentrations below that of normal air saturation. Similar to the fouling observed under conditions of partial oxygen consumption (Figs. 2 and 3), there are now obvious peaks in the deposition occurring in

Table 6 Carbon deposits and consumed dissolved O_2 for partial consumption conditions and fuel F2827

inlet O_2 concn. (ppm)	O_2 consumed heated block 1 (ppm)	O_2 consumed heated block 2 (ppm)	total O_2 consumed (ppm)	deposits-heated blocks (μg)	deposits-cooled block (μg)
JP-8					
70	4	7	11	2986	6179
30	1	5	6	5727	2407
JP-8A					
70	5	6	11	1357	8827
30	3	5	8	976	3161

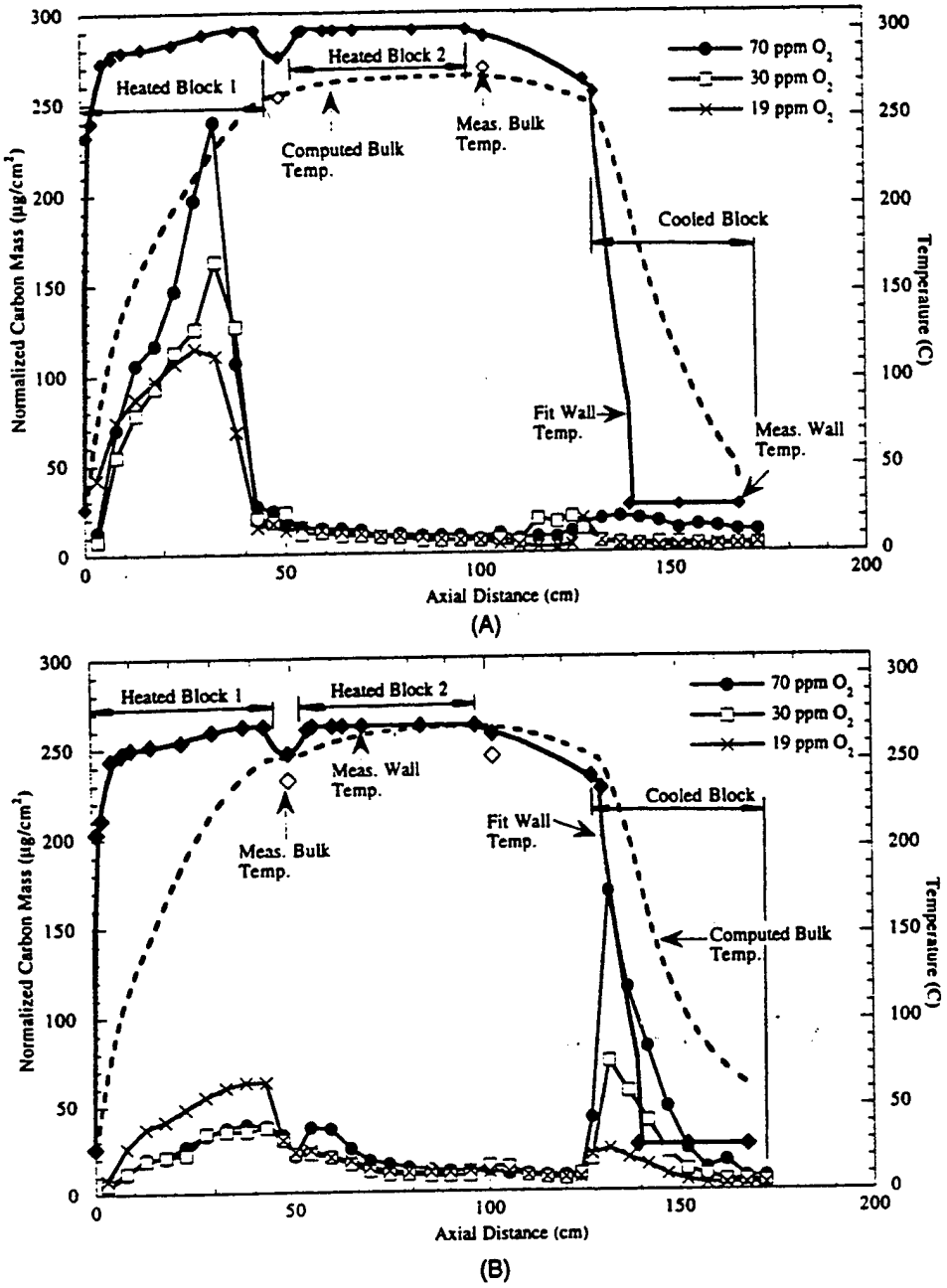

Fig. 4 Tube deposit and temperature profiles for complete O_2 consumption, JP-8 (F3119), and 16 ml/min: (*A*) 300°C block temperature; (*B*) 270°C block temperature

the cooled tube, and these peaks follow the inlet dissolved oxygen concentration.

Figure 4 shows that the heated block temperature affects the kind of oxidation products that are produced. The dissolved oxygen is consumed at a greater rate at the heated block temperature of 300°C than at the heated block temperature of 270°C. For example, Table 7 with 19 ppm dissolved oxygen and a block temperature of 300°C shows all dissolved oxygen is consumed within the first heated block. However at 270°C, 9 ppm is consumed within the second block. Although Table 7 does not show differences in oxidation rates between 270 and 300°C for the other dissolved oxygen concentrations, Heneghan et al. (1995) have observed that under conditions of complete oxygen consumption, greater temperatures result in greater rates of oxygen consumption. Furthermore, fewer solubles that deposit in cooled regions (Ervin et al., 1996) are produced with relatively high block temperatures. This has been observed previously (Heneghan et al., 1995) under conditions of complete oxygen consumption and different heated block temperatures.

An intriguing result found with JP-8 fuel is that increases in deposits in the heated sections may coincide with decreased oxygen consumption (Figs. 2–4). This observation is seemingly contrary to nearly all prior observations concerning the relation between deposit formation and oxygen consumption (Heneghan et al., 1995; Jones et al., 1995). Further, it conflicts with theories concerning the formation of deposits (Heneghan and Zabarnick, 1994; Hazlett, 1991). The mechanism proposed by Heneghan and Zabarnick (1994) for the autoxidation and antioxidant chemistry of jet fuels is:

Initiation Production of $R^{\cdot}$ (1)

Propagation $R^{\cdot} + O_2 \rightarrow RO_2^{\cdot}$ (2)

Table 7 Carbon deposits and dissolved O_2 consumption for complete consumption conditions, JP-8 (F3119)

inlet O_2 concn. (ppm)	O_2 consumed heated block 1 (ppm)	O_2 consumed heated block 2 (ppm)	total O_2 consumed (ppm)	deposits-heated blocks (μg)	deposits-cooled block (μg)
300 C					
70	70	0	70	3893	482
30	30	0	30	2974	139
19	19	0	19	2792	124
270 C					
70	70	0	70	1420	1673
30	30	0	30	1163	795
19	10	9	19	1837	302

$$RO_2^{\cdot} + RH \rightarrow RO_2H + R^{\cdot} \quad (3)$$

Termination $RO_2^{\cdot} + RO_2^{\cdot} \rightarrow$ Termination Products (4)

Transfer $RO_2^{\cdot} + AH \rightarrow RO_2H + A^{\cdot}$ (5)

$$AO_2^{\cdot} + RH \rightarrow AO_2H + R^{\cdot} \quad (6)$$

$$A^{\cdot} + O_2 \rightarrow AO_2^{\cdot} \quad (7)$$

$$AO_2^{\cdot} + AH \rightarrow AO_2H + A^{\cdot} \quad (8)$$

Deposition $AO_2^{\cdot} + AO_2^{\cdot} \rightarrow$ Deposit (9)

This mechanism is reconsidered in an attempt to explain the behavior observed here. Jet fuels are composed of hundreds of compounds. Thus, it is impractical to model the chemical changes of all components in the mixture. Here, the bulk fuel is modeled as a single hydrocarbon compound, *RH*. AH represents an antioxidant species, $R^{\cdot}$ is a hydrocarbon alkyl radical species, RO_2H is a hydroperoxide. O_2 represents the dissolved oxygen present in the fuel. In addition, $RO_2\cdot$ is a peroxy radical, $A\cdot$ is an antioxidant radical, and $AO_2\cdot$ is an antioxidant peroxy radical. The first four reactions constitute a simplified autoxidation mechanism for hydrocarbons in the liquid phase, and the remaining reactions include the chemistry of an antioxidant molecule. Reaction (9) is responsible for the production of insoluble deposits. From the results of the current work, it is desirable for a mechanism to account for increases in deposits in heated sections that occur with decreased oxygen consumption. It should also account for the presence of soluble deposits which form in cooled regions. Hence, reactions (6)–(9) are replaced with the following reactions:

Equilibrium $A^{\cdot} + O_2 \leftrightarrow AO_2^{\cdot} \rightarrow$ Soluble Products (6′)

Deposition $A^{\cdot} + PH \rightarrow$ Deposit (7′)

Thus, it is proposed that reaction (6′) is an equilibrium reaction that leads to soluble products, and a competiting reaction, (7′), leads to the formation of deposits in the heated regions. *PH* represents an unidentified molecule, but may be a phenol as Heneghan and Kauffman (1994) have shown a strong correlation between the formation of deposits in jet fuels and the presence of phenols. The equilibrium in reaction (6′) would be shifted to the right under large initial O_2 concentrations resulting in decreased deposits for each oxygen molecule consumed as shown in the heated regions of Figs. 2 and 3 and by Zabarnick et al. (1996). In addition, the equilibrium would be shifted to the left at high temperatures, causing increased deposition with temperature, a well-established trend (Hazlett, 1991). In future work, detailed computational kinetic modeling will be performed to verify the predicted behavior and establish values for the equilibrium constant in reaction (6′).

Conclusions

An understanding of the effect of the dissolved oxygen concentration on thermal stability is essential for the design of jet fuel systems. For this purpose, the dissolved oxygen concentration within the fuel at the inlet of a flowing system was varied. It was found that with JP-8 fuel under conditions of either partial or complete dissolved oxygen consumption there may be an increase in deposition for decreased inlet dissolved oxygen concentration. In addition, it was found that the thermal stability additive package improved the deposition characteristics of JP-8 fuel in the heated tube, but not necessarily in the cooled tube. From the results of this work, the following conclusions may be drawn:

- Deposit formation can be significantly affected by the upstream availability of the dissolved oxygen. Under certain conditions, more deposits can be produced with less dissolved oxygen. This is important for fuel system devices such as OBIGGS.
- Global chemistry models used in computational fluid dynamics computer codes to simulate jet fuel fouling do not presently account for the effects of dissolved oxygen availability observed here. A better understanding of the underlying chemical kinetics is needed for improved numerical simulation.
- Thermal stability tests are often conducted under conditions of high temperature and long residence time such that the influence of bulk dissolved oxygen availability on deposition is not observed. Thus, the testing of jet fuel thermal stability should be performed over a range of dissolved oxygen concentrations, residence times, and temperatures.

Acknowledgments

This work was supported by the U.S. Air Force, Fuels and Lubrication Division, Aero Propulsion and Power Directorate, Wright Laboratory, WPAFB, under Contract No. F33615-92-C-2207 (Technical Monitor: C. W. Frayne).

References

Anderson, S., Harrison, W., III, and Roquemore, W., 1994, "Development of Thermal Stability Additive Package for JP-8," *Proc. Fifth International Conference on the Handling and Stability of Liquid Fuels*, Rotterdam, Netherlands.

Baker, C. E., Bittker, D. A., Cohen, S. M. and Seng, G. T., 1983, NASA Tech Memorandum 83420.

Bradley, R., Bankhead, R., and Bucher, W., 1974, *High Temperature Hydrocarbon Fuels Research in an Advanced Aircraft Fuel System Simulator on Fuel AFFB-14-70* (AFAPL-TR-73-95), Air Force Aero Propulsion Laboratory, Wright-Patterson Air Force Base, Ohio.

Ervin, J. S., Heneghan, S. P., Martel, C. R., and Williams, T. F., 1996, "Surface Effects on Deposits From Jet Fuels," ASME JOURNAL OF ENGINEERING FOR GAS TURBINES AND POWER, Vol. 118, pp. 278–285.

Frankenfeld, J., and Taylor, W., 1980, "Deposit Formation From Deoxygenated Hydrocarbons. 4. Studies in Pure Compound Systems," *Ind. Eng. Chem. Prod. Res. Dev.*, Vol. 19, p. 65.

Harrison, W., Binns, K., Anderson, S., and Morris, R., 1993, "High Heat Sink Fuels for Improved Aircraft Thermal Management," SAE Paper No. 11E525.

Hazlett, R., 1991, *Thermal Oxidation Stability of Aviation Turbine Fuels*, American Society for Testing and Materials, Philadelphia, PA.

Heneghan, S., Martel, C., Williams, T., and Ballal, D., 1993, "Studies of Jet Fuel Thermal Stability in a Flowing System," ASME JOURNAL OF ENGINEERING FOR GAS TURBINES AND POWER, Vol. 115, p. 480.

Heneghan, S. P., and Zabarnick, S., 1994, "Oxidation of Jet Fuels and the Formation of Deposits," *Fuel*, Vol. 73, p. 35.

Heneghan, S. P., and Kauffman, R. E., 1994, "Analytic Tests and Their Relation to Jet Fuel Thermal Stability," *Proc. Fifth International Conference on the Stability and Handling of Liquid Fuels*, Rotterdam, Netherlands.

Heneghan, S., Martel, C., Williams, T., and Ballal, D., 1995, "Effects of Oxygen and Additives on the Thermal Stability of Jet Fuels," ASME JOURNAL OF ENGINEERING FOR GAS TURBINES AND POWER, Vol. 117, p. 120.

Jones, E. G., Balster, W. J., and Post, M. E., 1995, "Degradation of a Jet-A Fuel in a Single Pass Heat Exchanger," ASME JOURNAL OF ENGINEERING FOR GAS TURBINES AND POWER, Vol. 117, p. 125.

Katta, V. R., and Roquemore, W. M., 1993, "Numerical Method for Simulating Fluid Dynamic and Heat Transfer Changes in Jet Engine Injector Feed-Arm Due to Fouling," *J. of Thermophysics and Heat Transfer*, Vol. 7, p. 651.

Katta, V. R., Blust, J., Williams, T. F., and Martel, C. R., 1995, "Role of Buoyancy in Fuel-Thermal Stability Studies," *J. of Thermophysics and Heat Transfer*, Vol. 9, p. 159.

Rubey, W., Striebich, R., Anderson, S., Tissandier, M., and Tirey, D., 1992, "In Line Gas Chromatographic Measurement of Trace Oxygen and Other Dissolved Gases in Flowing High Pressure Thermally Stressed Jet Fuel," *Symposium on Structure of Jet Fuels III*, American Chemical Society, Div. Petr. Chem., San Francisco, California.

Taylor, W., 1974, "Deposit Formation from Deoxygenated Hydrocarbons. I. General Features," *Ind. Eng. Chem. Prod. Res. Dev.*, Vol. 13, p. 133.

Taylor, W., 1976, "Deposit Formation From Deoxygenated Hydrocarbons. II. Effect of Trace Sulfur Compounds," *Ind. Eng. Chem. Prod. Res. Dev.*, Vol. 15, p. 64.

Taylor, W., and Frankenfeld, J., 1978, "Deposit Formation From Deoxygenated Hydrocarbons. 3. Effects of Trace Nitrogen and Oxygen Compounds," *Ind. Eng. Chem. Prod. Res. Dev.*, Vol. 17, p. 87.

Taylor, W. F., 1979, "Jet Fuel Thermal Stability," NASA TM-79231.

Zabarnick, S., and Grinstead, R., 1994, "Studies of Jet Fuel Additives Using the Quartz Crystal Microbalance and Pressure Monitoring at 140°C," *Ind. Eng. Chem. Res.*, Vol. 33, p. 2771.

Zabarnick, S., Zelesnik, P., and Grinstead, R., 1996, "Jet Fuel Deposition and Oxidation: Dilution, Materials, Oxygen, and Temperature Effects," ASME JOURNAL OF ENGINEERING FOR GAS TURBINES AND POWER, Vol. 118, pp. 271–277.

Appendix L.

The Effects of Different Compounds on Jet Fuel Oxidation and Deposition

Robert E. Kauffman
University of Dayton
300 College Park
Dayton, OH 45469-0140

The Effects of Different Sulfur Compounds on Jet Fuel Oxidation and Deposition

R. E. Kauffman
University of Dayton Research Institute,
Dayton, OH 45469-0161

This paper presents research that supports a proposed fuel oxidation/deposition mechanism involving acid:base reactions between "oxidizable" sulfur compounds, "basic" nitrogen compounds, and oxygen-containing polymers. The reported research presents experiments that study the effects of different sulfur compounds on the high-temperature (160–220°C) oxidation products and deposition tendencies of jet fuel. Surface analyses incorporating elemental analyses and depth profiles of deposits formed on steel surfaces were performed to identify the species involved in the initial stages of deposition by jet fuels. Experiments to study the effects of acid neutralizing compounds on the deposition tendencies of jet fuels are also presented.

Introduction

Future engine designs will utilize fuel recirculation due to higher operating temperatures and improved fuel efficiency. Fuel recirculation and higher operating temperatures will require fuels (1) to operate at higher temperatures, (2) to operate for longer periods of time at elevated temperatures in the presence of dissolved oxygen, and (3) to undergo numerous heating and cooling cycles prior to combustion. These increased fuel requirements will result in increased fuel deposition at heated surfaces and increased bulk particles causing valves to stick and filters to clog. Although hydrotreating and other fuel treatments can be employed to reduce deposition at higher temperatures, hydrotreating is expensive and may result in reduced stability toward dissolved oxygen, allowing fuel to oxidize during recirculation, leading to gum formation on valves and filters.

Therefore, a multidirectional research program is being sponsored by the U.S. Air Force to develop additive packages capable of increasing the upper temperature limits of straight-run jet engine fuels by 100°F and capable of stabilizing the fuel against oxidation and bulk particle formation during recirculation. One of the goals of the research program is to gain a better understanding of the fuel reaction mechanisms, which produce the compounds responsible for the surface deposits and bulk particles. Additive packages can then be designed to inhibit or alter the specific reactions that produce the surface deposits and bulk particle precursors.

It is well known that dissolved oxygen must be present for deposition to occur and that fuel deposits contain concentrated levels of sulfur and nitrogen in comparison to the heated fuel. It has also been reported that phenol-containing compounds present in jet fuel inhibit fuel oxidation at elevated temperatures (Kauffman, 1994) and increase the deposition tendencies of jet fuels (Hazlett et al., 1986). Further research in our laboratory (Heneghan and Harris, 1992; Heneghan et al., 1992; Kauffman, 1992) has shown that straight-run (>500 ppm S) and hydrotreated (<10 ppm S) fuels oxidize at different rates (hydrotreated fuels oxidize faster) at elevated temperatures to produce different type soluble and insoluble compounds. The straight-run fuels produce phenols and bulk particles containing concentrated (~2–4 percent) levels of sulfur and nitrogen. The hydrotreated fuels produce soluble hydroperoxides, organic acids, and bulk particles with minimal levels (<0.2 percent) of sulfur and nitrogen. The bulk particles contain single carbon-to-oxygen bonds (ether type) for the straight-run fuels and contain both single and double carbon-to-oxygen bonds (carbonyl type) for the hydrotreated fuels.

Therefore, the reaction mechanism shown in Fig. 1 was proposed to explain the oxidation and deposition processes of hydrotreated and straight-run jet fuels.

Hydrotreated fuels that contain minimal levels of sulfur oxidize as detailed in reactions O1 through O4. Straight-run fuels that contain significant levels of sulfur oxidize as detailed in reactions O1 through O4, then deposit as detailed in reactions D1 through D5.

The proposed oxidation/deposition mechanism explains the need for oxygen to form deposits and explains the sulfur, nitrogen, and oxygen contents of deposits. The mechanism also explains the reported results (Hazlett et al., 1986) that phenols increase the tendency of fuels to form deposits. The proposed mechanism also predicts that the addition of sulfur compounds to hydrotreated fuels will decrease the hydroperoxide content and increase the phenol content of oxidized sulfur containing hydrotreated fuels. The sulfur-contaminated hydrotreated fuel should produce sulfur–nitrogen-containing bulk particles and deposits in which the sulfur compound is oxidized and should produce metal surface deposits that contain concentrated levels of the oxidized sulfur compounds. Also, the addition of sulfonic acids would be expected to increase deposits with minimal oxidation, as recently reported (Hazlett et al., 1991).

To evaluate the accuracy of the proposed oxidation/deposition mechanism, various sulfur compounds were dissolved in a hydrotreated jet fuel (Jet A-1). The neat Jet A-1 fuel, sulfur-contaminated Jet A-1 fuels, and a commercial straight-run fuel (Jet A) were heated in two different oxidation tests to determine the effects of the different sulfur compounds on fuel chemistry: soluble oxidation products (hydroperoxides versus phenols), bulk particles (S, N content of particulates), and initial deposits formed on steel wire surfaces (sulfur oxide content near metal surface). In an attempt to inhibit the deposition process of Jet A, various compounds with acid neutralizing capabilities were added to the Jet A fuel prior to oxidation to inhibit deposition reactions D3 and D5, which require acid/base reactions and acidic attack on metal surfaces, respectively. The results are reported herein.

Experimental

Sulfur Compounds. The sulfur compounds used in this study were 92–98 percent pure and were obtained from Aldrich

Contributed by the International Gas Turbine Institute and presented at the 40th International Gas Turbine and Aeroengine Congress and Exhibition, Houston, Texas, June 5–8, 1995. Manuscript received by the International Gas Turbine Institute February 27, 1995. Paper No. 95-GT-222. Associate Technical Editor: C. J. Russo.

Oxidation Process

Fuel + O_2 → Fuel Radical + • O_2H (O1)

Fuel Radical + O_2 → Hydroperoxide Radical (O2)

Hydroperoxide Radical + Fuel → Hydroperoxide + Fuel Radical (O3)

Hydroperoxide → Aldehydes, Organic Acids, → Polymers (O4)

Deposition Process

Hydroperoxide + Sulfur Compound → Phenol + Acidic Sulfur Oxide + Ketone (D1)

Phenol + Hydroperoxide Radical → Phenol Radicals + Hydroperoxide (D2)

Acidic Sulfur Oxide + Basic Nitrogen Compounds →S•N Compound (D3)

S•N Compound + Phenol Radicals → Bulk Particles (D4)

Acidic Sulfur Oxide + Metal Surface → Initial Deposition (D5)

Initial Deposition + Bulk Particles → Surface Deposition (D6)

Fig. 1 Proposed reaction mechanism for jet fuel oxidation and deposition processes

Chemical Company, Milwaukee, WI. The dodecylbenzene sulfonic acid (90+ percent purity) was obtained from Conoco Petroleum, Conostan Standards Div., Hammond, IN.

Fuels. The jet fuels used in this study were a straight-run, commercial fuel (Jet A) and a hydrotreated, commercial fuel (Jet A-1) provided by U.S. Air Force Wright Laboratory, Aero Propulsion and Power Directorate. The fuels' chemical and performance characteristics are listed in Table 1. The sulfur-contaminated hydrotreated fuels were produced by dissolving (room temperature, shaken by hand) the selected sulfur compounds into different portions of the Jet A-1 fuel. The weight of each sulfur compound added to the Jet A-1 fuel was determined based on producing a Jet A-1 fuel with a sulfur concentration of 1000 ppm (sulfur level of Jet A fuel, Table 1).

Oxidation Tests

Flask Test. The flask test was used to evaluate the tendencies of the jet fuels and sulfur compounds to produce bulk particles. The flask test was performed by heating 20 mL of fuel in a 50 ml erlenmeyer flask placed on a hot plate (200°C surface temperature) with stirring capability. The fuel was added to the flask and was heated with stirring (magnetic stir bar). When the fuel temperature reached 100°C, the test time was initiated and an air flow (0.5 liter per hour) was initiated through a disposable glass pipette situated on the bottom of the flask. The test was stopped at 30 minutes (bulk temperature: 160°C), the flask was removed from the hot plate, and the heated fuel was allowed to cool to room temperature. The oxidized fuel was stored in a glass vial for subsequent hydroperoxide and phenol analyses. All of the fuels had reached their maximum hydroperoxide values by 30 minutes. The phenol concentrations increased with time for the entire test period.

The phenol and hydroperoxide contents of the cooled fuels were determined by cyclic voltammetry and the remaining fuel was filtered through a 0.4 μm filter to isolate the bulk particles for elemental analysis by X-ray Photoelectron Spectroscopy (XPS). The isolated particles were washed with acetone/hexane (to remove residual fuel and soluble polymers) prior to XPS analysis. The filtered fuels were then heated under a stream of nitrogen to reduce the fuel volume causing the least soluble oxidation polymers to precipitate. The precipitated polymers were isolated by filtration and analyzed for elemental content by XPS.

Table 1 Chemical properties of studied fuels

	Jet A Fuel	Jet A-1 Fuel
Hydrotreated	No	Yes
Aromatics, Vol %. (D1319)	19	19
Mercaptan Sulfur, Wt %	0.001	0.000
Sulfur, Total Wt % (D4294)	0.10	0.00
JFTOT Breakpoint, °C	282	332
Hydroperoxides, mmole/L[a]	0.03	0.01
Phenols, mmole/L[a]	2.6	0.4

[a] by cyclic voltammetry

Sealed Ampoule Test. The sealed ampoule test was used to evaluate the tendencies of the fuels and sulfur compounds to produce deposits on metal surfaces. The sealed ampoule test was performed by pippetting 3 mL of fuel into a 4 mL glass ampoule. A low-carbon steel wire was then placed inside each ampoule ($\frac{3}{4}$ of wire covered by fuel). The prepared ampoules were sealed under an air atmosphere. The sealed vials were $\frac{3}{4}$ fuel and $\frac{1}{4}$ air (allow for fuel expansion during heating). The ampoules were heated for 10 minutes in an oven set to 210°C (fuel at 210°C after 5 minutes). The ampoules were removed and allowed to cool for 10 minutes to room temperature or for 24 hours to enhance deposit formation. The ampoules were then broken open, the wires removed and cleaned with acetone/hexane (to remove fuel and soluble polymers), and the cleaned wires were analyzed by Auger spectroscopy to determine deposit thickness and to determine elemental depth profiles.

Bulk Particle and Deposit Elemental Analyses. Auger electron spectroscopy (AES) was used to perform depth profiles of the deposits formed on metal surfaces. AES depth profiles were obtained from a Varian scanning Auger spectrometer using an electron beam energy of 5 keV to obtain spectra and a 1 keV argon ion beam to sputter the samples. The sputter rate for the deposits that formed on the steel wires was estimated to be 2 nm min^{-1} based on measurements of a thin silicon nitride film whose thickness had been measured with ellipsometry.

Nomenclature

C = carbon
L = liter
mmole = millimole
ml = milliliter
N = nitrogen
nm = nanometers
O = oxygen
ppm = parts per million
S = sulfur
V = volt
Vol = volume
wt = weight

Abbreviations

AES = Auger Emission Spectroscopy
ASTM = American Society of Testing Materials
Jet A = commercial, straight-run jet fuel
Jet A-1 = commercial, hydrotreated jet fuel
JFTOT = Jet Fuel Thermal Oxidation Tester
XPS = X-ray Photoelectron Spectroscopy

X-ray photoelectron spectroscopy (XPS) was used to perform elemental surface analyses (top 3 nanometers of compound) of the bulk particles and deposits. XPS spectra were obtained with an extensively modified AEI ES-100 photoelectron spectrometer. Modifications to this instrument have included the addition of a 2001 s^{-1} turbomolecular pump and a 1101 s^{-1} ion pump for evacuation of the sample chamber. This instrument is equipped with a magnesium X-ray source.

Cyclic Voltammetric Fuel Tests

Introduction. The theory of cyclic voltammetry has been described in detail (see Kauffman, 1992). The cyclic voltammetric tests were performed with a commercially available voltammograph equipped with a glassy carbon disk (3 mm diameter) working electrode, a platinum wire (0.5 mm diameter) reference electrode, and a platinum wire (0.5 mm diameter) auxiliary electrode. The cyclic voltammetric procedure applies a small voltage ramp (0–1 V) to a platinum wire electrode and measures the produced current (μamp) at the active surface of a glassy carbon electrode. If a species in the diluted fuel sample undergoes oxidation in the applied voltage range, the oxidation of the species causes an increase in the current measured by the cyclic voltammograph. The quantity of current increase is directly proportional to the concentration of the species in the fuel. The voltage at which the current increase occurs is indicative of the type of species present in the fuel, e.g., dihydroxyaromatics (0.5–0.6 V), primary and secondary aromatic amines (0.7–0.8 V), substituted phenols (0.8–1.0 V), and so on.

Two cyclic voltammetric-based tests, the new hydroperoxide method and the phenol test, were studied.

Hydroperoxide Method. The hydroperoxide method (Kauffman, 1994) uses the same aqueous potassium iodide and acetic/hydrochloric acid solutions as prepared in the current standard hydroperoxide test, ASTM D3703-85. Hydroperoxide analyses performed using the new hydroperoxide and ASTM D3703-85 test methods have been shown to be in good agreement (Kauffman, 1994). The hydroperoxides in the fuel sample react with the acidic potassium iodide solution to produce iodine. Consequently, the concentration of iodine produced is directly proportional to the concentration of hydroperoxides in the reacted fuel sample. The hand-held voltammetric instrument used to measure the produced iodine was calibrated using blank (0 mmole) and standard (1 mmole) iodine solutions.

The fuels were analyzed for hydroperoxide concentrations by dispensing 1 to 5 ml of fuel, 0.25 ml of aqueous potassium iodide solution, and 1 ml of acetic acid solution into a 10 ml vial. The vial was capped and shaken vigorously by hand for 30 seconds. The vial was opened, 1 ml of water added, the vial was recapped, and gently shaken for 2 seconds. The vial was allowed to sit undisturbed for approximately 10 seconds. The lower layer that formed was pipetted into a new vial. The iodine produced was determined by inserting the voltammograph electrode into the pipetted layer and scanning the voltage of the auxiliary electrode from 0.0 to −1.0 V (referenced to platinum reference electrode) at a rate of 0.1 V/s. The current produced by the glassy carbon electrode was compared against the blank and standard (1 mmole) to measure the produced iodine, and consequently, the concentration of hydroperoxide in the reacted fuel sample. The calculated concentrations of the hydroperoxides in the studied fuels are listed in Table 1.

Phenol Test. To determine the concentration of phenols present in the jet fuels, samples of the fuels (0.1 ml) were diluted with 3 ml of ethanol (fuel soluble) containing an inorganic base (potassium hydroxide: 0.25 percent) (Kauffman, 1994). The electrode was inserted into the diluted fuel and the voltage of the auxiliary electrode was increased from 0.0 to 1.0 V (referenced to the platinum reference electrode) at a rate of 0.05 V/s. The current produced by the glassy carbon electrode was plotted versus scan voltage by a strip chart recorder interfaced to the voltammograph. The height(s) of the peak(s) produced by the fuels were measured and compared to solutions containing known concentrations of ethyl phenol and 1-naphthol. The calculated concentrations of phenols in the studied fuels are listed in Table 1.

Results and Discussion

Introduction. Research was performed to evaluate five predictions of the proposed oxidation/deposition mechanism:

1. Addition of oxidizable sulfur compounds will reduce hydroperoxide content and increase phenol content of oxidized Jet A-1 (hydrotreated) fuel
2. Jet A-1 fuel (in the absence of oxidizable sulfur compounds) will produce bulk particles and soluble polymers, which contain minimal amounts of sulfur and nitrogen and contain double carbon-to-oxygen bonds (aldehyde-acid polymers)
3. Addition of oxidizable sulfur compounds will produce bulk particles from Jet A-1 fuel, which contain sulfur oxides, nitrogen, and single carbon-to-oxygen bonds (phenol polymers)
4. Addition of oxidizable sulfur compounds will produce initial deposits on metal surface that have concentrated levels of sulfur oxides.
5. Addition of acid neutralizing compounds to Jet A (straight run) fuel will inhibit metal surface deposits and bulk particle formation.

The chemical and performance characteristics of the Jet A and Jet A-1 fuels used in this study are listed in Table 1. The sulfur compounds used in this study included hexadecyl mercaptan, diphenyl disulfide, benzyl phenyl sulfide, diphenyl sulfoxide, diphenyl sulfone, and dodecyl benzene sulfonic acid. The acid-neutralizing compounds used in this study were laboratory grade and included ferric oxide powder (less than 0.1 μm particle size) and calcium oxide powder (less than 20 μm particle size).

Effects of Sulfur Compounds on Jet A-1 Oxidation Products. To test the effects of sulfur-containing compounds on the oxidation products of Jet A-1 fuel, Jet A-1 fuels containing the various sulfur compounds listed in Table 2 were oxidized for 30 minutes at a maximum temperature of 160°C using the flask oxidation test. Since the flask oxidation test is open to the air and a glass pipette is used to bubble air continuously through the heated fuel, oxygen is available for fuel oxidation during the entire test period. The hydroperoxide (reaction O3) and phenol (reaction D1) concentrations of the heated Jet A-1 fuels contaminated with the various sulfur compounds are listed in Table 2.

The results shown in Table 2 indicate that the presence of certain type sulfur compounds affects the hydroperoxide/phenol ratios of oxidized Jet A-1 fuel. The neat (uncontaminated) Jet A-1 fuel oxidized to produce hydroperoxides and very little phenols (reaction O3 dominant) (Table 2). The addition of a mercaptan compound to the Jet A-1 fuel inhibited oxidation (reaction O2 and O3 inhibited) and produced low levels of phenols (reaction D1 activated) and undetectable (below 0.01 mmole/L of fuel) levels of hydroperoxide. The disulfide and sulfide compounds inhibited oxidation to varying degrees and produced high levels of phenols (reaction D1 activated) and low levels of hydroperoxides (Table 2). In contrast to the other sulfur compounds, the sulfoxide and sulfone compounds did not affect the oxidation products (reaction D1 inactive) and produced primarily hydroperoxides. In agreement with the sulfide and disulfide compounds, the Jet A fuel oxidized to produce primarily phenol type compounds (reaction D1 activated).

Table 2 Effects of different sulfur compounds on the oxidation products of Jet A-1 and Jet A fuels obtained from the flask oxidation test

Fuel	Sulfur Compound [a]	Initial Oxidation Products mmoles/L of Fuel		Bulk Particle XPS Analyses (% Atomic Wt)		
		Peroxides	Phenols	% O	% N	% S
A-1	—	5.5	0.75	11[b]	< 0.2[b]	< 0.2[b]
	Hexadecyl Mercaptan	< 0.01	3.3	25	1.8	4.4 (>98%)[c]
	Diphenyl Disulfide	1.5	7.5	22	1.0	1.7 (>98%)[c]
	Benzyl Phenyl Sulfide	2.0	6.0	18	0.4	0.8 (57%)[c]
	Diphenyl Sulfoxide	6.0	0.75	13[b]	< 0.2[b]	< 0.2[b]
	Diphenyl Sulfone	8.0	0.75	12[b]	< 0.2[b]	< 0.2[b]
A	—	0.4	4.6	20	1.9	2.8 (>98%)[c]

a Concentration 1000 ppm by sulfur. b Polymer obtained by evaporating fuel. c % oxidized sulfur

Effects of Sulfur Compounds on Jet A-1 Bulk Particles. To test the effects of sulfur-containing compounds on the bulk particles produced by oxidized Jet A-1, the stressed fuels obtained from the flask oxidation tests (Table 2) were filtered to isolate the bulk particles produced during the oxidation of sulfur contaminated Jet A-1 fuels. The oxidized Jet A-1 fuel had to be evaporated to isolate soluble material formed by oxidation. The XPS elemental analyses of the bulk particles and soluble material isolated from the oxidized Jet A-1 fuels are also listed in Table 2.

The results given in Table 2 show that the soluble material isolated from the oxidized Jet A-1 fuel contains minimal amounts of sulfur and nitrogen. Infrared spectroscopy determined the soluble material contained a large number of carbonyl (C = O) type carbon-to-oxygen bonds (polymer resulting from reaction O4). The oxidized Jet A-1 fuels contaminated with mercaptan, disulfide, and sulfide compounds produced bulk particles (Table 2) containing significant levels of sulfur oxide (reactions D1 and D3) and significant levels of nitrogen (reaction D3). Infrared spectroscopy determined the bulk particles mainly contained ether (C-O) type carbon-to-oxygen bonds (polymers resulting from reactions D2 and D4). The oxidized Jet A-1 fuel contaminated with sulfoxide and sulfone compounds produced soluble material similar to the material produced by the neat oxidized Jet A-1 fuel, i.e., minimal amounts of sulfur and nitrogen and high levels of carbonyl type carbon-to-oxygen bonds.

In agreement with the mercaptan, sulfide, and disulfide compounds, the Jet A fuel oxidized to produce bulk particles that contain sulfur oxides, nitrogen, and primarily ether type carbon-to-oxygen bonds. The addition of dodecyl benzene sulfonic acid to Jet A fuel produced visible bulk particles within 24 hours at room temperature. The isolated particles had a significant nitrogen content (reaction D3), ether type carbon-to-oxygen bonds (reaction D4) and produced elemental analyses similar to the particles produced by the oxidized Jet A fuel (Table 2).

Effects of Sulfur Compounds on Initial Metal Surface Deposits. To test the effects of different sulfur compounds on the thickness and composition of the initial deposits formed on metal surfaces, Jet A-1 fuels containing the various sulfur compounds listed in Table 2, Jet A-1 fuel and Jet A fuel were heated at 210°C for 10 minutes in sealed glass ampoules containing low-carbon steel wires. After cooling to room temperature (about 10 minutes), the heated glass ampoules were opened so that the exposed wires could be removed and rinsed with hexane and acetone prior to analysis by Auger emission spectroscopy. The removed wires appeared to be clean or slightly tarnished and the Auger depth analyses (performed by ion sputtering) determined the produced deposits to be less than 6 nm in thickness (Fig. 2). Consequently, the thin deposits present on the metal surfaces represent the initial deposits formed by the heated fuels.

The Auger elemental analysis and depth profiles of the wires heated in the presence of neat Jet A-1 fuel (Fig. 2) indicate that the metal surface is covered by a thin oxide layer with minimal amounts of nitrogen and sulfur present. The Jet A-1 fuels containing mercaptan, sulfide, and disulfide compounds produced deposits 2–4 nm in thickness, which contain from 9 to 16 percent sulfur and less than 1 percent nitrogen (Fig. 2). The Jet A-1 fuels containing sulfoxide and sulfur compounds produced wires with metal oxide layers containing less than 1 percent nitrogen and sulfur (similar to Jet A-1 in Fig. 2). In agreement with the Jet A-1 fuels containing mercaptan, sulfide, and disulfide compounds, Jet A fuel produced a deposit 2 to 4 nm in thickness, which contained a maximum of 9 percent sulfur and 1 percent of nitrogen (Fig. 2).

For the fuels producing deposits in Fig. 2, the sulfur content of the deposit is at its maximum at the metal oxide surface of the steel coupon as predicted by reaction D5. XPS analyses determined the fuel deposits produced by the sulfur-contaminated Jet A-1 fuels and the Jet A fuel contained sulfur, which was >90 percent sulfur oxides as predicted by reaction D5.

Effects of Acid Neutralizing Compounds on Fuel Deposition. To study the effects of acid-neutralizing compounds on fuel deposition, Jet A fuels containing varying amounts of superfine iron oxide and calcium oxide powders were heated at 210°C for 10 minutes in sealed glass ampoules containing low-carbon steel wires. To increase the thickness of the deposits, the heated ampoules were allowed to cool for 24 hours prior to opening. The wires were removed from the opened ampoules, rinsed with hexane then acetone to remove residual fuel, and analyzed by Auger emission spectroscopy. The measured thicknesses of the produced deposits are listed in Table 3.

The results in Table 3 indicate that the iron oxide powder (<1 μm particle size) at 50 ppm and the calcium oxide powder (<20 μm particle size) at 100 ppm are capable of inhibiting the formation of deposits on the steel surface. The results in Table 3 also indicate that the deposition-inhibiting capabilities of the oxide powders decrease as the concentrations of the oxides decrease. Additional tests with other metal and oxide powders demonstrated that only powders with acid neutralizing capabilities were able to inhibit the deposition process. For instance, superfine alumina and silicon dioxide powders (unreactive toward sulfur containing acids) had no effect on the deposition process of Jet A even at concentrations of 1000 ppm powder. The addition of cyclohexane amine (a strong organic base) inhibited the deposition process in agreement with reported research (Hazlett et al., 1986).

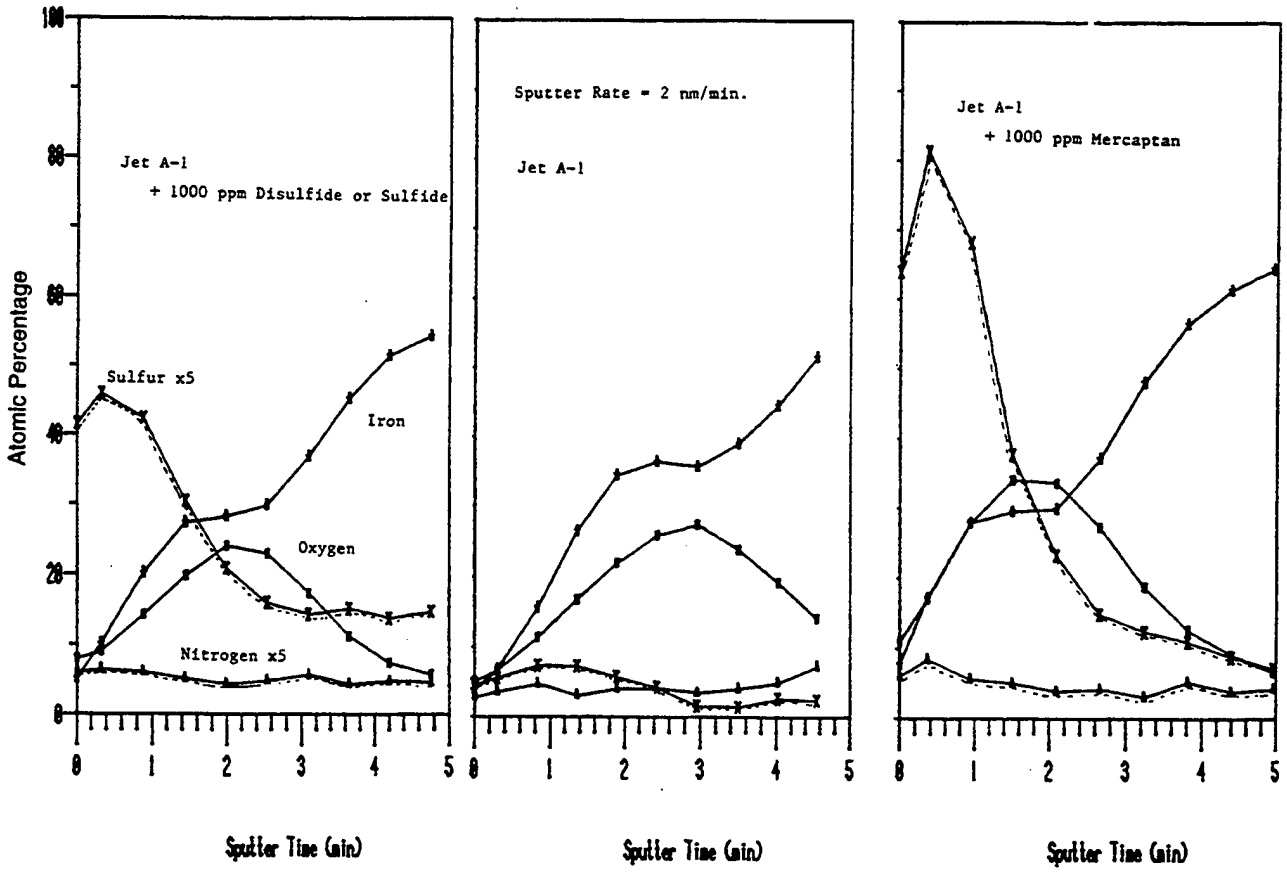

Fig. 2 Auger emission spectroscopic depth profiles of deposits formed on steel wires during sealed ampoule testing (ten minute cool down) at 210°C by Jet A-1 fuels containing different sulfur compounds (1000 ppm sulfur)

The fact that the deposits are much thicker for the 24 hour cooled steel wire than the 10 minute cooled wires, indicate that bulk particles are responsible for the thickness of the deposition (reactions D5 and D6). The fact that acid neutralizing powders are able to inhibit deposition thickness indicates that acid–base reactions are important in the formation of bulk particles (reaction D4). The acid-neutralizing powders heated in the Jet A fuel were isolated by filtration and analyzed for sulfur and nitrogen. All of the isolated powders contained significant levels of sulfur oxides and nitrogen, further indicating the powders had reacted with acidic sulfur compounds.

Table 3 Thickness measurements by AES depth profiling for deposits formed on steel surfaces by Jet A fuels with and without acid neutralizing powders

POWDER	Concentration (ppm)	Deposit Thickness [a] (nm)
Ferric Oxide	12	900
	25	300
	50	80
Calcium Oxide	50	400
	100	80
Aluminum Oxide	1000	1700
Silicon Dioxide	1000	1600
None	-	1800

a Sealed Ampoule Test (cooled 24 hours), Jet A-1 deposit thickness 70 nm

Summary

The results presented herein strongly support the oxidation (reactions O1–O5)/deposition (reactions D1–D6) reaction scheme proposed for jet fuels. The results show that the "oxidizable" sulfur compounds (mercaptan, sulfide, and disulfide) inhibit hydroperoxide production, increase phenol production, increase bulk particle formation, and increase surface deposition for sulfur contaminated Jet A-1 fuel. The "nonoxidizable" sulfur compounds, sulfoxide and sulfone, have very little effect on the oxidation/deposition processes of sulfur contaminated Jet A-1 fuel (in agreement with Mushrush et al., 1994). The results also show that the addition of "oxidizable" sulfur compounds to Jet A-1 fuel cause the contaminated Jet A-1 fuel to undergo oxidation/deposition processes similar to those of Jet A fuel. Consequently, the results herein demonstrate that "oxidizable" sulfur compounds have a very strong effect on the oxidation/deposition processes of jet fuels.

The exact identity of the oxidizable sulfur compounds responsible for the deposition processes cannot be assigned from this initial study due to the low purity levels (92–95 percent) of the mercaptan, disulfide, and sulfide compounds. However, XPS analyses were used to confirm that the sulfur contents of the "oxidizable" compounds were below 0.3 percent oxidized sul-

fur prior to use. Since the oxidized sulfur contents of the produced bulk particles were 57–98 percent (Table 2), the "oxidized" sulfur content was produced during the fuel oxidation reaction (reaction D1).

The fact that acid-neutralizing powders such as iron oxide and calcium oxide effectively inhibit surface deposition and the addition of sulfonic acid promotes bulk particles supports the acid (sulfur)/base (nitrogen) reaction proposed herein and previously (Hazlett et al., 1986) as an initial step of the deposition process. Dispersants or soluble compounds with acid-neutralizing capabilities will be studied in future work for inhibiting bulk particle formation as well as surface deposition.

Further research is also planned for identifying the "basic" nitrogen compounds, e.g., alkyl amines, aromatic amines, indoles, pyrroles, substituted pyridines, etc., which combine with the oxidized sulfur compounds to produce bulk particles and surface deposits. It is interesting to note that all of the "oxidizable" sulfur compounds produced bulk particles with significant nitrogen contents. An initial assessment of the XPS bulk particle analyses (Buckley, 1994) indicate that pyrrole and pyridine type nitrogen compounds are present. The XPS analyses also indicate that ionic type nitrogen compounds (salt from acidic sulfur: basic nitrogen reaction) are also present in the bulk particles, especially the particles from the Jet A fuel oxidation tests. The XPS analyses are in agreement with deposit-causing nitrogen compounds identified by other researchers (Hazlett et al., 1991).

The role of phenols in the bulk particle and deposition processes is more complicated than the roles of the "oxidizable" sulfur and "basic" nitrogen compounds. The phenols can act as both oxidation inhibitors (reaction D2) and deposition promoters (reaction D4). The high oxygen contents (12–17 percent) of the bulk particles and the ether type (C–O) carbon-to-oxygen bonds strongly indicate phenols or other type oxygenated compounds are involved in the deposition processes. Other researchers (Hazlett et al., 1986) have also proposed a role for phenols in the deposition process.

Acknowledgments

This research was supported by the U.S. Air Force Wright Laboratory, Aero Propulsion and Power Directorate, Wright-Patterson Air Force Base, Ohio under Contract No. F33615-92-C-2207 with W. M. Roquemore serving as Technical Monitor and D. R. Ballal serving as Principal Investigator. Tom Wittberg of the University of Dayton Research Institute performed the XPS and Auger analyses reported in this paper.

References

Buckley, A. N., 1994, "Nitrogen Functionality in Coals and Coal-Tar Pitch Determined by X-Ray Photoelectron Spectroscopy," *Fuel Processing Technology*, Vol. 37, pp. 165–179.

Hazlett, R. N., et al., 1986, "The Chemistry of Deposit Formation in Distillate Fuels," Report No. MRL-R-986, Materials Research Laboratories, Victoria, Australia.

Hazlett, R. N., et al., 1991, "Distillate Fuel Insolubles: Formation Conditions and Characterization," *Energy and Fuels*, Vol. 5, pp. 269–273.

Heneghan, S. P., and Harrison, W. E., 1992, "Antioxidants in Jet Fuels: A New Look," *Proc. 203rd National Meeting of the American Chemical Society, Division of Petroleum Chemistry, Symposium: Structure of Jet Fuels III*, pp. 404–411, San Francisco, CA.

Heneghan, S. P., Martel, C. R., Williams, T. F., and Ballal, D. R., 1992, "Studies of Jet Fuel Thermal Stability in a Flowing System," ASME Paper No. 92-GT-106; ASME JOURNAL OF ENGINEERING FOR GAS TURBINES AND POWER, Vol. 115, 1993, pp. 480–485.

Kauffman, R. E., 1992, "New Techniques to Predict and Evaluate the Effectiveness of Antioxidants in Jet Fuels," *Proc. 203rd National Meeting of the American Chemical Society, Division of Petroleum Chemistry, Symposium: Structure of Jet Fuels III*, San Francisco, CA, pp. 412–419.

Kauffman, R. E., 1994, "New, Rapid Techniques for Determining the Hydroperoxide Content, Oxidation Stability, and Thermal Stability of Jet Fuels," ASME Paper No. 94-GT-346.

Mushrush, G. W., et al., 1994, "Liquid Phase Oxidation of Organo-Sulfur Compounds by Tert-butyl Hydroperoxide and Fuel Instability Reactions," *Fuel*, Vol. 73, No. 9, pp. 1481–1485.

Appendix M.

System Evaluation of JP-8+100 Additives at High Bulk Temperatures

Gordon L. Dieterle
Kenneth E. Binns
University of Dayton
300 College Park
Dayton, OH 45469-0140

THE AMERICAN SOCIETY OF MECHANICAL ENGINEERS
345 E. 47th St., New York, N.Y. 10017

97-GT-71

SYSTEM EVALUATION OF JP-8+100 ADDITIVES AT HIGH BULK TEMPERATURES

Gordon L. Dieterle and Kenneth E. Binns
Aerospace Mechanics Division
University of Dayton
Dayton, OH

ABSTRACT

New tests were established early in the development of JP-8+100 fuel to provide system design information in addition to evaluating the JP-8 +100 additives. Preliminary evaluation of the JP-8+100 additives indicated that a thermal stability improvement for JP-8 of 100°F (56°C) was achieved for the wetted wall temperature. Specific tests were conducted to evaluate various additive concentrations and combinations for meeting the bulk fuel goal. Screening type tests were conducted in the Extended Duration Thermal Stability Test System. The promising additive candidates were then tested in the Advanced Reduced Scale Fuel System Simulator. These test systems were designed to provide information that is directly applicable to aircraft/engine fuel system designs. Based on the tests results of both the Extended Duration Thermal Stability Test and the Advanced Reduced Scale Fuel System Simulator, there were essentially zero deposits experienced at 385°F (196°C) bulk fuel temperatures with recirculation of JP-8+100 fuel. There were slight deposits experienced during tests of this fuel at 400°F (204°C) with recirculation. The description of the test systems and their operating characteristics along with the test results of the additive evaluations will be covered in this paper. A discussion of future fuel system applications and the potential payoff for JP-8+100 fuels will also be included.

INTRODUCTION

The United States Air Force embarked on a program[1] in 1989 to improve the thermal stability of JP-8 fuel. The technical approach was to develop an additive package for the JP-8 kerosene base fuel to improve its thermal stability. The specific goal established for this program is for the additive to provide a 100°F (56°C) increase in thermal stability for JP-8 fuel. Currently, the improved fuel is referred to as JP-8+100, but when the development is completed it is anticipated that the additive package will be listed in a Qualified Products List (QPL) for use in the JP-8 specification, Mil-T-83133. The cost goal for the additive is $0.001 per gallon of fuel.

Current research indicates that the additive package will contain four main ingredients; antioxidants, metal deactivators, detergents and dispersants. The Air Force contacted major additive manufacturers and oil companies to provide thermal stability improving additives for evaluation. To date over 300 additives have been screened and several show promise for meeting the thermal stability goals. A number of test devices have been developed or modified for screening of additives. The Extended Duration Thermal Stability Test (EDTST) system and Advanced Reduced Scale Fuel System Simulator (ARSFSS) are the primary test systems for evaluating the most promising additives identified by the screening tests. Additives that satisfactorily meet the requirements that are established for these tests are considered to be acceptable for material compatibility and engine testing.

FUTURE REQUIREMENTS FOR JP-8+100 FUEL

Integrated aircraft thermal management with fuel as the heat sink, is a basic design approach for today's high performance aircraft. The future trends are towards higher power avionics, hydraulic and electrical systems and more efficient, higher temperature engines. Fuel operating temperatures are increasing to accommodate the higher loads. Most current fighter aircraft recirculate fuel before it is arrives at the engine to maintain proper aircraft cooling and to maintain the aircraft/engine interface temperature to less than 200°F (93°C). Advanced fighters that will be produced early in the next decade will require increased cooling resources. Fuel will be subjected to higher temperature and thermal cycling due to increased heat loads imposed by the aircraft and engine systems. A potential design and thermal environment that a fuel will experience in next generation fighter aircraft fuel systems is shown in Figure 1. The significant areas of concern for these fuel systems are the higher bulk fuel temperatures, the recirculation of high temperature fuel from the engine back to the aircraft fuel tank, and the higher wetted wall temperatures to be experienced in the fuel nozzles. Another potential future aircraft fuel system and thermal environment that utilizes fuel/air heat exchangers to provide cooling for engine components and/or compressor bleed air is shown in Figure 2. A major advantage to the fuel/air heat exchanger approach is that the aircraft and engine fuel system components are not required to operate at higher temperatures with the associated weight and reliability penalties.

Presented at the International Gas Turbine & Aeroengine Congress & Exhibition
Orlando, Florida — June 2–June 5, 1997

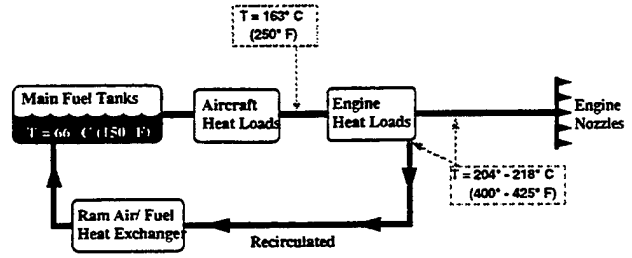

FIGURE 1: THE NEXT GENERATION FIGHTER AIRCRAFT FUEL SYSTEM

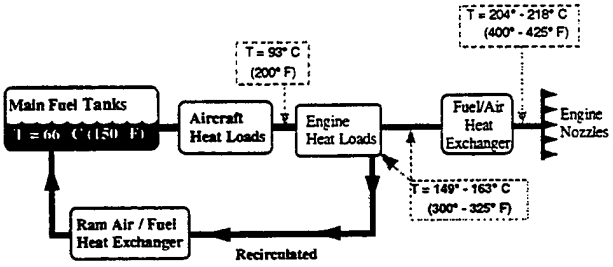

FIGURE 2: FUTURE AIRCRAFT FUEL SYSTEM

EXTENDED DURATION THERMAL STABILITY TEST SYSTEM (EDTST)

The Extended Duration Thermal Stability Test was established to provide fuel thermal stability information for designers in addition to evaluating fuels. This system was established by modifying an existing facility that was originally a "hydrotreater" for processing fuels. A schematic of the Extended Duration Thermal Stability Test system is shown in Figure 3. The system consists of a 60 gallon feed tank, an electrical motor driven gear pump, two clamshell furnace heaters, and a scrap tank. The first furnace heater (preheater) in the system is used to establish the desired fuel bulk temperature into the second heater and to establish the desired fuel bypass temperature. The fuel bulk temperature represents the temperature that results from aircraft and engine heat loads. The maximum bulk temperature used for present day JP-8 fuel systems is 300°F (149°C). A goal for JP-8+100 fuel is to provide a capability to operate at 400°F (204°C) bulk fuel temperatures. Temperature is established in the second furnace heater (main heater) to represent the wetted wall temperatures associated with engine injection nozzles. Another goal for JP-8+100 fuel is to provide a wetted wall temperature increase from 400°F (204°C), the present limit of JP-8, to 500°F (260°C) for engine fuel injection nozzle design.

Both furnace heaters are 0.81 meters long and resistance heated. They each have 5 heating element zones that are independently controlled. The fuel flows upward through a single stainless steel tube in each heater. The tube in the preheater has an outside diameter of 1.27 cm and a wall thickness of 0.0889 cm. The tube in the main heater has an outside diameter of 0.32 cm and a wall thickness of 0.0889 cm. Each tube is assembled inside a thick walled furnace tube that has an inside diameter of 2.54 cm and an outside diameter of 5.08 cm. The tubes have thermocouples attached to the outer wall for measuring wetted wall temperatures. The annular space between the furnace tube and heater tubes is filled with sand. A typical

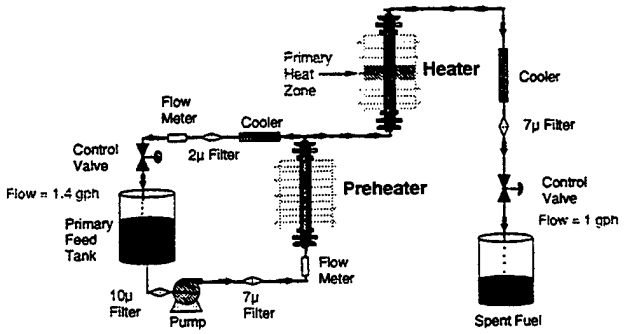

FIGURE 3. EDTST SCHEMATIC

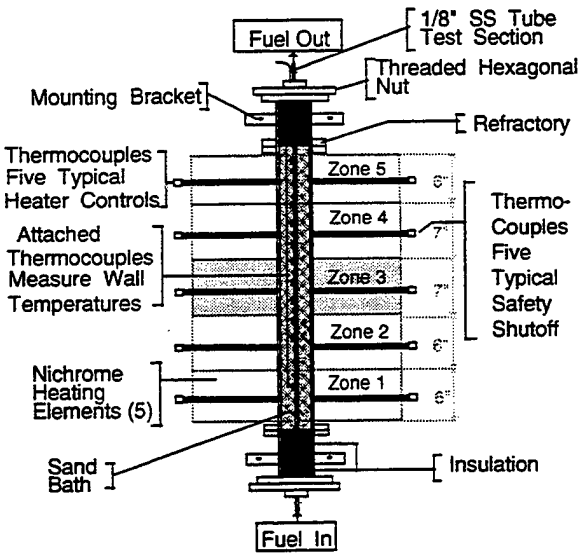

FIGURE 4. EDTST HEATER DIAGRAM

main heater assembly is shown in Figure 4. A fuel bypass line is installed downstream of the preheater to represent the aircraft recirculation line from the engine to the airframe tanks. A water/fuel cooler is installed in this line to represent the aircraft ram air heat exchanger cooler. A 2μ filter is also installed in the line for 4 hours to measure particles in the recirculated bulk fuel. Since effects of recirculation are one of the purposes of this test, the filter is installed for only a short duration. Aircraft fuel systems will probably not have a filter in the recirculation line. A 7μ filter is also installed downstream of the heater. This filter provides an indication of particles that the fuel nozzles will experience in the advanced system design as shown in Figure 2.

A flow rate out of the system of 1 gallon per hour (gph) and duration of 96 hours have been used for most tests. At the 1 gph flow rate and a bypass flow also at 1 gph, the residence time from the inlet of the preheater to the outlet of the main heater is 50 seconds. Similarly, the residence time from the inlet to the outlet of the main heater is 1.1 seconds with a Reynolds number of 2,400. These residence times are representative of those in aircraft and engine fuel systems. The Extended Duration Thermal Stability Test system is computer controlled and can run unattended for long periods of time.

Table 1
SUMMARY OF CARBON DEPOSIT COMPARISONS OF VARIOUS JP-8+100 ADDITIVE COMBINATIONS.

Fuel at 400°F Bulk, 500°F WWT	Maximum Segment Deposits (μgm/cm²) Heater	Preheater	Heat Exchanger	Filter Deposits (μgm) 2 μ	7 μ
POSF-3166 (JP-8)*	**8,386**	**181**	**63**	**720**	**90,700**
+8Q405/BHT/MDA	221	**30**	11	240	1,310
+125% (8Q405/BHT/MDA)	269	**28**	20	230	230
+8Q405/MDA	250	**15**	12	230	**51,700**
+200% (8Q405)/BHT/MDA	149	**19**	52	280	**103,000**
+150% (8Q405)/BHT/MDA	245	**22**	**78**	**2,930**	**155,000**
+8Q405/PDA (5ppm)/MDA	301	**36**	**265**	**5,360**	**198,000**
JPTS	**3,065**	**40**	**116**	**2,230**	**31,000**
Fuel at 350°F Bulk, 500°F WWT					
POSF-3166 (JP-8)					
+8Q405/BHT/MDA	42	3	8	210	1,020
Fuel at 385°F Bulk, 500°F WWT					
POSF-3166 (JP-8)					
+150% (8Q405)/BHT/MDA	153	10	7	264	410
Maximum Acceptable Deposit	250	10	15	300	2,000

BOLD - Considered to be unacceptable and/or unsatisfactory.
NOTE: All tests were for 96 hours except as noted.
* 24 Hours only.

Table 2.
PROPERTIES OF ADDITIVES STUDIED.

Additive Name	Classification	Type of Compound	Concentration (mg/l)	% Active Ingredient
BHT	Antioxidant	2,6 di-tert-butyl-4-methylphenol	24	100
MDA	Metal Deactivator	N,N'-disalicylidene -1,2-propanediamine	5.8	75-77
Betz 8Q405	Dispersant	Proprietary Dispersant	100	Proprietary

EDTST Test And Test Results

A test duration of 96 hours was selected for the evaluation of the JP-8+100 additive candidates to insure that there is a sufficient induction time for deposits to form. Previous evaluations[2] of the JP-8+100 additives at 400°F (204°C) bulk temperatures have resulted in deposits occurring in the preheater, bypass line cooler and in the bypass line filter. This test series was conducted with the POSF-3166* fuel plus the standard JP-8 additive package as the baseline. Most tests, unless otherwise specified, were conducted at bulk fuel temperatures out of the preheater of 400°F (204°C) and a heater wetted wall temperature of 500°F (260°C). A summary of the test results is shown in Table 1.

The test with JP-8 had to be stopped after 24 hours due to plugging of the 7-micron filter downstream of the heater. The test resulted in excess deposits throughout the system despite the abbreviated test duration. This test substantiates the finding of a coupling effect on tube deposits that result at high bulk fuel temperatures as reported in previous papers[3, 4]. A test was conducted on an additive package with Betz 8Q405, BHT and MDA at a concentration (Table 2) established by the additive supplier and verified as a viable JP-8+100 candidate by other tests[5]. This test resulted in satisfactory deposits except in the preheater tube. Since close tolerance valves downstream of the engine heat exchangers will be exposed to carbon deposits in an engine fuel system, any measurable deposits in this test component are considered to be a potential problem area and require further evaluation in actual components. Investigation of

* Each fuel acquired by the Air Force has been assigned a four-digit number (e.g., POSF-xxxx). These Air Force assigned numbers are used for identification.

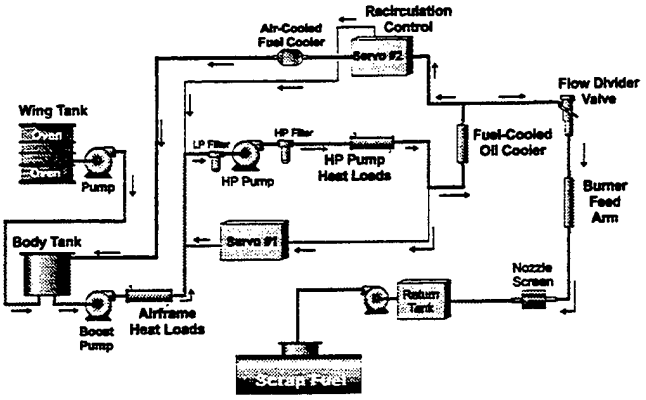

FIGURE 5. ADVANCED REDUCED SCALE SYSTEM SIMULATOR SCHEMATIC

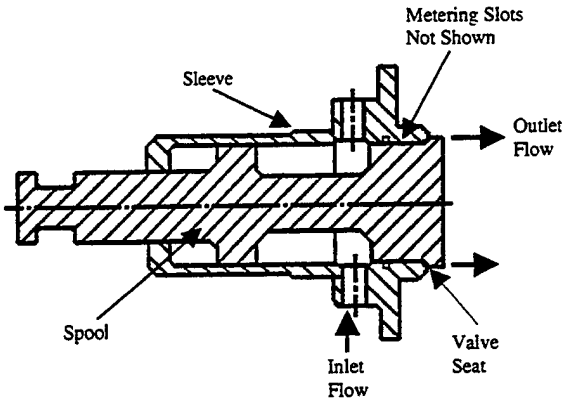

FIGURE 6. ARSFSS FLOW DIVIDER VALVE SPOOL & SLEEVE

different concentrations and additives was then initiated to determine if operation at 400°F (204°C) bulk fuel temperatures could be achieved with no carbon deposits. A test with 125% increase in the additive concentration resulted in essentially the same magnitude of deposits in the preheater.

To determine the effects of BHT, a test was conducted with the Betz 8Q405 and MDA additives only. The result of this test indicated that there was a reduction in the carbon deposits related to the bulk (preheater, heat exchanger, and 2-micron filter); however the deposits in the 7-micron filter were excessive. This is unacceptable since it would result in undesirable deposits in fuel nozzle valves for system designs as shown in Figure 2. The 150 % concentration of the Betz 8Q405 ingredient (187.5-ppm) along with the original amounts of BHT and MDA resulted in reduced deposits in the preheater and higher deposits in the other parts of the system. This same additive concentration was tested at 385°F (196°C) bulk temperature to determine its upper temperature limit. As shown in Table 1, the carbon deposition was acceptable throughout the system. An increase to 200% of the Betz 8Q405 additive resulted in lower deposits than the 150% test at the 400°F (204°C) bulk conditions. The deposits in the 7-micron filter and heat exchanger tube were still considered to be excessive for the 200% Betz test.

There was a concern that the additive package itself was not correct. A test was conducted at 350°F (177°C) bulk temperatures to validate this specific additive. As shown in Table 1, the deposits that resulted from this test throughout the system were extremely low. There was no problem with the additive itself based on this test. A test was then established for the Advanced Reduced Scale Fuel System Simulator to investigate the effects of this 200% Betz additive package on the valves and other components in that system. The results of that test are discussed later in this paper.

Based on the reduction of deposits in the bulk during the test with no BHT, it was decided to test another antioxidant. A phenylenediamine type antioxidant, denoted as AO-24, was tested with the Betz and MDA additives, based on results of one of the preliminary screening tests (Quartz Crystal Microbalance). As shown in Table 1, the deposits that were experienced during this test were considerably higher than all of the other JP-8 +100 additive candidates in this test series.

A test was also conducted with JPTS at these same conditions to provide comparison data. JPTS is a special -purpose jet fuel developed for the U-2 aircraft. Surprisingly, this test resulted in unacceptable deposits throughout the system. It should be noted that the JPTS tested has been stored in drums for over three years and is considered to be well aged. However, it did pass the JPTS specification test (JFTOT). Previous tests with no recirculation at 425°F (218°C) bulk temperatures with unaged fuel also indicated that JPTS was unsatisfactory. Based on these tests, JPTS also produces deposits at 400°F (204°C) bulk temperatures similar to the JP-8 +100 fuel.

ADVANCED REDUCED SCALE FUEL SYSTEM SIMULATOR

The Advanced Reduced Scale Fuel System Simulator has more extensive capability than the Extended Duration Thermal Stability Test. It is capable of simulating thermal and flow profiles of aircraft fuel systems. It also has valves that are representative of actual aircraft. The simulator consists of three major systems. These systems are the fuel conditioning system, the airframe fuel system simulator and the engine fuel system simulator. A schematic of this simulator is shown in Figure 5. The simulator is configured for simulating an F-22 aircraft with a F119 engine. The flow established for the simulator is approximately 1/72 scale of the F119 engine. The burn flow for the simulator is 1/3 of the flow for a single F119 fuel nozzle. The total flow that is required for each test is approximately 1,500 gallons.

The engine simulator contains the primary test articles that were used for this test series. The specific test articles are (1) the Fuel Cooled Oil Cooler (FCOC), (2) the flow divider valve, (3) the Burner Feed Arm (BFA), and (4) servovalves #1 and 2. The Fuel Cooled Oil Cooler represents the engine lube system cooler. It consists of an induction heater and a steel manifold with three, 3/8-inch diameter, 0.035-inch wall tubes and associated thermocouples. The tubes are connected and provide for three passes through the heater. The tube that is used for the final pass through the heater is removed after each test. It is then cut into 2-inch long segments and subjected to carbon analysis. The flow divider valve (Figure 6) is an actual F119 valve that has been modified by changing the slot width for the reduced flow. The materials, clearances (0.0003 inch nominal) and function is representative of the F119 flow divider valve. The performance of this valve is determined by hysteresis and visual inspection. The burner feed arm is RF induction heated. It consists of a steel clamshell with a 1/8-inch, 0.020-inch wall stainless steel tube

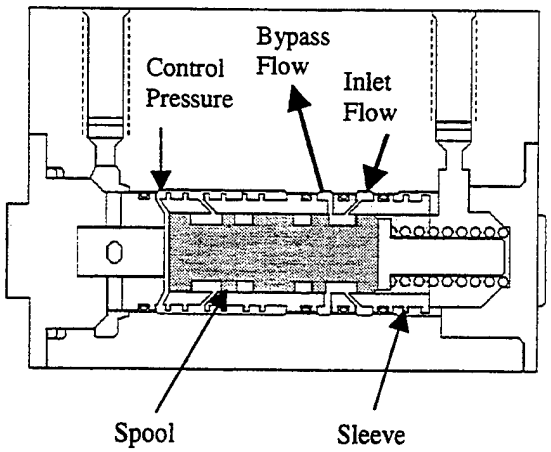

FIGURE 7. ARSFSS SERVO VALVE

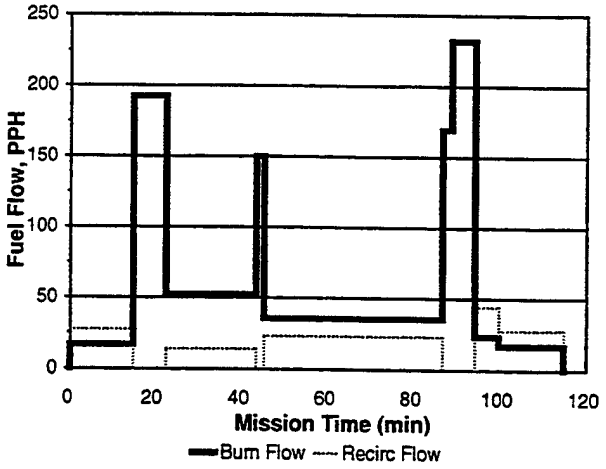

FIGURE 8. GENERIC MISSION CYCLE FOR F119

installed in middle of the clamshell. Thermocouples on the outside of the tube are located along the entire length to measure the temperature profile of the tube. At the end of the tests, this tube is cut up into 1-inch long sections and subjected to carbon burnoff. The servovalves (Figure 7) are modified F119 engine control valves. They are both the second stage valves of electrohydraulic valves used in the engine control system. The materials and clearances (0.00012 inch maximum) are representative of the actual engine valves. The performance of these valves is determined by hysteresis and visual inspection.

Advanced Reduced Scale Simulator Test And Test Results

The tests conducted on the Advanced Reduced Scale Fuel System Simulator were established to correlate the results of the Extended Duration Thermal Stability Test. A generic F119 test cycle profile (Figure 8) modified to evaluate the high bulk fuel temperatures was used for this series of testing. A summary of the tests and their results is shown in Table 3.

All tests were conducted with the same base fuel (POSF-3166) as tested in the Extended Duration Thermal Stability Test. The first test conducted was with the original concentrations of Betz 8Q405/BHT/MDA. The Fuel Cooled Oil Cooler bulk outlet fuel outlet temperature was 400°F (204°C) and the maximum wetted wall temperature for the Burner Feed Arm was 500°F (260°C) for this test. The flow divider valve and servovalve # 2 had visual deposits as a result of this test. A hysteresis shift of servovalve # 2 also was excessive after this test. The next test was conducted at the same conditions as the first test except the Fuel Cooled Oil Cooler bulk fuel temperature was 375°F (190°C) instead of 400°F (204°C). There were no significant deposits on the valves or hysteresis shift problems as experienced at the 400°F (204°C) conditions. The results of this test indicate that the additive package is acceptable for operation at 375°F (190°C) bulk temperatures. The system was the modified to reflect a potential future application as shown in Figure 2. The system was changed to provide fuel bypassing back to the airframe fuel tank upstream of the Fuel Cooled Oil Cooler. A test was then conducted with a bypassed fuel temperature of 330°F (165°C), a Fuel Cooled Oil Cooler bulk fuel outlet temperature of 400°F (204°C) and the Burner Feed Arm wetted wall temperature of 500°F (260°C). There were visual deposits on the flow divider valve after this test. However they did not appear as heavy as in the first test. The deposits on both the Fuel Cooled Oil Cooler and Burner Feed Arm were considerably less than in the first test. This is an indication of the adverse effect that results from recirculation at high temperatures. The last test in this series was a repeat of the first test with the 200% Betz additive package. This test resulted in less deposit in the Fuel Cooled Oil Cooler and valves than the baseline JP-8+100 fuel. However, any observable deposits on the valves are considered to be unacceptable for the relatively brief test. The desired service life for these valves for flight engines are over 4,000 hours. Therefore the higher Betz concentration is also not satisfactory for use at 400°F (204°C) bulk fuel conditions. The slight reduction in deposits that is provided by the higher concentrations of Betz 8Q405 is not considered sufficient to change from the original concentration.

SUMMARY

Based on the test results of both the Extended Duration Thermal Stability Test and the Advanced Reduced Scale Fuel System Simulator, there were essentially zero deposits experienced at 385°F (196°C) bulk fuel temperatures with recirculation with JP-8+100 fuel. There were slight deposits experienced during tests of this fuel at 400°F (204°C) bulk temperatures with recirculation. Slight deposits were also experienced with JPTS at 400°F (204°C) bulk temperatures.

The recirculation of high temperature fuel does result in accelerating the deposit rate of the fuel. Tests at 400°F (204°C) bulk temperature with recirculation at a lower temperature [315°F (157°C)] resulted in considerable less deposits than the tests with bulk and recirculation temperatures of 400°F (204°C). The higher bulk temperatures did not significantly affect the deposits associated with the 500°F (260°C) wetted wall.

The most promising JP-8+100 candidate, based on testing to date, is Betz 8Q405/BHT/MDA. Result of tests of this candidate have demonstrated that only slight deposits are experienced at bulk fuel temperatures of 400°F (204°C) and wetted wall temperatures of 500°F (260°C).

Table 3
SUMMARY OF ADVANCED REDUCED SCALE FUEL SYSTEM SIMULATOR TEST RESULTS.

Fuel	Temperature		Maximum Segment Deposits ($\mu gm/cm^2$)		Visual
	Bulk	Wetted Wall			Valve Deposits
	Fuel Cooled Oil Cooler (FCOC)	Burner Feed Arm (BFA)	Fuel Cooled Oil Cooler (FCOC)	Burner Feed Arm (BFA)	2 μ
3166 (JP-8)					
+8Q405/BHT/MDA	400°F (204°C)	500°F (260°C)	**115**	106	**Yes**
+8Q405/BHT/MDA	375°F (191°C)	500°F (260°C)	12	115	No
+8Q405/BHT/MDA Recirculated at 330°F (166°C)	400°F (204°C)	500°F (260°C)	**33**	59	**Yes**
+200% (8Q405)/BHT/MDA	400°F (204°C)	500°F (260°C)	**26**	73	**Yes**

BOLD - Considered to be unacceptable and/or unsatisfactory.

ACKNOWLEDGMENTS

This work was supported by the U.S. Air Force, Wright Laboratory, Fuels and Lubrication Division, Aero-Propulsion and Power Directorate, Wright-Patterson Air Force Base, Dayton, Ohio, under contract No. F33615-92-C-2207, with Mr. Charles W. Frayne serving as the Air Force Technical Monitor.

REFERENCES

1. S. P. Heneghan, S. Zabarnick, D. R. Ballal, and W. E. Harrison III, "JP-8+100: The Development of High-Thermal-Stability Jet Fuel," AIAA Paper No.96-0403, presented at the 34th Aerospace Sciences Meeting, Reno, NV., January 1996.

2. K. E. Binns, G. L. Dieterle, and T. F. Williams, "System Evaluation of Improved Thermal Stability Jet Fuels," *Proceedings of the 5th (Int.) Conference on the Stability and Handling of Liquid Fuels*, Vol.1, pp. 401, Rotterdam, Netherlands, 1995.

3. K. E. Binns, W. E. Harrison III, S. D. Anderson, and R. W. Morris, "High Heat Sink Fuels for Improved Aircraft Thermal Management," A paper presented at the International Conference on Environmental Systems, Colorado Springs, CO, July 11-13, 1993.--Published in *Transactions of the Society of Automotive Engineers, Journal of Aerospace*, 1994.

4. G. L. Dieterle and K. E. Binns, "Extended Duration Thermal Stability Test of Improved Thermal Stability Jet Fuel," ASME Paper No. 95-GT-69 presented at the ASME Turbo Expo '95, Houston, TX, June 1995.

5. Zabarnick and R. R. Grinstead, "Studies of Jet Fuel Additives Using a Quartz Crystal Microbalance and Pressure Monitoring at 140C," *Industrial and Engineering Chemistry Research*, Vol. 33, pp. 2771-77, 1994.

Appendix N.

Measurement of Dissolved and Total Water Content in Advanced Turbine Engine Fuels with a Gas-Liquid Chromatographic OTC Technique

Wayne A. Rubey
Richard C. Striebich
University of Dayton
300 College Park
Dayton, OH 45469-0140

Steven D. Anderson
Wright Laboratories POSF
1790 Loop Road North
Wright Patterson AFB, OH 45433-7103

6th International Conference
on Stability and Handling of Liquid Fuels
Vancouver, B. C., Canada
October 13-17, 1997

MEASUREMENT OF DISSOLVED AND TOTAL WATER CONTENT IN ADVANCED TURBINE ENGINE FUELS WITH A GAS-LIQUID CHROMATOGRAPHIC OTC TECHNIQUE

Steven D. Anderson[1], Wayne A. Rubey*[2], and Richard C. Striebich[2]

[1]Wright Laboratories, POSF, 1790 Loop Road North, Wright-Patterson AFB, OH 45433-7103.
[2]Environmental Sciences and Engineering Laboratory, Research Institute, University of Dayton, 300 College Park, Dayton, OH 45469-0132.

ABSTRACT

Significant capabilities have been developed over the past quarter century for detecting extremely trace quantities of organic compounds in water. However, accurate and precise analyses for water in complex organic mixtures continues to be an analytical challenge. Water is omnipresent and a thin film of adsorbed moisture usually coats every type particle and surface. The analysis for water content in a complex turbine engine fuel is complicated by water sorption onto fine particulate matter and also the presence of numerous fuel additives, e.g., corrosion inhibitors, fuel system icing inhibitors, static dissipators, metal deactivators, detergents, dispersants, etc. Many of these additives affect the interfacial surface tension and the water coalescing properties of the bulk fuel. Instrumental approaches for measuring water content in complex organic mixtures include titration techniques, optical spectroscopy, humidity sensing devices, diode lasers, light emitting diodes, liquid chromatography, and gas chromatography. There has been a real need for a laboratory technique that can provide appropriate water content measurements for turbine engine fuels which contain extensive additive packages. Accordingly, we pursued the gas chromatographic approach for measuring dissolved and free water. Initially, a reaction gas chromatography (RGC) technique was investigated in which water was converted to acetylene by way of a temperature controlled calcium carbide reactor. Although this RGC procedure exhibited considerable sensitivity via detecting water as acetylene using hydrogen flame ionization detection, significant irreproducibility was encountered. Accordingly, various gas-solid chromatographic (GSC) and gas-liquid chromatographic (GLC) scenarios were investigated. It was found that when a modified high-temperature splitter injector assembly is used in conjunction with a highly deactivated and low β value GLC open tubular column, that water can be well-behaved (symmetrical zone profile) and separated from other constituents. Measurement of water content in a variety of turbine engine fuels while using a modulating thermal conductivity detector was found to be both precise and sensitive, even into the sub-ppm region. Using standard addition procedures along with an internal standard, it is anticipated that this GLC analytical method can be simplified for eventual field-scale testing.

INTRODUCTION

Many analytical techniques have been developed for measuring trace levels of organic substances *in water*. Some of these instrumental procedures can measure certain organic constituents at the sub part-per-trillion level.[1,2] The situation is significantly different for measuring *water in* an organic mixture, as analytical techniques only have measurement capabilities down to the low ppm or high ppb measurement regions. Much of this difference in analytical capability is due to ease of contamination and the difficulty in quantitatively transporting trace quantities of water, particularly in various chromatographic scenarios.

With respect to advanced turbine engine fuels, dissolved and total water content represent important information with respect to transferring and refueling aircraft under a severe range of atmospheric conditions. There are many additives in advanced turbine engine fuels which can adversely affect the interfacial tension and the water coalescing properties of the bulk hydrocarbon fuel. They can also form emulsions or micelles as depicted in Figure 1. Example additives are fuel system icing inhibitors, static dissipators, metal deactivators, detergents, corrosion inhibitors/lubricant improvers, dispersants, etc. There has been a pressing need for a laboratory technique that can provide appropriate dissolved and total contained water measurements for turbine engine fuels, along with other complex organic mixtures which contain extensive additive packages.

Background. Under our earthly atmospheric conditions, water is omnipresent. Accordingly, precise measurement of water content is complicated by the physical and chemical nature of the various materials. A thin film of adsorbed moisture usually coats every type of particle and surface. In addition, water is present as a dissolved or dispersed contaminant in practically every organic mixture sample. Consequently, accurate measurement of low concentrations of water in an organic matrix needs to be accomplished with a minimum of atmospheric exposure, sample transfer, and further contamination.

There are a variety of instrumental techniques for measuring water in specific samples. However, an urgent need exists for a general technique which can address a wide range of organic matrices and particularly samples which contain fine particulate matter, assorted additives, and other interfering materials. The Karl Fischer titration procedure[3] has long been used for analyses where water can be liberated and reacted. Also, a variety of spectroscopy

procedures have found wide acceptance when water can be truly isolated from related materials, such as, alcohols, ketones, etc. A gas chromatographic technique was desired which could rapidly separate and detect low ppm concentrations of water in advanced turbine engine fuels. Initially, a precise laboratory procedure was desired in support of fuel research activities for high-performance aircraft. However, a field-portable unit would also be advantageous for monitoring fuel status at flight line facilities.

INSTRUMENTAL APPROACH

For several decades, ppm levels of water have been measured with a reaction gas chromatographic (RGC) procedure. Our laboratory and other research facilities have had considerable success measuring low levels of water using RGC techniques whereby water vapor is passed through a heated calcium carbide reactor.[4] This quantitatively converts the highly adsorbed water to acetylene which is thereafter readily transported and detected by a hydrogen flame ionization detector. High ppb levels of water in jet fuel can be measured using such a procedure. Even so, as the block diagram of the RGC system in Figure 2 shows, there are many stages involved in transporting water, acetylene, and the various associated inert and organic compounds through such an analytical system. It was found that significant and unpredictable error was associated with this particular multi-stage transport and RGC measurement procedure. Different forms of gas-solid chromatography (GSC) were also investigated and found to be unacceptable with respect to quantitatively transporting trace-levels of water. Consequently, a more straight forward gas-liquid chromatographic (GLC) analytical approach was pursued whereby inertness (relative to water) of the chromatographic flowpath was of primary concern.

Modified GLC-OTC Approach. Recent advances in column technology have permitted a different analytical approach for separating and measuring low levels of water. This instrumental approach utilized a modified GLC system which employed a highly deactivated and very thick film polydimethylsiloxane open tubular column (OTC). Detection was with the modulating thermal conductivity detector, although a variety of detection devices could be used, e.g., AED, PDID, etc. A special high-temperature splitter injector[5] was used for injecting approximately two microliters of fuel sample. This high- temperature split assembly used an inerted injector insert (with deactivated glass wool) which needed to be replenished after

approximately 50 injections. A high capacity, but coarse, in-line charcoal trap was used in the vent line of the injector.

The column specifics were the key to obtaining a separation of water from the other trace eluting constituents of the organic mixtures. Although the OTC was deactivated, the thick film of polydimethylsiloxane contributed significantly to the good symmetry of the emerging water zone. The importance of generating symmetrical solute zones is related to both the quantitative precision and accuracy. Specifically, Figure 3 presents a description of the various statistical moments that are associated with generating chromatographic zones. For this type of trace-water analysis, the third statistical moment describes the major criterion. The symmetry (or extent of asymmetry) that exists with an emerging zone is of extreme importance as the initiation and termination of the integration process is determined by the behavior of the extremities of the solute zone. Thus, symmetrical zone profiles always provide far better quantitative measurements in chromatography.

EXPERIMENTAL

We have a strong preference for the GLC separation mode. When chromatography is performed properly in the GLC mode, symmetrical elution profiles are generated.[6] Figure 4 shows a high resolution GC-MS tracing of a typical JP-8 fuel. Consequently, when water can be transported and eluted without skew (like these organic solutes) and analytically separated by GLC, then considerable instrumental simplifications can be obtained. Previously, most gas chromatographic procedures that involved a water separation (particularly the GSC methods) also included extensive solute zone "tailing", which would be extremely detrimental for precise quantitation of the trace amount of water.

The sample introduction mode is of major importance to a laboratory GLC analytical procedure. Two different procedures were investigated; an on-column injection technique, and a high-temperature split injection procedure. In both cases, an extremely thick film GLC-OTC was used as it has two distinct advantages for separating water from other constituents. By having a very thick film column, the water could be slightly retained relative to inert gases that would be dissolved in the jet fuel. Also, the thick film of stationary phase provides further deactivation of the fused silica OTC wall surface. Eventually, we decided upon the modified

high-temperature injector assembly shown in Figure 5. The instrumental arrangement for conducting water-in-fuel analyses consisted of a modified Hewlett Packard 5890 gas chromatograph with a reporting integrator (HP-3390A). This GC instrument had highly filtered helium as the carrier gas. With the splitter injector and a 15 meter megabore OTC having a polydimethylsiloxane substrate (of low phase ratio, or β value), water could be eluted with near-perfect symmetry (see Figure 6). Such an instrumental arrangement allowed water to be easily separated from the other constituents, and Figure 7 shows a typical chromatogram of a JP-8+100 fuel. Figure 8 also shows the early portion of chromatograms for other similar types of turbine engine fuels. These separations were performed with a GLC column temperature of 35°C. The only co-eluting species or interferent in this analysis scenario was propane. Consequently, a series of different jet fuels were analyzed for propane content using the highly sensitive hydrogen flame ionization detector, and here it was found that only extremely small quantities of propane (approximately 0.0l ppm) were encountered.

As water is an omnipresent contaminant, it was found that different syringe needles sorbed differing quantities of water. For example, while under laboratory conditions, a polyimide-clad fused silica needle could contain up to 100 nanograms of water, while a simple #26 stainless steel syringe needle sorbed approximately 10 nanograms of water. Recent information has shown that a special Silcosteel treated needle is especially inert with respect to water sorption, and only miniscule amounts of water have been detected using this syringe needle in conjunction with JP-8+100 fuels.

RESULTS

This particular gas-liquid chromatographic open tubular column method has been able to analyze a variety of turbine engine fuels. Thus far, measurements of water content have ranged from 33 to 144 ppm, by weight. The calibration procedure that is associated with this GLC method utilized a standard addition technique. The precision for the water measurement was found to be 2.48% RSD. It appeared that the largest source of error with the present method is associated with sample delivery. An automatic sampler or a digital syringe should reduce this error.

Water settling time has been observed to be a variable in high water-content analyses. The size of the formed water droplets appears to be especially important. Experiments are

planned for examining several aspects further. Investigations are underway to determine water settling time at different fuel temperatures and water/fuel equilibrium properties with various additive packages.

CONCLUSIONS

The measurement of water content in JP-8+100 fuel can be accomplished with precision using near-conventional GLC technology. Trace levels of water can behave well in an appropriate open tubular column and be measured to sub-ppm concentrations with the use of on-column injection. In this type of analytical work, precautions are needed for dealing with surface adsorbed water. Accurate calibrations for water are achievable using special standard addition procedures. With backflush capabilities, this measurement technique can be scaled down for field testing.

ACKNOWLEDGEMENTS

This work was supported by the Fuels Branch of the US Air Force Wright Laboratory. Part of this effort was performed under the Combustion and Heat Transfer Studies Program, F33615-87-C-2767.

REFERENCES

(1) Grob, K. *J. Chromatogr.* **1973**, *84*, 255-273.

(2) Tomkins, B. A. Griest, W. H., and Higgins, C. E. *Anal. Chem.* **1995**, *67*, 4387-4395.

(3) Fischer, K. *Angew. Chem.* **1935**, *48*, 394-399.

(4) Knight, H. S., and Weiss, F. T. *Anal. Chem.* **1962**, *34*, 749-751.

(5) Sandra, P. *Sample Introduction in Capillary Gas Chromatography: Volume 1*, Huthig: Heidelberg, 1985.

(6) Giddings, J. C. *Unified Separation Science*, Wiley: New York, 1991.

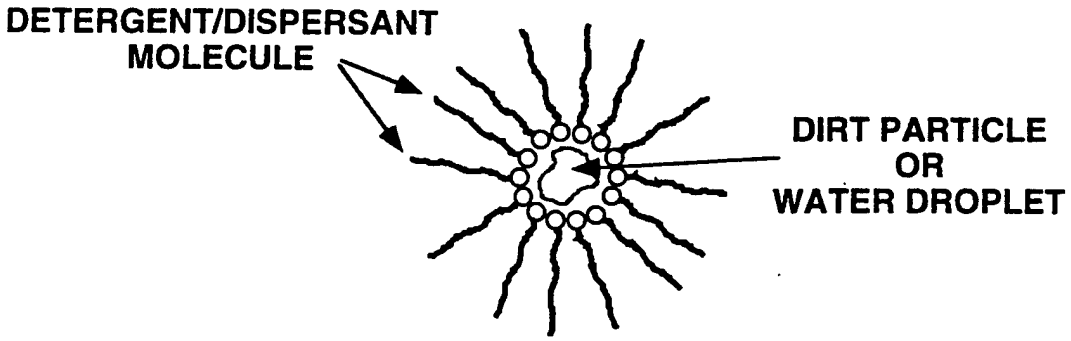

Figure 1. Detergent/dispersant additives can form micelles around dirt particles and water droplets. This prevents agglomeration of particles needed for removal in current filter/coalescer media.

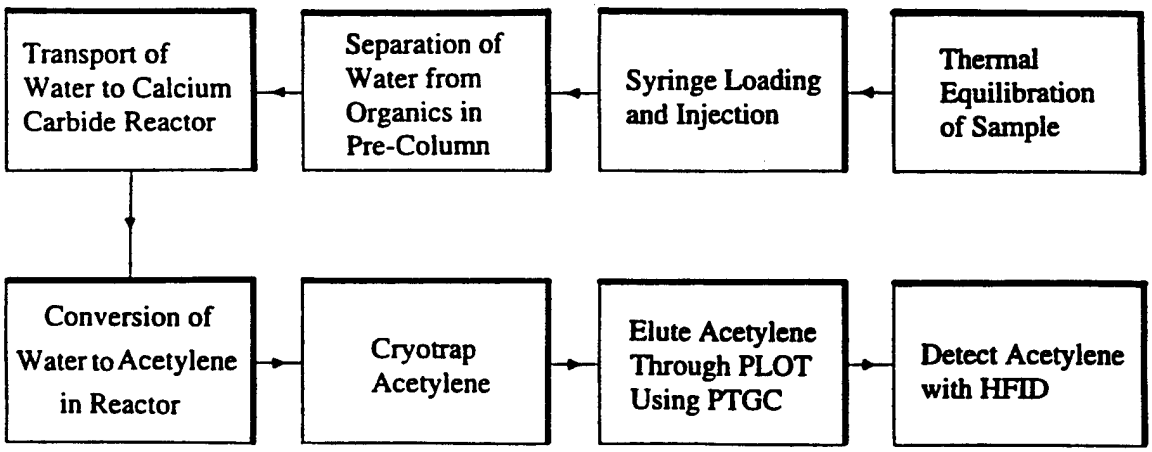

Figure 2. Block diagram of reaction gas chromatographic (RGC) procedure.

$$\bar{m}_k = \frac{\int_0^\infty c(\tau)(\tau - m_1)^k d\tau}{\int_0^\infty c(\tau) d\tau}$$

m_0 = zone area

m_1 = zone retention time

$\bar{m}_2$ = zone time variance

$\bar{m}_3$ = zone skew, or asymmetry

$\bar{m}_4$ = zone kurtosis, or flattening

Figure 3. Statistical moments of emerging GC solute zones.

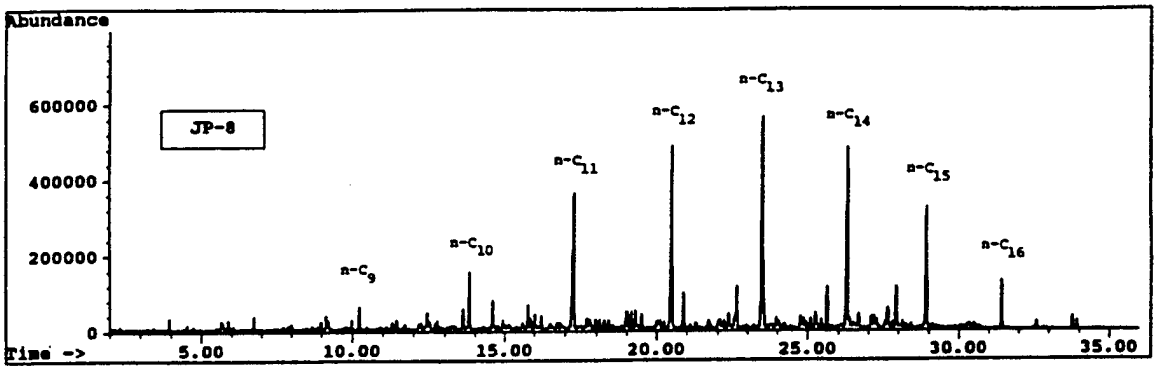

Figure 4. GC-MS output signal for a JP-8 fuel.

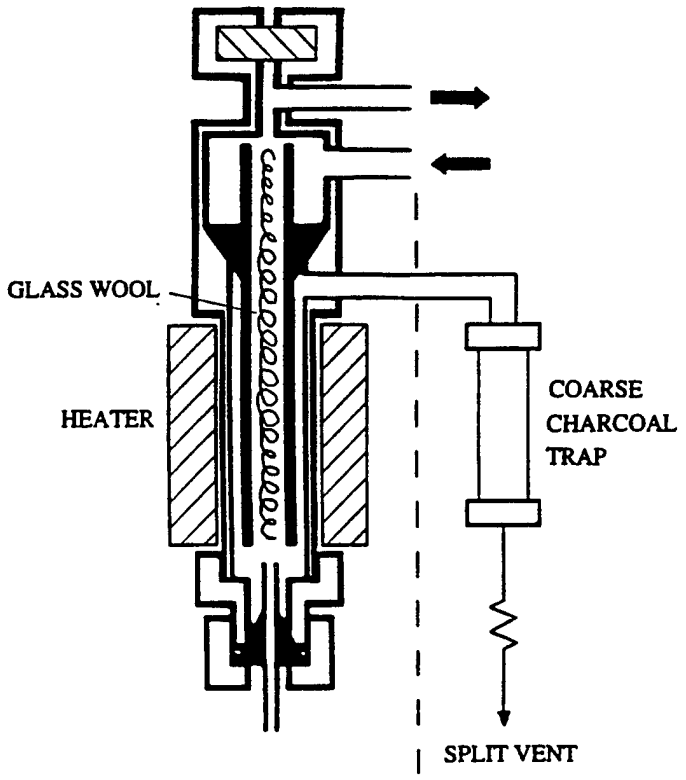

Figure 5. Modified high-temperature splitter injector assembly.

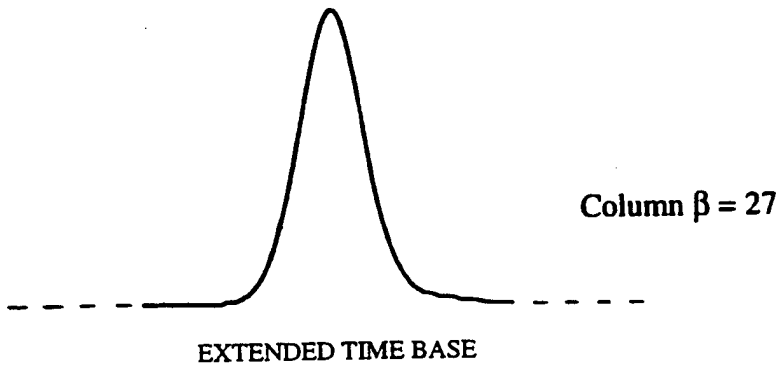

Figure 6. Near-perfect symmetry of water elution zone.

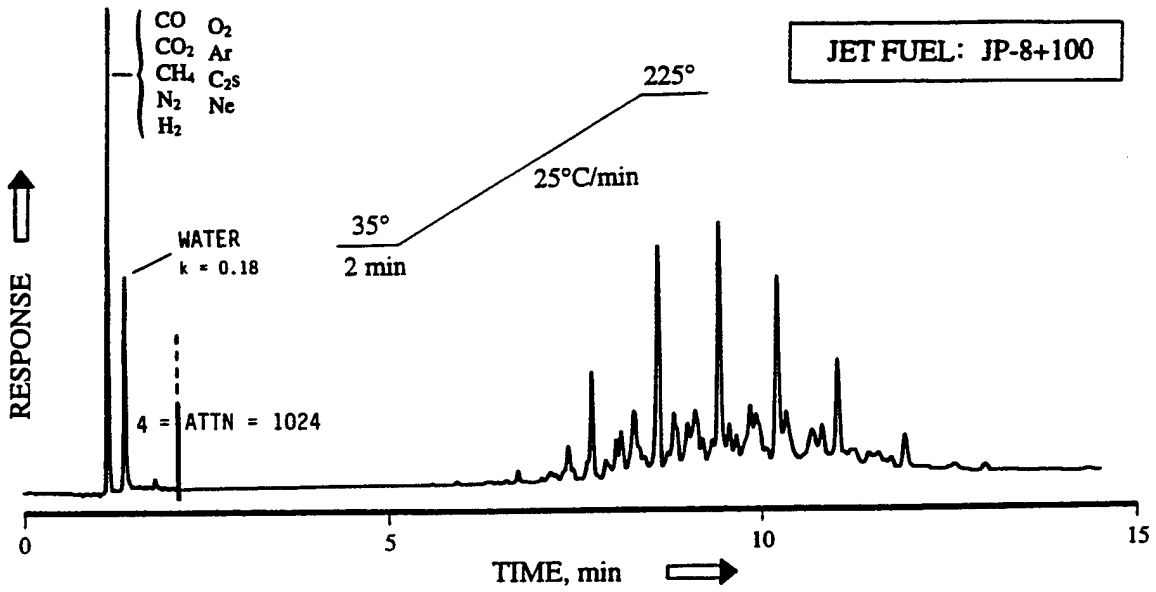

Figure 7. Typical GLC chromatogram of a JP-8+100 fuel.

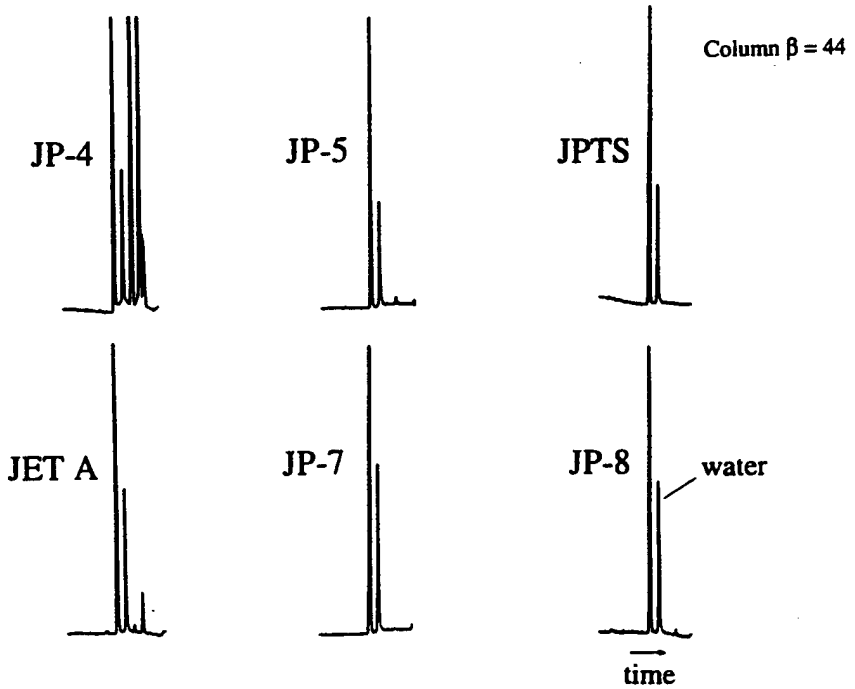

Figure 8. Early elution portion of GLC chromatograms of other types of jet fuels.

Appendix O.

List of Publications

University of Dayton
300 College Park
Dayton, OH 45469-0140

AWARDS, PUBLICATIONS, AND PRESENTATIONS
CONTRACT NO. F33615-92-C-2207
(June 1992 to December 1997)

Honors and Awards

1. R. E. Kauffman and J. D. Wolf (1992): R & D Top 100 Award for the Development of RULER Family of Instruments, Museum of Science & Industry, Chicago, IL.

2. F. Takahashi (1992): AIAA Best Paper Award (Combustion Section) AIAA Mini-Symposium, Dayton OH.

3. F. Takahashi (1992): Session Chairman, Central States Section, The Combustion Institute, Columbus, OH.

4. D. R. Ballal, S. P. Heneghan, J. C. Pan, and M. D. Vangsness (1992): ASME International Gas Turbine Institute (IGTI) Best Combustion and Fuels Research Paper Award.

5. D. R. Ballal (1992): Fellowship of ASME

6. R. E. Kauffman (1993): Wohlleben-Hochwalt Outstanding Professional Research Award, University of Dayton, Dayton, OH.

7. D. R. Ballal (1993): Fellowship of AIAA.

8. D. R. Ballal (1993): AIAA National Energy Systems Award.

9. J. Zelina (1993): AIAA Gordon C. Oates Graduate Fellowship Award.

10. M. D. Durbin (1993): AIAA Best Paper Award (Combustion Section) AIAA Mini-Symposium, Dayton OH.

11. F. Takahashi (1993): Session Chairman, Eastern States Section, The Combustion Institute, Princeton, NJ.

12. J. Zelina (1994): AIAA Best Paper Award (Combustion Section) AIAA Mini-Symposium, Dayton OH.

13. M. D. Durbin (1994): ASME Travel Fellowship Award.

14. W. A. Rubey (1994): Plenary Lecture Award, 16th International Symposium on Capillary Chromatography, Riva del Garda, Italy.

15. J. Zelina and D. R. Ballal (1994): AIAA Best Paper Award, AIAA Intersociety Energy Conversion Engineering Conference, Monterey, CA.

16. F. Takahashi (1994): "Laser Sheet Visualization of a Flame," Front Cover, Aerospace America, August.

17. R. E. Kauffman (1994): PERFECT-Added to Military Fuel Specification MIL-T-5624R.

18. USAF Improved Jet Fuel (1994): Aviation Week & Space Technology, December 12-19.

19. UDRI Fuels Team (1994): USAF Letter of Commendation, December. 20.

20. F. Takahashi and S. P. Heneghan (1995): Wohlleben-Hochwalt Outstanding Professional Research Award, April.

21. J. Zelina (1995): AIAA Best Paper Award (Combustion Section) AIAA Mini-Symposium, Dayton OH., June.

22. S. P. Heneghan (1995): Session Chairman, ASME Turbo Expo. '95, Houston, TX, June.

23. D. R. Ballal (1995): Chairman, Combustion and Fuels National Committee, ASME-International Gas Turbine Institute, July.

24. F. Takahashi (1995): Invited Foreign Researcher, National Institute for Resources and Environment, MITI, Japan, August.

25. D. Pestian (1995): Best Poster Paper, Gallery of Fluid Motion, American Physical Society Meeting, Irvine, CA, October.

26. F. Takahashi (1996): Session Chairman, Central States Section, The Combustion Institute, St. Louis, MO, May.

27. D. R. Ballal (1996): Program Chairman, ASME Turbo Asia '96 Congress, Jakarta, Indonesia, November.

28 J. Blust (1996): AIAA Best Paper Award (Combustion Section) AIAA Mini-Symposium, Dayton OH., October.

29. D. R. Ballal (1996): Faculty Award for Scholarship, School of Engineering, University of Dayton, Dayton, OH, August.

30. D. R. Ballal (1996): ASME Leadership Award, Presented by ASME President, Jakarta, Indonesia, November.

31. D. R. Ballal (1996): Invited Participant, Workshop on "Aviation Fuels & Fire Safety," National Research Council, Washington, D.C., November.

32. F. Takahashi (1997): Session Chairman, Central States Section, The Combustion Institute, Point Clear, AL, April.

33. D. R. Ballal (1997): Alumni Award In Scholarship, University of Dayton, Dayton, OH, April.

34. F. Takahashi (1997): Session Chairman, Second International Symposium on Scale Modeling, Lexington, KY, June.

35. F. Takahashi (1997): Session Chairman, 33rd AIAA/ASME/SAE/ASEE Joint Propulsion Conference, Seattle, WA, July.

36. S. P. Heneghan (1997): Invited Speaker, Ohio Valley Chromatography Symposium, Hueston Woods, June.

37. R. C. Striebich (1997): Invited Speaker, Ohio Valley Chromatography Symposium, Hueston Woods, June.

Patents

1. R. E. Kauffman, "Voltammetric Method for Measuring Peroxide Concentration,", U. S. Patent No. 5,480,808, January 1996.

2. R. E. Kauffman, "Freshness and Stability Test for Predicting Oxidation Degradation," U.S. Patent No. 5,239,258, August 1993.

3. W. A. Rubey and R. C. Striebich, "Method for Admitting and Receiving Samples in a Gas Chromatographic Column," U. S. Patent Applied For No. o8/851,888, May 1997.

Journal Publications

1. F. Takahashi and M. D. Vangsness, "Near-Field CARS Measurements and the Local Extinction of Turbulent Jet Diffusion Flames," *Dynamics of Heterogeneous Combustion and Reacting Systems,* AIAA Progress in Astronautics and Aeronautics Series, Vol. 152, pp. 37-55, 1993.

2. S. P. Heneghan, D. L. Geiger, S. D. Anderson, and W. D. Schultz, "Static Tests of Jet Fuel Thermal and Oxidative Stability," *AIAA Journal of Propulsion and Power,* **9**, 5 (1993).

3. S. Zabarnick, "Chemical Kinetic Modeling of Jet Fuel Autoxidation and Antioxidant Chemistry," *Industrial and Engineering Chemistry Research,* Vol. 32, pp. 1012-1017, 1993.

4. S. P. Heneghan, T. F. Williams, C. R. Martel and D. R. Ballal, "Studies of Jet Fuel Thermal Stability in Flowing Systems," *Transactions of ASME, Journal of Engineering for Gas Turbines and Power*, Vol. 115, pp. 480-486, (1993).

5. T. Edwards and S. Zabarnick, "Supercritical Fuel Deposition Mechanisms," *Industrial & Engineering Chemistry Research* **32**, 3117 (1993).

6. S. P. Heneghan, C. R. Martel, T. F. Williams, and D. R. Ballal, "Effects of Oxygen and Fuel Additives on The Thermal Stability of Jet Fuels," *Transactions of ASME, Journal of Gas Turbine and Power*, Vol. 117, pp. 120-124, 1995.

7. D. R. Ballal, M. D. Vangsness, S. P. Heneghan, and G. J. Sturgess, "Studies of Lean Blowout in a Research Combustor," NATO Advisory Group on Aerodynamics Research and Development, AGARD-CP-536, Paper Number 18, 1993.

8. S. P. Heneghan and S. Zabarnick, "Oxidation of Jet Fuels and the Formation of Deposits," *Fuel* **73**, 35 (1994).

9. M. D. Durbin and D. R. Ballal, "Studies of Lean Blowout in a Step Swirl Combustor," *Transactions of ASME, Journal of Gas Turbine and Power*, Vol. 118, pp. 72-78, Jan. 1996.

10. J. Blust, T. F. Williams, C. R. Martel, and V. R. Katta, "The Role of Buoyancy in Fuel Thermal Stability Studies," *AIAA Journal of Thermophysics and Heat Transfer*, Vol. 9, pp. 159-168, 1994.

11. S. Zabarnick, "Studies of Jet Fuel Thermal Stability and Oxidation Using a Quartz Crystal Microbalance and Pressure Measurements," *Industrial and Engineering Chemistry Research*, Vol. 33, pp.1348-1354, 1994.

12. J. Zelina and D. R. Ballal, "Combustion Studies in a Well Stirred Reactor," *AIAA Journal of Propulsion and Power*, Vol. 11, pp. 132-139, 1995.

13. F. Takahashi, W. J. Schmoll, and J. L. Dressler, "Characteristics of a Velocity-Modulated Pressure-Swirl Atomizing Spray Measured by the Phase-Doppler Method," *AIAA Journal of Propulsion and Power*, Vol. 11, pp. 955-963, 1995.

14. F. Takahashi, W. J. Schmoll, G. L. Switzer, and D. T. Shouse, "Structure of a Spray Flame Stabilized on a Production Engine Combustor Swirl Cup," *Proceedings of 25th Symposium (Int.) on Combustion*, The Combustion Institute, pp. 183-191, 1994.

15. F. Takahashi, W. J. Schmoll, and J. L. Dressler, "Characterization of a Velocity-Modulation Atomizer," *Reviews of Scientific Instruments*, Vol. 65, pp. 3563-68, 1994.

16. F. Takahashi, "Sooting Correlations for Premixed Combustion," *Physical & Chemical Aspects of Combustion: A Tribute to Irvin Glassman* (Eds. R. F. Sawyer and F. L. Dryer) Gordon & Breach, New York, NY, 1996.

17. F. Takahashi and V. R. Katta, "Numerical Experiments on the Vortex-Flame Interactions in a Jet Diffusion Flame," *AIAA Journal of Propulsion and Power*, Vol. 11, pp. 170-176, 1995.

18. S. Zabarnick and R. R. Grinstead, "Studies of Jet Fuel Additives Using a Quartz Crystal Microbalance and Pressure Monitoring at 140C," *Industrial and Engineering Chemistry Research*, Vol. 33, pp. 2771-77, 1994.

19. S. Zabarnick and R. R. Grinstead, "Studies of Jet Fuel Thermal Stability Using a Quartz Crystal Microbalance," PREPRINTS, *Division of Petroleum Chemistry*, American Chemical Society, pp. 51-57, 1994.

20. R. E. Kauffman, "Standard Test Method for Hydroperoxide Number of Aviation Turbine Fuels--An ASTM Standard," To appear in *Annual Book of the American Society of Testing and Materials (ASTM) Standards*, 1998.

21. S. Zabarnick and J. Zelina, "Chemical Kinetics of NOx Production in a Well Stirred Reactor," AIAA Paper No. 94-3828, *Proceedings of 29th Intersociety Energy Conversion Engineering Conference,* pp. 649-653, AIAA, Washington D.C., 1994.

22. M. D. Durbin and D. R. Ballal, "Optimizing the Combustion Performance of a Step Swirl Combustor," AIAA Paper No. 94-3825, *Proceedings of 29th Intersociety Energy Conversion Engineering Conference*, pp. 631-635, AIAA, Washington D.C., 1994.

23. J. Zelina, R. C. Striebich, and D. R. Ballal, "Pollutant Emissions Research Using a Well Stirred Reactor," AIAA Paper No. 94-3827, *in Proceedings of 29th Intersociety Energy Conversion Engineering Conference*, pp. 644-648, AIAA, Washington D.C., 1994.

24. M. D. Durbin and D. R. Ballal, "Studies of Combustion and Emissions in a Model Step Swirl Combustor," *Proceedings of the FACT Vol. 18, pp. 17-21, ASME (Int.) Joint Power Generation Conference,* New York, NY, 1994.

25. J. Zelina and D. R. Ballal, "Studies of Pollutant Emissions in a Well Stirred Reactor," *Proceedings of the FACT Vol. 18, pp. 12-16, ASME (Int.) Joint Power Generation Conference,* New York, NY, 1994.

26. S. P. Heneghan and R. E. Kauffman, "Analytic Tests and Their Relation to Jet Fuel Stability," *Proceedings of the 5th (Int.) Conference on the Stability and Handling of Liquid Fuels*, Vol. 1, pp. 29, Rotterdam, Netherlands, 1995.

27. S. P. Heneghan and L. P. Chin, "Autoxidation of Jet Fuels: Implications for Modeling and Thermal Stability," *Proceedings of the 5th (Int.) Conference on the Stability and Handling of Liquid Fuels*, Vol. 1, pp. 91, Rotterdam, Netherlands, 1995.

28. S. Zabarnick and R. Grinstead, "Studies of Jet Fuel Additives Using the Quartz Crystal Microbalance and Pressure Monitoring at 140C," *Proceedings of the 5th (Int.) Conference on the Stability and Handling of Liquid Fuels*, Vol. 1, pp. 275, Rotterdam, Netherlands, 1995.

29. K. E. Binns, G. L. Dieterle, and T. F. Williams, "System Evaluation of Improved Thermal Stability Jet Fuels," *Proceedings of the 5th (Int.) Conference on the Stability and Handling of Liquid Fuels*, Vol.1, pp. 401, Rotterdam, Netherlands, 1995.

30. W. A. Rubey, R. C. Striebich, M. D. Tissandier, and D. A. Tirey, "Gas Chromatographic Measurements of Trace Oxygen and Other Dissolved Gases in Thermally Stressed Jet Fuel," *Journal of Chromatographic Science*, Vol. 33, pp. 433-437, August, 1995.

31. F. Takahashi, M. D. Vangsness, and M. D. Durbin, "Stabilization of Hydrogen-Jet Diffusion Flames With and Without Swirl," *Transport Phenomenon In Combustion*, (S. H. Chan, Ed.) Vol. 1, pp. 593-604, Taylor & Francis, Washington D.C., 1996.

32. F. Takahashi, W. J. Schmoll, D. D. Trump, and L. P. Goss, "Vortex-Flame Interactions and Extinction of Turbulent Jet Diffusion Flames," *Proceedings of the 26th Symposium (Int.) on Combustion, The Combustion Institute*, pp. 145-152, 1996.

33. F. Takahashi and V. R. Katta, "Unsteady Extinction Mechanisms of Jet Diffusion Flames," *Proceedings of the 26th Symposium (Int.) on Combustion, The Combustion Institute*, pp. 1151-1160, 1996.

34. F. Takahashi, M. S. Anand, M. D. Vangsness, M. D. Durbin, and W. J. Schmoll, "An Experimental and Computational Study of Swirling Hydrogen Jet Diffusion Flames," *Transactions of ASME, Journal of Engineering for Gas Turbines and Power*, Vol. 119, pp. 305-314, 1997.

35. M. D. Durbin, M. D. Vangsness, D. R. Ballal, and V. R. Katta, "Study of Flame Stability in a Model Step Combustor," *Transactions of ASME, Journal of Engineering for Gas Turbines and Power*, Vol. 118, pp. 308-315, 1996.

36. S. Zabarnick, P. Zelesnik, and R. B. Grinstead, "Jet Fuel Deposition and Oxidation: Dilution, Materials, and Oxygen Effects," *Transactions of ASME, Journal of Engineering for Gas Turbines and Power*, Vol. 118, pp. 271-277, 1996.

37. J. S. Ervin, S. P. Heneghan, C. R. Martel, and T. F. Williams, "Surface Effects on Deposits from Jet Fuels," *Transactions of ASME, Journal of Engineering for Gas Turbines and Power*, Vol. 118, pp. 278-285, 1996.

38. J. Zelina and D. R. Ballal, "Combustor Stability and Emissions Research Using a Well Stirred Reactor," ASME Paper No. 95-GT-109, and *Transactions of ASME, Journal of Engineering for Gas Turbines and Power*, Vol. 119, pp. 70-75, 1997.

39. F. Takahashi, M. D. Vangsness, M. D. Durbin, and W. J. Schmoll, "Structure of Turbulent Hydrogen Jet Diffusion Flames with and without Swirl," *Transactions of ASME, Journal of Heat Transfer,* Vol. 118, pp. 877-884, 1996.

40. J. S. Ervin, S. P. Heneghan, T. F. Williams, and M. A. Hanchak, "Reduced Dissolved Oxygen and Jet Fuel Deposition," *Proceedings of the 30th Intersociety Energy Conversion Engineering Conference*, pp. 210-216, July 1995.

41. J. S. Ervin and T. F. Williams, "Dissolved Oxygen Concentration and Jet Fuel Deposition," *Industrial and Engineering Chemistry Research*, Vol. 35, pp. 899-904, 1996.

42. J. Zelina, J. Blust, and D. R. Ballal, "Combustion of Liquid Fuels in a Well Stirred Reactor," ASME Paper No. 96-GT-047, Presented at ASME Turbo Expo. '96, Birmingham, U.K., June 1996.

43. S. Zabarnick, P. Zelesnik, and S. Whitacre, "Silver Corrosion and Sulfur Detection using a Quartz Crystal Microbalance with Silver Electrode Surfaces," *Industrial and Engineering Chemistry Research,* Vol. 35, pp. 2576-2580, 1996.

44. S. P. Heneghan, S. Zabarnick, D. R. Ballal, and W. E. Harrison, III "JP-8+100: Development of a Thermally Stable Jet Fuel," *Transactions of ASME, Journal of Energy Resource Technology*, Vol. 118, pp. 170-179, October 1996.

45. S. Zabarnick, S. D. Whitacre, and P. Zelesnik, "Further Studies of JP-8+100 Additive Candidates in the QCM," PREPRINTS, Division of Petroleum Chemistry, Vol. 41, No. 2, pp. 438-441, March 1996.

46. J. S. Ervin, T. F. Williams, and V. R. Katta, "Global Kinetic Modeling of Aviation Fuel Fouling in Cooled Regions in a Flowing System," *Industrial and Engineering Chemistry Research,* Vol. 35, pp. 4028-4032, 1996.

47. S. P. Heneghan, S. Zabarnick, and D. R. Ballal, "Designing High Thermal Stability Jet Fuels for the 21st Century," *Proceedings of 31st Intersociety Energy Conversion Engineering Conference*, pp. 486-493, August 1996.

48. J. Zelina and D. R. Ballal, "Emissions Studies in a Well Stirred Reactor and Applications to Combustion Modeling," *Proceedings of FACT, Vol. 21, ASME (Int.) Joint Power Generation Conference*, pp. 255-263, October 1996.

49. G. J. Sturgess, A. L. Lesmerises, S. P. Heneghan, M. D. Vangsness, and D. R. Ballal, "Lean Blowout in a Research Combustor at Simulated Low Pressures," *Transactions of ASME, J. of Engineering for Gas Turbines and Power,* Vol. 118, pp. 773-781, 1996.

50. B. Beaver, R. DeMunshi, S. P. Heneghan, S. D. Whitacre, and P. Neta, "Model Studies Directed at the Development of New Thermal Oxidative Stability Enhancing Additives for Jet Fuels," *Energy and Fuels*, Vol. 11, pp. 396-408, 1997.

51. F. Takahashi and V. R. Katta, "A Numerical Study of a Methane Diffusion Flame over a Flat Surface," To appear in *Proceedings of the Second International Symposium on Scale Modeling*, 1998.

52. S. Zabarnick, "Pseudo-Detailed Chemical Kinetic Modeling of Antioxidant Chemistry for Jet Fuel Applications," *Energy and Fuels*, Vol. 12, pp. 547-553, 1998.

53. S. Zabarnick and S. D. Whitacre, "Aspects of Jet Fuel Oxidation," ASME paper NO. 97-GT-219, and *Transactions of ASME, Journal of Engineering for Gas Turbine and Power*, Vol. 120, pp. 519-525, 1998.

54. J. S. Ervin and S. P. Heneghan, "The Meaning of Activation Energy and Reaction Order in Autoaccelerating Systems," *Transactions of ASME, Journal of Engineering for Gas Turbine and Power*, Vol. 120, pp. 468-473.

55. R. E. Kauffman, "The Effects of Different Sulfur Compounds on Jet Fuel Oxidation and Deposition," *Transactions of ASME, J. of Engineering for Gas Turbines and Power,* Vol. 119, pp. 322-328, 1997.

56. S. P. Heneghan and W. E. Harrison, III, "JP-8 + 100: The Development of High Thermal Stability Jet Fuel," Proceedings of the Sixth International Conference on Stability and Handling of Liquid Fuels, Vancouver BC, Canada, Vol. 1, pp. 271-283, 1997.

57. S. P. Heneghan and M. D. Vangsness, "Additive Stability in JP-8—Metal Alloy Systems at Elevated Temperatures," Proceedings of the Sixth International Conference on Stability and Handling of Liquid Fuels, Vancouver BC, Canada, Vol. 1, pp. 285-293.

58. D. H. Kalt, "Evaluation of JP-8+100 Fuel Compatibility with Aircraft Fuel System Materials: The Effect of Detergent/Dispersant on Aircraft Materials," Proceedings of the Sixth

International Conference on Stability and Handling of Liquid Fuels, Vancouver BC, Canada, Vol. 1, pp. 251-269, 1997.

Presentations

1. S. P. Heneghan, D. L. Geiger and E. M. Steward, "Analysis of Sulfur Containing Compounds by Gas Chromatography (GC) Atomic Emission Detection," PittCon 93, Atlanta, GA, March 1993.

2. R. C. Striebich, S. Zabarnick, and W. A. Rubey, "Determination of Jet Fuel Compositional Changes in Flowing Heated Tube Experiments," PittCon 93, Atlanta, GA, March 1993.

3. W. A. Rubey, S. L. Mazer, P. C. Hayes, and E. M. Steward, "Analysis of Turbine Engine Fuels and Complex Industrial Organic Mixtures Using a Multidimensional GC and GC-MS System," 24th Ohio Valley Chromatographic Symposium, Hueston Woods, OH, June 1993.

4. S. D. Anderson and W. A. Rubey, "The Identification of Sulfur-Containing Compounds in Jet Fuel Using Multidimensional Gas Chromatography with Mass Selective Detection," 24th Ohio Valley Chromatographic Symposium, Hueston Woods, OH, June 1993.

5. S. Zabarnick, "Studies of Jet Fuel Thermal Stability using a Quartz Crystal Microbalance and GC Analysis," A paper presented at the CRC Fuels Meeting, Alexandria, VA, April, 1993.

6. S. P. Heneghan and B. Grinstead, "Analysis of Hetero-Atom compounds in Jet Fuels," Ohio Valley Chromatography Symposium, Heuston Woods, OH, June 1993.

7. K. E. Binns, W. E. Harrison III, S. D. Anderson, and R. W. Morris, "High Heat Sink Fuels for Improved Aircraft Thermal Management," A paper presented at the International Conference on Environmental Systems, Colorado Springs, CO, Reprint in *Transactions of the Society of Automotive Engineers, Journal of Aerospace*, 1994.

8. F. Takahashi, W. J. Schmoll, and M. D. Vangsness, "Structure of a Spray Flame Stabilized on a Production Engine Combustor Swirl Cup by Phase-Doppler Anemometer," Presented at the Eastern States Section/The Combustion Institute Meeting, October 1993.

9. M. D. Durbin, M. D. Vangsness, and F. Takahashi, "Stability of Hydrogen/Air Double-Concentric Jet Diffusion Flames with and without Swirl," Presented at the Eastern States Section/The Combustion Institute Meeting, October 1993.

10. S. P. Heneghan, S. Zabarnick, B. R. Grinstead, and D. L. Geiger, "Analysis of Fuel Deposit Precursors using Gas Chromatography/ Atomic Emission Detection," Federation of Analytic Chemistry and Spectroscopy Societies, Detroit, MI, October 1993.

11. S. Zabarnick, "Thermal Stability Measurements of Jet Fuel Using a Quartz Crystal Microbalance," ASTM D02 Meeting on Petroleum Products and Lubricants, Dallas, TX, December 1993.

12. R. E. Kauffman, "Development of a Rapid, Portable Hydroperoxide Test for Jet Fuels," ASTM D02 Meeting on Petroleum Products and Lubricants, Dallas, TX, December 1993.

13. R. C. Striebich and W. A. Rubey, "A Convenient Method for Analyzing Dissolved Oxygen in Hydrocarbon Matrices Using Gas Chromatography-Mass Spectrometry," Presented at the American Chemical Society Conference on Fuel Thermal Stability, San Diego, CA, March, 1994.

14. R. E. Kauffman, "Development of a Rapid, Portable Hydroperoxide Test for Jet Fuels," Presented at the American Chemical Society Conference on Fuel Thermal Stability, San Diego, CA, March, 1994.

15. S. Zabarnick and B. Grinstead, "Studies of Jet Fuel Thermal Stability using a Quartz Crystal Microbalance," Presented at the American Chemical Society Conference on Fuel Thermal Stability, San Diego, CA, March, 1994.

16. S. P. Heneghan, "Global Oxidation of Jet Fuels: Determining and Understanding the Parameters," Presented at The American Chemical Society Symposium on Autooxidation of Distillate Fuels, San Diego, CA, March, 1994.

17. P. H. Taylor, R. C. Striebich, L. Ostruska, and B. Dellinger, "Auto-Oxidation of N-Decane/Aniline/Thiophenol Mixtures," Presented at The American Chemical Society Symposium on Autooxidation of Distillate Fuels, San Diego, CA, March, 1994.

18. R. E. Kauffman, "Effect of Different Sulfur Compounds on the Deposition and Oxidation Mechanism of Hydrotreated Jet Fuels," Coordinating Research Council, Fuel Chemistry Group, Washington, D.C., April 1994.

19. R. E. Kauffman, "New, Rapid Techniques for Determining Hydroperoxide Contents, Oxidation Stability, and Thermal Stability of Jet Fuels," Presented at the 39th ASME (Int.) Gas Turbine Conference, Hague, Netherlands, June 1994.

20. R. C. Striebich and W. A. Rubey, "Surface Adsorption Studies Using Inverse Gas Chromatography and Inverse Liquid Chromatography," Presented at The American Chemical Society Symposium on Autooxidation of Distillate Fuels, San Diego, CA, March, 1994.

21. L. P. Chin, V. R. Katta, and S. P. Heneghan, "Computer Modeling of Deposits Formed in Jet Fuels," Presented at The American Chemical Society Symposium on Autooxidation of Distillate Fuels, San Diego, CA, March, 1994.

22. D. L. Geiger, R. Grinstead, and S. Zabarnick, "The Analysis of Thermally Stressed and Unstressed Jet Fuels for Sulfur, Nitrogen, and Oxygen by Solid Phase Extraction and Gas Chromatography-Atomic Emission Detection," Presented at the Society for Applied Spectroscopy, Ohio State University, Columbus, OH, February 1994.

23. R. E. Kauffman, "Oxidation Stability of California Diesel Engine Fuels," California State Legislature, Sacramento, CA, May 1994.

24. F. Takahashi, W. J. Schmoll, and J. L. Dressler, "Characterization of a Velocity-Modulation Atomizer," A paper for presentation at The Central States Section Meeting, The Combustion Institute, Madison, WI, June 1994.

25. M. Vangsness and W. J. Schmoll, "Applications of a Neural Net Simulator to CARS Temperature Measurements," A paper presented at The Central States Section Meeting, The Combustion Institute, Madison, WI, June 1994.

26. S. P. Heneghan, D. L. Geiger, and S. L. Locklear, "Quantifying Mass Transfer of Jet Fuels by Supercritical Fluid (CO_2) Extraction using Gas Chromatography and Atomic Emissions Detection," Ohio Valley Chromatographic Symposium, Heuston Woods, OH, June 1994.

27. F. Takahashi, M. D. Durbin, M. D. Vangsness, and W. J. Schmoll, "Structure of the Stabilizing Region of Hydrogen Jet Diffusion Flames," Poster presentation at The 25th Symposium (Int.) on Combustion, The Combustion Institute, July, 1994.

28. J. Zelina, R. C. Striebich, J. W. Blust, and L. F. Truett, III, "Studies of Halon Decomposition in the Well Stirred Reactor," A paper for presentation at The Central States Section Meeting, The Combustion Institute, Madison, WI, June 1994.

29. G. L. Dieterle and K. E. Binns, "Evaluation of High Thermal Stability Fuels for Future Aircraft," AIAA Paper No. 94-3171, presented at 30th AIAA/ASME/SAE/ASEE Joint Propulsion Conference, June 1994.

30. J. Zelina and D. R. Ballal, "Combustion and Emissions Studies Using a Well Stirred Reactor," AIAA Paper No. 94-2903, presented at 30th AIAA/ASME/SAE/ASEE Joint Propulsion Conference, June 1994.

31. M. D. Durbin and D. R. Ballal, "Characteristics of Swirl Flames in a Step Combustor," AIAA Paper No. 94-3272, presented at 30th AIAA/ASME/SAE/ASEE Joint Propulsion Conference, June 1994.

32. R. Grinstead, "Analysis of Jet Fuel Extracts and Deposits," Presented at the Coordinating Research Council Meeting, Washington, D.C., April 1994.

33. R. C. Striebich and W. A. Rubey, "A Convenient Method for Analyzing Dissolved Oxygen in Hydrocarbon Matrices Using Gas Chromatography-Mass Spectrometry," Submitted to *Journal of Energy and Fuels*, American Chemical Society, Washington, D.C. August 1994.

34. F. Takahashi, "Regression Analyses of the Soot Threshold Data for Premixed Combustion," Paper for presentation at the Eastern States Meeting, The Combustion Institute, Clearwater Beach, FL, December, 1994.

35. G. L. Dieterle and K. E. Binns, "Extended Duration Thermal Stability Test of Improved Thermal Stability Jet Fuel," ASME Paper No. 95-GT-69 presented at the ASME Turbo Expo '95, Houston, TX, June 1995.

36. R. E. Kauffman, "The Effect of Different Sulfur Compounds on the Oxidation and Deposition Mechanisms of Jet Fuel," ASME Paper No. 95-GT-222 for presentation at the ASME Turbo Expo '95, Houston, TX, June 1995.

37. S. P. Heneghan, D. R. Ballal, W. E. Harrison III, and H. C. Mongia, "Advanced Jet Fuels--JP-4 to JP-8 and Beyond," ASME Paper No. 95-GT-223, for presentation at the ASME Turbo Expo '95, Houston, TX, June 1995.

38. F. Takahashi, W. J. Schmoll, D. D. Trump, and L. P. Goss, "Vortex-Flame Interactions and the Local Extinction of Turbulent Jet Diffusion Flames," AIAA Paper No. 95-0139, Presented at 33rd Aerospace Sciences Meeting, Reno, NV, January 1995.

39. J. S. Ervin, R. E. Kauffman, and D. H. Kalt, "Effects of Thermal Stressed Jet Fuels on O-Rings," AIAA Paper No. 95-0287, Presented at 33rd Aerospace Sciences Meeting, Reno, NV, January 1995.

40. D. J. Pestian, J. P. Bons, R. B. Rivir, and C. D. MacArthur, "Effect of Unsteadiness on Film Cooling Effectiveness," AIAA Paper No. 95-0306, Presented at 33rd Aerospace Sciences Meeting, Reno, NV, January 1995.

41. F. Takahashi, M. D. Vangsness, and W. J. Schmoll, "Structure of the Stabilizing Region of the Methane Jet Diffusion Flames," Central States Section Meeting, The Combustion Institute, San Antonio, TX, April 1995.

42. J. Zelina and D. R. Ballal, "Model Predictions of Pollutant Emissions in a Well Stirred Reactor," ASME Paper No. 95-GT-48, to be presented at ASME COGEN Turbo Power 95 Conference, Vienna, Austria, Aug. 23-26, 1995.

43. J. S. Ervin, S. P. Heneghan, T. F. Williams, and M. A. Hanchak, "Effects of Reduced Dissolved Oxygen Concentration on Jet Fuel Deposit Formation," Presented at the American Chemical Society Symposium on Coke Formation and Mitigation, Chicago, IL, Aug. 1995.

44. F. Takahashi and V. R. Katta, "Numerical Experiments on the Local Extinction of Jet Diffusion Flames," Presented at the 15th International Colloquium on the Dynamics of Explosions and Reactive Systems, Boulder, CO, August 1995.

45. F. Takahashi, M. D. Durbin, and M. D. Vangsness, "Stabilization of Hydrogen Jet Diffusion Flames With and Without Swirl," Presented at the Eighth International Symposium on Transport Phenomenon in Combustion, San Francisco, CA, July 1995.

46. F. Takahashi, "Structure and Stability of Turbulent Diffusion Flames," Invited Lecture, Thermal energy and Combustion Department, National Institute for Resources and Environment, Ministry of International Trade and Industry, Tsukuba, Japan, August 1995.

47. F. Takahashi, "Vortex-Flame Interaction and Stability of Jet Diffusion Flames," Invited Lecture, Department of Chemical System Engineering, The University of Tokyo, Tokyo, Japan, August 1995.

48. F. Takahashi, "Vortex-Flame Interaction and the Local Extinction of Jet Diffusion Flames," Invited Lecture, Department of Mechanical Engineering, Keio University, Yokohama, Japan, August 1995.

49. R. Striebich, W. Rubey, and R. Grinstead, "Analysis of Halon-1301 Combustion Products Using GC-MS in a Wide- Bore Porous Layer Open Tubular (PLOT) Column," presented at the 17th International Symposium on Capillary Chromatography and Electrophoresis, Wintergreen, VA, May 1995.

50. R. Striebich, R. Grinstead, J. Zelina, and J. Blust, "Studies of Halon-1301 Decomposition in a Well Stirred Reactor," presented at the 4th International Congress on Toxic Combustion Byproducts," Berkeley, CA, June 1995.

51. S. Zabarnick and P. Zelesnik, "Studies of Jet Fuel Thermal Stability and Oxidation Applications of QCM," presented at the CRC-Aviation Group Meeting, Alexandria, VA, April 1995.

52. S. Zabarnick, P. Zelesnik, and R. Grinstead, "Jet Fuel Deposition and Oxidation: Dilution, Materials, Oxygen, and Temperature Effects," presented at the 21st Annual Mini-Symposium on Aerospace Science and Technology, Dayton, OH, March 1995.

53. R. Grinstead, R. Striebich, J. Blust, and J. Zelina, "Analytical Evaluation of Halon Combustion by FTIR and GC-MS," presented at the 21st Annual Mini-Symposium on Aerospace Science and Technology, Dayton, OH, March 1995.

54. F. Takahashi, J. W. Blust, J. Zelina, R. C. Striebich, and C. W. Frayne, "Soot Threshold Measurements Using a Well Stirred Reactor," Presented at the Eastern States Section Meeting, The Combustion Institute, Worcester, MA, October, 1995.

55. J. S. Ervin, T. F. Williams, S. P. Heneghan, and S. Zabarnick, "The Effects of Dissolved Oxygen Concentration, Fractional Oxygen Consumption, and Additives on JP-8 Thermal Stability," ASME Paper No. 96-GT-132, Presented at the ASME Turbo Expo., Birmingham, U.K., June 1996.

56. D. G. Holmberg and D. Pestian, "Wall Jet Turbulent Boundary Layer Heat Flux, Velocity, Temperature Spectra, and Time Scales," ASME Paper No. 96-GT-529, Presented at the ASME Turbo Expo., Birmingham, U.K., June 1996.

57. D. Pestian, R. B. Rivir, S. Gogineni, and D. Trump, "PIV Measurements of Periodically Forced Flat Plate Film Cooling Flows With High Freestream Turbulence," ASME Paper No. 96-GT-236, Presented at the ASME Turbo Expo., Birmingham, U.K., June 1996.

58. F. Takahashi, M. D. Vangsness, M. D. Durbin, and W. J. Schmoll, "Structure of Turbulent Hydrogen Jet Diffusion Flames With and Without Swirl," presented at ASME (Int.) Mechanical Engineering Congress and Exposition, Paper No. HTD-317-2, pp. 183-193, San - Francisco, CA, November 1995.

59. F. Takahashi and V. R. Katta, "Numerical Experiments on the Local Extinction of Jet Diffusion Flames," AIAA Paper No. 96-0521, presented at the 34th Aerospace Sciences Meeting, Reno, NV., January 1996.

60. D. Pestian, R. B. Rivir, S. Gogineni, and L. P. Goss, "PIV Measurements of Flat Plate Film Cooling Flows With High freestream Turbulence," AIAA Paper No. 96-0617, presented at the 34th Aerospace Sciences Meeting, Reno, NV., January 1996.

61. S. P. Heneghan, S. Zabarnick, D. R. Ballal, and W. E. Harrison III, "JP-8+100: The Development of High Thermal Stability Jet Fuel," AIAA Paper No.96-0403, presented at the 34th Aerospace Sciences Meeting, Reno, NV., January 1996.

62. J. S. Ervin, T. F. Williams, and V. R. Katta, "The Effects of JP-8 Thermal Stability Additives on Deposition in Heated and Cooled Regions in a Flowing System," Presented at the ACS Symposium on Structure of Jet Fuels, New Orleans, LA, March 1996.

63. S. Zabarnick, S. D. Whitacre, and P. Zelesnik, "Further Studies of JP-8 + 100 Additive Candidates in the QCM," Presented at the ACS Symposium on Structure of Jet Fuels, New Orleans, LA, March 1996.

64. S. P. Heneghan, T. F. Williams, S. D. Whitacre, and J. S. Ervin, "The Effects of Oxygen Scavenging on Jet Fuel Thermal stability," Presented at the ACS Symposium on Structure of Jet Fuels, New Orleans, LA, March 1996.

65. Binns and G. L. Dieterle, "Evaluation of the JP-8+100 Additive Candidates in the Extended Duration Thermal stability Test System," Presented at the American Chemical Society Symposium on Structure of Jet Fuels, New Orleans, LA, March 1996.

66. F. Takahashi and V. R. Katta, "A Numerical Study of the Stability of Methane Jet Diffusion Flames," Presented at the Central States Section, The Combustion Institute, St. Louis, MO, May 1996.

67. F. Takahashi, W. J. Schmoll, M. D. Vangsness, and V. R. Katta, "The Stabilizing Region of Methane-Jet Diffusion Flames," Poster presentation at the 26th International Symposium on Combustion, Naples, Italy, July 1996.

68. J. J. Schauer and D. J. Pestian, "Film Cooling Heat Transfer With High Free Stream Turbulence," Presented at the ASME (Int.) Mechanical Engineering Congress and Exhibition, Atlanta, GA, November 17-22, 1996.

69. F. Takahashi, M. D. Vangsness, M. D. Durbin, and W. J. Schmoll, "LDV and CARS Measurements in Swirling and Nonswirling Turbulent Jet Diffusion Flames," Proceedings of the International Workshop on Measurement and Computation of Turbulent Nonpremixed Flames, Naples, Italy, July 1996 (available on the internet: http: //www.ca.sandia.gov /tdf/Proceedings.html; http: //www.ca.sandia.gov /tdf /DataSums/TakahashiH2.html.).

70. F. Takahashi and V. R. Katta, "Further Analysis of the Stabilizing Region of Methane Jet Diffusion Flames," Eastern States Section Meeting, The Combustion Institute, Hilton Head, S.C., December 1996.

71. J. S. Ervin, S. P. Heneghan, S. Zabarnick, and W. E. Harrison III, "Development of Advanced Jet Fuels: Modeling Aspects," ASME (Int.) Mechanical Engineering Congress and Exhibition, Atlanta, GA, November, 1996.

72. J. S. Ervin and S. P. Heneghan, "The Meaning of Activation Energy and Reaction Order in Autoaccelerating Systems," ASME Paper No. 97-GT-224, presented at the ASME Turbo Expo., Orlando, FL, June 1997.

73. J. S. Ervin, T. F. Williams, and S. Zabarnick, "Modeling of Jet Fuel Oxidation at Low Temperature," AIAA Paper No. 97-0272, 35th AIAA Aerospace Sciences Meeting, Reno, NV, January 1997.

74. J. W. Blust, M. G. Getz, and S. Zabarnick, "Probe Design Optimization for the Well Stirred Reactor," AIAA Paper No. 97-0907, 35th AIAA Aerospace Sciences Meeting, Reno, NV, January 1997.

75. G. L. Dieterle and K. E. Binns, "System Evaluation of JP-8+100 Additives at High Bulk Temperature," ASME Paper No. 97-GT-071, presented at the ASME Turbo Expo., Orlando, FL, June 1997.

76. D. H. Kalt, "Evaluation of JP-8+100 Fuel Compatibility with Aircraft Fuel Systems Materials," Presented at the ASME Turbo Expo., Orlando, FL, June 1997.

77. F. Takahashi and V. R. Katta, "A Numerical Investigation of the Stabilizing Mechanism of Methane Jet Diffusion Flame," AIAA Paper No. 97-0251, 35th AIAA Aerospace Sciences Meeting, Reno, NV, January 1997.

78. F. Takahashi and V. R. Katta, "A Numerical Analysis of a Methane Diffusion Flame over a Flat Plate," To be presented at the Central States Section Meeting, The Combustion Institute, Point Clear, AL, April 1997.

79. S. Zabarnick, "UDRI Contributions to the JP-8+100 Program," JP-8+100 Program Review, WPAFB, OH, March 1997.

80. S. P. Heneghan, S. Zabarnick, and D. R. Ballal, "Designing High Thermal Stability Jet Fuels for the 21st Century," presented at the 31st Intersociety Energy Conversion Engineering Conference, Washington DC, August 1996.

81. R. C. Striebich and B. Ohler, "Surface Adsorption of Jet Fuel Metal Deactivator using Inverse Liquid Chromatography," presented at the Ohio Valley Chromatography Symposium, Hueston Woods, OH, June 1997.

82. M. Getz, J. Blust, J. M. Calo, T. Miller, J. O. Ballenthin, and R. Striebich, "Modeling of the Response of a Well Stirred Combustor to the Injection of Fire Suppressants," Presented at *The 5th International Congress on Toxic Combustion Byproducts*, Dayton, OH, June 1997.

83. J. O. Ballenthin, T. Miller, J. M. Calo, Striebich, J. Blust, and M Getz, "Free-Jet, Molecular Beam Mass Spectrometer System for Monitoring the Gas Phase Composition in a Well Stirred Reactor," presented at *The 5th International Congress on Toxic Combustion Byproducts*, Dayton, OH, June 1997.

84. J. M. Calo, J. O. Ballenthin, T. Miller, Striebich, J. Blust, and M Getz, "Transient Studies of the Effects of Fast Pulse Injections of Fire Suppressants into the Well Stirred Reactor," presented at *The 5th International Congress on Toxic Combustion Byproducts*, Dayton, OH, June 1997.

85. F. Takahashi and V. R. Katta, "A Numerical Study of a Methane Diffusion Flame Over a Flat Plate," Presented at the Second International Symposium on Scale Modeling, Lexington, KY, June 1997.

86. S. Zabarnick and S. D. Whitacre, "Aspects of Jet Fuel Oxidation," ASME Paper No. 97-GT-219, Presented at the ASME Turbo Expo, '97, Orlando, FL, June 1997.

87. R. E. Kauffman, "Simple Analytical Techniques to Determine the Dispersal Capacity and Metal Deactivator Additive Concentration of JP-8 + 100 and ther jet Fuels," ASME Paper No. 97-GT-77, Presented at the ASME Turbo Expo, '97, Orlando, FL, June 1997.

88. W. A. Rubey, R. C. Striebich, and S. D. Anderson, "Water Measurement Techniques: Analysis for Dissolved and Total Water in Turbine Engine Fuels," Presented at the JP-8 + 100 Program Review Conference, WPAFB, OH, March 1997.

UDRI Reports

1. F. Takahashi, M. D. Vangsness, and M. D. Durbin, "LDV Measurements in Swirling and Non-Swirling Coaxial Turbulent Air Jets--No. 5: 45 degree swirler, 100 m/s," University of Dayton Technical Report, UDR TR 93-22, May 1993.

2. F. Takahashi, M. D. Vangsness, and M. D. Durbin, "LDV Measurements in Swirling and Non-Swirling Coaxial Turbulent Air Jets--No. 6: 45 degree swirler, 25 m/s," University of Dayton Technical Report, UDR TR 93-23, June 1993.

3. F. Takahashi, M. D. Vangsness, and M. D. Durbin, "LDV Measurements in Swirling and Non-Swirling Coaxial Turbulent Air Jets--No. 7: 60 degree swirler, 25 m/s," University of Dayton Technical Report, UDR TR 93-24, July 1993.

4. F. Takahashi, M. D. Durbin, and M. D. Vangsness, "LDV Measurements in Swirling and Non-Swirling Coaxial Turbulent Hydrogen Jet Diffusion Flames--No. 1: No Swirl, 25 m/s," University of Dayton Technical Report, UDR TR 93-88, September 1993.

5. T. F. Williams, C. R. Martel, and J. W. Blust, "Studies of Thermal Stability of Jet Fuels--Volume I: Experimental Work," University of Dayton Technical Report, UDR TR 94-10, January 1994.

6. T. F. Williams, C. R. Martel, and J. W. Blust, "Studies of Thermal Stability of Jet Fuels--Volume II: Data Sets," University of Dayton Technical Report, UDR TR 94-11, January 1994.

7. S. P. Heneghan, R. R. Grinstead, R. C. Striebich, and S. Zabarnick, "Jet Fuel Thermal Stability and Analytic Test Data," University of Dayton Technical Report, UDR TR 94-20, February 1994.

8. S. Zabarnick, "Evaluation of Jet Fuels and Jet Fuel Additives Using the Quartz Crystal Microbalance and Pressure Measurements," University of Dayton Technical Report, UDR TR 94-63, March 1994.

9. R. Grinstead, "Evaluation of JP-8+100 Additives by the Isothermal Corrosion Oxidation Test and the Microcarbon Residue Test," University of Dayton Technical Report, UDR TR 94-85, May 1994.

10. F. Takahashi, M. D. Vangsness, M. D. Durbin, and W. J. Schmoll, "CARS Temperature Measurements in Swirling and Non-Swirling Coaxial Turbulent Hydrogen Jet Diffusion Flames," University of Dayton Technical Report, UDR TR 94-89, June 1994.

11. F. Takahashi, M. D. Durbin, W. J. Schmoll, and M. D. Vangsness, "LDV Measurements in Swirling and non-Swirling Coaxial Turbulent Hydrogen Jet Diffusion Flames--No. 2: No Swirl, 100 m/s," University of Dayton Technical Report, UDR TR 94-115, July 1994.

12. F. Takahashi, M. D. Durbin, W. J. Schmoll, and M. D. Vangsness, "LDV Measurements in Swirling and non-Swirling Coaxial Turbulent Hydrogen Jet Diffusion Flames--No. 3: 30-degree Swirl, 100 m/s," University of Dayton Technical Report, UDR TR 94-116, August 1994.

13. F. Takahashi, M. D. Durbin, W. J. Schmoll, and M. D. Vangsness, "LDV Measurements in Swirling and non-Swirling Coaxial Turbulent Hydrogen Jet Diffusion Flames--No. 4: 45-degree Swirl, 100 m/s," University of Dayton Technical Report, UDR TR 94-117, September 1994.

14. S. Zabarnick, P. Zelesnik, and S. D. Whitacre, "Evaluation of Jet Fuels and Jet Fuel Additives Using the Quartz Crystal Microbalance and Pressure Measurements-Part II," University of Dayton Technical Report, UDR TR 95-98, November 1995.

15. D. Kalt, "Fuel and Fuel System Materials Compatibility Test program for a JP-8+100 Fuel Additive: Vol 1: Betz/Dearborn-8Q462 Thermal Stability Additive Package," University of Dayton Technical Report No. UDR TR 97-01, January 1997.

16. S. Zabarnick, S. D. Whitacre, and M. S. Mick, "Evaluation of Jet Fuels and Jet Fuel Additives Using the Quartz Crystal Microbalance and Pressure Measurements: Part III" University of Dayton Technical Report No. UDR TR 97-108, June 1997.